Coral-based reconstructions of reef- to regional-scale ocean surface conditions in the Atlantic Warm Pool since the late 19th century

Korallenbasierte Rekonstruktionen riff- bis regionalmaßstäblicher Meeresoberflächenbedingungen im Atlantic Warm Pool seit dem späten 19. Jahrhundert

D i s s e r t a t i o n

zur Erlangung des Doktorgrades der Naturwissenschaften

Dr. rer. nat.

an der Mathematisch-Naturwissenschaftlichen Fakultät

der Christian-Albrechts-Universität zu Kiel

vorgelegt von

Jonas von Reumont

Kiel

2018

1. Gutachter:	Prof. Dr. Wolf-Christian Dullo
2. Gutachter:	Prof. Dr. Miriam Pfeiffer
Tag der Disputation:	29.11.2018
Zum Druck genehmigt:	29.11.2018

_____

Dekan

Erklärung

Hiermit erkläre ich an Eides statt, dass ich diese Dissertation selbständig und nur mit Hilfe der angegeben Quellen und Hilfsmittel erstellt habe. Weiterhin versichere ich, dass der Inhalt dieser Arbeit weder in dieser, noch in veränderter Form, einer weiteren Prüfungsbehörde vorliegt. Die Arbeit wurde unter Einhaltung der Regeln guter wissenschaftlicher Praxis der Deutschen Forschungsgemeinschaft verfasst.

Kiel, den 06.09.2018

_____

Jonas von Reumont

Abstract

Climate variability in the tropical Atlantic region produces numerous impacts on society and the environment of the surrounding continents on seasonal, interannual and multidecadal time scales through fluctuations in ocean and land temperature, rainfall and extreme events. A thorough knowledge of past variability of the climate system is mandatory for long-range climate forecasting and the assessment of the anthropogenic impact on climate and ecosystems from the local to the global scale. However, the current knowledge about climate variability is essentially based on observational climate data that are often too short to reliably determine and understand the underlying mechanisms with sufficient accuracy. Thus, understanding past tropical climate and environmental variability beyond the period of instrumental observations or within regions lacking instrumental data requires the use of proxy data, non-instrumental sources of indirect climatic information. Large colonies of massive growing tropical reef corals have been proven to sensitively monitor environmental fluctuations in ambient seawater and large scale climate variability with a fidelity and temporal resolution comparable to instrumental climate data. Stable oxygen isotopic composition ($\delta^{18}O$) and trace elemental ratios (e.g., Sr/Ca) incorporated in the aragonitic coral skeleton can reveal a detailed history of past environmental conditions, e.g., sea surface temperature (SST). However, decade-long and continuous subseasonally resolved coral records from the Atlantic region have lagged behind the extensive work published using coral records from the Indo-Pacific Ocean. The principal objective of this thesis is the development of seasonal-scale proxy records of surface ocean conditions in order to study past changes in tropical Atlantic climate variability as well as reef scale environmental variability extending beyond the period of instrumental data. For this purpose, monthly resolved geochemical coral records from the lagoon and fore reef of Little Cayman (Cayman Islands, central Caribbean) were generated using the massive growing, hermatypic species *Diploria strigosa* (Dana, 1846).

The first study compares two coral Sr/Ca records from the two different reef environments and gridded reanalysis SST data from 1970 to 2012 and shows that reef-scale SST variability can be much larger and site specific than suggested by satellite SST measurements. Based on Sr/Ca data the study also indicates that the two corals respond differently to El Niño related short-term thermal stress depending on their position in the reef. The coral from the fore reef is more susceptible to short-term high temperature events and consequently reacts with stress symptoms, while the coral from the shallow lagoon environment shows a higher level of resilience because it may already be adapted to an environment with rapid thermal fluctuations and higher maximum temperatures. Additionally, the shallow lagoon coral showed decadal variations in Sr/Ca, supposedly related to the modulation of lagoonal temperature through a varying volume of tidal water, forced by the 18.6-year period lunar nodal cycle.

The following study expands the scope beyond the local level. The fore reef coral record is extended in time and completed with $\delta^{18}O$ measurements, representing the longest continuous, seasonally resolved record from a *Diploria strigosa* coral in the Atlantic to date (1887–2012 = 125 years). Both geochemical proxies show decreasing long-term trends, indicating long-term warming. Sr/Ca indicates much stronger regional warming than large-scale grid-SST data, while $\delta^{18}O$ also tracks large-scale SST changes in the Atlantic Warm Pool. Seawater $\delta^{18}O$ variations, which are linked to the hydrological cycle, are reconstructed from paired Sr/Ca and $\delta^{18}O$ measurements ($\Delta\delta^{18}O_{sw\text{-}center}$), indicating a drying trend over the past century. The (spatial) relationships of geochemical coral proxy data with SST are

investigated, along with the feasibility of the coral record to track the impact of modes of external forcing (North Atlantic Oscillation, NAO; El Niño-Southern Oscillation, ENSO) on north tropical Atlantic SST and climate variability. The results show that coral $\delta^{18}O$ tracks decadal and multidecadal North Atlantic Oscillation variability in the region of the Loop Current and Gulf Stream system. In Addition, a combined evaluation of the fore reef record with two other coral records from different Caribbean sites reveals valuable SST information for large sparsely sampled Atlantic regions beyond the Caribbean.

The following short study explores coral nitrogen isotopes, which only recently have been used in biogenic carbonate skeletons as a proxy for nitrogen fixation in tropical oceans. Based on material from the fore reef core the development of the first centennial-scale record of annual nitrogen isotopes in a Caribbean coral is described. The results show changing nitrogen fixation that correlates with multidecadal variability in North Atlantic Ocean SST. A decreasing trend in reconstructed nitrogen fixation during the 20th century suggests a connection to a supposed slowdown of the Atlantic Meridional Overturning Circulation (AMOC).

The fourth and final study contributes to the current and incomplete knowledge of the distribution and living conditions of cold and dark dwelling warm water coral relatives and draws attention to the global aspect of scleractinian corals as climate and paleoceanographic archive for surface ocean to deep ocean conditions. The study reports on the newly discovered Eugen Seibold cold-water coral (CWC) province between 678 and 863 m water depth off western Morocco, covering an area of more than 410 km^2. The province was successfully discovered based on Conductivity-Temperature-Depth (CTD) reconnaissance applying seawater density as a potential indicator of CWC occurrences, followed by hydroacoustic mapping. Box core based ground-truthing of selected sites revealed a thin cover of living corals, dominated by *Lophelia pertusa,* but much larger accumulations of dead thickets and fragmented coral rubble within the province. Living CWC colonies occur within the deeper part of the North Atlantic Central Water (NACW). Buried coral material from box core samples yield absolute ages dating back to the late Holocene. These initial geochronological results and a patchy distribution of the cold-water corals suggest recolonization of this area by *Lophelia pertusa*, rather than the continuous evolution of large flourishing reef build-ups.

Zusammenfassung

Klimaschwankungen in der Region des tropischen Nordatlantiks haben einen großen Einfluss auf die menschliche Gesellschaft sowie auf die Umweltbedingungen auf den umliegenden Kontinenten. Auf saisonalen, interannualen und multidekadischen Zeitskalen macht sich dieser Einfluss vor allem durch Schwankungen der Temperatur der Meeres- und Landoberfläche, des Niederschlags und durch Extremereignisse bemerkbar. Eine gründliche und umfassende Kenntnis der Variabilität des Klimasystems in der Vergangenheit ist zwingend notwendig, um langfristige Klimaprognosen formulieren und die anthropogenen Auswirkungen auf Klima- und Ökosysteme von der lokalen bis zur globalen Ebene bewerten zu können. Das derzeitige Wissen über die Variabilität des Klimas basiert hingegen im Wesentlichen auf instrumentell aufgezeichneten Klimadaten, die oft zu kurz sind, um die zugrunde liegenden Mechanismen mit hinreichender Genauigkeit zuverlässig ermitteln und verstehen zu können. Das Verständnis tropischer Klima- und Umweltbedingungen in der Vergangenheit, über die Zeit instrumenteller Beobachtungen hinaus und auch innerhalb von Regionen, in denen keine instrumentellen Daten vorhanden sind, erfordert die Nutzung von Proxyarchiven, nicht-instrumentellen Quellen indirekter Klimainformationen. Es ist beispielsweise bekannt, dass große Kolonien massiv wachsender tropischer Riffkorallen physikochemische Veränderungen im sie umgebenden Meerwasser mit einer Genauigkeit und zeitlichen Auflösung aufzeichnen, die mit instrumentellen Klimadaten vergleichbar ist. Im aragonitischen Korallenskelett eingebaute stabile Sauerstoffisotope ($\delta^{18}O$) und Spurenelemente (z.B. Sr/Ca) können ein detailliertes Bild über vergangene Änderungen in den Umweltbedingungen (z.B. der Temperatur an der Wasseroberfläche, SST) liefern. Die Anzahl der auf Korallen aus dem tropischen Atlantik basierenden Proxy-Zeitreihen mit saisonaler und höherer zeitlicher Auflösung ist jedoch relativ gering im Vergleich zu den zahlreichen Studien, die auf Korallen aus dem Indischen und Pazifischen Ozean basieren. Das Hauptziel der vorliegenden Arbeit ist die Entwicklung von saisonal aufgelösten Proxy-Zeitreihen der Oberflächenozeanbedingungen, um Klima- und Umweltveränderungen im tropischen Atlantik als auch im Riffsystem untersuchen zu können, die über den verfügbaren Zeitraum instrumenteller Daten hinausgehen. Zu diesem Zweck wurden monatlich aufgelöste Korallen-Zeitreihen aus der Lagune und dem Vorriff von Little Cayman (Cayman Islands, zentrale Karibik) aus schnellwachsenden, hermatypischen Korallen massiver Wuchsform der Art *Diploria strigosa* (Dana, 1846) erzeugt.

Die erste Studie vergleicht Korallen-Sr/Ca-Zeitreihen aus den zwei verschiedenen Riffumgebungen mit Reanalyse-SST-Daten von 1970 bis 2012 und zeigt, dass die Riff-SST-Variabilität standortspezifisch deutlich größer sein kann, als dies durch Satelliten-SST-Messungen vermittelt wird. Basierend auf den Sr/Ca-Daten zeigt die Studie auch, dass die beiden Korallen in Abhängigkeit von ihrer Position im Riff unterschiedlich auf mit El Niño in Verbindung stehende, kurzfristige thermische Belastungen reagieren. Die Koralle aus dem Vorriff ist hierbei anfälliger und reagiert mit Stresssymptomen, während die Koralle aus der flachen Lagune eine höhere Widerstandsfähigkeit aufweist, da sie möglicherweise bereits an eine Umgebung mit schnellen thermischen Schwankungen und höheren Maximaltemperaturen angepasst ist. Zusätzlich zeigt die Koralle aus der Lagune dekadische Schwankungen im Sr/Ca, die vermutlich mit der Modulation der Wassertemperatur durch ein variierendes Volumen des Gezeitenwassers zusammenhängen, welches wiederum durch den Nodal-Zyklus der Partialtiden des Mondes von 18.6 Jahren gesteuert wird.

Die folgende Studie erweitert das Blickfeld über die lokale Ebene hinaus. Die Korallen-Zeitreihe aus dem Vorriff wird hier verlängert und durch $\delta^{18}O$-Messungen ergänzt.

Hierdurch ergibt sich die derzeit längste kontinuierliche und saisonal aufgelöste Proxy-Zeitreihe aus einer *Diploria strigosa* Koralle (1887–2012 = 125 Jahre). Beide geochemischen Proxies weisen abnehmende Langzeittrends auf, was auf eine langfristige Erwärmung hindeutet. Sr/Ca zeigt eine wesentlich stärkere regionale Erwärmung an als großflächige Reanalyse-SST-Daten dies wiedergeben. Die $\delta^{18}O$-Zeitreihe verfolgt außerdem großräumige SST-Veränderungen in der Region des Atlantic Warm Pool. Vom hydrologischen Kreislauf abhängige Meerwasser-$\delta^{18}O$-Schwankungen werden aus gepaarten Sr/Ca- und $\delta^{18}O$-Messungen ($\Delta\delta^{18}O_{sw\text{-}center}$) rekonstruiert, die einen Trend zu trockeneren Bedingungen über das letzte Jahrhundert anzeigen. Die (räumlichen) Beziehungen von Korallen-Proxydaten und SST werden untersucht, gemeinsam mit der Möglichkeit, den Einfluss externer Modi des Klimaantriebs (Nordatlantische Oszillation, NAO; El Niño-Southern Oscillation, ENSO) auf SST und Klimavariabilität im tropischen Nordatlantik zu verfolgen. Die Ergebnisse zeigen, dass anhand des Korallen-$\delta^{18}O$ dekadische und multidekadische Schwankungen der NAO im Bereich des Loop Current und Golfstromsystems nachvollzogen werden können. Darüber hinaus zeigt eine kombinierte Auswertung der Vorriff-Zeitreihe und zweier weiterer Korallen-Zeitreihen aus verschiedenen karibischen Gebieten, dass diese Kombination wichtige zusammenhängende Informationen über sie SST für weite, wenig beprobte Regionen des Atlantiks außerhalb der Karibik liefern kann.
Die folgende Kurzstudie untersucht die Zusammensetzung stabiler Stickstoffisotope, welche erst seit kurzem in biogenen Karbonatskeletten als Proxy für die Stickstofffixierung in tropischen Ozeanen verwendet werden. Anhand von Material aus dem Vorriffkern wird die erste etwa 100 Jahre umfassende Stickstoffisotopen-Zeitreihe aus einer Karibikkoralle vorgestellt. Die Ergebnisse zeigen eine veränderliche Stickstofffixierung, die mit multidekadischer Variabilität der SST im Nordatlantik korreliert. Ein abnehmender Trend in der rekonstruierten Stickstofffixierung während des 20. Jahrhunderts weist auf einen Zusammenhang mit einer Verlangsamung der Atlantic Meridional Overturning Circulation (AMOC) hin.
Die vierte und letzte Studie trägt zum aktuellen und unvollständigen Wissen über die Verbreitung und die Lebensbedingungen von kalt und dunkel lebenden Verwandten der Warmwasserkorallen bei und lenkt die Aufmerksamkeit auf den globalen Aspekt der Steinkorallen als Klimaarchiv bzw. als paläozeanographisches Archiv für die physikochemischen Bedingungen im Ozean, vom Oberflächenwasser bis in die Tiefsee. Die Studie beschreibt die neu entdeckte Eugen Seibold Kaltwasserkorallen (CWC) Provinz vor Westmarokko in einer Wassertiefe von 678 bis 863 m und mit einer Ausdehnung von mehr als 410 km^2. Die Provinz wurde mit Hilfe von CTD-Erkundungen und hydroakustischen Kartierungsverfahren entdeckt, wobei die Meerwasserdichte als potenzieller Indikator für das CWC-Vorkommen verwendet wurde. Großkastengreiferproben weisen eine dünne Abdeckung von lebenden Korallen auf, die von *Lophelia pertusa* dominiert wird. Die lebenden CWC-Kolonien kommen innerhalb des tieferen Teils des Nordatlantischen Zentralwassers (NACW) vor. Innerhalb der Provinz befinden sich jedoch viel größere Ansammlungen von toten Dickichten und fragmentiertem Korallenschutt. Absolute Alter von vergrabenem Korallenmaterial aus Großkastengreiferproben reichen bis ins späte Holozän. Diese ersten geochronologischen Ergebnisse und eine uneinheitliche Verteilung der Kaltwasserkorallen lassen auf eine Wiederbesiedlung dieses Gebiets durch *Lophelia pertusa* schließen, anstatt auf eine kontinuierliche Entwicklung von großen und gedeihenden Riffansammlungen.

Acknowledgements

I doubt any dissertation could be completed without extensive support and assistance from a large crowd of people, and this one is no exception.

I am especially grateful to Prof. Wolf-Christian Dullo for giving me the opportunity to carry out this thesis and for being a patient and helpful supervisor in every circumstance. His door was always open for me and I appreciated that.

I am also grateful to Prof. Miriam Pfeiffer for being the second reviewer of this thesis.

Special thanks go to Steffen Hetzinger, my „little supervisor", for the comprehensive introduction to coral paleoclimatology and numerous valuable discussions. I hugely benefited from his knowledge, experience and inexhaustible support. Thank you Steffen!

I am greatly indebted to Carrie Manfrino for giving me the opportunity to work and do research at the Central Caribbean Marine Institute. Rob Hedges, Jon Clamp and Lowell Forbes are thanked for logistical support and assistance during fieldwork on land and under water. Of course, thank you also to Emily Lopez aka "Miss Em", whose range of deliciously home cooked Caribbean style food was always a welcome treat after strenuous fieldwork.

Furthermore, I would like to thank Tsuyoshi Watanabe at the University of Hokkaido for inviting me to Japan for the exchange of ideas and valuable discussions as well as for some inspiring onsen "温泉" visits.

Craig Grove and Rik Tjallingii are thanked for their assistance with digital X-raying and luminescence scanning at NIOZ, as well as for the cheerful company on the island of Texel.

For the introduction to laboratory work and the assistance during numerous stable isotope measurements and the analysis of trace elemental ratios I would like to thank Sebastian Fessler and Ana Kolevica at GEOMAR, as well as Dieter Garbe-Schönberg and Karen Bremer at the University of Kiel.

Atsuko Yamazaki and Netramani Sagar is deeply thanked for encouragement, support and uncountable discussions.

I would like to thank "my" REU-Program students Kelly Luis and Sam Degregory for their support and the opportunity to learn how to teach and attract young people in science.

I am also grateful to my colleagues Stefan Reißig, David Poggeman, Silke Glogowski, Anna Jentzen, Anne Osborne, Zeynep Erdem, Veit Dausmann, Kristin Doering, Jacqueline Bertlich and Ed Hathorne for the exchange of ideas, helpful discussions and for providing an enjoyable working environment. Thank you also to Martina Hars and all the other colleagues at GEOMAR who made this time an enjoyable one.

Life would not be the same without my closest friend! Thank you Syawoch!

I deeply thank my parents for love and inspiration throughout my life.

Finally, this work could not have been completed without the support and encouragement of my wife Anne, who is always there for me, and my two sons, Frederik and Fridolin, who give everything its right dimension. Thank you for your love! I love you too!

Table of Contents

List of Figures

List of Tables

List of Acronyms

AMO	Atlantic Multidecadal Oscillation
AMOC	Atlantic Meridional Overturning Circulation
AVHRR	Advanced Very High Resolution Radiometer
AWP	Atlantic Warm Pool
CAC	Caribbean Current
CAR	Carbonate Accumulation Rates
CREWS	Coral Reef Early Warning System
CSW	Caribbean Surface Water
CTD	Conductivity-Temperature-Depth
CW	Central Water
CWC	Cold-water coral
DHW	Degree Heating Weeks
ENSO	El Niño-Southern Oscillation
GC	Guyana Current
GoC	Gulf of Cadiz
GS	Gulf Stream
ICON	Integrated Coral Observing Network
ICP-OES	Inductively coupled plasma optical emission spectrometry
ITCZ	Intertropical Convergence Zone
LC	Loop Current
MC-ICP-MS	Multi-collector inductively coupled plasma mass spectrometry
MOW	Mediterranean Outflow Water
MSP	Mean square potential
NACW	North Atlantic Central Water
NADW	North Atlantic Deep Water
NAO	North Atlantic Oscillation
NBC	North Brazilian Current
NEC	North Equatorial Current
NTA	North Tropical Atlantic
ONI	Oceanic Niño Index
PAR	Photosynthetically-active radiation
SACW	South Atlantic Central Water
SCUBA	Self-contained underwater breathing apparatus
SLP	Sea Level Pressure
SSS	Sea Surface Salinity
SST	Sea Surface Temperature
SUW	Subtropical Under Water
VPDB	Vienna-Pee Dee Belemnite
VSMOW	Vienna Standard Ocean Mean Water
WTC	Wavelet Coherence
XRD	X-Ray diffraction

1. Introduction

A sound understanding of the climate system is essential for the prediction of climate variability and change. Decadal to centennial climate variations are of particular importance because these are the typical time scales over which long-term projections of climate change and anthropogenic impact on climate and ecosystems are assessed (Delworth & Mann, 2000; Enfield & Cid-Serrano, 2010; Latif & Keenlyside, 2011; IPCC, 2013). Instrumental records that could be used to understand climate system variability and underlying mechanisms do not span much more than the 20th century. In the tropics, which are known to affect climate variability worldwide, instrumental records of environmental parameters are both spatially and temporally sparse even until the 1950s. These records are too short to detect and investigate statistically significant relationships between different climate parameters over long-term periods. Proxy archives, non-instrumental sources of indirect climatic information, are essential means for complementing and significantly extending instrumental records back in time and space (Jones et al., 2001). The majority of high-resolution (i.e., annual to subannual) climate and environmental proxy archives comes from the terrestrial realm and largely captures atmospheric and/or continental conditions (e.g., treerings, speleothems, ice cores). By contrast, paleoenvironmental and paleoclimate records from marine settings are sparse and often have poor temporal resolution such as laminated marine sediments. To draw a more detailed picture of past climate variability that very often exhibits strong seasonality, seasonally to annually resolved, precisely chronologically aligned and quantifiable proxy data are required. Well-constrained subannually resolved archives for the marine environment do exist in the form of coral sclerochronological archives, i.e. physicochemical variations in periodically growing hard tissues of scleractinians (stony corals) (Oschmann, 2009). Scleractinians are colonial organisms that secrete calcareous skeletons composed primarily of Aragonite, a modification of calcium carbonate. In many species, the coral skeletons possess internal annual density banding, which records the growth rate of the colony, and provide chronological control. Regular changes in the rate of skeletal formation determined by environmental factors such as light, food, tides etc. are responsible for the formation of density bands. In conjunction with the annual banding the chemical composition of the skeleton contains temporal records based on isotopic ratios and trace elemental concentrations that are a function of environmental changes in the ambient seawater (e.g.,

changes in water temperature, salinity, nutrients and pH) as well as in site specific factors (e.g., turbidity, runoff, upwelling intensity). Coral colonies can have a lifespan of hundreds of years and therefore provide important annual geochemical proxy data, which can be used to reconstruct past environmental and climatic conditions. The present dissertation lays the main focus on tropical corals as archives of past environmental and climate variability but also sheds light on their deep and dark dwelling relatives: cold-water corals.

1.1. Tropical corals as archives of climate variability

Tropical coral reefs are amongst the most productive and diverse ecosystems on earth that have existed in tropical and subtropical oceans for millions of years to form prominent geological structures. Modern tropical coral reefs are dominated by hermatypic (reef-building) corals in the order Scleractinia. The individual coral animal (polyp) of scleractinian corals contains zooxanthellae, unicellular endosymbiotic and photosynthetic algae, which are essential to the growth and survival of most zooxanthellate corals and which impart corals with their characteristic vivid coloration. These algae provide oxygen and essential nutrients for the polyp (e.g., glucose, glycerol and amino acids) while gaining shelter and waste products from the coral. On average, zooxanthellate corals obtain around 70 % of their nutrient requirements from zooxanthellae photosynthesis but may additionally feed on zooplankton (Veron, 2000). The geographic distribution of highly consolidated reefs is confined to shallow warm water regions. Mean annual water temperatures above 24 °C and winter temperatures above 18 °C are warm enough to facilitate polyp replication, gametogenesis, and skeletogenesis. Solar radiation needs to be sufficient to sustain the photosynthetic activity of the zooxanthellae. For these reasons, zooxanthellate corals are rare and reefs are absent at latitudes above 35° north or south of the equator (Veron, 1995). It should be pointed out here that modern tropical coral reef ecosystems are affected by a phenomenon known as coral bleaching. This is the whitening of corals due to the loss of zooxanthellae, mainly as a response to sustained high temperatures above the corals thermal tolerance (Glynn, 1993; Brown, 1997). Coral bleaching may result in the death of affected corals depending on the severity and duration of the environmental stressor. Bleaching before the 1980s was recorded only at a local scale of a few tens of kilometers because of small-scale stressors such as unusually cold or hot weather, freshwater inundation or sedimentation (Glynn, 1993; Wellington & Glynn, 2007; Oliver et al., 2009). Today, recurrent regional-scale (> 1000 km) bleaching and mortality of corals is being observed, a

phenomenon caused by the anthropogenic global rise in sea temperature (Hughes et al., 2003; Carilli et al., 2010; Donner et al., 2017; Hughes et al., 2018).

Their longevity, continuous growth (ranging from about 0.5 to 2 cm a^{-1}) and large geographical distribution in the tropical oceans make massive-growing tropical corals a unique marine archive for the reconstruction of seasonal to multidecadal variability of environmental variables in the tropical surface oceans (e.g., Cobb et al., 2003; Pfeiffer & Dullo, 2006; Kilbourne et al., 2008; Scott et al., 2010; DeLong et al., 2014; Cole et al., 2016). Tropical coral records are therefore a very promising tool for the development of accurate oceanic records of ocean-atmosphere variability beyond the period of instrumental observations but with fidelity and temporal resolution comparable to instrumental climate data (e.g., Gagan et al., 2000; Zinke et al., 2008; Eakin et al., 2009). However, only few coral records have been calibrated with multi-year in-situ monitoring data. Hence, investigators usually rely on gridded (reanalysis) climate data sets for calibration of the coral-derived geochemical proxy records, or standardized indices of major climate phenomena.

The most widely used climate proxies that tropical corals provide are stable isotopes (e.g., $\delta^{18}O$, $\delta^{13}C$) and trace elemental ratios (e.g., Sr/Ca, Mg/Ca, U/Ca, B/Ca). The incorporation of stable isotopes and trace elements is predominantly controlled by thermodynamic factors, although modified by biological processes. The majority of coral-based climate studies are based upon oxygen isotopes ($\delta^{18}O$) because they are relatively straightforward to measure and interpret. The $\delta^{18}O$ of coral aragonite reflects the temperature and $\delta^{18}O$ value of the ambient seawater ($\delta^{18}O_{sw}$) at the time of carbonate precipitation. This has led to information about sea surface temperatures, the hydrological cycle and tropical wind systems (Gagan et al., 1994; Juillet-Leclerc & Schmidt, 2001; Ren et al., 2002; Corrège et al., 2004; Pfeiffer et al., 2006b). In settings where $\delta^{18}O_{sw}$ co-varies with salinity, coral $\delta^{18}O$ also records these changes (Dunbar & Wellington, 1981; Gagan et al., 1994) and thus can be used to reconstruct salinity variations (Linsley et al., 1994; McCulloch et al., 1994; Gagan et al., 1998).

The Sr/Ca ratio in coral aragonite is perhaps the best characterized and most established trace elemental indicator in coral studies and appears to be a robust thermometer in tropical reef corals (e.g., Beck et al., 1992b; de Villiers et al., 1994; Shen et al., 1996b; Alibert & McCulloch, 1997; Gagan et al., 1998; Marshall & McCulloch, 2002). The U/Ca, Mg/Ca, and B/Ca SST proxies show higher variability between sites and corals, and so are generally considered less reliable for SST reconstructions than Sr/Ca (Fallon et al., 2003).

However, the coral skeleton not only provides a record of physical environmental parameters but also has been proposed to be a high-resolution recorder of past nutrient dynamics in the open ocean. In particular, the nitrogen isotope of organic matter contained in coral skeletons ($\delta^{15}N_{Coral}$) is a promising tool to record the origin of nitrogenous nutrients (i.e., ocean circulation, mixed-layer dynamics, atmospheric deposition, influences of the biological pump) with their own nitrogen isotope compositions and is also used as a proxy for nitrogen fixation in tropical oceans (Straub et al., 2013; Sherwood et al., 2014). Common nutrient proxies such as Ba/Ca, Cd/Ca and P/Ca have been used to reconstruct upwelling events (Lea et al., 1989; LaVigne et al., 2008) in the tropical ocean but they have limitations in reconstructing the various other nutrient sources. Only recently, nitrogen isotopes in biogenic carbonate skeletons have been used as a proxy for nitrogen fixation in tropical oceans (Yamazaki et al., 2011; Straub et al., 2013; Sherwood et al., 2014).

A steadily growing number of subseasonally resolved climate reconstructions using massive growing scleractinian reef corals has significantly improved the understanding of past tropical and subtropical climate variability (e.g., Cole et al., 1993; Gagan et al., 1998; Felis et al., 2000; Tudhope et al., 2001; Cobb et al., 2003; Felis et al., 2004; Linsley et al., 2006; Abram et al., 2007; Hetzinger et al., 2008; Hetzinger et al., 2010b; Kilbourne et al., 2010; Vásquez-Bedoya et al., 2012; DeLong et al., 2014; Tierney et al., 2015; Brocas et al., 2016; Sagar et al., 2016). The majority of coral-based reconstructions of climate variability have focused on the use of long-lived coral heads from the Pacific and Indian Ocean (Figure 1-1) because of the importance of the ENSO system (e.g., Cole & Fairbanks, 1990; Cole et al., 1993; Dunbar et al., 1994; Linsley et al., 1994; Tudhope et al., 1995; Wellington & Dunbar, 1995; Shen et al., 1996a; Evans et al., 1999; Cobb et al., 2001; Cobb et al., 2003; Linsley et al., 2006; Quinn & Taylor, 2006; Quinn et al., 2006; Shen et al., 2006; DeLong et al., 2012) and Indian Ocean Dipole (e.g., Charles et al., 1997; Charles et al., 2003; Pfeiffer et al., 2004a; Pfeiffer et al., 2004c; Pfeiffer & Dullo, 2006; Tierney et al., 2015) to large-scale climate variability. Consequently, massive growing species of the genus *Porites*, which are abundant in the tropical Indo-Pacific Ocean, have become the primary source of coral paleoclimate data (e.g., Cole et al., 1993; Quinn et al., 1998; Cole et al., 2000; Pfeiffer et al., 2004c; Pfeiffer et al., 2006b; Zinke et al., 2008; Grove et al., 2010; Lough, 2011; Sagar et al., 2016; Clarke et al., 2017).

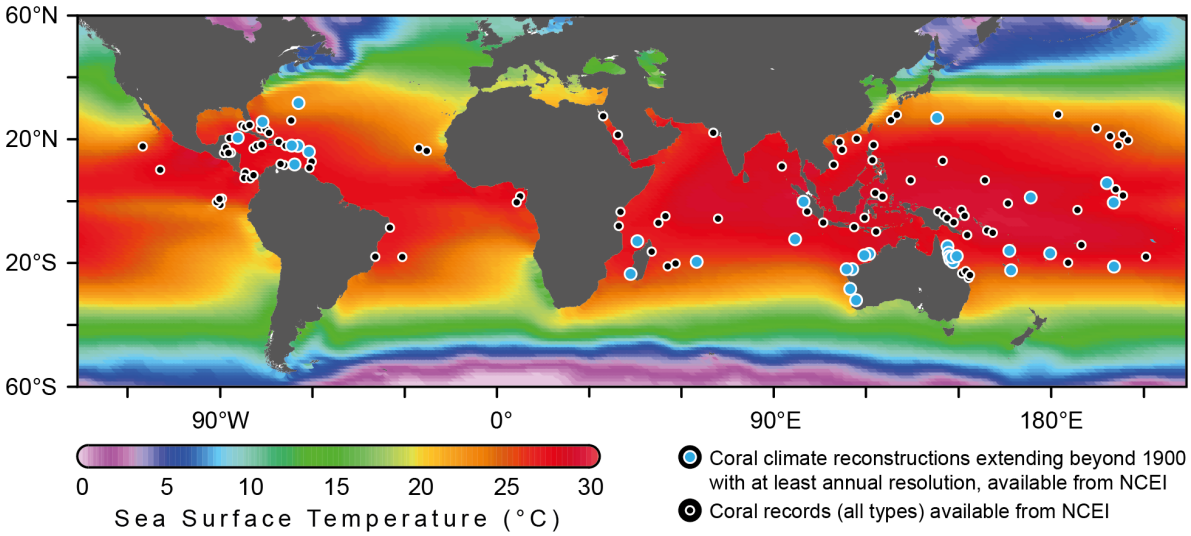

Figure 1-1. Annual 1° × 1° SST data from the World Ocean Atlas 2013 (Locarnini et al., 2013). Circles represent locations of published coral records (see legend for details) from World Data Center for Paleoclimatology at NOAA's National Center for Environmental Information (NCEI).

However, decade-long and continuous subseasonally resolved coral records from the Atlantic region have lagged behind the extensive work published using coral records from the Indo-Pacific Ocean. In the Atlantic, primarily corals of the genus *Montastraea* (Blainville, 1830) and *Siderastrea* (Blainville, 1830) have been used for climate reconstructions (e.g., Swart et al., 1996; Winter et al., 2000; Swart et al., 2002; Carricart-Ganivet, 2004; Carilli et al., 2010; DeLong et al., 2011) as well as the species *Diploria labyrinthiformis* (Linnaeus, 1758). However, the development of coral-based climate records from the tropical Atlantic have long been hindered by questioning the validity of geochemical proxies measured in these corals due to either their more complex skeletal architecture or problems arising from slow annual growth (Leder et al., 1996; Veron, 2000; Watanabe et al., 2001; Watanabe et al., 2002; Moses et al., 2006). Complex decade-long subseasonal coral-based climate records from the Caribbean and western Atlantic are therefore still underrepresented with respect to the Indo-Pacific. Hence, the development of continuous long-term coral-based proxy records is highly necessary for a better understanding of interannual to centennial-scale climate variability in the tropical Atlantic, including the Caribbean, which is influenced by (and possibly influences) a number of climate modes (e.g., NAO, AMO, ENSO) and is a key region in the Northern Hemisphere when it comes to the reconstruction of long-term climate variations. Therefore it is necessary to find suitable, easily accessible coral archives in order to assess the natural range of seasonal to interdecadal climate variability in this region. A couple of studies have recently demonstrated the potential of fast-growing massive Caribbean brain corals of the

species *Diploria strigosa* (Figure 1-2) as reliable recorders of seasonal to interannual temperature and hydrology variability that can be used to detect the seasonal impact of dominant large-scale climate signals (ENSO, NAO, AMO) on the northern tropical Atlantic (Hetzinger et al., 2006a; Hetzinger et al., 2008; Giry et al., 2010; Hetzinger et al., 2010b) (see chapter 1.7.1 for additional information). Thus, Caribbean *Diploria strigosa* holds the potential to expand the understanding of western tropical Atlantic climate variability and was selected as appropriate coral paleoclimate archive for the present thesis.

Figure 1-2. Living *Diploria strigosa* brain coral in the lagoon of Little Cayman.

Most of the published coral records exhibit strong correlations to local environmental and climatic variables and, in addition, provide information about large-scale climate variability. The most common approach to reconstructing past climates from corals is to collect a core from a live (modern) coral on a reef. Records from modern corals usually extend back no longer than a few centuries and are limited by the time the coral started to grow. A relatively new approach is to combine coral records from live and dead colonies by cross-dating proxy variations to produce records extending back multiple centuries from the present day (Hendy et al., 2002; Nyberg et al., 2007; Lough & Cooper, 2011; DeLong et al., 2012; DeLong et al., 2014). An emerging alternative approach is to use well-preserved fossil corals to reconstruct climate during periods much further back in time (e.g., Cobb et al., 2003; Corrège et al., 2004; McGregor & Gagan, 2004; Abram et al., 2007; Giry et al., 2012;

Felis et al., 2015b; Brocas et al., 2018). Although the complications of using fossil corals as paleoclimate archives are greater than using modern corals (e.g., often potential diagenetic changes must be considered, radiocarbon or U-series dating is required for age control, proxy calibration is difficult), the produced records are of great importance, since they provide a "snap shot" of the climate system under different boundary conditions (Tudhope et al., 2001).

1.2. Cold-water corals

Coral reefs have long been recognized as large ecosystems restricted to warm and shallow tropical to subtropical seas. Recent deep-ocean exploration using advanced acoustics and submersibles has revealed unexpectedly widespread and diverse coral ecosystems in deep waters on continental shelves, slopes, seamounts and ridge systems around the world. Like their warm-water relatives some cold-water coral (CWC) species also form large and extensive reefs. CWC reefs seem to be most abundant on the continental margins in the eastern North Atlantic where they form a dense band stretching from the Barents Sea down to Northwest Africa (Figure 1-3) (Zibrowius, 1980; Freiwald et al., 2004; Roberts et al., 2006b). However, CWC reefs have also been discovered in the Caribbean Sea and the Gulf of Mexico but also in parts of the Mediterranean Sea and in the Pacific and Indian Ocean (Zibrowius, 1973; Cairns, 1984). The currently observed distribution is likely biased by the predominance of research activities of certain countries (Roberts et al., 2006b) while ecoenvironmental prediction models probably more reliably indicate the true global distribution (e.g., UNEP-WCMC, 2009). In fact, there is growing evidence, that on a global scale, CWC reefs could equal, or even exceed, the coverage of all warm-water tropical coral reefs (Freiwald et al., 2004). As outlined in chapter 1.1 shallow-water corals have been used to reconstruct high resolution records of ocean surface conditions from the tropics. CWCs are less utilized but show potential to significantly increase the knowledge of paleoenvironmental variability in other portions of the ocean, in particular extratropical intermediate-ocean environments on glacial–interglacial timescales (Sakai et al., 2009; Ruggeberg et al., 2016). The relevance of such data becomes evident when considering that the extratropical oceans play a major role in global heat exchange (Manabe & Stouffer, 1999; Levitus et al., 2000; Visbeck, 2002), host major carbon sinks (Sabine et al., 2004) and govern quasi-decadal to multidecadal climate variability (Rodwell et al., 1999; Sutton & Hodson,

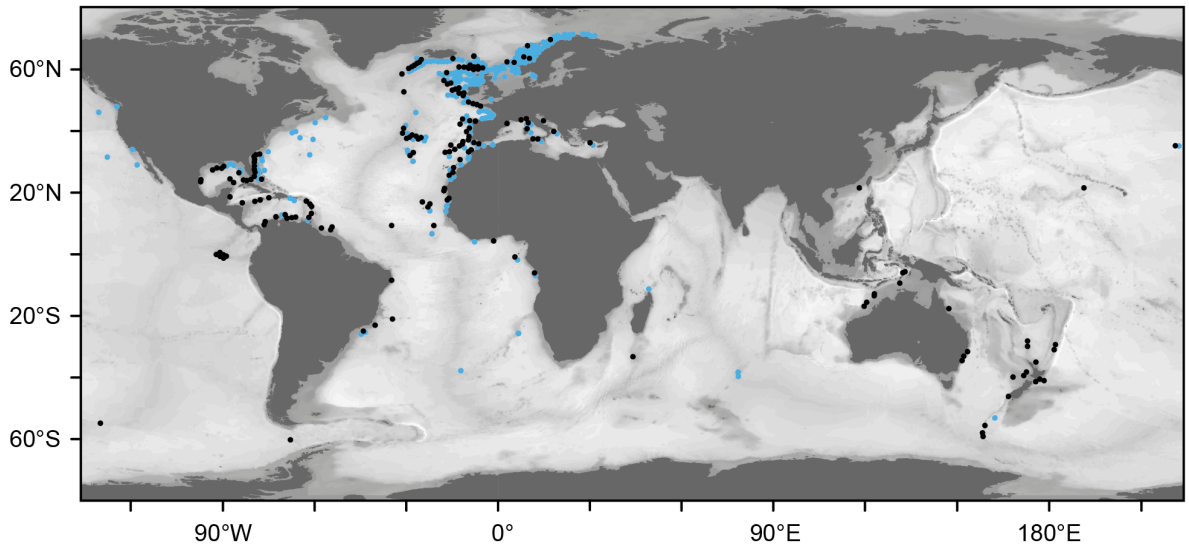

Figure 1-3. Global distribution of the most important cosmopolitan reef-builders *Lophelia pertusa* (blue) and *Madrepora oculata (black)*. Redrawn after Roberts et al. (2009). Note, due to the high research effort in the NE-Atlantic this distribution pattern is presumably biased and the full geographic extend of these species is still unknown.

2005; Keenlyside et al., 2008). Scleractinian CWCs, like the most important cosmopolitan reef-builders *Lophelia pertusa* (Linnaeus, 1758) and *Madrepora oculata* (Linnaeus, 1758) (Figure 1-1) (Messing et al., 2008; Roberts et al., 2009), are azooxanthellate corals. It is the lack of photosymbiotic algae that enables the CWCs to occupy a much larger realm than the photic zone in which their zooxanthellate tropical relatives dwell. For example, the shallowest occurrence of live *Lophelia pertusa* is in about 40 m water depth in Trondheimsfjord, Norway (Rapp & Sneli, 1999) while the deepest is in 3383 m water depth on the New England Seamount Chain in the North Atlantic (Zibrowius, 1980). Besides the large bathymetrical range *Lophelia pertusa* also has a very large latitudinal distribution. So far *Lophelia pertusa* has been found as far north as the Hjelmsøybank at about 71°N in the south-western Barents Sea (Fosså et al., 2002) and as far south as the Antarctic Macquarie Ridge at 51°S (Cairns & Stanley, 1982). These scleractinian CWCs are sessile suspension feeders, requiring large organic fluxes and strong bottom currents. Initially the corals need a hard substrate to settle on and prefer bathymetric features like mound structures, oceanic ridges, or the summits and flanks of seamounts where strong water currents and high productivity typically occur (Genin et al., 1986; Frederiksen et al., 1992; Thiem et al., 2006). Flourishing cold-water colonies have been observed in water masses with a certain range of physicochemical properties. For example, occurrences of *Lophelia pertusa* are associated with temperatures of 4–14 °C (Freiwald, 2002; Freiwald et al., 2009) and salinity values of 32–38.8 psu (Freiwald et al., 2004; Roberts et al., 2006a; Davies et al., 2008), where the higher

values for temperature and salinity are related to the Mediterranean Sea (Taviani et al., 2005a; Taviani et al., 2005b). Furthermore, *Lophelia pertusa* tolerates values of dissolved oxygen ranging from 3.75 to 6.65 ml l^{-1} (Dodds et al., 2007; Dullo et al., 2008). Moreover, living reef ecosystems of CWCs in the north-eastern North Atlantic seem to prefer a narrow interval of potential seawater density (σ_Θ) between 27.35 and 27.65 kg m^{-3} (Dullo et al., 2008). This concept of defining the overall habitat range of CWC however needs to be adjusted to regional conditions regarding σ_Θ interval boundaries (Flögel et al., 2014). Furthermore, sustained CWC growth seems to depend on steep density gradients at water mass boundaries, favouring the concentration of suspended particles and the development of a nepheloid layer (Dickson & McCave, 1986; Rice et al., 1991; Dullo et al., 2008; Mazzini et al., 2012; Hebbeln et al., 2014). Enhanced horizontal energy forces the flux of nutrients to the corals and may even influence the distribution of larvae (Dullo et al., 2008; Henry et al., 2014). The species *Lophelia pertusa* and *Madrepora oculata* show surprisingly high growth rates between 3 and 33 mm a^{-1}. Apart from differences in the shape of the corals framework (Figure 1-4), both species can grow up to several decimetres in height and, under optimal conditions, can form enormous structures like CWC reefs with a lateral extension of several kilometers as discovered in Norway (e.g., the approximately 40 km long Rœst reef) (Fosså et al., 2005) or coral carbonate mounds which are reported from all over the Atlantic margin. On geological time scales the geographical distribution and sustained development of such CWC structures have been strongly related to changes in bottom currents, nutrient availability and density gradient paced by climatic changes during glacial–interglacial times (Dorschel et al., 2005; Roberts et al., 2006b; Wienberg et al., 2010; Frank et al., 2011;

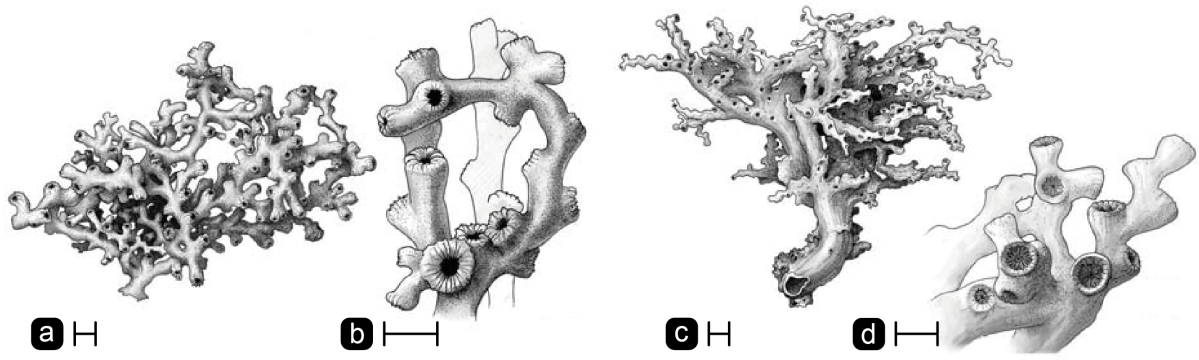

Figure 1-4. Drawings of the scleractinian cold-water coral species *Lophelia pertusa* (a, b) and *Madrepora oculata* (c, d), showing the framework formed by the coral colony (a, c) and the details of individual polyp calices (b, d) Scale bars: 10 mm (a-c), 4 mm (d). Modified after Roberts et al. (2009).

Hebbeln et al., 2016; Ruggeberg et al., 2016). Thus, records of CWC reef and mound development, especially in the Northeast Atlantic, represent important tools to better understand environmental change on geological time scales corresponding to recurrent glacial cycles.

The CWC aspect of the present thesis is limited to the report of a newly discovered CWC mound province and its oceanographic and bathymetric boundary conditions so that considerations on the application of geochemical climate proxies in scleractinian CWCs are beyond the scope of this thesis. However, for the sake of completeness it should be pointed out that paleoenvironment proxies in CWCs have successfully been applied to reconstruct oceanographic boundary conditions. These include elemental ratios for reconstruction of temperature (Li/Mg), nutrients and melt water (Ba/Ca), changes in the carbonate system (U/Ca) as well as isotopic composition for the reconstruction of temperature ($\delta^{88/86}Sr$) and water masses (ε_{Nd}) (Montagna et al., 2005; Rüggeberg et al., 2008; Case et al., 2010; Van de Flierdt et al., 2010; Anagnostou et al., 2011; Inoue et al., 2011; Raddatz et al., 2013; Montagna et al., 2014; Raddatz et al., 2014; DeCarlo et al., 2015; Raddatz et al., 2016). Nevertheless, geochemical proxies including carbon isotopes, oxygen isotopes and Sr/Ca ratios appear to be strongly affected by physiological processes during biomineralization in the skeletons of CWCs (Smith et al., 2000; Adkins et al., 2003; Shirai et al., 2005; Sinclair et al., 2006; Blamart et al., 2007; Gagnon et al., 2007; Montagna et al., 2007) and are thus not as commonly used as in tropical warm-water corals.

1.2.1. Cold-water coral mounds – Development and importance

Cold-water coral mounds are morphological features on the sea floor ranging from a height of a few to several hundred meters. They occur as isolated mounds as well as in clusters of mounds, which in some places form large distinct provinces. CWC mounds are created on millennial and longer time scales by repetitive growth of scleractinian CWCs in complex interaction with biological, geological and sedimentological as well as oceanographic and climatic processes (De Mol et al., 2002; Freiwald, 2002; Dorschel et al., 2005; Rüggeberg et al., 2005; Rüggeberg et al., 2007; Roberts et al., 2009). The result is a structure build up by the corals framework, hemipelagic sediments and bioclastic material (Dorschel et al., 2007; Wheeler et al., 2007). The majority of CWC mounds described so far has been discovered in the north-eastern Atlantic, where they are widespread along the Irish (De Mol et al., 2002; Wheeler et al., 2007) and British margins (Roberts et al., 2000). They have also been

discovered in regions further south, e.g., along the Moroccan margin (Foubert et al., 2008; Wienberg et al., 2009), off Mauritania (Colman et al., 2005) and off Angola (Le Guilloux et al., 2009) and in the western Atlantic, e.g., in the Straits of Florida (Grasmueck et al., 2006), on the West Florida Slope (Newton et al., 1987; Grasmueck et al., 2006), off Colombia (Reyes et al., 2005) and off Brazil (Viana et al., 1998; Sumida et al., 2004; Mangini et al., 2010). Growth dynamics of CWC mounds are linked to environmental conditions such as a dynamic hydrographic regime. Coral thickets are capable of trapping and accumulating suspended sediments that have a supporting effect on the coral framework. Over time this can lead to vertical mound growth varying between less than 5 cm ka^{-1} and up to 220 cm ka^{-1} (Frank et al., 2009). However, with an environmental regime unfavorable for the corals, mound growth can stagnate and ultimately even erosion may occur (Dorschel et al., 2005; Roberts et al., 2006b; Kano et al., 2007). As changes in mound growth are strongly moderated by overall climatic variability (Roberts et al., 2006b) CWC mounds provide an archive for the reconstruction of environmentally-driven growth dynamics of cold-water coral ecosystems over thousands to millions of years (Dorschel et al., 2005; Mienis et al., 2006; Kano et al., 2007; Eisele et al., 2008; Frank et al., 2009; Wienberg et al., 2010; Eisele et al., 2011).

Cold-water coral mounds make up a significant volume within the continental margin sedimentary system and as the growth rates of the constituting scleractinian CWCs can be as high as those of their warm-water relatives, CWC mounds might play a notable role in the global carbonate budget. This assumption is corroborated by the wide distribution of CWC mounds, which only recently has been discovered, and a very likely growing number of discoveries in the future. It has been shown that the content of background-sediment-derived carbonate within CWC mounds is several times higher compared to the carbonate content of adjacent and underlying deposits (Dorschel et al., 2007; Titschack et al., 2009; Titschack et al., 2015). This selective enrichment might be caused by the effective baffling of marine fluff rich in calcareous detritus by the coral framework and/or the active catch of the calcareous plankton by the corals. Studies from the Norwegian Sea and the Irish continental margin revealed carbonate accumulation rates (CAR) of CWC mounds of up to 25 g cm^{-2} ka^{-1} (Lindberg & Mienert, 2005; Dorschel et al., 2007; Titschack et al., 2009). These rates are at most 12 % of the accumulation rate of tropical warm-water reefs but exceed those of continental slopes by a factor of up to 11 (Milliman, 1993; Schneider et al., 2006; Smith & Mackenzie, 2016). This suggests that in a global context CWC mounds are a

significant carbonate sink, which has, so far, not been considered in any global carbonate budget estimation or any model of the distribution of CO_2 (Milliman, 1993; Milliman & Droxler, 1996; Vecsei, 2004; Lindberg & Mienert, 2005; Schneider et al., 2006; Dorschel et al., 2007; Titschack et al., 2009).

Taking into account that the favourability of environmental conditions regarding mound growth varied on long time scales, it is likely that their influence was even larger at times in the geological past. For example, new hydroacoustic subseafloor data from a coral mound region off Nortwest Morocco reveal six times more buried mounds that have no expression at the seafloor compared to still exposed mounds along the investigated hydroacoustic lines (Hebbeln et al., 2017). The number of more than $3 \cdot 10^3$ coral mounds detected in the swath bathymetry data from that region implies that the total number of all mounds, buried and unburied, might reach about $2 \cdot 10^4$. In conjunction with recent results from CWC deposits off Norway, emphasizing the potential of CWCs as a globally significant carbonate factory with CARs in the range of tropical shallow-water reefs (Titschack et al., 2015), the question arises whether CWC systems even might have contributed to the global carbonate budget to the same extent as the tropical reef forming corals.

However, to evaluate the contribution of CWC mounds and other CWC factories to the global carbonate budget today and in the past, the global area of living and dead CWCs as well as extensive data of CARs of CWC ecosystems would be necessary. Both are currently lacking. Consequently, there is an urgent need for high-resolution seafloor mapping to identify and spatially quantify CWC systems as well as for accumulation rate estimates of the CWC factory. The present thesis makes an important contribution to the former aspect by providing hydroacoustic data of a newly discovered CWC mound province off western Morocco.

1.3. Coral $\delta^{18}O$ as a proxy for temperature and the hydrological cycle

The partitioning of oxygen isotopes between reef carbonates and seawater has been investigated extensively over recent decades, and reviews of this relationship can be found for example in (Swart, 1983) and (Swart et al., 1996), (Aharon, 1991), and (Leder et al., 1996). It is common practice to express isotopic composition in terms of delta (δ) values:

$$\delta = \left(\frac{R_{sample}}{R_{standard}} - 1 \right) \times 10^3 (‰) \quad (1)$$

where δ is the oxygen isotopic composition ($\delta^{18}O$) of a carbonate sample, R_{sample} is the ratio of the heavy stable oxygen isotope ^{18}O and the light stable isotope ^{16}O ($^{18}O/^{16}O$) of a carbonate sample and $R_{standard}$ is the defined isotope ratio of a standard sample, such as the Vienna Pee Dee Belemnite (VPDB) carbonate. The isotopic composition of slowly precipitated carbonates is governed by temperature dependent thermodynamic isotope fractionation (McCrea, 1950) and the isotopic composition of the fluid. It is well known that the aragonite of the coral skeleton is not precipitated in isotopic equilibrium with ambient seawater (Weber & Woodhead, 1970; Swart, 1983; McConnaughey, 1989a; Swart et al., 1996). Comparison of experimental equilibrium isotope fractionation and isotope determinations on coral aragonite using a large collection of hermatypic coral genera has shown that the isotopic composition of coral aragonite is invariably depleted relative to equilibrium precipitation at any given temperature (e.g., Weber & Woodhead, 1972). Kinetic and metabolic factors have been identified as the causes that lead to isotopic disequilibria or so called "vital effects" during biological calcification (Weber & Woodhead, 1970; Erez, 1978; McConnaughey, 1989a, 1989b; Juillet-Leclerc & Reynaud, 2010). The degree of this disequilibrium is constant within a coral colony but varies between colonies belonging to the same genus and among different coral taxa (Weber & Woodhead, 1972; McConnaughey, 1989a; Aharon, 1991; Suzuki et al., 2005). Furthermore, for large-polyped corals like *Diploria strigosa* with a relatively coarse skeletal structure compared to small-polyped corals (e.g., *Porites* sp.), Giry et al. (2010) emphasize the importance of the vital effect in controlling the isotopic composition of different skeletal elements. These different vital effects observed between mesoskeletal elements are to some extent linked to different calcification and photosynthesis rates (Erez, 1978; Juillet-Leclerc & Reynaud, 2010). This has implications for microsampling, which are considered in chapter 1.7.2. In contrast to *Diploria strigosa*, small-polyped corals have less pronounced differences in density between individual skeletal elements and are therefore expected to be less or not affected by this mesoscale geochemical heterogeneity. However, in slower growing portions of the coral skeleton (e.g., the lateral less sunlight receiving surface, compared to the upper surface of a coral head) the isotopic composition may gradually approach equilibrium, indicating that large variations in growth rate may bias environmental signals (McConnaughey, 1989a) (Figure 1-5). However, it has been suggested that the effect of growth rate variations on the isotopic composition is much reduced in coral skeleton growing at a rate greater than 0.5 to

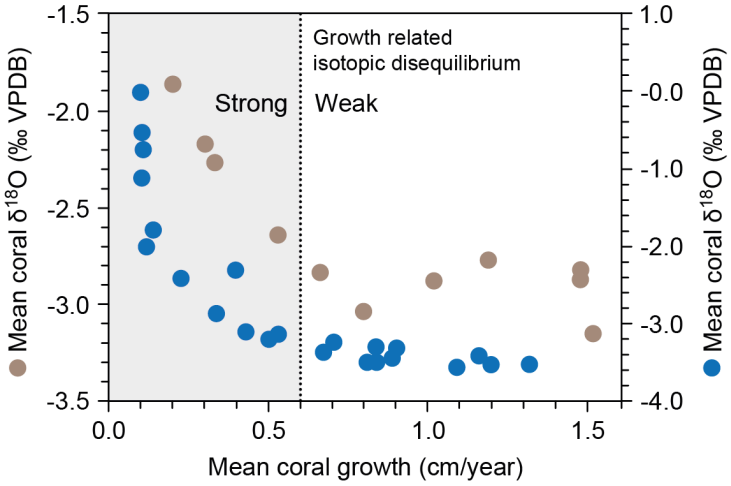

Figure 1-5. Relationship between coral $\delta^{18}O$ and coral growth rate for lateral to upper surface samples from a *Pavona clavus* coral head (blue dots) from San Cristobal Island, Galápagos (McConnaughey, 1989) and for *Porites* sp. coral colonies from the Gulf of Aqaba, Red Sea (brown dots) (Felis et al., 2003). Stippled line indicates lower limit growth rate value (0.6 cm a^{-1}) from where growth rate related kinetic isotopic disequilibria have reduced effect on mean coral $\delta^{18}O$ (Felis et al., 2003).

0.6 cm a^{-1} (Felis et al., 2003) (Figure 1-5). Despite these observations the degree of influence of vital effects on coral $\delta^{18}O$ appears to be stable over time and over different environmental settings (Gagan et al., 2000) enabling the development of well applicable coral oxygen isotope paleotemperature equations. For example, calibration slopes obtained for frequently deployed *Porites* sp. from various locations in the Indo-Pacific appear to be nearly constant at about -0.2 ‰ $°C^{-1}$ (slopes range from -0.18 to -0.22 ‰ $°C^{-1}$) (Weber & Woodhead, 1972; Gagan et al., 1994; Wellington et al., 1996; Juillet-Leclerc & Schmidt, 2001). This is in general agreement with the slope of inorganic experiments. The $\delta^{18}O$ of calcium carbonate precipitated in equilibrium with seawater decreases by about 0.22 ‰ per 1 °C rise (Epstein et al., 1953). However, the coral $\delta^{18}O$ is not only a function of water temperature but also of $\delta^{18}O$ of ambient seawater ($\delta^{18}O_{sw}$) (e.g., Ren et al., 2002; Corrège et al., 2004; Pfeiffer et al., 2004b; Pfeiffer et al., 2006a). $\delta^{18}O_{sw}$ is strongly related to the hydrological cycle, with higher values observed in regions where evaporation exceeds precipitation and lower values in regions characterized by high precipitation and/or river runoff. Consequently $\delta^{18}O_{sw}$ is also strongly related to sea surface salinity (SSS). Both variables covary in the surface waters of the oceans, which makes this relation an important estimating tool in paleoclimate studies. Apart from the local hydrological balance, variable atmospheric fluxes at certain latitudes and ocean basins as well as oceanic advection and diffusion processes also affect $\delta^{18}O_{sw}$ of surface waters (Craig & Gordon, 1965; Schmidt, 1999; Bigg & Rohling, 2000; Delaygue et al., 2000). For example, the advection of surface waters originating in the Caribbean and Gulf of Mexico into the North Atlantic basin leads to an enrichment in $\delta^{18}O_{sw}$, which is then

transported poleward of 60° N by the North Atlantic Drift. However, due to its strong dependence on the evaporation-precipitation balance (Delaygue et al., 2000), reconstructions of $\delta^{18}O_{sw}$ could yield important information about past changes in the hydrological cycle. Since the $\delta^{18}O$ composition of scleractinian corals is a multivariable function of $\delta^{18}O_{sw}$ and SST, a single-variable (SST) proxy is necessary to reconstruct $\delta^{18}O_{sw}$ from coral $\delta^{18}O$. One great advantage of corals for paleoclimatic studies is that they possess a remarkable array of chemical tracers that contain information on past environmental variations. The skeletal Sr/Ca ratio in many corals appears to be mainly influenced by SST, and it appears that coral Sr/Ca is linearly related to SST (Smith et al., 1979; Beck et al., 1992b; Gagan et al., 1998; Linsley et al., 2000; Marshall & McCulloch, 2002; Pfeiffer et al., 2006b). Several studies have shown that paired measurements of $\delta^{18}O$ and Sr/Ca in coral skeletons can provide information on $\delta^{18}O_{sw}$ variability of surface water through removing the temperature component of the $\delta^{18}O$ variations which is derived from the Sr/Ca measurements (McCulloch et al., 1994; Gagan et al., 1998; Ren et al., 2002; Zinke et al., 2004; Sun, 2005; Linsley et al., 2006; Pfeiffer et al., 2006a; Cahyarini et al., 2008; Deng et al., 2009; Felis et al., 2009; Hetzinger et al., 2010b). First attempts to quantitatively separate the effects of SST from those of $\delta^{18}O_{sw}$ based on paired analysis of coral $\delta^{18}O$ and Sr/Ca used equations obtained by univariate linear regression of proxy data against local SST:

$$\delta^{18}\mathrm{O}_{\mathrm{coral}}\,(\mathrm{Sr/Ca}_{\mathrm{coral}}) = m \times \mathrm{SST} + b \qquad (2)$$

For $\delta^{18}O$ the equation obtained in this way may not represent the true $\delta^{18}O$-SST relationship because there may also be effects of $\delta^{18}O_{sw}$ variation, which could alter the relationship (Linsley et al., 1999; Felis et al., 2003; Suzuki et al., 2005). For a general function of two variables, the effects of them acting at the same time generally are not the simple sum of the effects of two variables acting separately. This is because the effect of one variable is generally influenced by changes of the other. Specifically, at least the intercept in the $\delta^{18}O$-SST equation must be different under different $\delta^{18}O_{sw}$ conditions (even if the slope does not change). Consequently, Ren et al. (2002) proposed to omit the intercept values of the calibration regressions by calculating the first derivatives of the two proxies. Cahyarini et al. (2008) reduced mathematical complexity of this approach through centering of the linear regression equation by removing the mean value from its variables. In this way variations of $\delta^{18}O_{sw}$ can be defined relative to the mean value of $\delta^{18}O_{sw}$ ($\Delta\delta^{18}O_{sw\text{-}center}$):

$$\Delta\delta^{18}O_{sw-center} = \left(\delta^{18}O_{coral_i} - \overline{\delta^{18}O_{coral}}\right) - \frac{\gamma}{\beta}\left(Sr/Ca_{coral_i} - \overline{Sr/Ca_{coral}}\right) \quad (3)$$

where $\Delta\delta^{18}O_{sw\text{-}center}$ is the centered $\delta^{18}O_{sw}$ contribution to $\delta^{18}O_{coral}$, $\delta^{18}O_{coral_i}$ (Sr/Ca_{coral_i}) is the measured coral $\delta^{18}O$ (Sr/Ca), $\overline{\delta^{18}O_{coral}}$ ($\overline{Sr/Ca_{coral}}$) is the mean value of all measurements of $\delta^{18}O$ (Sr/Ca), and γ (β) is the regression slope of coral $\delta^{18}O_{coral}$ (Sr/Ca_{coral}) against SST. Thus, it is possible to insert the known slope of the $\delta^{18}O$ (Sr/Ca)-SST relationship and to calculate relative variations of $\delta^{18}O_{sw}$. Applied to corals from the Cayman Islands this approach can provide insights into long-term variability of the hydrological cycle in the Central Caribbean region.

1.4. Coral Sr/Ca as a proxy for temperature

Coral skeletal Sr/Ca is used as paleothermometer because the partition coefficient of the Sr^{2+} ions between seawater and coral aragonite

$$K_d = \frac{Sr/Ca_{coral}}{Sr/Ca_{sw}} \quad (4)$$

is understood to be temperature dependent (Beck et al., 1992a; Marshall & McCulloch, 2002). Sr is one of various trace elements incorporated into the corals skeleton. In the process of aragonite secretion from the calcifying fluid Sr^{2+} ions are thought to replace Ca^{2+} ions due to their similar ionic radii (1.31 Å and 1.18 Å, respectively) (Shannon, 1976; Watson, 1996; Allison et al., 2005; Gabitov & Watson, 2006). The Sr/Ca ratio is the most commonly used geochemical temperature proxy in coral archives (Weber, 1973; Beck et al., 1992a; de Villiers et al., 1994; McCulloch et al., 1994; Alibert & McCulloch, 1997; Cohen et al., 2001; Cohen et al., 2002; Ferrier-Pages et al., 2002; Swart et al., 2002; Fallon et al., 2003; Gagnon et al., 2007; Reynaud et al., 2007; Maupin et al., 2008; Mitsuguchi et al., 2008; Hetzinger et al., 2010a; Gagan et al., 2012; Gagnon et al., 2013; Raddatz et al., 2013; DeLong et al., 2014; Clarke et al., 2017; Pfeiffer et al., 2017). Strong correlations have been observed between instrumental SST records and skeletal Sr/Ca in modern corals over seasonal to decadal timescales (Quinn & Sampson, 2002; Linsley et al., 2004; Stephans et al., 2004) providing a reliable proxy for the reconstruction of multi-centennial SST variations and valuably extending the record of many natural climate oscillations back to the 16th Century

(Linsley et al., 2000; Hendy et al., 2002; DeLong et al., 2012). However, the reliability of this proxy has been called into question. For instance, over millennial timescales SST estimates from Sr/Ca ratios in fossil corals frequently yield improbably cool or spatially inconsistent values (Beck et al., 1997; Corrège et al., 2004; DeLong et al., 2010). Regional oceanographic dynamics can explain some of these inconsistencies (Asami et al., 2009) but other possible influences on skeletal Sr/Ca in corals remain unresolved. For example, Sr/Ca is correlated with growth rate in some (de Villiers et al., 1995; Kuffner et al., 2012), but not all corals (Allison & Finch, 2004; Hayashi et al., 2013) and may be influenced by diagenesis (Allison et al., 2005; Allison & Finch, 2007), skeletal ultrastructure (Allison, 1996; Allison & Finch, 2004), metabolic cycles (Meibom et al., 2003), and potential variations in seawater Sr/Ca (Stoll & Schrag, 1998), pH and pCO_2 (Cohen et al., 2009; Gagnon et al., 2013; Tanaka et al., 2015; Cole et al., 2016). However, a number of studies have concluded that calcification and growth rate have little effect on coral Sr/Ca as long as microsampling is confined to the main axis of coral growth (Mitsuguchi et al., 1996; Shen et al., 1996b; Alibert & McCulloch, 1997; McCulloch et al., 1997; Gagan et al., 1998; Swart et al., 2002; Allison & Finch, 2004; Corrège et al., 2004). For *Diploria strigosa* microsampling should additionally be confined to a single skeletal element, preferentially the theca as with $\delta^{18}O$ (Giry et al., 2010) (see also chapter 1.7.2). The sensitivity of Sr/Ca to temperature change may differ among species and within a single species sampled from different reef locations, suggesting that species- and even colony-specific calibrations are needed (e.g., Alpert et al., 2016). Coral palaeoproxy relationships are derived by correlating SST variations with coral Sr/Ca measured in modern specimens. The relationship between coral Sr/Ca and SST is parameterised as a linear function of the form given in Equation (2). Ideally, the correlation of coral Sr/Ca ratio and temperature should be based on an in-situ instrumental SST record from the same time period from the same reef. In fact, due to the lack of availability of such data, only a few studies exist (e.g., Alibert & McCulloch, 1997; Crowley et al., 1999; Hetzinger et al., 2010a; DeLong et al., 2012) that use in-situ SST data. Most studies must rely on data from either SST stations that are remote to the coral site, or gridded SST datasets that are based on measurements from satellites and ships-of-opportunity (Gagan et al., 2000). This is considered to be a significant uncertainty in deriving accurate Sr/Ca-SST relationships. Calibrations are available for a number of coral species, mostly for the genus *Porites* from the Indo-Pacific Ocean. For the tropical Atlantic published relationships between Sr/Ca from different coral genera and water temperatures show slopes ranging from -0.023

to -0.084 mmol mol^{-1} $°C^{-1}$ (Cardinal et al., 2001; Swart et al., 2002; Cohen et al., 2004; Goodkin et al., 2005; Smith et al., 2006; Maupin et al., 2008; DeLong et al., 2011). Previously published slopes for modern Caribbean *Diploria strigosa* from Guadeloupe (Hetzinger et al., 2006a) and Bonaire (Giry et al., 2012) range from -0.034 to -0.042 mmol mol^{-1} $°C^{-1}$. Overall, there are large differences between slope values for coral Sr/Ca-SST relationships between different studies. Although Sr/Ca seems to be a reliable proxy for the reconstruction of multi-centennial SST variations, the lack of a robust universal Sr/Ca-SST calibration for a single species of coral must be considered a downside of coral strontium-paleothermometry.

1.5. Coral $\delta^{15}N$ as a proxy for the marine nitrogen cycle

Coral-based paleoceanographic studies have long focused on the inorganic compound of the coral skeleton, while the organic matter within the skeleton got attention only recently (e.g., LaVigne et al., 2008). This is primarily due to the analytical challenges regarding the relatively organic-poor aragonite skeleton. Several studies have investigated the isotopic composition of organic nitrogen bound in the coral skeleton as a potential high-resolution archive of nitrogen cycle dynamics (e.g., Marion et al., 2005; Muscatine et al., 2005; Yamazaki et al., 2011). The nitrogen isotopic composition is expressed in delta notation following Equation (1), where δ is the nitrogen isotopic composition ($\delta^{15}N$) of a sample, R_{sample} is the ratio of the heavy nitrogen isotope ^{15}N and the light isotope ^{14}N ($^{15}N/^{14}N$) of a sample and $R_{standard}$ is the isotope ratio of atmospheric N_2, which serves as standard. Marine primary production, which influences climate processes and biogeochemical cycles, is largely dependant on the availability of nutrients in ocean surface water (Falkowski et al., 1998; Behrenfeld et al., 2006). Nitrogen is introduced into surface waters by exchange with the atmosphere. Nitrogen gas dissolved as molecular N_2 in the ocean is biologically almost inert and generally participates very little in marine biological processes. It can, however, be converted to "fixed nitrogen" by algae and cyanobacteria, which, in turn, can be used by biota and degraded to simple nitrogen compounds such as nitrate (NO_3^-) and ammonium (NH_4^+). Thus, microorganisms are responsible for all major conversions in the biological nitrogen cycle, which generally is divided into fixation, nitrification and denitrification. These main processes involved in the biological utilization of nitrogen are all associated with kinetic fractionation effects, although they exhibit different magnitudes.

The $\delta^{15}N$ of marine organic matter produced in the photic zone depends on the isotope ratio of NO_3^-, which dominates the oceanic pool of dissolved inorganic nitrogen, and the degree

to which this inorganic pool is utilized (Wada & Hattori, 1976; Altabet et al., 1991; Voss & Richardson, 2006). The dominant and lighter isotope ^{14}N is preferentially taken up by photosynthetic organisms, leaving behind the much less abundant heavier isotope ^{15}N. Subsequently, the remaining nitrogen pool becomes progressively enriched in ^{15}N, according to Rayleigh fractionation kinetics (Cifuentes et al., 1988). Thus, $\delta^{15}N$ can be used as an indicator of nutrient dynamics and ocean ventilation (e.g., Farrell et al., 1995). Understanding oceanic nutrient dynamics is essential for, e.g., the estimation of primary productivity. In oligotrophic open oceans the spatial and continuous observation of nutrients has been limited even though these regions represent more than 75 % of the global ocean surface. Coral reefs are widely distributed in oligotrophic seas and the organic matter bound in the coral skeleton reflects the carbon and nitrogen sources of the coral-zooxanthellae symbiotic system (Drake et al., 2013) and may thus provide insights into past biogeochemical conditions of these ocean regions and/or the physiological and ecological history of corals. Organic matrix in coral skeletons is biosynthesized in a prerequisite step of the calcification process (Allemand et al., 1998), and preserved over a timescale of centuries (Ingalls et al., 2003). Because most methods used to measure coral $\delta^{15}N$ require large quantities of skeletal material (Muscatine et al., 2005; Uchida et al., 2008; Yamazaki et al., 2013), for *Diploria strigosa* the theca, as the skeletal element with the highest proportional mass, should be chosen for sampling. This also complies with the sampling strategy for $\delta^{18}O$ and Sr/Ca of the present work. However, there are methodological issues regarding the measurement of coral $\delta^{15}N$. Different methods have been used to measure this relatively new proxy and these either require large quantities of skeletal material and/or have low precision (Marion et al., 2005; Muscatine et al., 2005; Uchida et al., 2008; Yamazaki et al., 2013). A more recent study by Wang et al. (2015) could, however, show some improvements regarding these issues using yet another method on samples from a *Diploria labyrinthiformis* colony. In addition, the controlling factors on $\delta^{15}N$ remain poorly understood: the $\delta^{15}N$ of source nitrogen and the internal nitrogen cycle of the coral-zooxanthellae symbiosis may both be important (Muscatine et al., 2005; Swart & Szmant, 2005; Yamazaki et al., 2011; Wang et al., 2015).

Several studies have explored the skeleton-bound $\delta^{15}N$ of hermatypic symbiotic corals and revealed different aspects of this proxy. Muscatine et al. (2005) compared modern coral species and found that the $\delta^{15}N$ in symbiotic corals (4.09 ± 1.51 ‰, n = 24) is substantially lower than in non-symbiotic corals (12.28 ± 1.81 ‰, n = 17). They suggested that $\delta^{15}N$ is an

indicator for the coral host-zooxanthellae symbiosis, using their data to argue that this symbiosis may have started as early as the Triassic. Marion et al. (2005) interpret a coral $\delta^{15}N$ signal from Bali, Indonesia, as an indicator for the $\delta^{15}N$ of fixed nitrogen sources to the reef and found that synthetic low-$\delta^{15}N$ fertilizer has been affecting coastal coral reefs since the 1970s. Yamazaki et al. (2011) also interpreted coral $\delta^{15}N$ as a proxy for the $\delta^{15}N$ of nitrogen sources. On Ishigaki Island, Japan, where the riverine nitrate is the dominant nitrogen source to the reef, they observed a correlation between an onshore-offshore coral $\delta^{15}N$ gradient and the gradient in surface water nitrate $\delta^{15}N$.

1.6. Regional setting of the study area

1.6.1. Geography and Geology

Little Cayman (19.68° N, 80.05° W) is one of the three islands that form the Cayman Islands archipelago in the Caribbean Sea (Figure 1-6). The other islands are Grand Cayman and Cayman Brac. The Cayman Islands are the most remote of the West Indian islands and are part of the Greater Antilles. The main island Grand Cayman is located about 700 km south of Florida and 300 km from both Jamaica and Cuba. Little Cayman and Cayman Brac, the "Sister Islands", lie within 7 km of each other about 130 km north-west of Grand Cayman and some 200 km from Jamaica and Cuba. Little Cayman is the smallest and least developed island of the archipelago, with a human population of less than 200. It is 17 km long and from little more than a kilometer to 3 km wide. With the highest point 13 m above sea level it is a very flat island. The marine environment is characterized by an almost continuously developed fringing reef.

The three Cayman Islands are the peaks of the Cayman Ridge, which forms the southern margin of the North American Plate and stretches from the Sierra Maestra of Cuba to the Gulf of Honduras. This ridge forms the northern margin of the Cayman Trough, which is 100 to 150 km wide and reaches depths of more than 6000 m (Brunt & Davies, 2012). It is the deepest region in the Caribbean Sea and part of the tectonic boundary between the North American Plate and the Caribbean Plate containing Jamaica and the rest of the Caribbean islands. The islands are formed entirely from calcareous marine deposits (limestone and dolostone), no volcanic or other rocks being found (Stoddart, 1980; Jones, 1994). They rose above sea level by uplifting and block faulting during the late Miocene (Stoddart, 1980; Woodroffe et al., 1983). According to the few available studies each of the

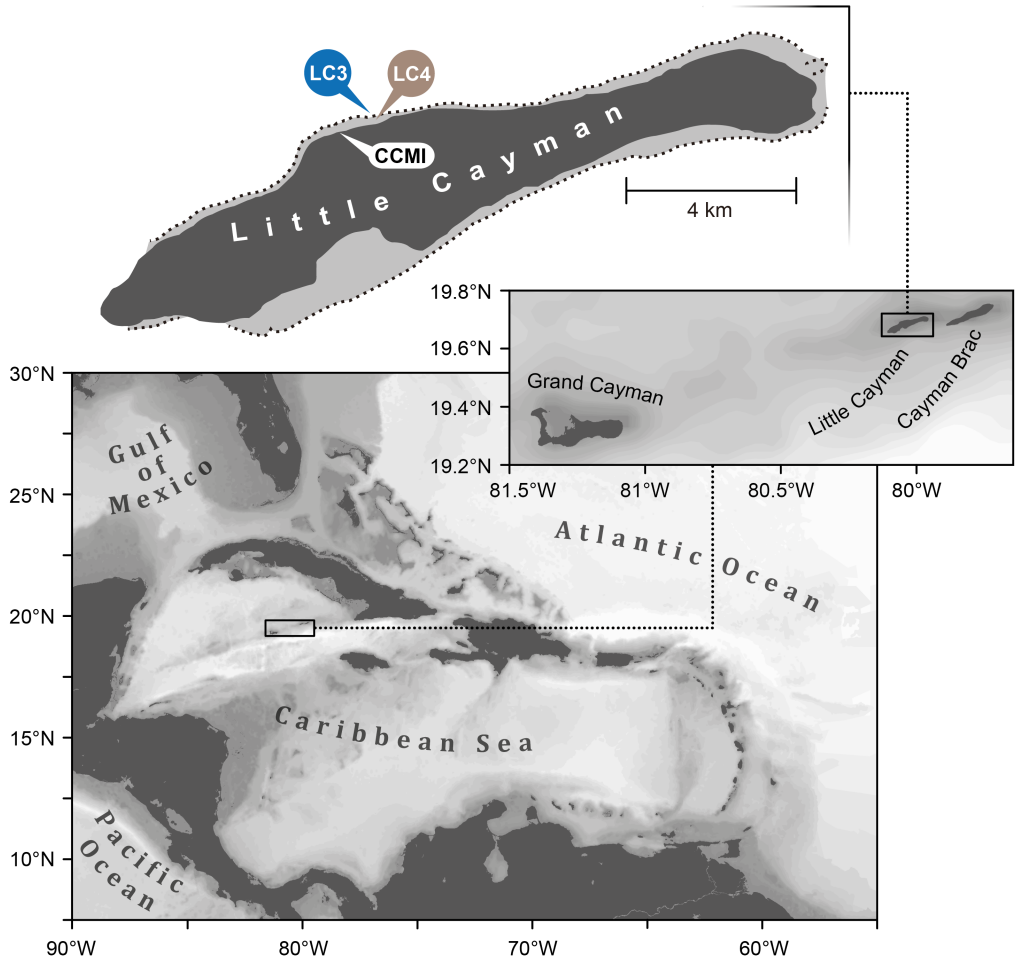

Figure 1-6. Map of the eastern Caribbean Sea with the location of the study area and close ups of the Cayman Islands and Little Cayman. Sampling sites of coral cores LC3 and LC4 are marked with blue and brown indicators, respectively. The location of the Central Caribbean Marine Institue (CCMI) is also indicated. Stippled contour in Island map represents reef crest.

three Cayman Islands appears to be based on a granodiorite foundation succeeded by a cap of basalt and then by Tertiary carbonates (Emery & Milliman, 1980; Stoddart, 1980; Woodroffe et al., 1983; Woodroffe, 1988; Brunt & Davies, 2012).

1.6.2. Climate

Annual cycle. Seasonal climate variability in the Caribbean Sea and tropical North Atlantic is primarily forced by the covarying pattern of trade wind convergence (Hastenrath, 1976, 1984; Peterson et al., 1991), the migration of the Intertropical Convergence Zone (ITCZ), and the underlying cross-equatorial SST gradient (Carton et al., 1996). However, the Cayman Islands are too far north to be reached by the zonal band of maximum rainfalls during the northernmost extent of the Atlantic ITCZ. At between 19 and 20° N the Cayman Islands lie within the center of the northeast trade winds belt and are subject to a sub-humid tropical climate. Due to their remote location the climate is strongly moderated by the sea

with a restricted range in air temperature, rather high humidities and generally stable weather patterns. Seasonal change is most strongly marked by variations in precipitation (Figure 1-7). The year is characterized by a summer wet season from May to November and a winter dry season from November/December to April (Figure 1-7). Minimum rainfall and

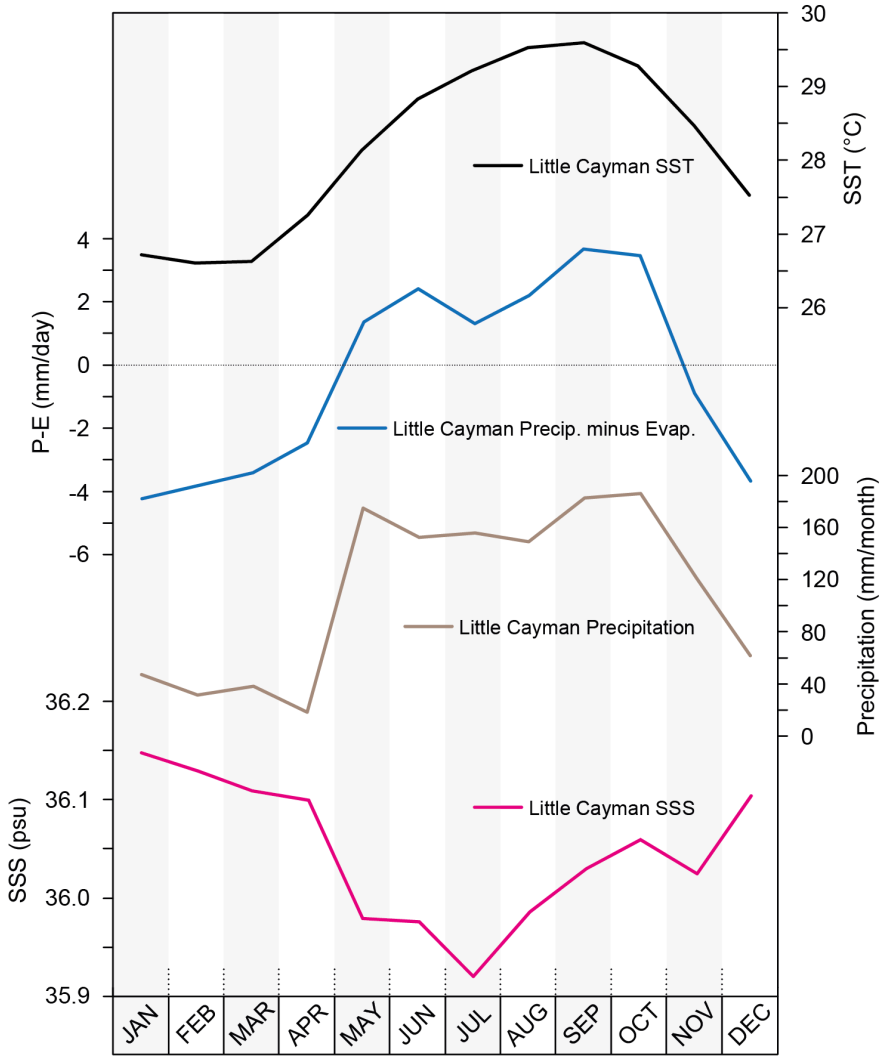

Figure 1-7. Monthly mean climatology of environmental parameters at the study site, Little Cayman: black curve: Sea Surface Temperature (SST) climatology for 1950-2012 from HadISST1 in a 1° × 1° grid box (Rayner et al., 2003); blue curve: Precipitation minus Evaporation (P-E) for 1979-2012 from ECMWF ERA-interim (Berrisford et al., 2011), note that negative values indicate net evaporation; brown curve: climatology of monthly mean precipitation for 1950-2012 from CRU TS3.25 (Harris & Jones, 2017); pink curve: Sea Surface Salinity (SSS) climatology from World Ocean Atlas 2013 (Zweng et al., 2013); SST, P-E and Precipitation in a 1°× 1°, SSS in a 0.7° × 0.7° grid box including the study site.

maximum evaporation coincide in March and April, while heaviest rains usually occur in October. The high evaporation results from the enhancement of the trade winds associated with the southward displacement of the ITCZ at this time and rising air temperatures. During the summer months and the northward movement of the ITCZ the Islands are frequently affected by low-pressure systems moving west across the Caribbean. These range

from weak tropical waves, through depressions and tropical storms to hurricanes and are often accompanied by heavy rainfall. SST displays a well marked seasonal cycle of 3 °C in amplitude, ranging from 26.6 °C in February to 29.6 °C in September with an annual mean of 28.2 °C (Rayner et al., 2003) (Figure 1-7). SSS data from World Ocean Atlas 2013 (Zweng et al., 2013) indicate a small annual amplitude of only about 0.25 psu, with more saline conditions during the winter dry season and less saline conditions during the summer wet season (Figure 1-7).

Interannual to decadal variability. Unlike the tropical Pacific, where climate variability on seasonal to decadal timescales is dominated by a single mode, the El Niño Southern Oscillation, the tropical Atlantic is dominated by the competing influence of modes of climate variability originating from local (internal) processes as well as from regions remote from the tropical Atlantic. (Sutton et al., 2000; Marshall et al., 2001; Czaja et al., 2002; Czaja, 2004; Hurrell et al., 2006). Interannual to decadal variability of Caribbean climate is known to be influenced by both tropical Pacific as well as tropical and extratropical North Atlantic variability (Taylor et al., 2002). SST over the north tropical Atlantic (NTA) exhibits substantial interannual to decadal variability, and is arguably one of the most important climate parameters on these time scales. Several mechanisms have been proposed to explain the origin of this variability (e.g., Marshall et al., 2001; Xie & Carton, 2004; Kushnir et al., 2006). These mechanisms include local coupled ocean-atmosphere interaction and forcing from the Pacific El Niño-Southern Oscillation (ENSO) (Figure 1-8) and the North Atlantic Oscillation (NAO) (Figure 1-9), both having significant teleconnections to the NTA (Curtis & Hastenrath, 1995; Giannini et al., 2001a; Giannini et al., 2001b; Czaja et al., 2002; Ruiz-Barradas et al., 2003; Hurrell et al., 2006). ENSO and NAO modulate the strength of the trade winds that affects SST through latent heat exchange at the ocean surface as well as the distribution and intensity of rainfall over the surrounding landmasses (Enfield & Mayer, 1997; Giannini et al., 2000; Giannini et al., 2001b; Chiang, 2002; Czaja et al., 2002). The relative importance of both modes for SST variability in the NTA appears to be frequency dependent, with ENSO dominating at interannual and the NAO at interdecadal time scales (Czaja et al., 2002). Both modes also influence SST variability in the Caribbean Sea which is linked to sea level pressure (SLP) variations in the North Atlantic region (Hastenrath, 1984) mainly through changes in surface winds (Wang et al., 2007, 2008b). Through the influence on SST, wind stress and rainfall ENSO also modulates the occurrence of hurricanes in the Caribbean (Gray, 1984; Enfield & Mayer, 1997; Giannini et al., 2000; Tang & Neelin, 2004).

The El Niño Southern Oscillation is a system of combined oscillations of temperature in the eastern Pacific and atmospheric pressure in the western and south-central Pacific. El Niño is an ocean circulation pattern that interrupts the normal circulation of water in the Pacific Ocean typically every 3 to 7 years and is marked by significantly warmer than average SSTs in the eastern tropical Pacific off the west coast of South America. The opposite state of the system is named La Niña and is associated with significantly cooler temperatures than average. Although theses events are typically characterized by a significant deviation from average SSTs, they are also associated with changes in wind, pressure, and rainfall patterns. In the NTA and Caribbean region SSTs act in concert with SSTs in the eastern Tropical

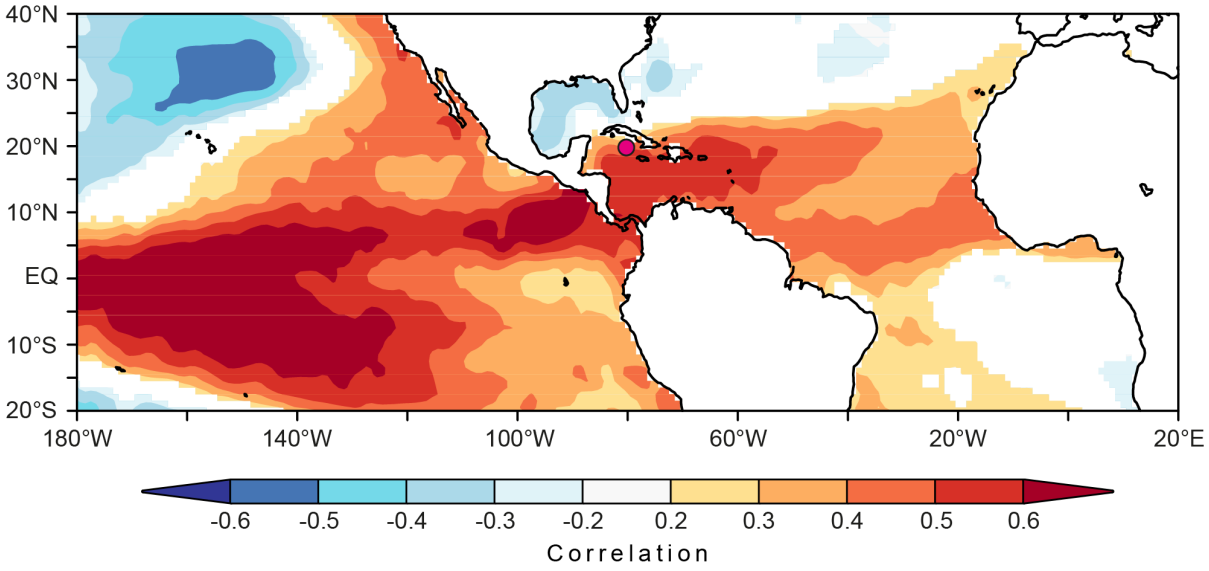

Figure 1-8. Spatial distribution of correlations between December-January-February Nino3.4 index and March-April-May SST data (Rayner et al., 2003). Data cover the period 1950–2012. Location of Little Cayman is indicated with pink dot.

Pacific during El Niño/La Niña years, although lagged in time by several months (Saravanan & Chang, 2000) (Figure 1-8). The Southern Oscillation is a naturally occurring fluctuation in which changes in lower atmospheric surface pressure in the far western Pacific, near northern Australia, are opposite in sense to those in the south-central Pacific, near Tahiti. During an El Niño event, surface pressure tends to be lower in the eastern Pacific and higher in the western Pacific while the opposite scenario tends to occur during a La Niña event. The Pacific ENSO system influences seasonal climate variability (such as rainfall and temperature) on a global scale (Philander, 1990). That means, depending on the region and season, certain climate conditions are more likely to happen during El Niño events or during La Niña events than at other times. ENSO related climate conditions play an important role in connection with the observed rapid global decline of coral reefs (Hoegh-

Guldberg, 1999; Hughes et al., 2003; Pandolfi et al., 2003; Pandolfi et al., 2011). This decline has been attributed largely to an increase in the frequency and severity of widespread coral bleaching events as a result of the increased occurrence of acute, regional ocean-warming events superimposed on longer-term trends in global warming (Hoegh-Guldberg, 1999; Veron et al., 2009). Warm SST anomalies related to El Niño brought on recurrent regional bleaching events in the Caribbean, the Indo-Pacific and Red Sea and caused three mass coral bleaching events across the globe so far (1998, 2010 and the most widespread and longest 2014-2017) (Hughes et al., 2003; Oliver et al., 2009; Eakin et al., 2010; Hughes et al., 2018; National Oceanic and Atmospheric Administration (NOAA), 2018). A comprehensive review of the El Niño phenomenon and the Southern Oscillation can be found in the studies of (Trenberth, 1997; Cane, 2005).

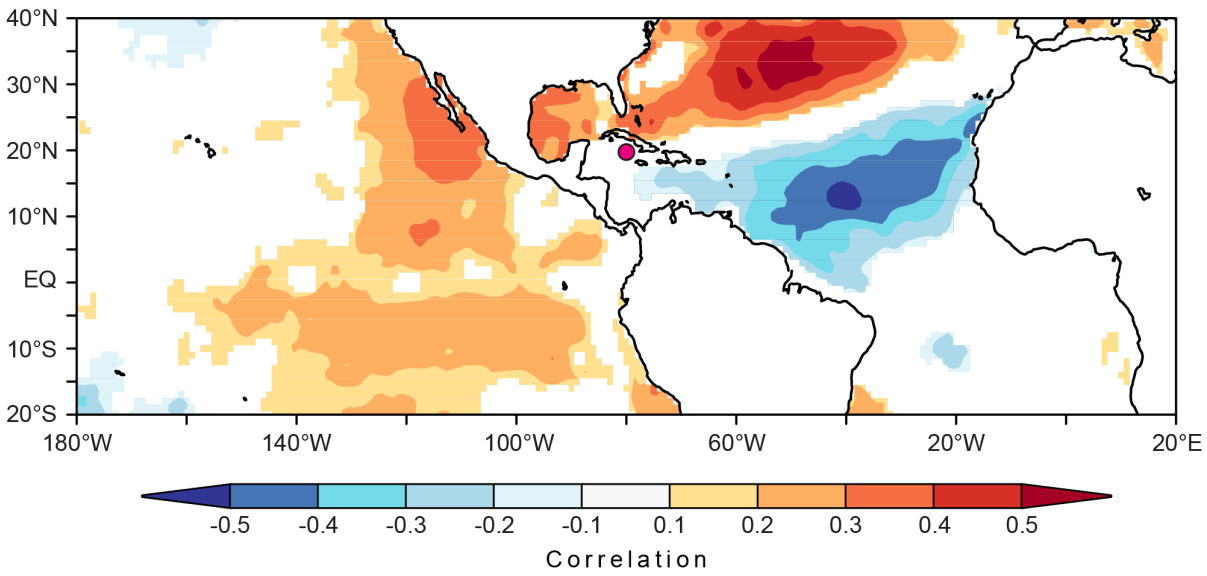

Figure 1-9. Spatial distribution of correlations between December-January-February North Atlantic Oscillation (NAO) index (Jones et al., 1997) and March-April-May SST data (Rayner et al., 2003). Data cover the period 1950–2012. Location of Little Cayman is indicated with pink dot.

While ENSO shows an important intertropical teleconnection pattern with the Caribbean, the NAO forcing is of extratropical origin (Figure 1-9). The NAO is defined as the normalized sea-level pressure difference between the Azores and Iceland (Jones et al., 1997). This gradient affects the strength of the tropical North Atlantic trade winds (George & Saunders, 2001) and thus the sensible and latent heat flux that in turn influences north tropical Atlantic SST (George & Saunders, 2001; Giannini et al., 2001a) and the extent of the Atlantic Warm Pool (AWP) comprising the Gulf of Mexico, the Caribbean Sea, and the western tropical North Atlantic (Wang & Enfield, 2001; Wang et al., 2007, 2008b). On decadal timescales the NAO influences climate in the North Atlantic basin and the

surrounding continents. NAO-related impacts on winter climate extend from Florida to Greenland, from northwestern Africa to Europe, and as far as into northern Asia (Visbeck et al., 2001). A detailed review of the North Atlantic Oscillation can be found in (Hurrell et al., 2003a, 2003b).

Multidecadal variability. Fluctuations of North Atlantic SST on decadal to multidecadal timescales are linked with decadal climate fluctuations, such as Indian and Sahel rainfall (Zhang & Delworth, 2006), European summer precipitation (Sutton & Dong, 2012), tropical Atlantic hurricane behavior (Goldenberg et al., 2001; Knight et al., 2006) and variations in global temperatures (Chen & Tung, 2014) and may mask or augment warming due to anthropogenic causes (Latif et al., 2006b). The multidecadal portion of this SST variability is commonly referred to as the Atlantic Multidecadal Oscillation (AMO) (Kerr, 2000) (Figure 1-10). The AMO has been identified as a coherent pattern of oscillatory changes in North Atlantic SST with a period of about 60 to 90 years (Kushnir, 1994; Schlesinger & Ramankutty, 1994). Indices of the AMO have traditionally been based on average annual

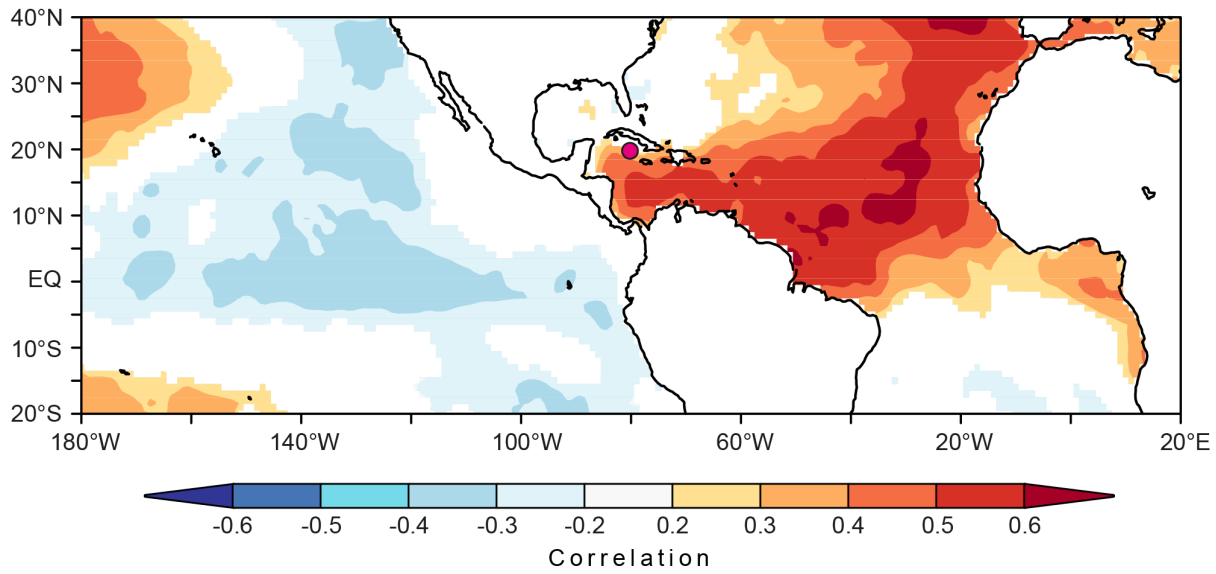

Figure 1-10. Spatial distribution of correlations between annual Atlantic Multidecadal Oscillation (AMO) index (Enfield et al., 2001) and annual SST data (Rayner et al., 2003). Data cover the period 1950–2012. Location of Little Cayman is indicated with pink dot.

SST anomalies in the North Atlantic region (Kaplan et al., 1998). To account for the influence of the recent global warming trend on North Atlantic SST, revised AMO indiceshave subsequently been defined by including global mean SSTs (Trenberth & Shea, 2006; Parker et al., 2007). It is widely believed that ocean circulation drives the phase changes of the AMO by controlling ocean heat content (Delworth & Mann, 2000; McCarthy et al., 2015). Observational data and model simulations suggest that the AMO is a persistent

mode of internal ocean variability which is associated, at least partly, with natural changes in the strength of the Atlantic Meridional Overturning Circulation (AMOC) (Dong & Sutton, 2005; Knight et al., 2005; O'Reilly et al., 2016). However, because the instrumental SST records only span about 150 years, it remains a matter of debate whether the observed SST variability merely reflects a transient feature on a "red noise" background or a truly oscillatory phenomenon (Xie & Carton, 2004; Latif et al., 2006a; Kilbourne et al., 2008; Knudsen et al., 2011). For example, 440-year coral-based SST reconstructions from Bermuda suggest that multidecadal variability in the low-latitude Atlantic Ocean may not be a persistent feature but becomes significant only after 1730 (Saenger et al., 2009). Answering this controversy requires a longer perspective based on multiple proxy records from different parts of the Atlantic Ocean that extends significantly further back in time.

1.6.3. Oceanography

The Caribbean Sea is a semi-enclosed basin bounded on the south and west by South and Central America, and fringed on the east and north by the chain of Antilles Islands and the Atlantic Ocean. Outflow from the Caribbean promotes the transequatorial heat transfer to higher latitudes (Schmitz et al., 1993; Schmitz & McCartney, 1993; Sato & Rossby, 1995) and acts as a source of the Gulf Stream (GS) (Hogg & Johns, 1995). Most Atlantic water infiltrates the Caribbean Sea through the Grenada, St. Vincent, and St. Lucia Passages in the southeast (Johns et al., 2002) sourced from the meandering North Brazil (NBC) and Guyana Current (GC) (Figure 1-11) that bear fresh water from the Amazon and Orinoco Rivers. North of 15°N inflow water is primarily Gulf Stream water returning southwestward in the North Equatorial Current (NEC), passing through the Leeward Islands of the Lesser Antilles, through the Windward Passage and through the Mona Passage (Richardson, 2005). Overall, thermohaline circulation combines with wind-driven circulation from the subtropical gyre to form an inflow of about 28 Sv (1 Sv = 1 Sverdrup = 106 $m^3 s^{-1}$) to the Caribbean (Schmitz & Richardson, 1991; Johns et al., 2002). The water then continues westward as the Caribbean Current (CAC), the main surface circulation in the Caribbean Sea, at about 0.5 m s^{-1} within latitudes 13°–16° N (Wüst, 1964; Gordon, 1967; Molinari et al., 1981; Roemmich, 1981; Kinder et al., 1985; Hernandez-Guerra & Joyce, 2000; Fratantoni, 2001). It turns northwest between Nicaragua and Jamaica, with a branch forming the counter clockwise Panama Gyre (Roemmich, 1981; Hernandez-Guerra & Joyce, 2000). The westward current exits via the Yucatan Channel entering warm water to the Gulf of Mexico

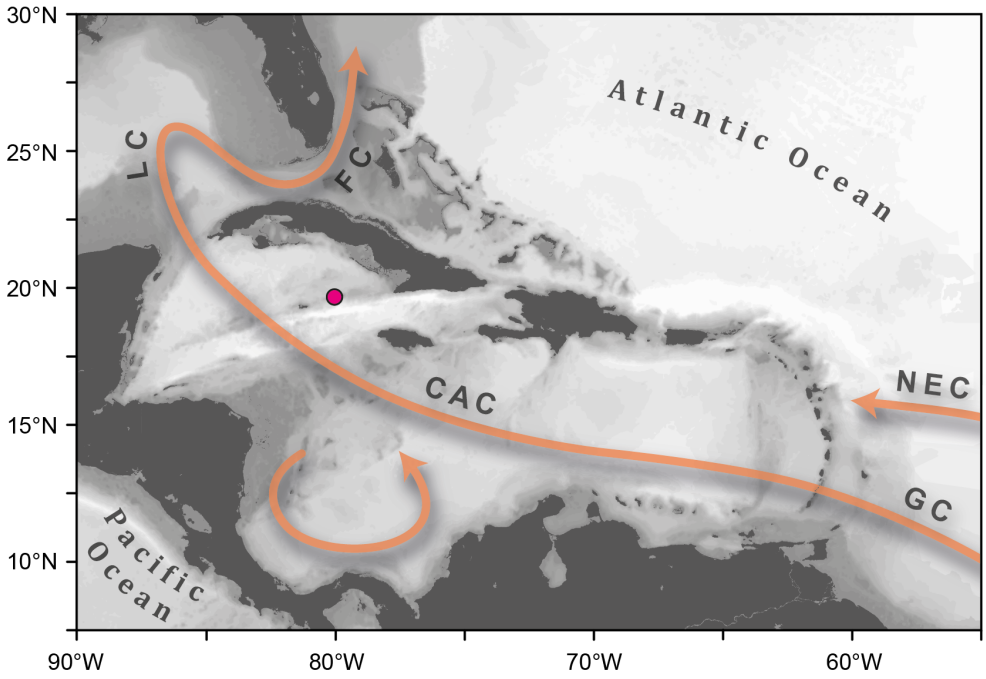

Figure 1-11. Oceanographic setting of the Caribbean region schematically showing the major surface current systems. Surface currents are indicated as orange arrow based on the Mariano Global Surface Velocity Analysis (MGSVA) (http://oceancurrents.rsmas.miami.edu): CAC: Caribbean Current; LC: Loop Current; FC: Florida Current; GC: Guyana Current; NEC: North Equatorial Current. Location of Little Cayman is indicated with pink dot.

via the Loop Current (LC) and to the Florida Strait via the Florida Current (FC) (Figure 1-11) eventually to be drawn into the GS, which receives contributions from the Antilles Current and its Atlantic sources (Gunn & Watts, 1982; Lee et al., 1996). The CAC builds an important branch of the upper part of the northward-flowing AMOC (Schmitz & Richardson, 1991; Schmitz & McCartney, 1993), since this is the major route by which South Atlantic water flows into the FC and GS. It also is the major current affecting the Cayman Islands (Scheltema, 1971) and of some importance to coral colonization of these islands. Currents are the major means of widespread dispersal of coral larvae and the CAC can distribute larvae from the Antilles west-northwest to the Cayman Islands on its northern border, but not directly from the Jamaican area (Brunt & Davies, 2012).

Surface current patterns and hydrography in the Caribbean are subject to seasonal fluctuations that are mainly controlled by the seasonal migration of the ITCZ. In summer, with the ITCZ displaced to the north, the Caribbean hydrography is characterized by enhanced rainfall and fluvial freshwater input. Also, the North Equatorial Counter Current establishes during that time. It is mainly driven by a combination of the southeast trade winds and the diverting Coriolis force, which forces equatorial Atlantic surface waters towards the east and leads to strengthened inflow into the Caribbean (Richardson & McKee, 1984). The uppermost layer of Caribbean seawater (upper 80 m), the Caribbean Surface

Water (CSW) (Wüst, 1964), is believed to be a mixture of tropical Atlantic surface waters and fresh water from the Amazon and Orinoco Rivers, which flows to the Caribbean as the Guyana Current. Due to the influence of this riverine water, salinity of the CSW is relatively low at around 35.5 psu (Hernandez-Guerra & Joyce, 2000). About 80 % of the CSW originates from South Atlantic water, while the remainder has a North Atlantic source (Schmitz & Richardson, 1991). Underneath the CSW is the more saline (36.5 psu) and cooler Subtropical Under Water (SUW; 22–23 °C compared to 28 °C of CSW) (Wüst, 1964; Morrison & Nowlin, 1982; Schmitz & McCartney, 1993). This water mass originates in the central tropical Atlantic, where evaporation exceeds precipitation, and forms the permanent upper thermocline in the Caribbean (Wüst, 1964).

1.7. Coral archives from Little Cayman

Little Cayman and its reef environment meet several requirements for successfully studying large-scale climate as well as local natural environmental variability from coral archives. The island is located in the pathway of the Caribbean Current and due to its isolated position around 150 km away from the nearest major land mass its climate is strongly moderated by the sea. Live coral cover around the island has been documented to be equivalent to or higher than in other locations in the Caribbean (Gardner et al., 2003). Two key factors contribute to this status, i.e., the lack of freshwater rivers on the island and minimal anthropogenic stress due to nutrient inputs, commercial fishing, groundings or other activities undertaken by less than 200 permanent residents. Since the mid-1980s, marine protected areas have been enforced along more than 50 % of the island's coast, including two no-take marine parks. Hence, Little Cayman corals are not affected by factors that can potentially introduce signals related to local anthropogenic or terrestrial influences, which could hamper the detection of natural environmental and (large-scale) climate signals. The Little Cayman Research Center (LCRC) of the Central Caribbean Marine Institue (CCMI) is located on the northern shore of Little Cayman (Figure 1-6) and provides all facilities needed for coral research (e.g., diving equipment, field guides, boat, wet lab for initial sample processing). Extensive surveys have been conducted by CCMI marine biologists and reef ecologists of the reefs inside the Marine Park on a regular basis for more than a decade (Atlantic and Gulf Rapid Reef Assessment (AGRRA) Program, pers. comm. Dr. Manfrino; Coelho & Manfrino, 2007). As a result, detailed information on species, size and location (including water depth) of coral colonies is available for numerous Little Cayman sites.

Furthermore, near real-time in-situ water temperature data is available from the Coral Reef Early Warning System (CREWS) station LCIY2 located within the fore reef zone of the Bloody Bay Marine Park. The station is part of the Integrated Coral Observing Network (ICON) of the National Oceanic and Atmospheric Administration (NOAA) and is in operation since July 2009. At the time of coral core collection three full years of in situ recordings where available for the adjustment of gridded SST data products to match the in-situ SST mean and variance for the subsequent calibration of geochemical coral proxies (see chapter 2.2.5 for details).

1.7.1. Diploria strigosa (Dana, 1846)

The scleractinian coral *Diploria strigosa* (Dana, 1846) (Figure 1-2) is the most common of three *Diploria* species, all of which are endemic to the Atlantic-Caribbean region (Figure 1-12). This species forms massive usually spherical boulders (especially in shallow water) or crusts across a wide depth distribution (0 to 35 meters) and is abundant in Little Cayman reefs and across most reef habitats in the Caribbean region. The coral surface is even with sinuous valleys resembling the brain of higher animals, hence its trivial name "brain coral" (Figure 1-14c). *Diploria strigosa* is a simultaneous hermaphrodite (i.e., a single individual functions as both male and female at the same time) and a broadcast spawner, releasing gamete bundles during the summer, with a single gametogenic cycle per year. In broadcast spawners gametes are released into the water and fertilization takes place in the water column. Planulae develop, free-swimming larvae, which are transported by surface currents until they reach an algae free substrate where they settle, undergo metamorphosis into individual coral polyps and begin secreting a calcium carbonate skeleton (Fadlallah, 1983) called the corallite (Weil & Vargas, 2010). Over successive generations the individual

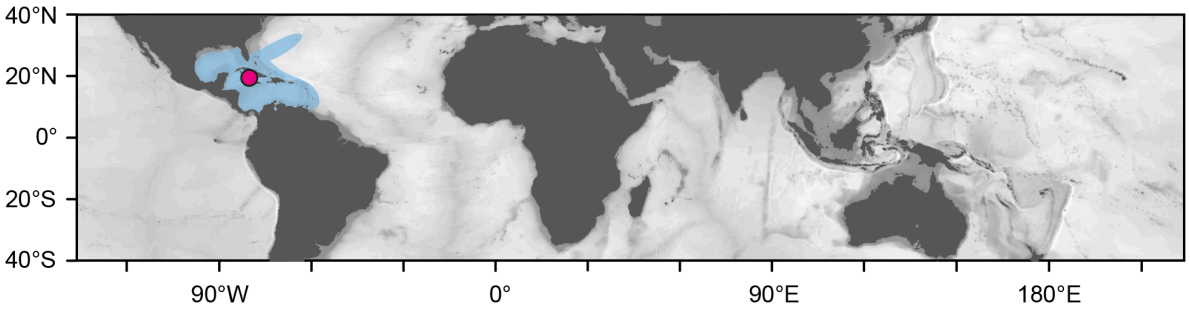

Figure 1-12. Distribution map of *Diploria strigosa*. The map indicates the general regions where *Diploria strigosa* has been recorded (Veron, 2000). Location of Little Cayman is indicated with pink dot.

corallite contributes to the formation of the coral colony and, on a larger scale, of a coral reef. The coral skeleton forms the bulk of the colony, while the polyp tissue comprises only a thin veneer. Polyps are often connected and usually convoluted except near the colonies edge. The sinuous continuous corallite valleys are usually 6 to 9 mm wide and separated by a solid skeletal wall called the theca (Figure 1-13). Adjacent valleys, or rows of polyps, share a common theca and therefore, no exothecal structures are present. The thinner vertical inner walls are called septa. They extend from the theca towards the center of the corallite where they join and form a spongy structure that is called the columella (Figure 1-13). As the coral colony grows, the polyps lift their basal surface and secrete new basal floors, the dissepiments (Helmle et al., 2002). The identification of different skeletal elements is important in the process of microsampling. The sampling should be restricted to a single structure of the coral skeleton for geochemical analysis in order to obtain robust unbiased results (e.g., Leder et al., 1996; Giry et al., 2010).

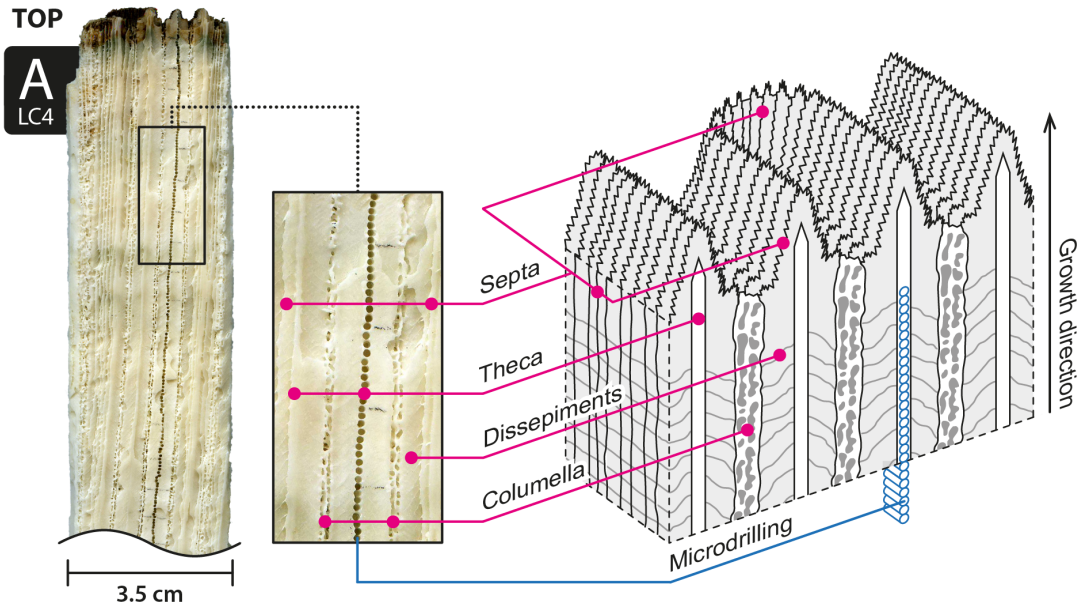

Figure 1-13. Image of upper part of sectioned coral slab from Little Cayman *Diploria strigosa* core LC4 (left). Enlarged section: Major elements of the coral skeleton are indicated; line of small holes observable from top to bottom represents the microsampling transect. Right: spatial scheme of major skeletal elements of *Diploria strigosa* clearly showing the microsampling approach (redrawn and modified from/after Giry et al. (2010)).

1.7.2. Coral core collection and microsampling

The coral cores investigated in this thesis were collected as part of a field sampling campaign in July 2012. Criteria such as size and shape, water depth and reef zone as well as vicinity to research facilities on land determined the selection of coral colonies. Two hemispherical colonies of *Diploria strigosa* on the north central coast of Little Cayman were sampled. The

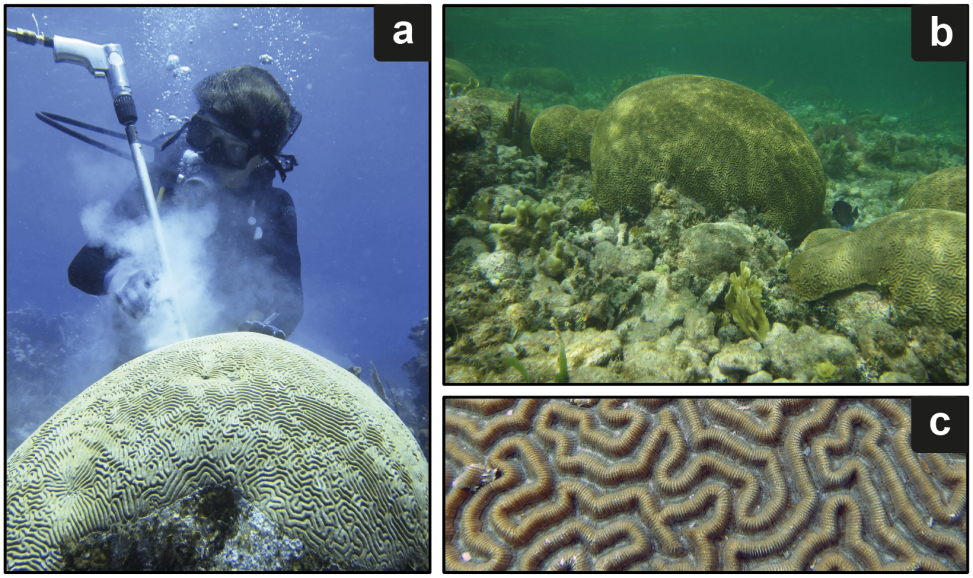

Figure 1-14. Images of coral colonies LC3 (a), LC4 (b) and close up of the surface of colony LC3 (c). All *Diploria strigosa*.

colonies grow 500 m apart from each other in different parts of the reef. Colony LC3 (Figure 1-14a) had a diameter of 0.8 m and grows in a water depth of 9 m in the fore reef (19.7° N, 80.06° W; Figure 1-6), 200 m off the fringing reef, while colony LC4 (Figure 1-14b) had a diameter of 1 m and grows in a water depth of 1.5 m in the backreef inside the lagoon (19.7° N, 80.05° W; Figure 1-6). The corresponding coral cores LC3 and LC4 have a length of 69 cm and 61.5 cm, respectively. Only one coral core from each colony and part of the reef could be drilled due to limited permission by the Cayman Islands Department of Environment, making replication studies with several cores impossible. The coral cores used in this thesis were drilled using SCUBA (self-contained underwater breathing apparatus) and a hand held pneumatic drill gun, air-powered by SCUBA tanks. The core barrel used was a diamond-tipped steel tube with an inner core barrel diameter of 3.6 cm and a length of 30 cm. Through the use of extension rods, the collection of longer coral cores (in 30 cm-segments) was possible. The cores were drilled vertically, in parallel orientation to the axis of maximum growth. During this process the corer cut through the concentric layers of colony growth and when the core was removed, a hole through the colony was created from the living surface to the base. The living tissue of *Diploria strigosa* only occupies the outer 0.5 to 1.0 cm of the colony (the layers below are dead but retain their physical structure). Thus, extracting the cores 3.6 cm in diameter removed approximately 10 cm^2 of live coral from the colonies surface.

Holes left by coring activities create opportunities for boring organisms to invade a colony and provide a place for sediment to collect. Both possibilities may cause long term damage

to the colony (Matson, 2011). Therefore drill holes were plugged immediately after drilling using a specific biocompatible underwater glue (ORCA glue), which is widely used in aquariums. The glue was applied to seal the drill hole up to the living coral surface (Figure 1-15a). During a survey in 2014, two years later, the corals were revisited and it could be confirmed that overgrowth of the glue plugs was occurring (Figure 1-15b). After collection, the cores were rinsed with freshwater and then air-dried. The coral core segments were

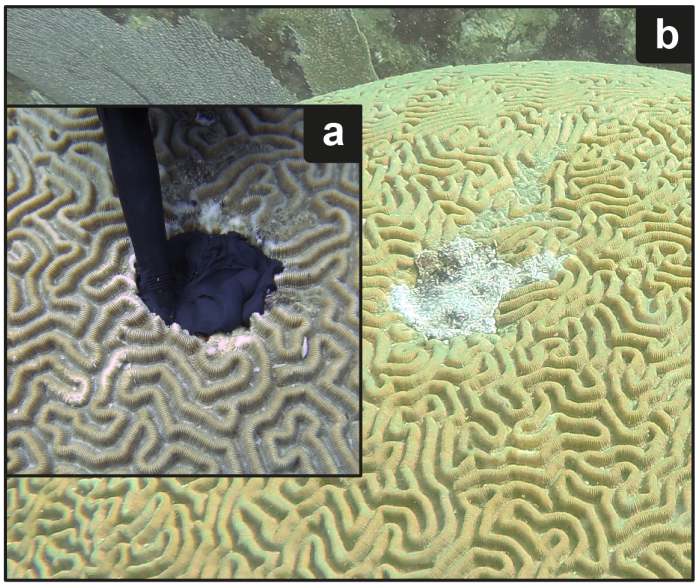

Figure 1-15. Core hole with underwater glue (ORCA) plug in coral colony LC3 (*Diploria strigosa*). (a) Freshly plugged drill hole and (b) the same hole two years later.

sectioned longitudinally into two sets of 7 mm thick slabs. The coral slabs were then cleaned in an ultrasonic bath with deionized water to remove saw cuttings and were oven dried at 50 °C for 24 hours. Afterwards the slabs were x-rayed at 60 kVp tube voltage and an exposure time of 15 seconds using digital radiography at the Royal Netherlands Institute for Sea Research (NIOZ) in order to expose annual density banding (Figure 1-16 and Figure 1-17). The X-radiographs were also used to measure mean annual skeletal growth rates and to determine optimal sampling transects for the following collection of microsamples. Samples for stable isotope and trace element analysis were collected using a low-speed micro drill (Proxxon Micromot E50 mounted on Drill Stand MB200) with a 0.5 mm diameter drill bit. The slabs were sampled along the theca, in order to avoid mixing of sample powder from different skeletal elements (Figure 1-13). A study by Helmle et al. (2002), who analyzed the complex skeletal architecture and density banding of *Diploria strigosa* using X-ray computed tomography (Figure 1-18), approved that the theca wall of this species is not influenced by secondary thickening processes, which could dampen the annual signal in the

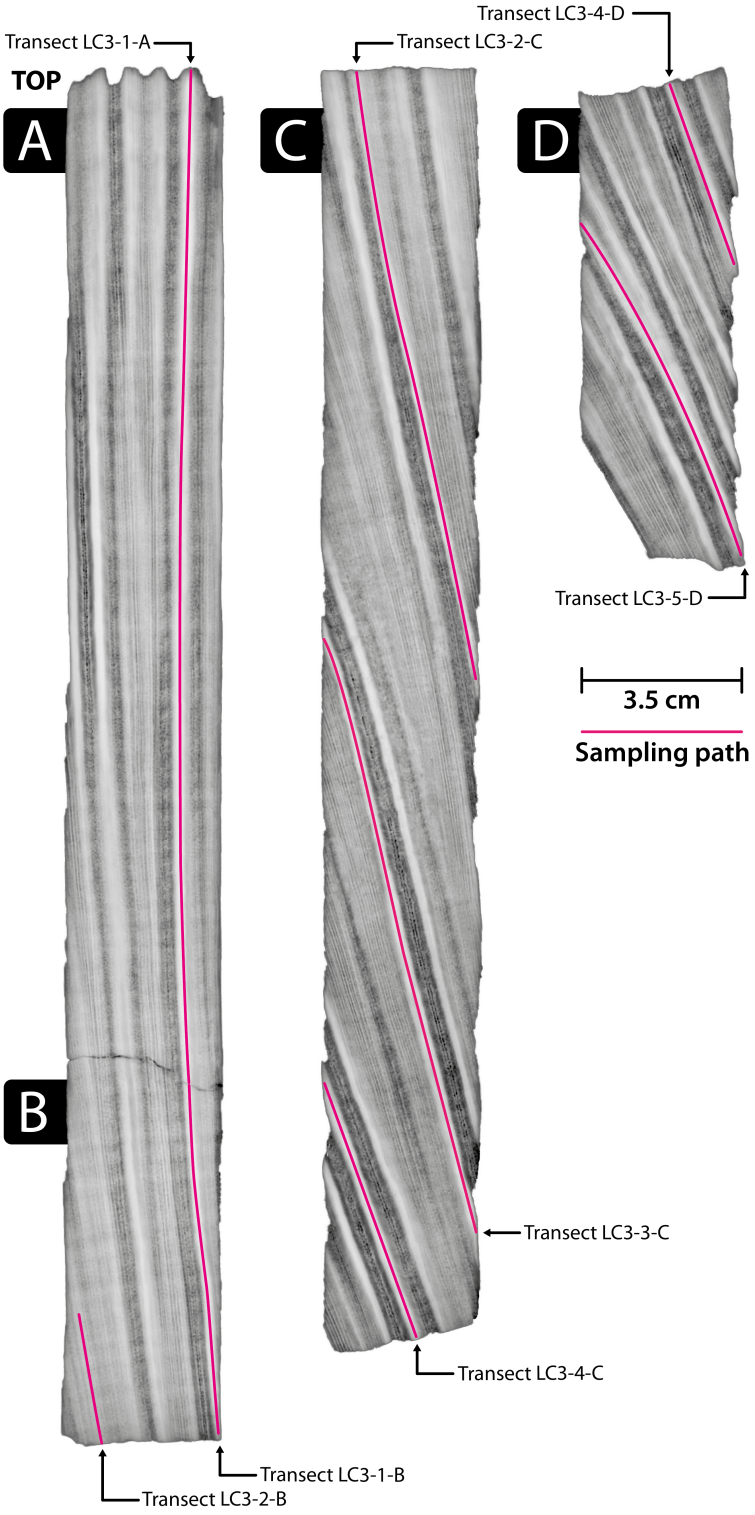

Figure 1-16. X-radiographs of the slabs from core LC3 recovered from a *Diploria strigosa* colony. Lighter regions in negative X-radiographs are denser and vice versa. Sampling transects are indicated by pink solid (sub-)vertical lines on each slab.

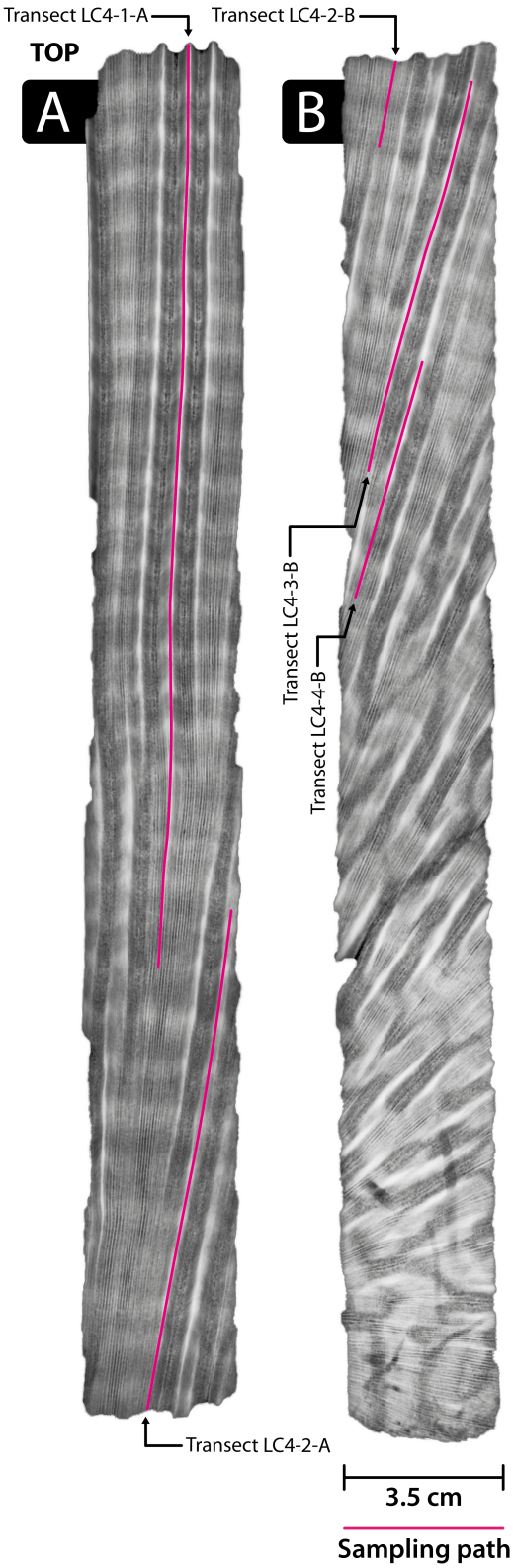

Figure 1-17. X-radiographs of the slabs from core LC4 recovered from a *Diploria strigosa* colony. Lighter regions in negative X-radiographs are denser and vice versa. Sampling transects are indicated by pink solid (sub-)vertical lines on each slab.

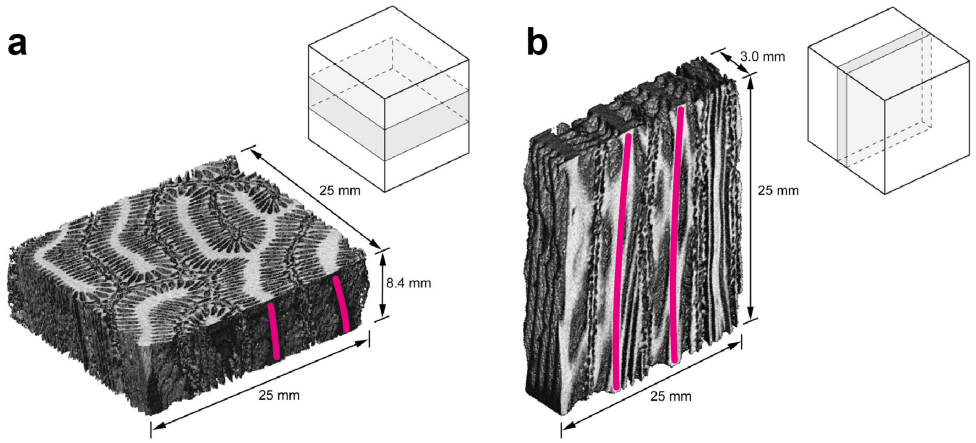

Figure 1-18: Three-dimensional skeletal reconstructions of X-ray computed tomography (CT) images and their relative positions within a diagram of a 25 x 25 x 25 mm coral cube from a *Diploria strigosa* colony retrieved off Florida. (a) plan-view image, and (b) longitudinal-view image. Coral cube diagrams are oriented with the growth trajectory running vertically. From Helmle et al. (2002), slightly modified. Pink lines schematically indicate the position of theca walls used for microsampling within the skeletal framework.

proxy time series (e.g., as observed in slow-growing specimens of *Diploria labyrinthiformis* from Bermuda by Cohen et al. (2004)). Furthermore, Giry et al. (2010) performed microsampling experiments along different skeletal elements of *Diploria strigosa* and revealed that microdrilling along the center of the theca is the method that best captures the annual SST cycle in both Sr/Ca and $\delta^{18}O$ and provides more realistic proxy–SST relationships. These differences in the geochemical composition of mesoskeletal elements might be controlled by vital effects that are to some extent linked to different calcification and photosynthesis rates (Erez, 1978; Juillet-Leclerc & Reynaud, 2010). Consequently, the sampling of cores LC3 and LC4 was confined to the theca of the coral skeleton. Microsamples were retrieved continuously at approximately 0.5 mm intervals along transects following the axis of maximum growth (Figure 1-13), yielding on average 10 (LC3) to 19 (LC4) samples per year of growth. Possible problems arising from annual variations in coral growth, i.e., an overrepresentation (underrepresentation) of coral aragonite formed during periods of fast (slow) growth and corresponding climate signals are considered in chapter 2.3. As a next step, the sample material was split into separate aliquots for stable isotope ($\delta^{18}O$ and $\delta^{13}C$) and trace element (Sr/Ca and Mg/Ca) analysis, respectively. Only the records of $\delta^{18}O$ and Sr/Ca ratios will be discussed herein. Analysis data series from different mircrosampling transects were spliced using the overlapping parts of these transects. Further details on Sr/Ca and $\delta^{18}O$ analysis are given in chapters 2.2.3. and 3.2.3. A second set of coral slabs of core LC3 was sent to Japan for sampling and analysis of $\delta^{15}N_{Coral}$ by colleagues at Hokkaido University. Details are described in chapter 4.4. Chronologies for

the individual coral records were established based on two methods: the counting of annual density bands on the coral X-radiographs and the alignment of coral Sr/Ca variations to a SST time series. Coral Sr/Ca was used for the age model generation because of a higher correlation of coral Sr/Ca with in situ SST data from the CREWS station. The conversion from depth to time domain was achieved by matching coral Sr/Ca maxima (minima) to SST minima (maxima) for each annual cycle using AnalySeries software (Paillard et al., 1996). The SST reference used for alignment was an artificial monthly SST time series representing average seasonality calculated from the HadISST1.1 data set (Rayner et al., 2003) for the 1° × 1° grid box at 19-20° N and 79-80° E including the coral sites. The uncertainty of this approach is approximately ± 2 months in any given year (non-cumulative) due to interannual differences in the exact timing of maximum (minimum) SST. However, this is the most objective method (Charles et al., 1997), and the resulting proxy time series is independent of instrumental or gridded data. Subsequent visual comparison between Sr/Ca years and density band years confirmed the accuracy of conversion to the time domain. The Sr/Ca age model for each core was applied to the $\delta^{18}O$ record from the same core and numerically resampled to even monthly intervals. The depth-time relationship could also be transferred to the coral slabs used for $\delta^{15}N_{Coral}$ analysis because both sets of slabs share one sectional plane and feature the same skeletal structures at their cutting surfaces. Thus, the position of microsampling transects and age information from one slab could directly be transferred to the corresponding slab.

1.8. Motivation and Objectives

Climate variability in the tropical ocean regions produces numerous impacts on society and the environment of the surrounding continents on seasonal, interannual and multidecadal time scales through fluctuations in ocean and land temperature, rainfall and extreme events. Records of past sea surface parameters from the tropical oceans are essential for the understanding of past and future climate and environmental variations. High-resolution long-term data of past sea surface conditions are required to calibrate and validate numerical climate models, which promote an enhanced understanding of internal variability in the coupled ocean-atmosphere system (e.g., the Northern Hemisphere ocean circulation, including the Caribbean Current, the Gulf Stream system, and the North Atlantic Thermohaline Circulation (Latif et al., 2000; Latif, 2001a; Vellinga & Wu, 2004a). Furthermore, a thorough knowledge of past variability of the climate system and a high

spatiotemporal resolution of observational data is important for long-range climate forecasting (Delworth & Mann, 2000) and the assessment of the anthropogenic impact on climate and ecosystems. However, especially in the tropics, observational records are limited to the last 140 years and become sparser and spatiotemporally lacking before 1950 (Smith & Reynolds, 2003). Consequently, the interpretation of climate signals exhibiting decadal or longer scale variability and trends is complicated. Furthermore, globally rising ocean temperatures are not only influencing the global climate system, but also affect coral reef ecosystems by increasing the frequency and severity of bleaching and mortality events. The susceptibility of corals to temperature stress varies on local and regional scales. However, insights into potential controlling parameters are hampered by a lack of long term in situ data in most coral reef environments and gridded sea surface temperature products often do not resolve reef-scale variations. Thus, understanding past tropical climate and environmental variability beyond the period of instrumental observations or within regions lacking instrumental data requires the use of proxy data. Hetzinger et al. (2006a) have demonstrated that the geochemistry of the skeleton of massive fast-growing Caribbean corals of the species *Diploria strigosa* can provide such accurate, monthly resolved and century-long proxy records of climate and environmental variability in the Caribbean and the tropical North Atlantic, which is a key region for reconstructing long-term Northern Hemisphere climate variations. Long-term reconstructions are also highly needed to assess superimposed long-term trends related to global warming. Empirical evidence and climate model simulations indicate that the Caribbean is a prime area for the reconstruction and study of global temperature trends and variability (e.g., Hoerling et al., 2001; Wang et al., 2007).

The principal objective of this thesis is the development of seasonal-scale proxy records of surface ocean conditions in order to study past changes in tropical Atlantic climate variability as well as reef scale environmental variability extending beyond the period of instrumental data. For this purpose, monthly resolved coral records from the central Caribbean (Little Cayman, Cayman Islands) are generated using the massive growing hermatypic species *Diploria strigosa*.

In the first step the potential of geochemical proxy ($\delta^{18}O$, Sr/Ca) time series derived from *Diploria strigosa* to capture local environmental signals is assessed. These time series are used to examine how local environmental parameters may affect and be imprinted in the

coral record and which may be specific for different reef environments. For this task the isotopic and trace elemental composition of two coral cores drilled in adjacent but distinct reef environments (fore reef and lagoon) are examined sharing 40 years of information with high-temporal sampling resolution. The measured geochemical proxies are compared to in situ and gridded SST data and used to reconstruct seasonal- to decadal-scale SST variations. In the next step the potential of Little Cayman as a qualified reference site for the investigation of past large-scale climate signals (e.g., SST, hydrological cycle) and of the influence of external climate modes (e.g., ENSO, NAO) on the Caribbean and regions beyond is assessed. For this purpose the geochemical record of the longer coral core from the fore reef environment is extended to full length of 125 years, analyzed for decadal to multidecadal signals of climate variability and examined in combination with coral proxy records from other Caribbean sites.

As a secondary objective coral nitrogen isotopes ($\delta^{15}N$), a newly developed proxy for the reconstruction of past nitrogen cycling, are tested for the first time on a coral from the tropical Atlantic. The analyzed coral material was derived from the fore reef core in up to annual resolution in order to assess the ability of *Diploria strigosa* to detect changes in past nitrogen fixation rates in the surface ocean at Little Cayman.

Finally, as a tidbit, this thesis reports on the discovery of a cold-water coral province off western Morocco and explores its oceanographic and bathymetric boundary conditions. In this way, the thesis sheds light on the currently observed distribution of warm water coral relatives hidden in the dark deep and draws attention to the global aspect of scleractinian corals as climate and paleoceanographic archive for surface ocean to deep ocean conditions.

1.9. Dissertation Outline

The remainder of this dissertation consists of five chapters. In **chapter 2**, coral Sr/Ca data are used to reconstruct seasonal- to decadal-scale SST variations in the fore reef and in the lagoon to investigate potential differences between environments. Coral Sr/Ca data from the shallow lagoon successfully record high summer temperatures, whereas coral Sr/Ca from the deeper fore reef is strongly affected by thermal stress events. The results indicate that two massive *Diploria strigosa* corals responded differently to past warming events depending on the reef environment and that reef-scale SST variability can be much larger than suggested by satellite SST measurements. Furthermore, decadal variations in Sr/Ca from the shallow lagoon coral are discussed with regard to long-term background tidal effects.

Chapter 3 expands the scope beyond the local level. The fore reef coral record from chapter 2 is extended in time and completed with $\delta^{18}O$ measurements to asses the major climatic signals recorded in this century-long coral record, that are known to have strong influence on climate variability of the tropical Atlantic region on different time scales. Seawater $\delta^{18}O$ variations are reconstructed from paired Sr/Ca and $\delta^{18}O$ measurements, which indicate a drying trend over the past century. The (spatial) relationships of geochemical coral proxy data with SST are discussed, along with the feasibility of the coral record to track the impact of modes of external forcing (NAO, ENSO) on north tropical Atlantic SST and climate variability. The results show that coral data tracks decadal and multidecadal NAO variability in the region of the Loop Current and Gulf Stream system. In addition, a combined evaluation of the fore reef record with two other coral records from different Caribbean sites reveals SST information for large sparsely sampled Atlantic regions beyond the Caribbean.

While chapter 2 and 3 are based on commonly used geochemical proxies, **chapter 4** explores coral nitrogen isotopes, which only recently have been used in biogenic carbonate skeletons as a proxy for nitrogen fixation in tropical oceans. Based on material from the fore reef core the development of the first centennial-scale record of annual nitrogen isotopes in a Caribbean coral is described. The results show changing nitrogen fixation that correlates with multidecadal variability in North Atlantic Ocean SST. A decreasing trend in reconstructed nitrogen fixation during the 20^{th} century suggests a connection to the slowdown of the AMOC.

Chapter 5 dives down to a deep and dark coral habitat on the opposite side of the Atlantic and reports on a new cold-water coral mound province covering about 410 km^2 off western Morocco at 678 to 863 m water depth. The province was successfully discovered by CTD reconnaissance applying seawater density as a potential indicator of CWC occurrences, followed by hydroacoustic mapping. Box core based ground-truthing of selected sites revealed a thin cover of living corals but much larger accumulations of dead thickets and fragmented coral rubble within the province. Buried coral material from box core samples yield absolute ages dating back to the late Holocene.

In **chapter 6**, the major conclusions resulting from this thesis are summarized and, in **chapter 7**, future research perspectives are proposed.

2. Impact of warming events on reef-scale temperature variability as captured in two Little Cayman coral Sr/Ca records

Jonas von Reumont[1], Steffen Hetzinger[1], Dieter Garbe-Schönberg[2], Carrie Manfrino[3,4], Christian Dullo[1]

[1]*GEOMAR Helmholtz-Zentrum für Ozeanforschung Kiel, Wischhofstr. 1-3, 24148 Kiel, Germany*
[2]*IfG, Institute of Geosciences, Christian-Albrechts-University, Ludewig-Meyn-Str. 10-14, 24118 Kiel, Germany*
[3]*Department of Geology and Meteorology, Kean University, 1000 Morris Ave., Union, NJ 07083, USA*
[4]*Central Caribbean Marine Institute, PO Box 1461, Princeton, NJ 08542, USA*

Published in *G*[3] | *Geochemistry, Geophysics, Geosystems*

The rising temperature of the world's oceans is affecting coral reef ecosystems by increasing the frequency and severity of bleaching and mortality events. The susceptibility of corals to temperature stress varies on local and regional scales. Insights into potential controlling parameters are hampered by a lack of long term in situ data in most coral reef environments and sea surface temperature (SST) products often do not resolve reef-scale variations. Here we use 42 years (1970–2012) of coral Sr/Ca data to reconstruct seasonal- to decadal-scale SST variations in two adjacent but distinct reef environments at Little Cayman, Cayman Islands. Our results indicate that two massive *Diploria strigosa* corals growing in the lagoon and in the fore reef responded differently to past warming events. Coral Sr/Ca data from the shallow lagoon successfully record high summer temperatures confirmed by in situ observations (> 33 °C). Surprisingly, coral Sr/Ca from the deeper fore reef is strongly affected by thermal stress events, although seasonal temperature extremes and mean SSTs at this site are reduced compared to the lagoon.

The shallow lagoon coral showed decadal variations in Sr/Ca, supposedly related to the modulation of lagoonal temperature through varying tidal water exchange, influenced by the 18.6-year lunar nodal cycle. Our results show that reef-scale SST variability can be much larger than suggested by satellite SST measurements. Thus, using coral SST proxy records from different reef zones combined with in situ observations will improve conservation programs that are developed to monitor and predict potential thermal stress on coral reefs.

Citation: von Reumont, J., Hetzinger, S., Garbe-Schönberg, D., Manfrino, C., & Dullo, W. C. (2016). Impact of warming events on reef-scale temperature variability as captured in two Little Cayman coral Sr/Ca records. *Geochemistry, Geophysics, Geosystems*, 17(3), 846-857, https://doi.org/10.1002/2015GC006194.

2.1. Introduction

Sea surface temperature (SST) in the tropical oceans is an important component in understanding tropical ocean-atmosphere dynamics and a key parameter for climate models in assessing future climate evolution linked to anthropogenic climate change (Deser et al., 2010; Enfield & Cid-Serrano, 2010; Latif & Keenlyside, 2011; IPCC, 2013). Understanding past tropical climate variability beyond the period of instrumental observations or within regions lacking instrumental data requires the use of climate proxies. The geochemistry of coral skeletons provides such proxies. Corals record environmental fluctuations in ambient seawater and large scale climate variability during growth. Geochemical records from corals offer reliable data on dominant large-scale climate modes and are used to detect impacts in the northern tropical Atlantic including the El Niño Southern-Oscillation (ENSO), the North Atlantic Oscillation (NAO) (Kuhnert et al., 2005; Hetzinger et al., 2006a; Goodkin et al., 2008) or the Atlantic Multidecadal Oscillation (AMO) (Hetzinger et al., 2008). One of the most commonly used geochemical parameters measured in coral aragonite are Sr/Ca ratios. Relative variations of coral Sr/Ca ratios follow thermodynamic principles and are influenced by temperature and the Sr/Ca of seawater. Over the past several hundred years seawater Sr/Ca changes are negligible (Gagan et al., 2000) and several studies have used the Sr/Ca ratios as paleothermometers for the reconstruction of SSTs on timescales ranging from seasonal and interannual to decadal in local to regional dimensions (Smith et al., 1979; Beck et al., 1992a; de Villiers et al., 1994; Alibert & McCulloch, 1997; Gagan et al., 2000; Marshall & McCulloch, 2002; DeLong et al., 2012). Coral Sr/Ca records are typically calibrated against SST records from local in situ measurements or reanalysis data and ideally resemble SST variability over the calibration period. In most cases local SST records are not available and reanalysis products calculated over a relatively large area are used. However, water temperatures can vary significantly at individual reef sites over small spatial and temporal scales because of the bottom topography and variable forcing parameters (e.g., tides, currents and insolation) (Monismith et al., 2006; McCabe et al., 2010). Tidal forcing can play a role in coral Sr/Ca variability on a daily and monthly scale (Cohen & Sohn, 2004). Consequently, local effects on SST may hamper the use of coral colonies as recorders of regional/large-scale environmental variability. This study presents Sr/Ca time series from two *Diploria strigosa* coral cores drilled in different reef environments, the shallow lagoon and the fore reef of Little Cayman, Cayman Islands. These time series are used to examine

how local environmental parameters may be imprinted in the coral record and which may be specific for each environment.

The questions addressed in this study include: (1) does satellite-based instrumental temperature data accurately capture the local- to regional-scale temperature variability? (2) which mechanisms influence seawater temperature and coral Sr/Ca in reef environments on a local scale (e.g., tides, insolation, water depth)? and (3) how does local-scale environmental variability affect the applicability of coral proxy data for regional and large-scale temperature reconstructions?

2.2. Materials and Methods

2.2.1. Setting of the study area

Little Cayman (Figure 2-1) is the smallest and least developed island of the three Cayman Islands with a human population of less than 200. It is a 17 km long and 1.6 km wide low-lying island with a maximum elevation of 13 m located in the pathway of the Caribbean Current. The islands climate is strongly moderated by the sea since no major land masses are present within a radius of 200 km. An almost continuously developed fringing reef encircles the island. The fore reef shelf is shallow and narrow and its edge is marked by the 20 m isobath from where it drops to great depths outside the euphotic zone. The width of

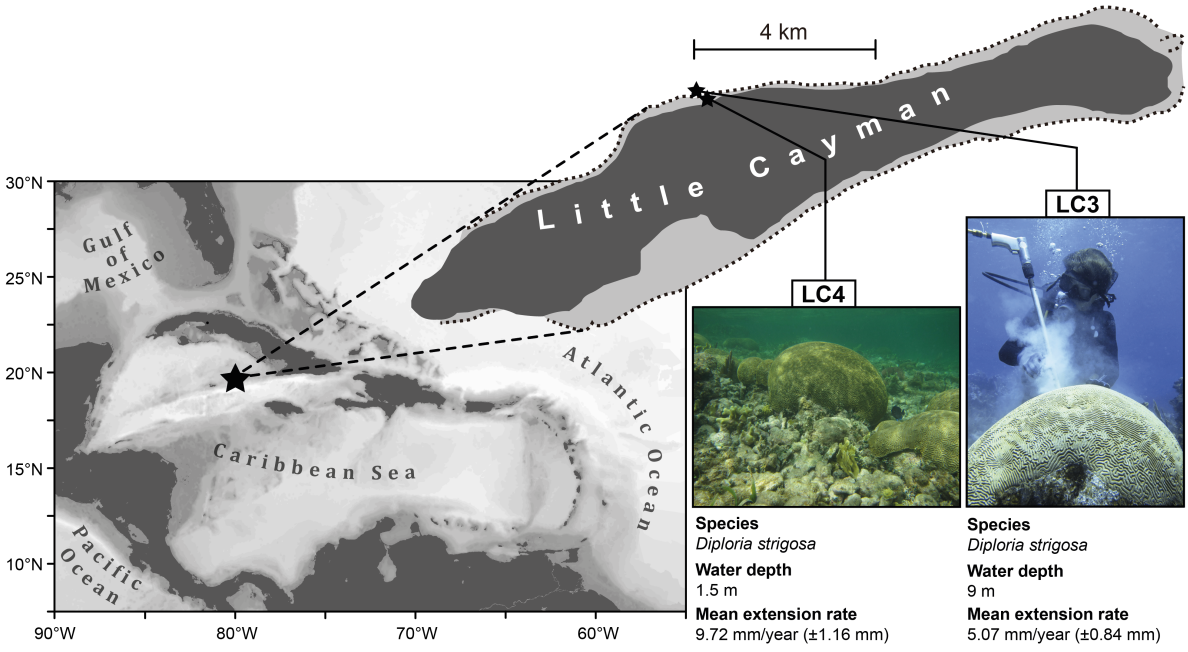

Figure 2-1. Location of coral cores LC3 and LC4 (small stars) at Little Cayman, Cayman Islands (large star), Caribbean Sea. Coral cores are located 500 m apart. Images of the two colonies together with water depth and mean extension rates of the colonies over their common 42-year period. Stippled contour in Island map represents reef crest.

the shelf averages 500 m, but extends to 1700 m off the east end of Little Cayman. Freshwater is scarce and the island lacks rivers and streams. Land based discharge of erosional products into lagoonal waters seems to be insignificant. Little Cayman has an average tidal amplitude of 26 cm while the range between highest and lowest tidal elevation is 1 m, representing a micro tidal environment typical for the Caribbean region (Kjerfve, 1981). The tidal cycle generally shows a semidiurnal pattern allthough the diurnal component is often dominant. More than 50 % of the nearshore waters are designated as marine park or no-take zone, ensuring minimal direct anthropogenic stress.

2.2.2. Coral sampling

In July 2012 coral cores LC3 and LC4 were extracted from two separate hemispherical colonies of *Diploria strigosa* on the north central coast of Little Cayman. Colonies are located 500 m from each other. LC3 had a diameter of 0.8 m and grows in a water depth of 9 m in the fore reef (Figure 2-1) 200 m off the fringing reef. LC4 had a diameter of 1 m and grows in a water depth of 1.5 m in the backreef inside the lagoon. At this site the lagoon is shallow and only 140 m wide. Here tidal currents are believed to be relatively strong despite the micro tidal environment owing to the lagoons shallow cross section and the proximity to a tidal inlet 300 m to the east of the corals location. Both cores were drilled approximately parallel to the central growth axis of the colony. The pneumatic drill was equipped with a 3.6 cm diameter core drill. Cores LC3 and LC4 have a length of 69 cm and 61.5 cm, respectively. The coral slabs were x-rayed in order to expose annual density band couplets, which are slightly inclined. A chronology was generated by counting the well developed annual density bands. Core LC3 extends continuously from 1871 to 2012, core LC4 from 1970 to 2012. For this study only the chronologically overlapping parts of both cores were considered. The skeletal growth rate measured from the annual density bands averages 5.07 mm a^{-1} (± 0.84 mm) and 9.72 mm a^{-1} (± 1.16 mm) for LC3 and LC4, respectively.

2.2.3. Coral Sr/Ca

Powdered samples were collected for trace element analysis using a low-speed micro drill with a diamond-coated 0.5 mm diameter drill bit. The samples where drilled every 0.5 mm along the corallite walls (parallel to the growth axis), yielding on average 10 samples per year for LC3 and 19 samples per year for LC4. Since the longitudinal axis of either core was slightly inclined to the growth axis of the coral, it was necessary to track jump downcore to

stay in the growth axis. The molar Sr/Ca ratios were determined by inductively coupled plasma optical emission spectrometry (ICP-OES, Spectro Ciros SOP) at the University of Kiel. Element emission signals were simultaneously collected and subsequently drift corrected by sample-standard bracketing every five samples following a combination of technics described by Schrag (1999) and de Villiers et al. (2002). Analytical precision on Sr/Ca determinations was 0.15 % RSD or 0.01 mmol mol^{-1} (1σ). The average Sr/Ca value of the JCp-1 standard (Inoue et al., 2004) from multiple measurements on the same day and on consecutive days was 8.855 mmol mol^{-1} with a RSD of 0.09 %.

2.2.4. Coral chronology

The coral chronologies were developed based on the pronounced seasonal cycle in the Sr/Ca record. The highest (lowest) measured Sr/Ca value was assigned to February (September) of any given year, which on average is the coldest (warmest) month according to HadISST. The Sr/Ca time series were linearly interpolated between these anchor points using the Analyseries software (Paillard et al., 1996) to obtain monthly proxy time series. The uncertainty of the age model is approximately 1-2 months in any given year due to interannual differences in the exact timing of maximum (minimum) SST.

2.2.5. In situ and gridded temperature data

In situ water temperature data for Little Cayman Island are available from the Coral Reef Early Warning System (CREWS) station located within the fore reef zone of the Bloody Bay Marine Park < 300 m off the reef crest and < 400 m apart from coral colony LC3. The station is part of the Integrated Coral Observing Network (ICON) of the National Oceanic and Atmospheric Administration (NOAA) and is equipped with a variety of meteorological and oceanographic instruments. Hourly water temperatures were recorded by an NXIC-CTD (Conductivity, Temperature, Depth) from Falmouth Scientific at a depth of approximately 5 m. The employed data set comprises 3 years of measurements. The record starts in August 2009 when the station was newly brought into service and ends in October 2012 due to storm damage 3 months after retrieval of the coral cores. For this study the water temperature data were averaged to produce a monthly time series. Mean annual SST for the time interval is 28.21 °C with an average seasonal variation of 3.91 °C. Monthly SST data for the calibration of the Sr/Ca record were extracted from the HadISST data set for the 1° × 1° grid box at 19–20° N and 79–80° E including the coral sites (Rayner et al., 2003). A

comparison of the CREWS and HadISST data for the 2009-2012 period reveals similar mean annual SSTs but different average seasonal variations with the gridded SST product underestimating the in situ data by almost 0.8 °C (Table 2-1). Accordingly these data were adjusted using an ordinary least squares (OLS) regression relationship between the HadISST and the CREWS data to create an augmented SST data set (referred to as such hereafter) following previous examples (e.g., Smith et al., 2006; Maupin et al., 2008). The discrepancy in the average seasonal variation between the (augmented) gridded and the in situ data could thus be reduced to 0.2 °C. A regression of monthly augmented and in situ SST yields a high correlation coefficient of 0.98.

Table 2-1. Basic statistics of the (calibrated) Sr/Ca and temperature data sets for the seasonal cycle and full records for the 1969-2011 and the 2009-2012 time period[a].

		Seasonal Cycle											
Data Set	Period	Summer	Winter	Δ_S	Δ_W	Average	Range	Δ_{Range}	Max	Min	Range	Δ_{Range}	σ_{AMV}
Sr/Ca													
LC4	1969-2011	9.182	9.024			9.111	0.158		9.330	8.899	0.431		0.05
LC3	1969-2011	8.941	8.867			8.901	0.074		9.029	8.814	0.215		0.02
SST													
CREWS	2009-2012	30.26	26.35	-	-	28.21	3.91	-	30.50	25.79	4.71	-	0.01
HadISST	2009-2012	29.74	26.61	0.25	-0.30	28.26	3.13	0.78	30.16	26.37	3.79	-0.92	0.03
$HadISST_{aug}$	2009-2012	29.97	26.25	-0.10	-0.10	28.22	3.71	0.20	30.46	25.97	4.50	-0.21	0.04
$HadISST_{aug}$	1969-2011	29.74	26.25	-	-	28.08	3.49	-	30.52	25.73	4.79	-	0.19
LC4	1969-2011	30.35	26.40	0.61	0.15	28.17	3.95	0.46	33.48	22.71	10.78	5.98	1.13
LC3	1969-2011	29.28	25.36	-0.46	-0.89	27.49	3.92	0.43	32.05	20.74	11.32	6.52	1.12

[a]Sr/Ca in mmol/mol; SST in °C; Δ is difference to CREWS (HadISST*); σ_{AMV} is standard deviation of annual mean values

Since no systematic tidal measurements from tide gauges were available for Little Cayman, tidal data were generated using the Mr. Tides software (Hahn Software, Seattle, WA, USA). The program predicts tides based only on harmonics data for a particular location and the used algorithm does not take into account anything other than the Sun and the Moon.

2.3. Results and Discussion

2.3.1. Calibration of coral Sr/Ca records with temperature

Both LC3 and LC4 show clear seasonal cycles in the monthly time series (Figure 2-2). The two records strongly correlate over the entire length on the monthly scale ($r = 0.75$, $p < 0.0001$). However, the correlation is much reduced ($r = 0.24$, $p < 0.05$) on the mean annual scale. To evaluate the applicability of Sr/Ca ratios as a proxy for regional temperature

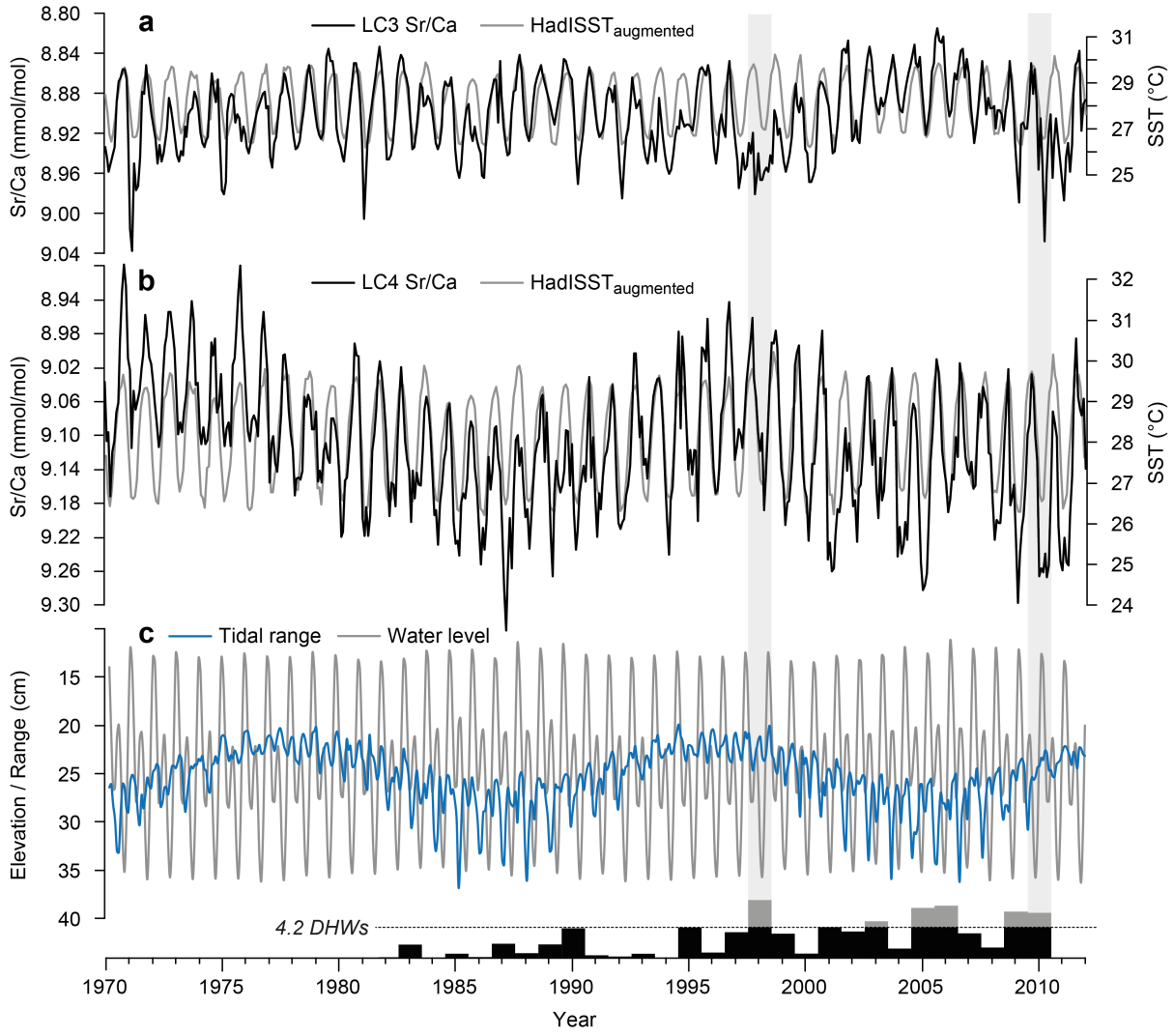

Figure 2-2. Monthly mean Sr/Ca time series of coral cores (a) LC3 and (b) LC4 together with monthly mean SST time series from the HadISST reanalysis data set. SST has been scaled according to each cores regression equation. (c) Tidal range and water level for Little Cayman. Note that for better comparison with Sr/Ca and SST variability tidal ranges are shown with inverse scale. Black bars represent Maximum Degree Heating Weeks (DHW) per year for the period 1982-2010 calculated from OISST v2 data at Little Cayman (van Hooidonk et al., 2012). The horizontal line is the optimal bleaching threshold of 4.2 DHWs. DHWs above this threshold are grey, indicating that bleaching is predicted. Light grey bars mark the El Niño years 1998 and 2010.

variability, both records were calibrated against the augmented SST data set. A comparison of the resulting transfer functions for monthly, annual mean, and extreme values is given in Table 2-2.

Regressions of monthly Sr/Ca with gridded SST yield significant relationships for both records ($r = -0.67$ and -0.70, LC3 and LC4 respectively; $p < 0.0001$). The resulting regression slopes show significant differences between coral records with -0.04 mmol mol^{-1} $°C^{-1}$ for LC4 and -0.019 for LC3. A regression using only the warmest and coldest months in SST (September and February) and the corresponding minimum and maximum Sr/Ca values further enhances the relationship and also confirms the regression slopes obtained using

Table 2-2. Linear regression equations between coral Sr/Ca ratios and augmented HadISST data set[a].

Coral Core	Data Set	Period	Resolution	Regression Equation	r	r^2	p	σ[b]
LC3	$HadISST_{aug}$	1969-2011	monthly	Sr/Ca = -0.019(0.001) x SST + 9.423(0.028)	-0.67	0.45	<0.0001	0.028
			extreme	Sr/Ca = -0.021(0.002) x SST + 9.497(0.048)	-0.83	0.69	<0.0001	0.026
			annual	Sr/Ca = 0.003(0.019) x SST + 8.823(0.539)	0.03	0.00	0.86	0.022
LC4	$HadISST_{aug}$	1969-2011	monthly	Sr/Ca = -0.04(0.002) x SST + 10.238(0.051)	-0.70	0.49	<0.0001	0.055
			extreme	Sr/Ca = -0.045(0.004) x SST + 10.369(0.099)	-0.81	0.66	<0.0001	0.057
			annual	Sr/Ca = -0.037(0.037) x SST + 10.163(1.03)	0.16	0.03	0.30	0.046

[a]Equations are computed using ordinary least squares (OLS) regression with zero-lag, 95% confidence limits for slope and intercept are given.
[b]The residual standard errors are given as σ.

monthly data (Table 2-2). The correlation of annual mean Sr/Ca values to SST, however, is weaker (Table 2-2) and insignificant for both records. Published relationships between Sr/Ca from different tropical Atlantic coral genera and water temperatures show slopes ranging from -0.023 to -0.084 mmol mol^{-1} $°C^{-1}$ (Cardinal et al., 2001; Swart et al., 2002; Cohen et al., 2004; Goodkin et al., 2005; Smith et al., 2006; Maupin et al., 2008; DeLong et al., 2011). Previously published slopes for modern Caribbean *Diploria strigosa* from Guadeloupe (Hetzinger et al., 2006a) and Bonaire (Giry et al., 2012) range from -0.034 to -0.042 mmol mol^{-1} $°C^{-1}$. The Sr/Ca-SST slope from the lagoon coral LC4 obtained in this study falls within this range while that from the fore reef coral LC3 is notably lower. The applicability of these calibrations, however, needs to be scrutinized, e.g., Smith et al. (2006) explained similar differences in calibrations (for *Montastraea*) with variations in water chemistry not accounted for in the regression analysis. Their explanation is supported by the work of several investigators indicating that Sr/Ca of seawater, especially in the realm where corals grow, cannot be considered constant through time and space (de Villiers et al., 1994; Shen et al., 1996a; de Villiers, 1999; De Deckker, 2004). Furthermore, the strength and pattern of surface water circulation and therefore heat fluxes and associated heat accumulation within a reef system are strongly dependent on the systems morphology and its exposure to the open ocean (Roberts et al., 1975; Farrow & Patterson, 1993; Monismith et al., 2006; McCabe et al., 2010). As a result, the maximum temperatures in shallow lagoon waters, which are separated from the open ocean, can be several degrees higher than in the fore reef environment. In situ temperature logger data from a survey in summer 2014 at Grape Tree Bay, Little Cayman, confirm this assumption, indicating that daily maximum temperatures are much higher in the lagoon than in the fore reef environment at the same water depth exceeding 33 °C during the summer (unpublished data). Water exchange of lagoonal waters with the open ocean is limited at this location through the shallow water

depth on the reef crest (0.5–1 m). Particularly a calibration of the lagoon Sr/Ca record with gridded SST, although augmented with in-situ fore reef data, will therefore lead to an underestimation of the true temperature range in the surrounding waters.

2.3.2. Comparison of coral Sr/Ca between the fore reef and the lagoon record

Due to their location within different sectors of the reef (Figure 2-1) the two *Diploria strigosa* colonies are exposed to different environmental conditions (e.g., tides, seawater temperature, water depth, insolation) causing apparent differences between both records. Different seasonal amplitudes in coral Sr/Ca, for instance, point to local temperature variability in distinct reef sectors, which is not captured by reanalysis SST data. Other differences include disparities in linear growth, mean Sr/Ca values (LC3 = 8.901 and LC4 = 9.111 mmol mol^{-1}) and deviating variability of Sr/Ca on decadal scales (Table 2-1 and Figure 2-2).

2.3.3. Differences in mean values

The incorporation of Sr into the coral skeleton is partially related to the annual growth rate (Emiliani et al., 1978; de Villiers et al., 1995; Felis et al., 2003; Goodkin et al., 2007). Considering the mean value of each entire coral record (overall mean) considerable differences exist between both coral cores regarding Sr/Ca and growth, with higher values for LC4 for both parameters (Table 2-1 and Figure 1-1). This points to a direct relation between growth rates and Sr/Ca, in which the nearly two times faster growing coral LC4 is more enriched in Sr than the slower growing coral LC3. This observation is in good agreement with results of other studies (Oomori et al., 1982; Cross & Cross, 1983; de Villiers et al., 1995; DeLong et al., 2011). In the present context, water depth seems an important factor of influence since light intensity is reduced with increasing water depth causing corals to grow more slowly (Huston, 1985). Weber (1973) named this relationship the "depth effect", although he observed a direct relation between Sr/Ca and depth contrary to the result of the present study. His observation may be explained by pronounced influence of temperature on the overall mean coral Sr/Ca, assuming colder temperatures in the fore reef and warmer mean temperatures in the lagoon. However, in the present case growth may be the more important parameter causing the differences between overall mean Sr/Ca values of LC3 and LC4. Differences in growth may also have been affected by the coral microbiology. For example, studies on coral response to increased temperature extremes could show that

some corals can shuffle or substitute symbiont types and that this may be a mechanism of thermal acclimatization/adaptation to a changing environment (Berkelmans & van Oppen, 2006; Edmunds & Gates, 2008; Weis, 2010) (see further discussion on this topic in section 3.1.4). Distinct lineages of *Symbiodinium* differ in the contribution of photosynthetic products to the coral host (Loram et al., 2007) and calcification is considered to be a "photosynthesis-driven" process (Colombo-Pallotta et al., 2010). These considerations also lead to the question of how growth rate related kinetic effects (Cohen & McConnaughey, 2003) as well as vital effects (Urey et al., 1951) affect the quality of the Sr/Ca records as monitors of local- to regional-scale, temperature variability. Several authors recommend some level of replication of geochemical proxies at each site to enhance the reliability of the coral paleoclimate record (Lough, 2004; DeLong et al., 2007; Pfeiffer et al., 2009). For example, Cahyarini et al. (2009) averaged Sr/Ca records from three different coral cores taken from the lagoon of Tahiti (French Polynesia) resulting in a better correlation with grid-SST and a lower residual SST compared to any of the single-core Sr/Ca records. In the present study only one coral record from each part of the reef was available due to limited sampling permits, making replication with several cores impossible. However, DeLong et al. (2007) and Pfeiffer et al. (2009) also found that multiple single-core Sr/Ca records from the same reef location are highly reproducible. Their results indicate that coral Sr/Ca variations from multiple cores from the same location are recording the same Sr/Ca signal.

Another factor that could potentially influence the overall mean Sr/Ca values is the width of the thecal wall and the exact position of the sampling line. In order to identify complications associated with the complex skeletal architecture of *Diploria strigosa*, Giry et al. (2010) performed micro-sampling experiments along and across individual skeletal elements. The study showed that the thecal wall is systematically depleted in Sr while samples derived from the center of the theca exhibited enriched Sr/Ca values. This observation may be relevant for interpreting the present results even though the corals were sampled along the center of the thecal wall. The slower growing coral LC3 displayed a generally thicker structure of its skeletal elements, with specifically the thecal wall being much wider than in the faster growing coral. Consequently the sampled portion of depleted material from the center of the theca was relatively larger, possibly leading to the reduced mean Sr/Ca values when compared to the faster growing coral LC4.

A comparison of annual Sr/Ca and annual growth variability reveals a moderate, but still apparent, direct relationship between both parameters for LC3 ($r = 0.4$, $p = 0.02$), whereas it

is weak and insignificant for LC4 ($r = 0.23$, $p = 0.14$). Similar results are provided by studies from *Diploria strigosa* from Guadeloupe and Bonaire which found positive but weak relationships between annual mean Sr/Ca and annual mean growth rate (Hetzinger et al., 2006a; Giry et al., 2010; Hetzinger et al., 2010a; Giry et al., 2012). This is also in good agreement with results from Cohen and Gaetani (2010) who, under controlled experimental conditions, could show that coral Sr/Ca ratios increased with increasing crystal growth rate and decreased with increasing seawater temperature. Furthermore, Hayashi et al. (2013) and Hirabayashi et al. (2013) found that the skeletal Sr/Ca ratio from cultivated and non-cultivated *Porites* is stable in relation to temporal intracolony variation in the skeletal growth rate. Accordingly, a reasonable explanation for the direct relation between annual mean Sr/Ca and annual mean growth rate observed in the present study is that in a given year the coral grew faster when the years mean SST was lower (and *vice versa*) as it is the case with other genera from different locations in the western Atlantic (Dodge & Vaisnys, 1975; Carricart-Ganivet, 2004; Crueger et al., 2006; Saenger et al., 2009). For LC3 this assumption is supported to some extent by a weak inverse correlation ($r = -0.3$) between linear growth and HadISST, significant at the 90 % level. The correlation for LC4 is also negative but very weak and insignificant ($r = -0.16$, $p = 0.28$).

2.3.4. Seasonal scale differences

The slower growing coral LC3 has a seasonal Sr/Ca cycle with only half the amplitude of the faster growing coral LC4 (Figure 2-2, Table 2-1). Due to the shallower water in lagoon environments, short-scale temperature variability from diurnal solar forcing and cooling is amplified (McCabe et al., 2010; Zhang et al., 2013) while in the deeper fore reef temperature amplitudes are dampened and mean values are lower. Hence, the observed differences between the coral Sr/Ca records are reasonable. However, there are most likely additional reasons, which would also explain the unusually reduced slope of the Sr/Ca-SST relationship of colony LC3. Referring to a similar case (Cardinal et al., 2001), DeLong et al. (2011) suggested a significant influence of the sampling strategy on measured amplitude differences between records derived from corals with different growth rates. Cohen et al. (2004) could show that micro-sampling two colonies of *Diploria labyrinthiformis* with the same interval would lead to a damped amplitude of the seasonal Sr/Ca cycle in the slower growing colony as a result of more time averaging. Consequently each Sr/Ca record would also be biased to the season of higher growth with a possibly larger effect for the slower growing coral.

2.3.5. Decadal variability

On longer time scales, however, a pronounced decadal variation of Sr/Ca values is apparent in core LC4 that is not seen in LC3 or the augmented SST data set (Figure 2-2). The disparity between the records indicates that LC4, the lagoon record, is responding to a forcing not present or negligible in the fore reef of LC3 at greater depth. Inside the lagoon the corals physical environment is subject to the tides, which change the water level and flush water into and out of the lagoon. Cohen and Sohn (2004) proposed that variations in tidal water level within shallow lagoonal settings might indirectly influence Sr/Ca by modulation of photosynthetically-active radiation (PAR), which in turn drives large changes in zooxanthellate photosynthesis. This means that skeletons accreted during phases of low water level and high photosynthesis have lower Sr/Ca ratios (Cohen & McConnaughey, 2003). However, the tidally varying depth of the lagoon and the volume of relatively cooler ambient water masses from the ocean entering the lagoon can significantly influence the mean lagoon temperature through tidal mixing (Smith & Kierspe, 1981; McCabe et al., 2010; Zhang et al., 2013), which has an additional effect on coral Sr/Ca values. To evaluate a potential tidal effect on Sr/Ca two aspects of tidal variability were considered: water level and tidal range (Figure 2-2). The mean water level provides information about water depth while the mean tidal range is an indicator for the water volume exchange between the lagoon and open waters, although it is not a direct relation since water volume is also dependent on the cross-section/topography of the lagoons basin. Mean water level and mean tidal range have an inverse relationship, i.e., high (low) water levels correspond to low (high) tidal ranges. Coral Sr/Ca and tidal data were filtered and normalized (Figure 2-3a) to allow a direct comparison of signal variability in the low frequency band. The time series show a clear covariance over the largest part of the record, with the LC4 record directly (inversely) mimicking the oscillating tidal signals. However, before 1977 Sr/Ca show persistently low mean values with the result that tidal and Sr/Ca signals are not covarying like in the subsequent part of the record (Figure 2-2). This oldest portion of the core is from near the basement of the coral, which corresponds to the corals post-settlement juvenile period. Ourbak et al. (2008) found significant differences in the magnitude of the Sr/Ca signature between the modern part and the basement of a New Caledonian *Porites* sp. coral that could unlikely be caused by environmental factors alone. Similar differences were observed between small juvenile *Porites* sp. and their larger, more mature counterparts in New Caledonia (Ourbak et al., 2006) and the Great Barrier Reef (Marshall & McCulloch,

2002). Both studies conclude that the differences seem to be caused by ontogenic effects and that temperature does not have the same effect on Sr incorporation at the early stage of the corals life compared to today. Therefore, in the case of LC4 the divergence between Sr/Ca and the tidal signal, restricted only to the oldest portion of the core, possibly is a result of ontogenic effects altering the geochemistry. In the low pass filtered data this leads to Sr/Ca being slightly out of phase with water level and out of a half phase shift with tidal range, respectively (Figure 2-3).

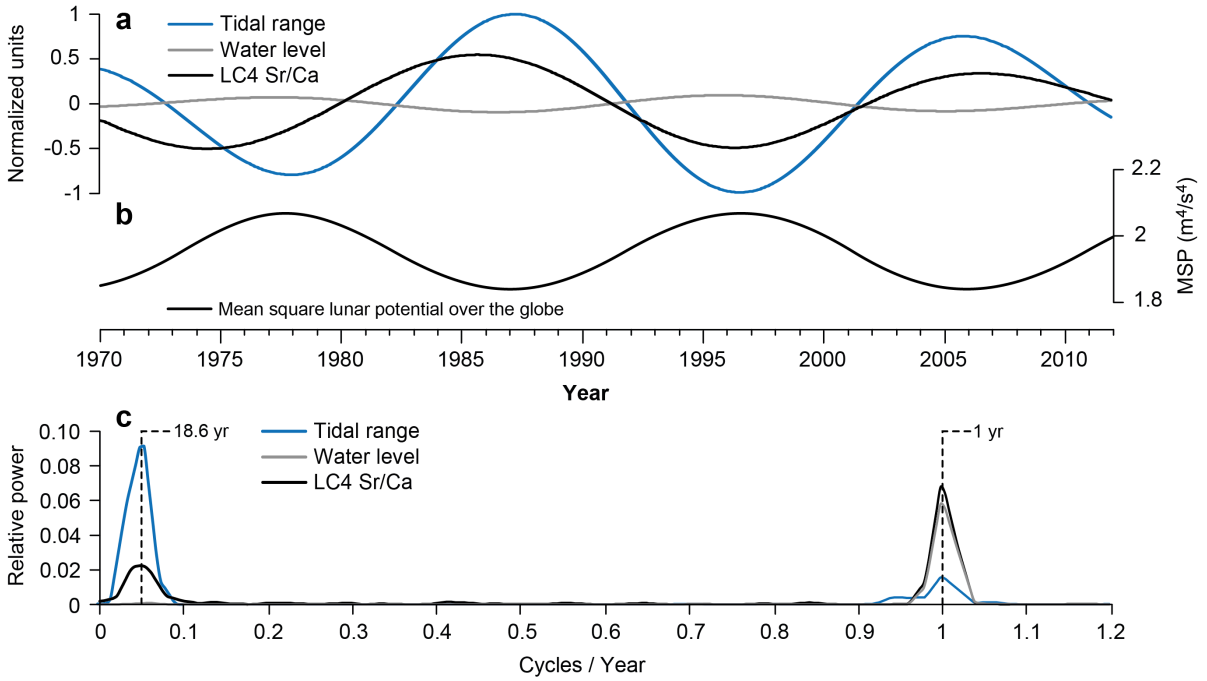

Figure 2-3. (a) Filtered and normalized (zero mean, unit variance) data records of tidal range, water level and LC4 Sr/Ca. A Low-pass filter (band-pass Gaussian filter with a center frequency of 0.05 and a bandwidth of 0.02) was applied. (b) Mean square potential (virtually the tidal force exerted by the moon) over the globe averaged over each year for semidiurnal tides (after Ray (2007)) with the 18.6-year modulation being the main feature. (c) Power-Spectral-Density of normalized monthly data. Spectral estimates formed using the simple periodogram method. Dashed lines indicating 1-year seasonal cycle and 18.6-year lunar nodal cycle.

The observed direct relation between coral Sr/Ca and tidal range potentially shows the modulation of temperature inside the lagoon through a varying volume of entering ambient water masses. Modulation by PAR on the other hand does not seem to play a significant role because the relation of Sr/Ca and water level is negative. Cohen and Sohn (2004) found Sr/Ca to correlate with both water temperature and water level at subannual periods > 50 days. This was not observed in the present study over the much longer periods.

To express the combined lunar plus solar potentials/tidal forces integrated over the earths surface Ray (2007) calculated the mean square potential (MSP) which is shown in Figure 2-3b, it has a period of 18.6 years. From the figure it can clearly be seen that the tidal force is

virtually in phase with the water level and out of phase with the tidal range. Thus, the 18.6-year period nodal tidal cycle is a potential cause of the decadal Sr/Ca variability since it considerably modulates the amplitude of the tide on this time scale (Doodson, 1928; Loder & Garrett, 1978). This assumption is corroborated by the analysis of the Power-Spectral-Density (PSD) of the water level, tidal range and LC4 Sr/Ca data (Figure 2-3c), which reveals two major frequency domains: around 1 and around 0.05 cycle(s) per year representing the seasonal cycle and a variation with a period of about 20 years, respectively.

2.3.6. Coral susceptibility to positive thermal anomalies

Coral reefs in Little Cayman have shown different levels of coral bleaching during phases of sustained high temperatures. Bleaching has been reported since 1987 with subsequent observations in 1995, 1998, 2003, 2005 and 2009 (Ghiold & Smith, 1990; Coelho & Manfrino, 2007; Eakin et al., 2010; van Hooidonk et al., 2012). In 2002, 2004 and 2007 low levels of bleaching were reported when less than 5 % of colonies under observation where affected. In order to improve the forecast of imminent bleaching van Hooidonk and Huber (2009) and van Hooidonk et al. (2012) refined the Degree Heating Weeks (DHW) method (Goreau & Hayes, 1994; Gleeson & Strong, 1995), an accumulative stress index based on the sum of the positive anomalies above the maximum summertime temperature of the previous 12 weeks, by establishing a local threshold above which bleaching was expected to occur at Little Cayman. By combining the reanalysis of the existing reports with own observations from the bleaching year 2009 and OISST V2 temperature data for the period 1982-2010 van Hooidonk et al. (2012) has established a site specific optimal bleaching threshold of 4.2 DHW's with SST's above 29.5 °C. From observations of site-specific recovery in March 2010 they also found the corals with a prevalence (number of affected colonies divided by total number of colonies) of bleaching or paling of more than 25 % to be *Siderastrea siderea*, *Montastraea annularis*, *Montastraea faveolata*, *Diplora strigosa* and *Agaricia* spp.. The bleaching extent was quantified at different spur and groove reef sites at a depth between approximately 10 and 18 m in the fore reef zone. While van Hooidonk et al. (2012) distinguished between coral species, the present study assesses different responses and their geochemical imprints within one coral species as a function of the colonies environment. On the assumption of a local optimal bleaching threshold of 4.2 DHW the considered colonies/corals may show signs of stress either in Sr/Ca or calcification or both in years when the threshold was passed.

Within the reconstructed DHW period 1982–2010 the years in which bleaching is predicted are confined to a period limited by the years 1998 and 2010, both coincident with recorded El Niño events in the tropical Pacific. There is no direct evidence that either of the two sampled corals bleached during these years. However, these two thermal events (high SST) are characterized in LC3 by considerably reduced seasonal amplitudes and increased Sr/Ca ratios during the warm summer season when lower Sr/Ca values are expected. At very high temperatures the corals Ca-transport enzymes may become less efficient, thereby lowering the active Ca^{2+} transport and decreasing calcification (Sinclair, 1999). The observed elevated Sr/Ca ratios could be a result of passively transported Sr^{2+}, which would not be affected in the same way as Ca^{2+} (Ip & Lim, 1991; Sinclair, 1999; Fallon et al., 2003). Interestingly, above threshold DHW's in 2001, 2003, 2005 and 2006 do not seem to inhibit the Sr/Ca "recorder". The coral presumably could tolerate the persisting high temperatures in the respective 4 years between the two El Niño events. This does not contradict the corals behavior during the El Niño years. Although *Diploria strigosa* was found to be one of the more susceptible corals, its observed prevalence of bleaching was about 37 % (van Hooidonk et al., 2012), implying that not all colonies of this species are affected equally. Additionally, in the years 2001 and 2006 none of the coral colonies observed where reported bleached, only some were reported pale or patchy (van Hooidonk et al., 2012). Different from the fore reef record, the lagoon Sr/Ca record (LC4) does not show the pronounced response to the thermal events in 1998 and 2010. These discrepancies between the records together with generally higher thermal maxima inside the lagoon suggest that LC4 may be equipped with an improved tolerance for thermal extremes relative to LC3. Oliver and Palumbi (2011) summarized three mechanisms corals and their endosymbionts may deploy to raise thermal tolerance: *coral adaption* and *Symbiodinium adaption* through the natural selection for heat-tolerant lineages of either partner and physiological *acclimatization* to differences in the thermal climate by living individuals of either or both partners (Gates & Edmunds, 1999; Edmunds & Gates, 2008; Weis, 2010). As LC3 and LC4 were both drilled from colonies of the same species, differences between cores may partly be explained by the presence of distinct lineages of *Symbiodinium* incorporated within the coral host. However, there are likely additional factors. The apparent differences in seasonal Sr/Ca amplitudes and overall mean Sr/Ca ratios between both cores point to processes leading to physiological acclimatization of the coral as suggested by results from experimentally applied long-term treatments (Coles & Jokiel, 1978; Middlebrook et al., 2008). These results imply that corals which are exposed

to elevations in mean temperatures for long (56 days) or short (2 days) periods develop elevated thermal stress tolerances. Furthermore, comparisons of corals from habitats with more rapid thermal fluctuations and higher daily thermal maxima with those from thermally moderate fore reefs indicate that temperature fluctuations resulting from daily or tidal changes expose corals to extreme temperatures below a critical amount of time avoiding coral mortality but for a beneficial amount of time stimulating acclimatization or adaption processes (Coles, 1975; Warner et al., 1996; Castillo & Helmuth, 2005) Thus, exposure to an environmentally variable microhabitat adds substantially to coral-algal thermal tolerance (Oliver & Palumbi, 2011). Arguing from these findings and from the observations of the present study it seems plausible to suggest that at Little Cayman *Diploria strigosa* from an environment with more rapid thermal fluctuations and higher maximum temperatures may be less susceptible to exceptionally high temperatures during a thermal event also because it is accustomed to extreme temperatures, while *Diploria strigosa* from the thermally moderate fore reef is not and hence reacts with stress symptoms.

2.4. Conclusions

A comparison between Sr/Ca variability from massive *Diploria strigosa* corals growing in different reef environments and augmented SST data from 1970 to 2012 point to local temperature variability in the respective reef sectors, which cannot be resolved by augmented instrumental SST data. More specifically, our data show that a calibration of the lagoon Sr/Ca record with gridded SST, although augmented with in-situ observations from the fore reef, would lead to an underestimation of the true temperature range in the lagoon. The two corals respond differently to El Niño related thermal events influencing the magnitude of Sr/Ca ratios and seasonal amplitudes: *Diploria strigosa* from the fore reef seems to be more susceptible to such short-term events displaying significantly reduced seasonal amplitudes and increased Sr/Ca ratios in the same year suggesting cooler SSTs than expected. In contrast the lagoon Sr/Ca record does successfully capture the expected seasonal temperature variability during the thermal events in 1998 and 2010 related to El Niño.

The results suggest that *Diploria strigosa* from the deeper fore reef, where seasonal temperature amplitudes are dampened compared to the lagoon, is more susceptible to short-term high temperature events and consequently reacts with stress symptoms (high

mean Sr/Ca and reduced seasonal amplitude). *Diploria strigosa* from the shallow lagoon environment shows a higher level of resilience because it may already be adapted to an environment with rapid thermal fluctuations and higher maximum temperatures.

On longer time scales the lagoon coral shows decadal variations in Sr/Ca, which are absent in the fore reef coral. A comparison of the coral Sr/Ca record and tidal data indicates that modulation of temperature inside the lagoon through a varying volume of entering ambient water masses is presumably the underlying mechanism. The 18.6-year period lunar nodal cycle may be the forcing factor.

Further studies concerning coral physiology and bleaching thresholds could benefit from a systematic investigation of potential controls of these shallow lagoon sites where environmental conditions appear to promote coral resilience during thermal events. This could also help to improve monitoring systems such as NOAA's Coral Reef Watch, which provides coral reef managers and other stakeholders with tools to understand, monitor and better manage the complex interactions leading to coral bleaching.

2.5. Acknowledgments

The authors would like to thank Karen Bremer for the lab assistance and Lowell Forbes for diving assistance as well as two anonymous reviewers for their thorough review, which helped to improve this manuscript. This work was supported with funding from the DFG (through project HE 6251/2-1). The data plotted in all figures will be available to the public over the Paleoclimatology Branch of NOAA's National Center for Environmental Information (NCEI) (http://www.ncdc.noaa.gov/data-access/paleoclimatology-data) after the completion of the dissertation of J. von Reumont.

3. Tracking interannual to multidecadal-scale climate variability in the Atlantic Warm Pool using central Caribbean coral data

Jonas von Reumont[1], Steffen Hetzinger[1,2], Dieter Garbe-Schönberg[3], Carrie Manfrino[4,5], Christian Dullo[1]

[1]GEOMAR Helmholtz-Zentrum für Ozeanforschung Kiel, Wischhofstr. 1-3, 24148 Kiel, Germany
[2]Institut für Geologie, Universität Hamburg, Bundesstr. 55, 20416 Hamburg, Germany
[3]IfG, Institute of Geosciences, Christian-Albrechts-University, Ludewig-Meyn-Str. 10-14, 24118 Kiel, Germany
[4]Department of Geology and Meteorology, Kean University, 1000 Morris Ave., Union, NJ 07083, USA
[5]Central Caribbean Marine Institute, PO Box 1461, Princeton, NJ 08542, USA

Published in *Paleoceanography and Paleoclimatology*

Atlantic Warm Pool (AWP) climate variability is subject to multiple influences of remote and local forcing. However, shortage of observational data before the mid-20th century and of long-term sea surface temperature (SST) and climate records has hampered the detection and investigation of decadal- and longer-scale variability. We present new seasonally resolved 125-year records of coral $\delta^{18}O$ and Sr/Ca variations in the Central Caribbean Sea (Little Cayman, Cayman Islands; *Diploria strigosa*). Both geochemical proxies show decreasing long-term trends, indicating long-term warming. Sr/Ca indicates much stronger regional warming than large-scale grid-SST data, while $\delta^{18}O$ tracks large-scale SST changes in the AWP. Seawater $\delta^{18}O$ variations are reconstructed, indicating a drying trend over the past century.

High spatial correlation between coral $\delta^{18}O$ and SST in the region of the Loop Current and Gulf Stream system suggests that Little Cayman is a sensitive location for detecting past large-scale temperature variability beyond the central Caribbean region. More specifically, our $\delta^{18}O$ data track changes in North Atlantic Oscillation (NAO) variability on decadal and multidecadal time scales providing insights into the temporal and spatial nonstationarity of the NAO. A combination of our $\delta^{18}O$ record with two coral records from different Caribbean sites reveals high spatial correspondence between coral $\delta^{18}O$ and SST variability in the North Atlantic subtropical gyre, where few instrumental measurements and proxies are available prior to the twentieth century. Our results clearly demonstrate the potential of combining proxy data to provide information from sparsely sampled areas, helping to reduce uncertainty in model-based projections.

Citation: von Reumont, J., Hetzinger, S., Garbe-Schönberg, D., Manfrino, C., & Dullo, C. (2018). Tracking interannual- to multidecadal-scale climate variability in the Atlantic Warm Pool using Central Caribbean coral data. Paleoceanography and Paleoclimatology, 33, 395–411. https://doi.org/10.1002/2018PA003321

3.1. Introduction

Climate variability in the tropical Atlantic region produces numerous impacts on society and the environment of the surrounding continents on seasonal, interannual and multidecadal time scales through fluctuations in ocean and land temperature, rainfall and extreme events (Moura & Shukla, 1981; Enfield & Alfaro, 1999; Giannini et al., 2000; Hurrell et al., 2006). Improving the assessment of the range of future climate fluctuations and their predictability relies on a better understanding of these fluctuations.

Unlike the tropical Pacific, the tropical Atlantic is dominated by the competing influence of modes of climate variability originating from tropical and extratropical oceans (Sutton et al., 2000; Marshall et al., 2001; Czaja et al., 2002; Czaja, 2004; Hurrell et al., 2006). Interannual variability of north tropical Atlantic (NTA) climate is associated with the Pacific El Niño Southern Oscillation (ENSO) and the North Atlantic Oscillation (NAO) (Curtis & Hastenrath, 1995; Giannini et al., 2001a; Giannini et al., 2001b; Czaja et al., 2002; Ruiz-Barradas et al., 2003; Hurrell et al., 2006), both having significant teleconnections to the NTA. ENSO and NAO modulate the strength of the trade winds that affects SST through latent heat exchange at the ocean surface as well as the distribution and intensity of rainfall over the surrounding landmasses (Enfield & Mayer, 1997; Giannini et al., 2000; Giannini et al., 2001b; Chiang, 2002; Czaja et al., 2002). The relative importance of both modes for SST variability in the NTA appears to be frequency dependent, with ENSO dominating at interannual and the NAO at interdecadal time scales (Czaja et al., 2002). Both modes also influence SST variability in the Caribbean Sea which is linked to sea level pressure (SLP) variations in the North Atlantic region (Hastenrath, 1984) mainly through changes in surface winds which in turn affect the dynamics of the Atlantic Warm Pool (AWP) (Wang et al., 2007, 2008b). The AWP is a large body of warm water that comprises the Gulf of Mexico, the Caribbean Sea, and the western tropical North Atlantic. During its maximum extent in boreal summer, the AWP affects summer climate of the western hemisphere (Wang et al., 2006; Wang et al., 2007) and can induce significant stress to Caribbean coral colonies during phases of sustained high temperatures as reported, e.g., in 1995, 1998, 2003, 2005, and 2009 (Ghiold & Smith, 1990; Coelho & Manfrino, 2007; Eakin et al., 2010; van Hooidonk et al., 2012). As expected, the AWP fluctuates with the ENSO and NAO on interannual to decadal timescales (Enfield et al., 2006), but also on the timescale of the Atlantic Multidecadal Oscillation (AMO) (Wang et al., 2008a). The AMO has been identified as the leading large-scale pattern of oscillatory changes in North Atlantic SST with

a period of about 60-90 years (Schlesinger & Ramankutty, 1994; Kerr, 2000; Enfield et al., 2001) over the last 150 years of instrumental observations. SST variations related to the AMO have been suggested to drive climate and precipitation patterns over regions including North America and the Caribbean (Enfield et al., 2001; Sutton & Hodson, 2005; Hu & Feng, 2008) as well as tropical hurricane activity (Goldenberg et al., 2001; Hetzinger et al., 2008). Ocean circulation in the Caribbean and Gulf of Mexico region of the AWP plays an important role in the heat transport from low to high latitudes. It is the source area of warm water masses leaving the low latitudes. The outflow via the Loop and Florida Current promotes the transequatorial heat transfer to higher latitudes through the Gulf Stream (Schmitz & McCartney, 1993; Hogg & Johns, 1995; Sato & Rossby, 1995; Lund et al., 2006). It is widely accepted that the Gulf Stream system is of fundamental importance to the climatic evolution in high northern latitudes and thus, to the living conditions in NW Europe. However, the lack of long-term SST and climate records has hampered the detection and investigation of variability and relationships between climate properties in the North Atlantic, especially on decadal and longer time scales (Dommenget & Latif, 2000). Observational records are limited to the last 140 years and become sparser and spatiotemporally lacking before 1950 (Smith & Reynolds, 2003). High-resolution climate proxy records from long-lived marine biota such as corals, bivalves and coralline algae can help to complement and significantly extend instrumental records back in space and time (Jones et al., 2001; Wanamaker et al., 2011; Hetzinger et al., 2012; Svendsen et al., 2014; Zinke et al., 2014; Hetzinger et al., 2016; Sagar et al., 2016). Additionally, these proxy records provide necessary input data for the calibration and validation of numerical climate models, which have the objective to enhance the understanding of internal variability in the coupled ocean-atmosphere system (e.g., the Northern Hemisphere ocean circulation, including the Caribbean Current, the Gulf Stream system, and the North Atlantic thermohaline circulation (Latif et al., 2000; Latif, 2001b; Vellinga & Wu, 2004b)). An improved understanding of past variability of the climate system is also important with regard to long-range climate forecasting (Delworth & Mann, 2000), and to assess the anthropogenic impact on climate and ecosystems (Delworth & Mann, 2000; Enfield & Cid-Serrano, 2010; Latif & Keenlyside, 2011; IPCC, 2013).

Due to their long lifetime (up to several centuries) and rapid growth (typically more than 1 cm per year), corals can provide an ideal archive for the reconstruction of seasonal-to-multidecadal variability of environmental variables in the tropical surface oceans. Several

studies have used geochemical proxies ($\delta^{18}O$ and Sr/Ca) as paleothermometers for the reconstruction of SSTs (Smith et al., 1979; Beck et al., 1992a; de Villiers et al., 1994; Alibert & McCulloch, 1997; Gagan et al., 2000; Marshall & McCulloch, 2002; Zinke et al., 2004; Maupin et al., 2008; DeLong et al., 2012). Coral $\delta^{18}O$ is a combined signal of the temperature and the $\delta^{18}O$ of seawater, whereas coral Sr/Ca is primarily influenced by seawater temperature (Smith et al., 1979).

This study presents a 125-year record of coral $\delta^{18}O$ and Sr/Ca variations from a *Diploria strigosa* coral drilled off Little Cayman (Cayman Islands, Central Caribbean Sea). We compare geochemical variations of the coral record with observational data and climate indices as well as other Caribbean coral records over the past 125 years to address questions including the following: (1) do the coral proxies record local and/or regional climate variability (i.e., SST and the hydrological cycle) and trends in long-term climate evolution? (2) Do the coral proxies capture impacts of major climate modes onto the Caribbean? (3) Does the geochemical record show the potential to track climate variability on large spatial scales, for example within the AWP region and the Gulf Stream system? (4) If so, how does the coral proxy record compare to other Caribbean coral records in terms of their references to possibly different regions and do they complement each other?

3.2. Materials and Methods

The most recent 42 years of Sr/Ca variations from this Little Cayman coral record were already examined in an earlier study by von Reumont et al. (2016) who compared this fore reef record to a record from the adjacent lagoon environment. Here, a new $\delta^{18}O$ and extended Sr/Ca record is presented: core LC3 spans 125 years, from 1887 to 2011.

3.2.1. Setting of the Study Area

Little Cayman is the smallest and least developed island of the three Cayman Islands with a human population of less than 200. It is 17 km long and from little more than a kilometer to 3 km wide. With the highest point 13 m above sea level it is a very flat island. The marine environment is characterized by an almost continuously developed fringing reef. Little Cayman is situated in the Central Caribbean Sea, where it is sheltered by Cuba and Hispaniola from substantial wave input from the Atlantic. However, it is in a position to receive the full impact of a moderately strong unidirectional trade wind and wave field. Freshwater is scarce and the island lacks rivers and streams. Land based discharge of

erosional products into lagoonal waters seems to be insignificant. More than 50 % of the nearshore waters are designated as marine park or no-take zone, ensuring minimal direct anthropogenic stress. Little Cayman is bathed in waters of the Caribbean Current, the main surface current in the Caribbean Sea (Wüst, 1964; Gordon, 1967; Hernandez-Guerra & Joyce, 2000). The island's climate is strongly moderated by the sea since no major land masses are present within a radius of 200 km. Overall Caribbean Sea climate, surface current patterns, and hydrography are subject to seasonal fluctuations, which are mainly controlled by the covarying pattern of trade wind convergence (Hastenrath, 1976, 1984), the seasonally northward and southward migration of the Intertropical Convergence Zone, and the underlying cross-equatorial SST gradient (Carton et al., 1996).

3.2.2. Coral sampling

In July 2012 coral core LC3 was extracted from a hemispherical colony of *Diploria strigosa* on the north central coast of Little Cayman (19.7° N, 80.06° W). The colony had a diameter of 0.8 m and grew in a water depth of 9 m in the fore reef 200 m off the fringing reef. The core was drilled vertically approximately parallel to the central growth axis of the colony. The pneumatic drill was equipped with a 3.6 cm diameter core drill. Core LC3 has a length of 69 cm. The core was sectioned longitudinally into 7 mm thick slabs. The coral slabs were x-rayed (Figure S3-1) in order to expose annual density band couplets. A preliminary chronology was generated by counting the annual density bands. Core LC3 extends continuously from 1887 to 2011. The skeletal growth rate measured from the annual density bands averages 5.07 mm a^{-1} (± 0.84 mm). Core LC3 was drilled as part of a field campaign during which the recovery of only one coral record from each part of the reef (lagoon, fore reef etc.) was permitted by the local environmental authority, making replication with several cores impossible.

3.2.3. Coral $\delta^{18}O$ and Sr/Ca

Powdered samples were collected for stable isotope and trace element analysis using a low-speed micro drill with a diamond-coated 0.5 mm diameter drill bit. The samples where drilled every 0.5 mm along the corallite walls (parallel to the growth axis), yielding on average 10 samples per year. Since the longitudinal axis of our core was slightly inclined to the growth axis of the coral, it was necessary to track jump downcore to stay in the growth

axis. The molar Sr/Ca ratios were determined by inductively coupled plasma optical emission spectrometry (ICP-OES, Spectro Ciros SOP) at the University of Kiel. Element emission signals were simultaneously collected and subsequently drift corrected by sample-standard bracketing every five samples following a combination of technics described by Schrag (1999) and de Villiers et al. (2002). Analytical precision on Sr/Ca determinations was 0.15 % RSD or 0.01 mmol mol^{-1} (1σ) (n = 1350). The average Sr/Ca value of the JCp-1 standard (Hathorne et al., 2013) from multiple measurements on the same day and on consecutive days was 8.855 mmol mol^{-1} with a RSD of 0.09 %.

Oxygen isotope measurements were conducted on a Thermo Scientific MAT-253 mass spectrometer equipped with a CARBO Kiel IV device. The isotopic ratios are reported in ‰ relative to the Vienna Pee Dee Belemnite (VPDB) based on calibration directly to NBS-19 standard (National Bureau of Standards). Analytical uncertainty on $\delta^{18}O$ determinations was 0.06 ‰ (1σ) (n = 1350; 2 standards after every 10 samples).

3.2.4. Coral chronology

The coral chronology was developed based on the pronounced seasonal cycle in the Sr/Ca record. The maximum (minimum) Sr/Ca value was tied to February (September) of any given year, which on average is the coldest (warmest) month in the study area. Coral $\delta^{18}O$ and Sr/Ca time series were linearly interpolated between these anchor points using the Analyseries software (Paillard et al., 1996) to obtain age assignments for all other measurements. This approach creates a non-cumulative error of 1–2 months in any given year due to interannual differences in the exact timing of maximum (minimum) SST.

3.2.5. In-situ and gridded temperature data

In-situ water temperature data for Little Cayman Island is available from the Coral Reef Early Warning System (CREWS) station located within the fore reef zone < 400 m apart from coral colony LC3. The station is part of the Integrated Coral Observing Network (ICON) of the National Oceanic and Atmospheric Administration (NOAA). Hourly water temperatures were recorded by an NXIC-CTD (Conductivity, Temperature, Depth) from Falmouth Scientific at a depth of approximately 5 m. The employed dataset comprises 3 years of measurements. The record starts in August 2009 when the station was newly brought into service and ends in October 2012 due to storm damage 3 months after retrieval of the coral core. Monthly SST data for the calibration of the proxy records were extracted

from the HadISST1 data set for the 1° × 1° grid box centered on 19.5° N and 79.5° W, including the coral site (Rayner et al., 2003). These data were adjusted using an ordinary least squares (OLS) regression relationship between the HadISST and the CREWS data to create an augmented SST data set (referred to as such hereafter) (von Reumont et al., 2016). Augmented SST variability agrees very well with the local in-situ SST data set (r = 0.98) over the interval from 2009 to 2012.

3.3. Results and Discussion

3.3.1. $\delta^{18}O$ and Sr/Ca Records

The time series of monthly $\delta^{18}O$ and Sr/Ca variations extend from 1887 to 2011 and show clear seasonal cycles. The seasonality in monthly $\delta^{18}O$ has a mean amplitude of 0.27 ‰ while in monthly Sr/Ca it is 0.09 mmol mol^{-1}. The two time series correlate significantly over the entire length on the monthly ($r = 0.63$; $p < 0.0001$) and on the mean annual scale ($r = 0.62$; $p < 0.0001$).

Regressions of monthly $\delta^{18}O$ and Sr/Ca with augmented SST yield significant relationships for both proxies (r = -0.54 and -0.56, $\delta^{18}O$ and Sr/Ca respectively; $p < 0.0001$) (Table 3-1). Annual mean proxy values also correlate well with gridded SST (r = -0.56 and -0.54, $\delta^{18}O$ and Sr/Ca respectively; $p < 0.0001$). The resulting regression slopes show notable differences depending on temporal resolution. At monthly resolution regression slopes for $\delta^{18}O$ and Sr/Ca are -0.082 (± 0.003) ‰ $°C^{-1}$ and -0.021 (± 0.001) mmol mol^{-1} $°C^{-1}$ respectively, while at annual resolution they are clearly larger with -0.292 (± 0.039) ‰ $°C^{-1}$ and -0.069 (± 0.012) mmol mol^{-1} $°C^{-1}$. Slopes for published equations relating $\delta^{18}O$ and Sr/Ca

Table 3-1. Linear regression equations between coral $\delta^{18}O$ (Sr/Ca ratios) and $HadISST_{aug}$ data seta for the 1887–2011 time period.

Data Set	Resolution	Regression Equation[a]	r	r^2	p	σ[b]
$\delta^{18}O$	monthly	$\delta^{18}O$ = -0.082(0.003) x SST - 1.915(0.093)	-0.54	0.29	<0.0001	0.172
	extreme values	$\delta^{18}O$ = -0.082(0.006) x SST - 1.901(0.17)	-0.65	0.42	<0.0001	0.171
	annual	$\delta^{18}O$ = -0.292(0.039) x SST + 3.973(1.081)	-0.56	0.32	<0.0001	0.117
Sr/Ca	monthly	Sr/Ca = -0.021(0.001) x SST + 9.546(0.023)	-0.56	0.31	<0.0001	0.043
	extreme values	Sr/Ca = -0.027(0.001) x SST + 9.703(0.041)	-0.76	0.58	<0.0001	0.041
	annual	Sr/Ca = -0.069(0.012) x SST + 10.875(0.331)	-0.46	0.22	<0.0001	0.036

[a] Equations are computed using ordinary least squares (OLS) regression with zero-lag, 95% confidence limits for slope and intercept are given. Results from a test between the OLS technique and orthogonal regression did not significantly differ. [b]The residual standard errors are given as σ.

Table 3-2. Basic statistics of the calibrated $\delta^{18}O$ (Sr/Ca) and augmented HadISST data sets for the seasonal cycle and mean annual values[a].

		Seasonal Cycle				*Mean Annual Values*			
Data Set	Period	Summer	Winter	Average	Range	Max	Min	Range	σ
$HadISST_{aug}$	1887-2011	29.59	26.11	27.93	3.48	28.50	27.17	1.33	0.27
$\delta^{18}O$	1887-2011	29.42	26.08	27.80	3.34	29.28	27.01	2.27	0.48
Sr/Ca	1887-2011	30.76	26.39	28.56	4.37	29.16	26.55	2.62	0.58

[a]In °C; σ is standard deviation of annual mean values

from different tropical Atlantic coral genera to SST range from -0.101 to -0.22 ‰ $°C^{-1}$ (Leder et al., 1996; Smith et al., 2006; Maupin et al., 2008) and from -0.023 to -0.084 mmol mol^{-1} $°C^{-1}$ (Swart et al., 2002; Cohen et al., 2004; Goodkin et al., 2005; Smith et al., 2006; Maupin et al., 2008; DeLong et al., 2011; Xu et al., 2015) respectively. Previously published slopes for modern Caribbean *Diploria strigosa* (Hetzinger et al., 2006a; Giry et al., 2012; Xu et al., 2015) range from -0.184 to -0.196 ‰ $°C^{-1}$ for $\delta^{18}O$-SST and from -0.034 to -0.063 mmol mol^{-1} $°C^{-1}$ for Sr/Ca-SST relationships. Compared with the published data our coral $\delta^{18}O$-SST and Sr/Ca-SST slopes of the monthly data are in the lower range while those of the annual data are in the higher range of slope values. Basic statistics of the calibrated proxy records in comparison to gridded SST are given in Table 3-2.

3.3.2. Long-Term Trends

Both geochemical proxy records show a pronounced centennial scale trend of decreasing $\delta^{18}O$ and Sr/Ca values over the time period from 1887 to 2011 (Figure 3-1a, b). The trend in Sr/Ca is equivalent to a warming of 1.60 °C whereas in $\delta^{18}O$ it is 1.06 °C (Table 3-3) if interpreted completely in terms of temperature (using the slope of the regression equations). However, in contrast to Sr/Ca, $\delta^{18}O$ variability is influenced not only by water temperature but also by seawater $\delta^{18}O$ ($\delta^{18}O_{sw}$), which primarily reflects the regional precipitation-evaporation balance (Zinke et al., 2008) and might account for the discrepancy in the magnitude of the temperature trends. Compared to the proxy records the $HadISST_{aug}$ data show a weaker warming of 0.62 °C which is in the lower portion of globally averaged surface temperature data analyzed by the IPCC (2013) that indicate a warming of 0.65 to 1.06 °C over the period 1880 to 2012. Warming calculated from $\delta^{18}O$ matches the upper IPCC warming estimate. Similar results, i.e., stronger proxy-derived warming trends than indicated by gridded SST data, have also been found in other coral-based SST

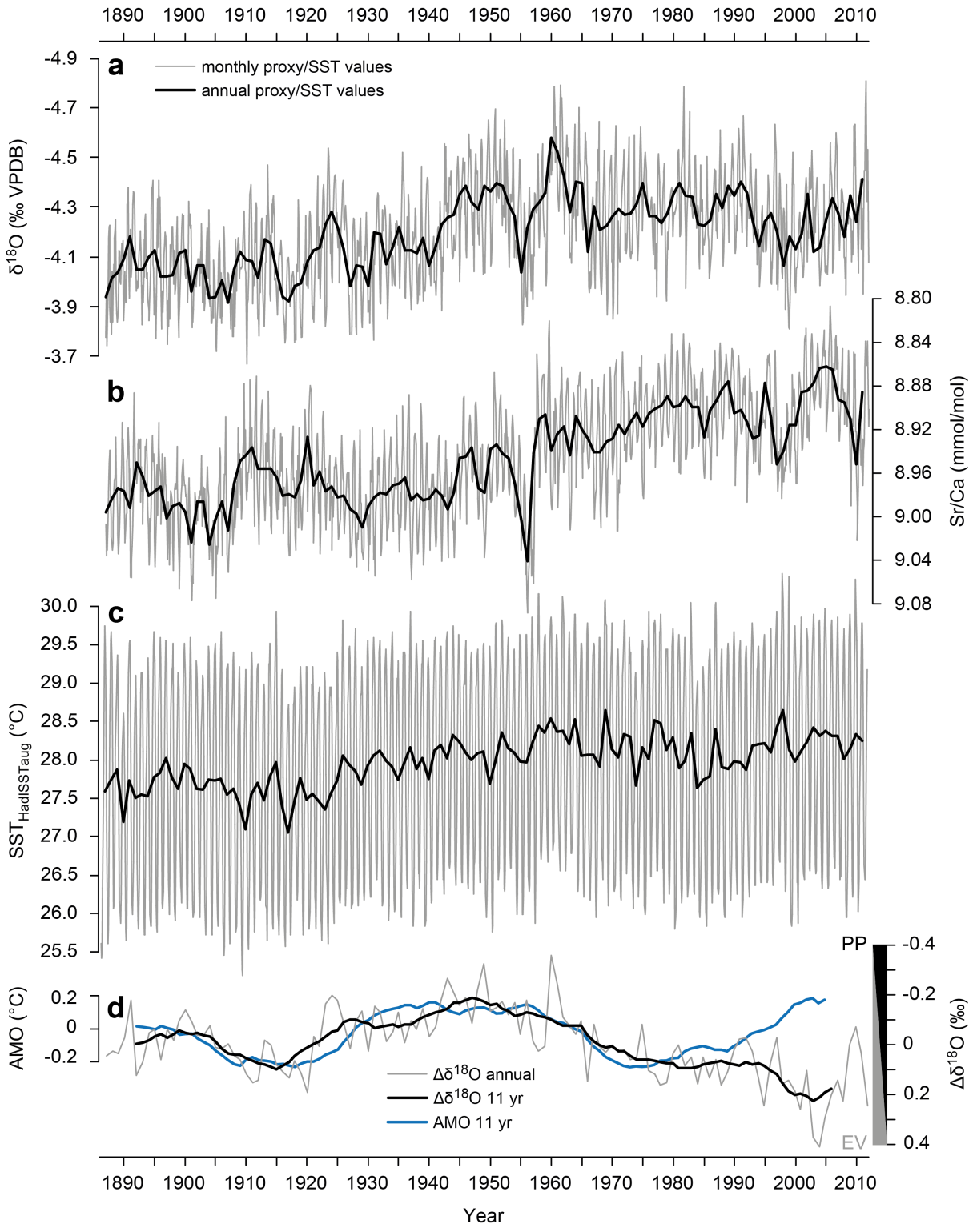

Figure 3-1. Monthly and annual mean time series (1887-2011) of (a) coral $\delta^{18}O$, and (b) coral Sr/Ca from core LC3 and of (c) the augmented HadISST reanalysis data for the grid box centered on 19.5°N and 79.5°W, including the coral site. (d) Comparison between 11-year moving average data of coral $\Delta\delta^{18}O_{sw\text{-}center}$ and AMO. Guadeloupe coral $\Delta\delta^{18}O_{sw\text{-}center}$ generated by removing the Sr/Ca-derived temperature component of the coral $\delta^{18}O$ signal. The resultant $\Delta\delta^{18}O_{sw\text{-}center}$ is an estimate of seawater $\delta^{18}O$. Note divergence of the $\Delta\delta^{18}O_{sw\text{-}center}$ signal from the AMO from the late 1970s resulting from atmospheric circulation alterations and changing precipitation patterns in the tropics. PP: Precipitation; EV: Evaporation.

Table 3-3. Trend analysis of SST and coral proxy time series (Sr/Ca and $\delta^{18}O$) for the time interval 1887–2011 for three different locations. Trends were computed based on proxy temperature relationships determined in the reference studies and linearly extrapolated where necessary for the overall trend. Original length of records: LC3: 1887–2011, Gua1: 1896–1998, TR: 1751–2004.

		Overall Trend (°C)			
Location	Coral Core / Data Set	Sr/Ca-SST	$\delta^{18}O$-SST	Gridded SST	Reference
Cayman Islands	LC3	*1.60*	1.06	0.62[a]	*this study*
Guadeloupe	Gua1	*1.63*	0.62	0.64[b]	*Hetzinger et al., 2010*
Puerto Rico	Turrumote Reef	*1.24*	1.63	0.60[c]	*Kilbourne et al., 2008*
		Warming per Decade (°C)			
Location	Coral Core / Data Set	Sr/Ca-SST	$\delta^{18}O$-SST	Gridded SST	Reference
Cayman Islands	LC3	*0.13*	0.08	0.05[a]	*this study*
Guadeloupe	Gua1	*0.13*	0.04	0.05[b]	*Hetzinger et al., 2010*
Puerto Rico	Turrumote Reef	*0.13*	0.10	0.05[c]	*Kilbourne et al., 2008*

[a]$HadISST_{aug}$ (augmented with CREWS data), [b]ERSST, [c]HadISST

reconstructions from this region. For example, coral proxy data from Puerto Rico (Kilbourne et al., 2008) and Guadeloupe (Hetzinger et al., 2010a) yield temperature trends that are also up to 2 times larger than what the corresponding grid SST data suggest (Table 3-3). Such records have been found not only in corals but also in sclerosponges from Jamaica (Rosenheim et al., 2005) and the Bahamas (Rosenheim et al., 2004). However, there are exceptions to these records from the Florida Keys (Maupin et al., 2008; DeLong et al., 2014) where coral records do not match this larger trend. In context of the larger trend, recently published observations from Little Cayman suggest that grid-SSTs, which are averaged over a large area and often computed from multiple data sources (Smith & Reynolds, 2003), do not sufficiently represent local SST variability within the reef system from which the coral cores and thus the geochemical records have been retrieved (von Reumont et al., 2016). Furthermore, Hetzinger et al. (2010a) showed that temperature trends derived from the coral Sr/Ca data of Guadeloupe *Diploria strigosa* are clearly consistent with those of local air temperature measurements starting in 1951 while grid-SST shows no warming in the same time period. The magnitude of the trend in Little Cayman Sr/Ca derived temperature is consistent with the observed increase in temperature at the other two Caribbean coral sites. This consistency indicates that the annual mean Sr/Ca values from our Little Cayman coral record yield a robust warming signal that is much stronger than suggested by large-scale grid-SST data, but of similar magnitude as other coral-derived proxy reconstructions. These trends in the coral temperature reconstructions together with the aforementioned coral records from the Florida Keys support the findings

of a study of decadal SST trends (1985–2009) that includes the Caribbean Sea and the south-eastern Gulf of Mexico and uses Advanced Very High Resolution Radiometer (AVHRR) (Chollett et al., 2012). According to the AVHRR data the region of the Caribbean records is warming whereas the southeastern Gulf of Mexico including the Florida Keys is not warming as quickly. One possible explanation of the spatial heterogeneity is reduced transport of warm water from the Caribbean into the Gulf of Mexico, at least on centennial time scales (Lund et al., 2006), which may be further linked to reduced AMOC transport as suggested in a high-resolution simulation study by Liu et al. (2012). However, this is not an explanation for the larger proxy-derived warming trends, which need to be further investigated by means of additional high-resolution proxy records and model simulations.

The comparison of the proxy results suggests that Sr/Ca is a better indicator of local changes in temperature, while $\delta^{18}O$ seems to be a better indicator of large-scale/regional scale SST changes. At the seasonal scale this assumption is corroborated by a good agreement of the seasonal cycle range between the gridded SST and $\delta^{18}O$-SST, whereas Sr/Ca-SST shows a clearly larger range (Table 3-2). Furthermore, the monthly Sr/Ca record shows a distinct positive excursion around the years 1955-1956 (Figure 3-1b). This suggests a cooling event, which coincides with the timing of a moderate La Niña event (-1.46) according to the Oceanic Niño Index (ONI, 1950 to present), which measures departures from average SST in the Pacific Nino3.4 region. On the other hand $\delta^{18}O$ and SST show no deviation from general interannual variability at that time. The reasons for this singular Sr/Ca excursion cannot be completely determined here and may be due to several different factors related either to the coral proxy itself or to local variability. However, diagenetic alteration, which has been observed in some modern corals (e.g., *Porites*) (Hendy et al., 2007; Sayani et al., 2011), is not considered to be the cause. The skeletal mesoarchitecture of large-polyped *Diploria strigosa* facilitates microsampling that strictly follows a single skeletal element, the solid and thick theca wall. Different to the sampling in small-polyped corals such as *Porites*, sampling does not integrate over different skeletal elements and vacated skeleton where secondary aragonite infilling may occur. Here, microsampling was constrained to the central part of the theca, where the admixture of secondary cements, if present somewhere in the skeletal structure, is unlikely. Additionally, no indications of secondary aragonite overgrowth were found in X-ray images of the core slabs that could point to diagenetic alteration effects. Although a singular feature, the Sr/Ca excursion potentially is a true local

temperature signal that points to the higher sensitivity of Sr/Ca towards local SST changes compared to the $\delta^{18}O$ signal.

In addition to trends in both proxy records with a focus on SST, we investigate long-term changes in the hydrologic balance by using paired coral $\delta^{18}O$ and Sr/Ca measurements to calculate changes in seawater $\delta^{18}O$ ($\delta^{18}O_{sw}$). Several studies have demonstrated that past $\delta^{18}O_{sw}$ variations can be reconstructed by removing the temperature component of the $\delta^{18}O$ signal by using Sr/Ca derived temperature (McCulloch et al., 1994; Gagan et al., 1998; Ren et al., 2002; Kilbourne et al., 2004; Cahyarini et al., 2014). We calculate relative changes in annual $\delta^{18}O_{sw}$ following the method described in Cahyarini et al. (2008), assuming a coral $\delta^{18}O$-SST relationship of -0.29 ‰ $°C^{-1}$ and a coral Sr/Ca-SST relationship of -0.069 mmol mol^{-1} $°C^{-1}$ based on our calibrations. Variations in $\delta^{18}O_{sw}$ are defined relative to the mean value of $\delta^{18}O_{sw}$ and are given as $\Delta\delta^{18}O_{sw\text{-}center}$ (Cahyarini et al., 2009) (Figure 3-1d). Given the positive long-term trend in proxy derived temperatures total precipitation is expected to increase in conjunction with increasing tropical temperature since, in theory, increased heating leads to greater evaporation and thus higher precipitation (Mitchell et al., 1987). The long-term perspective on the $\Delta\delta^{18}O_{sw\text{-}center}$ data is inconsistent with this assumption. At our study site generally increasing $\Delta\delta^{18}O_{sw\text{-}center}$ suggests an overall reduction in precipitation from 1887 to 2011. However, the $\Delta\delta^{18}O_{sw\text{-}center}$ signal does not evolve in a linear way. From the beginning of the record until the mid-1970s the $\Delta\delta^{18}O_{sw\text{-}center}$ data shows a high inverse correlation with the AMO, ($r = -0.88$; $p < 0.0001$) (van Oldenborgh et al., 2009) (Figure 3-1d), thus being consistent with the above assumption that when temperature increases precipitation increases and vice versa. Starting in the mid-1970s the $\Delta\delta^{18}O_{sw\text{-}center}$ record seems to decouple from the AMO signal and shifts to a steadily increasing regime, i.e. precipitation decreases while temperature increases. Gauge data from the Global Historical Climatology Network data set (National Climatic Data Center summarized by Trenberth et al. (2007)) showed that for the period from 1979 to 2005 precipitation patterns have developed such that the higher latitudes have become wetter and the subtropics and much of the tropics including the central Caribbean region have indeed become drier. Alterations in atmospheric circulation are associated with these patterns (Trenberth et al., 2007), namely increases in the westerly winds at mid-latitudes and a strengthening of the northeasterly trade winds (Kalnay et al., 1996). These alterations should theoretically cause more evaporation and advection of moisture from the region, thereby increasing the $\Delta\delta^{18}O_{sw\text{-}center}$. A combination of higher evaporation and increasing

temperature, as captured by our coral, could have negative long-term consequences on the Cayman Islands and similar low-lying islands with few fresh water resources. Empirical evidence and climate model simulations indicate that warmer climates, owing to increased water vapor, lead to more intense precipitation events, even when the total annual precipitation is reduced (Trenberth et al., 2003; Allan & Soden, 2008). Additionally more atmospheric moisture is available for tropical storms to feed upon (Bender et al., 2010). These factors often occur together, thereby increasing the potential incidence and severity of flooding events (Trenberth, 2011). The warming on the other hand accelerates drying of land surfaces as the evaporation of moisture takes in heat, eventually leading to an increased risk of extended dry or even drought periods (Dai et al., 2004).

Interestingly, while we observe a strong relationship between $\Delta\delta^{18}O_{sw\text{-}center}$ and AMO, this does not hold true for the individual $\delta^{18}O$ and Sr/Ca records. Hetzinger et al. (2008) and Kilbourne et al. (2008) have found a strong relationship between coral $\delta^{18}O$ and AMO in their records from Guadeloupe and Puerto Rico. However, these records come from locations in the southern and eastern Caribbean. Spatial distribution of correlations between annual mean SST and the AMO index over the time period from 1887 to 2011 shows that Guadeloupe and Puerto Rico are situated within a field of significant agreement (Figure S3-2). In contrast, no correlation exists in the northwestern part of the Caribbean, north of the latitude of Jamaica where the Cayman Islands are situated. The high correlation between our coral $\delta^{18}O$ and Sr/Ca records indicates a dominant role of SST in coral $\delta^{18}O$ variability at Little Cayman, and consequently, both proxy records show no significant relationship to AMO. Observational and model data provide evidence for a major role of atmospheric processes in generating the tropical portion of AMO variability (Brown et al., 2016; Yuan et al., 2016). Observational analyses suggest that the focus of North Atlantic SST anomalies is in the midlatitudes during the mature stage of AMO and SST anomalies subsequently propagate into the tropics (Guan & Nigam, 2009; Kavvada et al., 2013; Hodson et al., 2014). In response to a warm middle latitude SST anomaly tropical trade wind speed weakens which in turn reduces evaporation in the tropics (Chiang & Friedman, 2012; Qu et al., 2014). This AMO related atmospheric effect on the hydrological balance might be an explanation for the observed coral $\delta^{18}O_{sw}$ signal with no necessary causal connection to local SST.

Hetzinger et al. (2008) could also show that their estimate of $\delta^{18}O_{sw}$ contribution to the $\delta^{18}O$ signal and precipitation are highly correlated at low frequencies to the AMO, implying that

multidecadal $\delta^{18}O_{sw}$ variations in Guadeloupe are primarily atmosphere-driven. Presumably, this observation applies to a wider region and perhaps also to the Puerto Rico and Little Cayman site.

3.3.3. Regional to Large Scale Variability

Spatial distribution of correlations between annual mean Sr/Ca and SST exhibit strong relations mainly restricted to the local level and not on regional to large scales (Figure S3-3). In contrast, annual mean coral $\delta^{18}O$ reveals strong negative relations to SST in the eastern Sargasso Sea, but especially to SST in the Loop Current region (SST_{LC}; Figure 3-2), where the clockwise surface flow extends northward into the Gulf of Mexico and joins the Yucatan Current and Florida Current. Strong correlations of coral $\delta^{18}O$ are also found to SST in the Gulf Stream region (SST_{GS}) upstream of Cape Hatteras, where the Florida Current ceases to follow the continental shelf. Our observation is consistent with results from Hetzinger et al. (2010a) who found that $\delta^{18}O$ appears to be a better indicator of large scale SST variability in the tropical North Atlantic, while Sr/Ca appears to be a better indicator of local temperature variability. Consequently we focus on $\delta^{18}O$ variability for the investigation of regional to large scale SST variability. The observed relationships between $\delta^{18}O$ and SST_{LC} / SST_{GS} potentially make our study site a sensitive location for the detection of past regional scale variability within the Gulf Stream System. To validate/verify this assumption we determine one comparative grid-SST cell from the field with the strongest correlation for the Loop Current region and the Gulf Stream region, respectively. Figure 3-3 confirms that interannual variations in coral $\delta^{18}O$ agree very well with SST from the two selected regions. Both coral $\delta^{18}O$ and SST show a clear multidecadal variation with a period of about 80 years. However, phase and thus period of the variation differ from AMO variability. A comparison of low-pass-filtered data yields strong negative relationships between $\delta^{18}O$ and both SST time series from 1887 to the mid-1970s (Gulf Stream: $r = -0.98$; Loop Current: $r = -0.96$; $p < 0.0001$). Between the mid-1970s and 1990s the $\delta^{18}O$ signal is characterized by a departure from decreasing SST signals. This coincides with the behavior of $\Delta\delta^{18}O_{sw\text{-}center}$, which contributes to the $\delta^{18}O$ signal. During this time period three strong (> +1.5 °C; 1972–1973, 1986–1987 and 1991–1992) and two very strong (> +2.0 °C; 1982–1983, 1997–1998) El Niño events developed according to the ONI. Together with the 2015–2016 El Niño the 1982–1983 and 1997–1998 events are the strongest on the ONI record, covering the period from 1950 to now. The El Niño Southern-Oscillation (ENSO) originates in the tropical

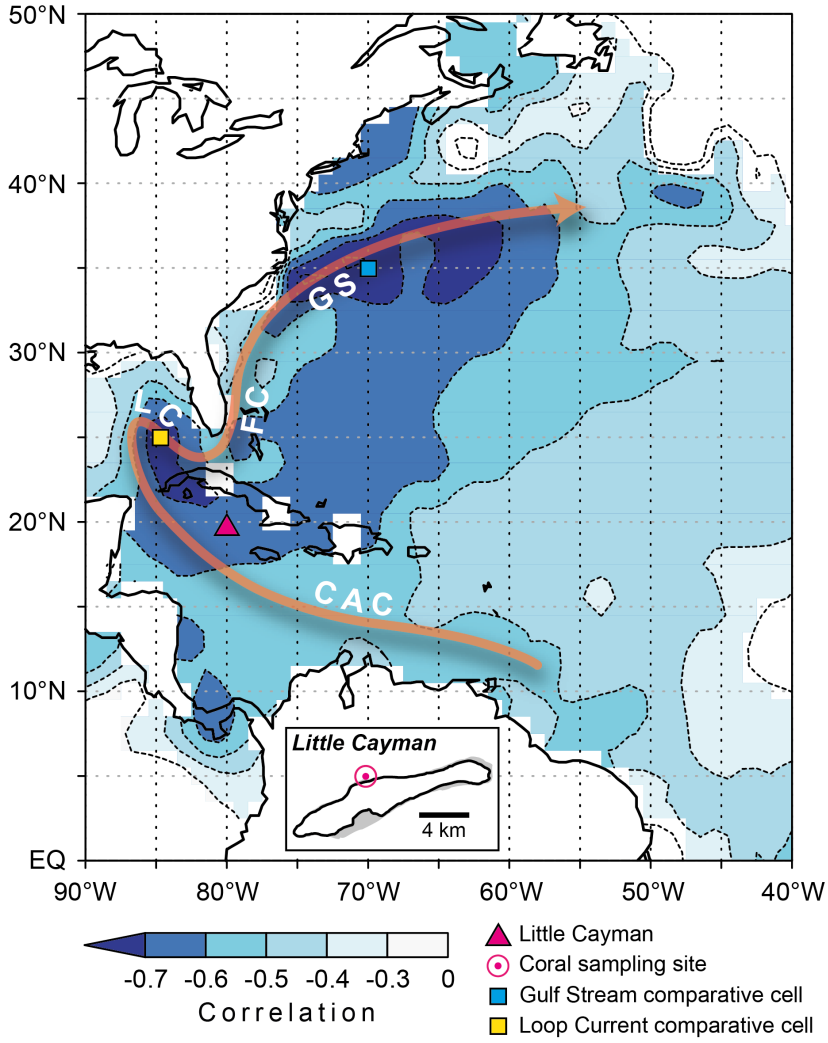

Figure 3-2. Oceanographic setting of the western North Atlantic and Caribbean region showing major surface currents in the Caribbean and flowing out of it. Surface currents are indicated as orange arrow based on the Mariano Global Surface Velocity Analysis (MGSVA) (http://oceancurrents.rsmas.miami.edu): CAC: Caribbean Current; LC: Loop Current; FC: Florida Current; GS: Gulf Stream. Blue colors represent the spatial distribution of correlations between annual mean coral $\delta^{18}O$ and HadISST data (Rayner et al., 2003). Data cover the period 1887–2011 and were detrended. Note that correlation of coral $\delta^{18}O$ and HadISST is high and significant at the 1 % level especially in the Gulf Stream and Loop Current region. Spatial distribution of correlations was computed and plotted at http://climexp.knmi.nl/.

Pacific Ocean but is known to exert a strong influence on climate variability in the northern tropical Atlantic and the Caribbean region (Curtis & Hastenrath, 1995; Enfield & Mayer, 1997; Giannini et al., 2000; Saravanan & Chang, 2000; George & Saunders, 2001; Giannini et al., 2001a; Giannini et al., 2001b; Czaja et al., 2002). A spatial correlation of the ONI record with HadISST data over the time period from 1970 to 2000 (Figure S3-4) yields moderate values ($0.4 \leq r \leq 0.6$, $p < 0.1$) for the northeast Caribbean while for the Gulf Stream and Loop Current region no or only weak correlations can be observed ($0 \leq r \leq 0.2$, $p < 0.1$). Consequently we assume that ENSO can have a measurable impact on local SST and thus coral $\delta^{18}O$ at Little Cayman, which already has been shown for corals from other Caribbean sites (Smith et al., 2006; Maupin et al., 2008), while SST in the comparative regions seems to

be unaffected. The frequency and magnitude of El Niño events likely have contributed to the $\delta^{18}O$ signal remaining at low values at Little Cayman compared to decreasing SSTs in the Gulf Stream and Loop Current region in Figure 3-3. Another prominent mode of external forcing on northern tropical Atlantic climate variability is the North Atlantic Oscillation (NAO) (Czaja et al., 2002). The NAO is associated with basin-wide variations in atmospheric circulation (Hurrell, 1995), which in turn result in changes in the regional distribution of temperature and rainfall over the North Atlantic and surrounding continents (including the Caribbean) (Walker & Bliss, 1932; van Loon & Rogers, 1978; Rogers & Van Loon, 1979). We investigate the relationship between coral $\delta^{18}O$ and the two modes of climate variability, ENSO and NAO, to eventually identify forcing of corresponding variability between $\delta^{18}O$ at Little Cayman and SST in the Gulf Stream and Loop Current region. In order to do this, we perform wavelet coherence (WTC) analyses, which find regions in time frequency space where two time series co-vary (but do not necessarily have high power) (Grinsted et al., 2004). Results from WTC between coral $\delta^{18}O$ and the Nino3.4 index show only one significant ($p \leq 0.05$) field of covariance (Figure S3-5), which appears on interannual time scales with a period between 1 and 2 years around 1900. Elevated but insignificant values of annual to interannual covariation can be observed from 1940 into the 1990s comprising the time period of higher El Niño activity between the mid-1970s and 1990s considered above. While the ENSO systems effect on annual $\delta^{18}O$ is generally insignificant an examination of NAO variability gives a different picture. Strong and persisting covariation between $\delta^{18}O$ and NAO exists on decadal time scales in a band

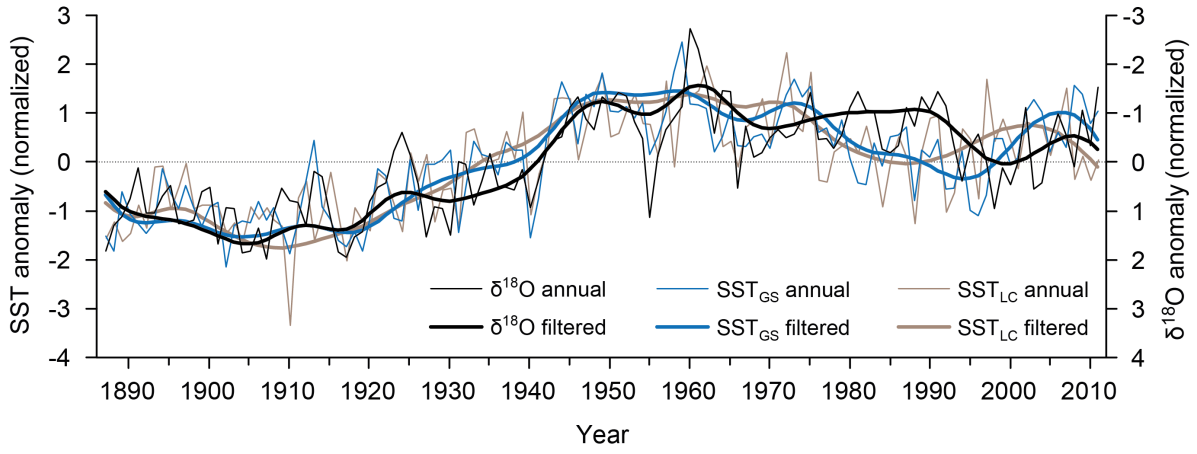

Figure 3-3. Coral $\delta^{18}O$ time series and its relation to sea surface temperature in the Gulf Stream (GS) and Loop Current (LC) comparative grid cells (see Figure 3-2). Data were normalized to unit variance for comparison by subtracting the mean and dividing by standard deviation. Filtering was done with a 15-year low-pass Gaussian filter.

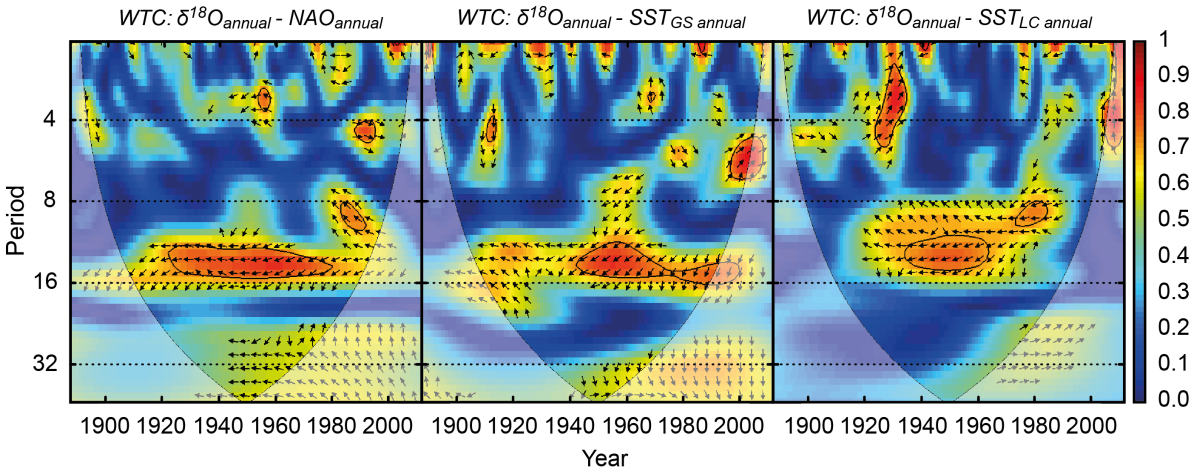

Figure 3-4. Results from wavelet coherence spectra between annual coral $\delta^{18}O$ and NAO index data as well as between annual coral $\delta^{18}O$ and SST from the Gulf Stream (GS) and the Loop Current (LC) (see Figure 3—2). The black contour designates the 5% significance level against red noise and the cone of influence where edge effects might distort the picture is shown as a lighter shade. The plots were computed using wavelet coherency software by (Grinsted et al., 2004).

between 1920 and 1980 with periods around 12–16 years (Figure 3-4). This significant region is surrounded by elevated but insignificant values even reaching from around 1900 to around 2000. After 1980 into the 1990s significant covariation seems to switch to shorter, interannual periods between around 8–11 and 5–6 years. Additionally, we compute WTCs between annual $\delta^{18}O$ and SST_{GS} and SST_{LC}, respectively (Figure 3-4), to investigate whether the two SST time series share time frequency patterns with $\delta^{18}O$ that also exist between $\delta^{18}O$ and NAO. Covariation in periods around 12–16 years is also present in both WTCs although not to similar extent. Both share a region of significant covariation between around 1940 and 1960 although covariation between $\delta^{18}O$ and SST_{GS} lasts longer, until around 2000. If elevated but not significant values are included, covariation between $\delta^{18}O$ and SST_{GS} coincides primarily with the region from 1900 and 2000 observed in the WTC between $\delta^{18}O$ and NAO. In contrast, covariation between $\delta^{18}O$ and SST_{LC} shows a narrower region on decadal scales, with no covariation existing before 1920 and after 1990. Here, the shift to shorter, interannual periods around the 1980s, as observed in WTC between $\delta^{18}O$ and NAO, also exists. The pattern of decadal variation is the dominant feature in all WTCs. This corresponds very well to results of Hurrell and van Loon (1997) and Hurrell et al. (2003b), which indicate that while no preferable time scale of NAO variability is detectable, the NAO exhibit considerable variability at quasi-biennial periods and in the decadal band. More importantly, the studies show that variability in the decadal band was enhanced over the twentieth century and has become especially pronounced in the second half of it. However, despite the good agreement with our observations from Little Cayman on decadal

time scales, evident multidecadal variability in $\delta^{18}O$ still needs to be addressed. In this context earlier studies have observed that wintertime NAO exhibits significant multidecadal variability (Hurrell, 1995; Chelliah & Bell, 2004; Goodkin et al., 2008; Woollings et al., 2015). Interestingly, multidecadal variability observed in both SST and $\delta^{18}O$ (Figure 3-3) agrees very well with multidecadal variability of wintertime NAO (wintertime NAO to: $\delta^{18}O$, $r = 0.74$; SST_{GS}, $r = 0.73$; SST_{LC}, $r = 0.79$; $p < 0.0001$; comparison of low-pass filtered annual data), suggesting a relation to wintertime NAO. Decadal variability also seems to be influenced by wintertime NAO in such a way that when wintertime NAO (not shown) is low during 1920–1970, covariance between NAO and $\delta^{18}O$/SST is significantly increased in the decadal band (Figure 3-4). Results from observations and models point to distinct patterns of ocean-atmosphere variability on decadal and multidecadal scales of the NAO (Deser & Blackmon, 1993; Delworth & Mann, 2000; Sutton & Hodson, 2003; Shaffrey & Sutton, 2006). On the decadal time scale NAO is dominated by meridional shifts of the jet stream and associated storm track, whereas on the multidecadal time scale variability is dominated by changes in their strength (Woollings et al., 2015). Recent studies suggest that the two timescales thereby express non-stationary relationships between NAO and regional impacts on temperature (Pozo-Vazquez et al., 2001; Haylock et al., 2007; Comas-Bru & McDermott, 2014) and precipitation (Vicente-Serrano & Lopez-Moreno, 2008; Raible et al., 2014) and different relationships to SST (Raible et al., 2001; Walter & Graf, 2002; Raible et al., 2005; Alvarez-Garcia et al., 2008). Especially in Europe the multidecadal component of NAO variability has a clear and distinct influence on surface temperatures and precipitation, so that decadal forecasts of this variability could be of practical use (Woollings et al., 2015). However, model predictability may be hampered by the assumption of stationarity of the NAO signal, which is commonly used in reconstruction methods(Küttel et al., 2010; Woollings et al., 2015). This problem is compounded by the complexity of the observed low-frequency variability in the Atlantic, which is subject of intense debate (Enfield & Mayer, 1997; Xie & Tanimoto, 1998; Dommenget & Latif, 2000; Marshall et al., 2001; Huang et al., 2004; Xie & Carton, 2004).

Our analyses suggest that the coral, due to its position, tracks changes in NAO variability on both the decadal and the multidecadal time scales in the important Loop Current and Gulf Stream regions (Figure 3-2). Hence, proxy data from this location may contribute new insights into the temporal and spatial nonstationarity of the NAO and can help to specifically investigate its impact on the western Caribbean and the Gulf Stream region.

Moreover, these new proxy reconstructions can be compared with model-generated fields of forced (external and internal) and natural variability over the last centuries. Evaluation of model simulations against paleodata indicates that models are capable of reproducing trends and large-scale patterns of past climate changes but tend to underestimate or lack distinct signatures of regional changes related to NAO and ENSO (Küttel et al., 2010; Braconnot et al., 2012; Woollings et al., 2015). Here, higher density of proxy data and distribution over larger geographical areas potentially provide more internally consistent and spatially coherent insights into past climatic variability not covered by instrumental data. However, there are regions of the ocean with naturally low density of available proxy archives due to, e.g., a lack of landmass and associated shallow waters housing potential biogenic proxy archives. Our coral $\delta^{18}O$ record is a clear example for the potential of proxy records to fill these gaps by tracking climate variables, such as SST, over larger regions. To obtain missing information it is crucial to localize the proxy record that potentially contains this information. We compare our $\delta^{18}O$ record to other Caribbean $\delta^{18}O$ data from the Venezuelan Archipelago Los Roques (Hetzinger et al., 2008) and from Puerto Rico (Kilbourne et al., 2008) to visualize geographical differences of SST variability representation between records. Figure 3-5 shows the spatial correlation patterns of those three records. For more clarity only high negative correlations with $r \leq -0.6$ are considered. Data from Los Roques show a pronounced correlation between coral $\delta^{18}O$ and large-scale SST variability in the northern tropical Atlantic (NTA), the Caribbean Current as well as the Canary Current region, representing the northeastern to southwestern portion of the North Atlantic subtropical gyre. Hence, while our observations and results from earlier studies (Hetzinger et al., 2006b; Hetzinger et al., 2008) indicate that the south-eastern Caribbean record is sensitive to changes in SST and seawater $\delta^{18}O$ in waters upstream from Los Roques (entering the Caribbean from the southeast) our central Caribbean isotope record seems to track SST-changes mainly in waters downstream from the sampling site (leaving the Caribbean in northerly direction). Interestingly, the Puerto Rico record shows highest correlations mainly in two separate regions remote from the location, i.e., the eastern sector of the Equatorial Counter Current and a region including the Azores and Portugal Current and the northern branch of the Canary Current. There is much overlap between the correlation fields of the Puerto Rico and Los Roques records. Despite the overlap additional information is still obtained, specifically in the north, because spatial correlations of the Puerto Rico record extend farther into the western central part of the North Atlantic gyre. Our analysis shows

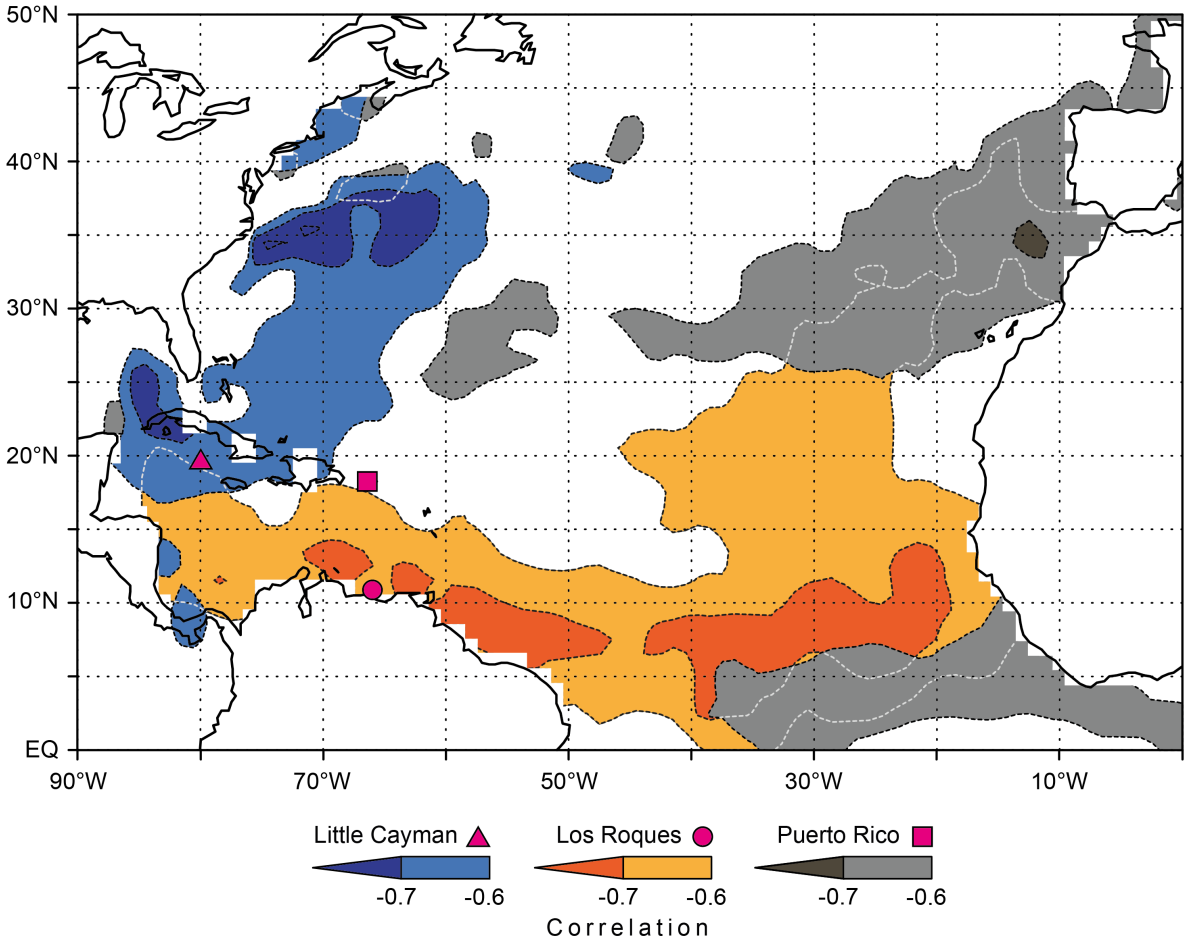

Figure 3-5. Spatial distribution of correlations between annual mean coral $\delta^{18}O$ and HadISST data (Rayner et al., 2003) for Little Cayman, Los Roques (Hetzinger et al., 2008) and Puerto Rico (Kilbourne et al., 2008). Data cover the period 1887–2011 (Little Cayman), 1918–2003 (Los Roques) and 1751–2004 (Puerto Rico) and were detrended. For more clarity only high negative correlations with $r \leq -0.6$ are shown. Correlations are significant at the 1 % level and were computed and plotted at http://climexp.knmi.nl/. White dashed lines represent the continuing contour line of a correlation field where fields overlap. A three-panel version depicting the correltations to the different corals in full in each panel is provided in Figure S3-6.

that the total acquired spatial coverage of high correspondence between $\delta^{18}O$ and SST variability is large, including principal elements of the North Atlantic subtropical gyre, even though it is based only on three records from three different Caribbean sites. The spatial distribution of correlations of these records clearly demonstrates the potential of proxy data to provide information on SST variability for regions where no instrumental measurements or proxy archives are available and to reconstruct the climate system in periods prior to the instrumental record. A focused application of proxy data from such areas, which also have been identified as "areas of uncertainty" in model based projections by the IPCC (2013), has the potential to greatly reduce that uncertainty.

3.4. Summary and Conclusions

Here we describe and interpret a 125-year record of coral $\delta^{18}O$ and Sr/Ca variations in the Central Caribbean Sea (Little Cayman, Cayman Islands), representing the longest continuous seasonal resolution record from a *Diploria strigosa* coral to date.
Both geochemical proxies show a decreasing long-term trend. The calculated warming from $\delta^{18}O$ is within the range of globally averaged surface warming estimates of the IPCC (2013), while Sr/Ca indicates a much stronger regional warming in comparison to large-scale grid-SST data. In conjunction with earlier studies (Kilbourne et al., 2008; Hetzinger et al., 2010a; von Reumont et al., 2016) our results suggest that Sr/Ca is a better indicator of local changes in temperature, while $\delta^{18}O$ seems to be a better indicator of large-scale/regional scale SST changes and that grid-SSTs do not sufficiently represent local SST variability within the reef system.

Seawater $\delta^{18}O$ variations ($\Delta\delta^{18}O_{sw\text{-}center}$) at Little Cayman are successfully captured by the coral proxy record by removing the Sr/Ca derived temperature component from coral $\delta^{18}O$. High inverse correlation with the AMO indicates that when temperature increases precipitation increases and vice versa. After the mid-1970s however, the $\Delta\delta^{18}O_{sw\text{-}center}$ signal decouples from the AMO signal and shifts to a steadily increasing regime, i.e., precipitation decreases, while temperature increases. An overall linear trend towards higher $\Delta\delta^{18}O_{sw\text{-}center}$ also indicates a drying trend over the past century. Through its environmental implications a continued drying and increase in temperature could have important socioeconomic consequences in the Cayman Islands and in the whole region.

The $\delta^{18}O$ and Sr/Ca time series show different potential in tracking SST variability on large spatial scales. While Sr/Ca exhibits strong relations with SST restricted to the local level, $\delta^{18}O$ shows high correlation with SST in the Gulf Stream region east of Cape Hatteras and the Loop Current region. Therefore, Little Cayman potentially is a sensitive location for the detection of past regional scale SST variability within the Gulf Stream System. More specifically, our $\delta^{18}O$ data track changes in NAO variability on both the decadal and the multidecadal time scales in that region. The data may contribute to a basic understanding of the temporal and spatial nonstationarity of NAO and can help to investigate the impact of NAO on the western Caribbean and the Gulf Stream region.

The combined evaluation of our coral $\delta^{18}O$ record and two other records from different Caribbean sites reveals a large total spatial coverage of high correspondence between coral $\delta^{18}O$ and SST variability, comprising principal elements of the North Atlantic subtropical gyre. This result is a clear demonstration of the potential of proxy data to provide information on SST variability for regions where no instrumental measurements or proxy archives are available and to reconstruct the climate system in periods prior to the instrumental record. Thereby, our new Central Caribbean proxy reconstructions help to increase the density and distribution of proxy data over larger geographical areas, which is important for gaining more internally consistent and spatially coherent insights into past climatic variability not covered by instrumental data.

3.5. Acknowledgments

The authors would like to thank Karen Bremer for the lab assistance and Lowell Forbes for diving assistance. This work was supported with funding from the DFG (through project HE 6251/2-1). Data are available to the public from World Data Center for Paleoclimatology www.ncdc.noaa.gov/paleo at NOAA's National Center for Environmental Information (NCEI): https://www.ncdc.noaa.gov/paleo/study/23850. The authors declare that they have no conflict of interest.

3.6. Supporting information

The supporting information on the following pages includes additional figures.

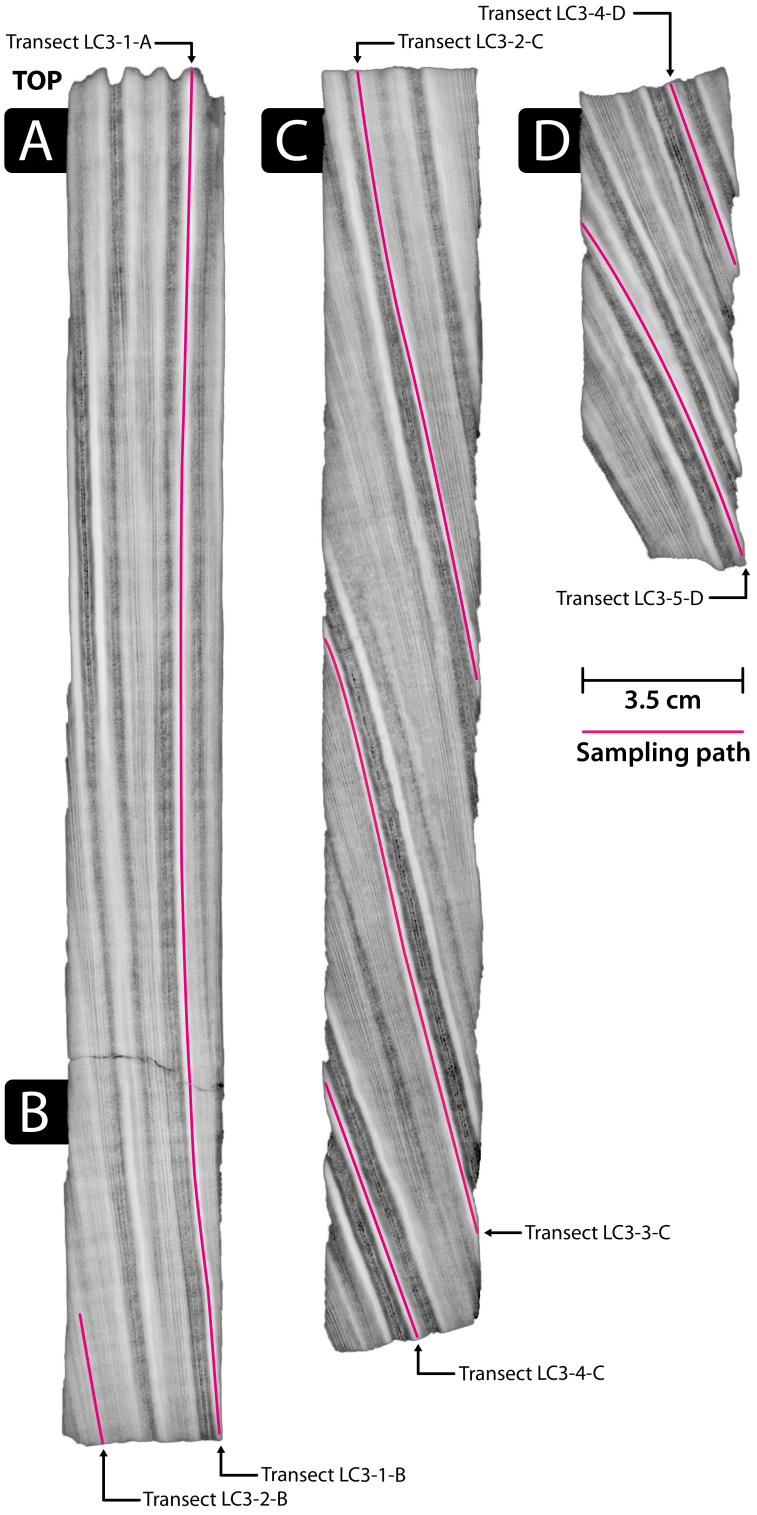

Figure S3-1. X-radiographs of the slabs from core LC3 recovered from a *Diploria strigosa* colony. Lighter regions in negative X-radiographs are denser and vice versa. Sampling transects are indicated by pink solid (sub-)vertical lines on each slab.

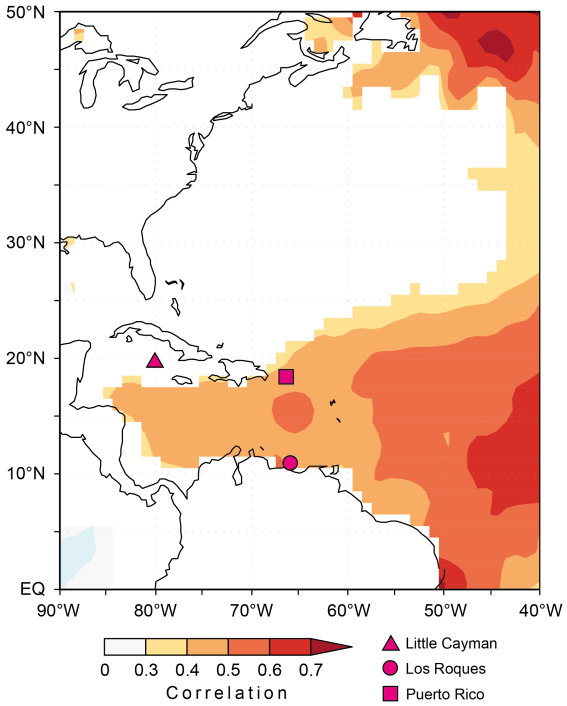

Figure S3-2. Spatial distribution of correlations between annual mean HadISST data (Rayner et al., 2003) and the AMO index (van Oldenborgh et al., 2009). Data cover the period 1887–2011. Note that Guadeloupe and Puerto Rico are situated within a field of significant agreement. In contrast, no correlation exists in the northwestern part of the Caribbean, north of the latitude of Jamaica where the Cayman Islands are situated. Correlations are significant at the 1% level and were computed and plotted at http://climexp.knmi.nl/.

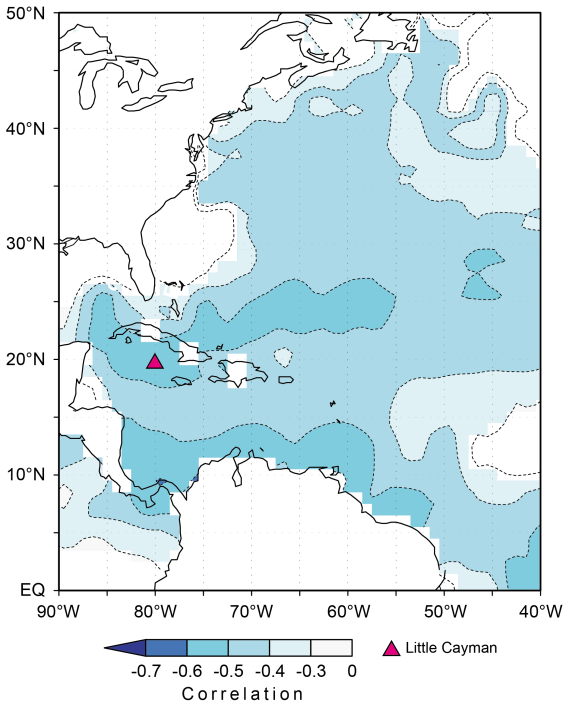

Figure S3-3. Spatial distribution of correlations between annual mean coral Sr/Ca and HadISST data (Rayner et al., 2003). Data cover the period 1887–2011 and were detrended. In contrast to annual mean coral $\delta^{18}O$, which reveals strong negative relations to SST in the Loop Current region and the Gulf Stream region, annual mean Sr/Ca and SST exhibit strong relations mainly restricted to the local level and not on regional to large scales. Correlations are significant at the 1% level and were computed and plotted at http://climexp.knmi.nl/.

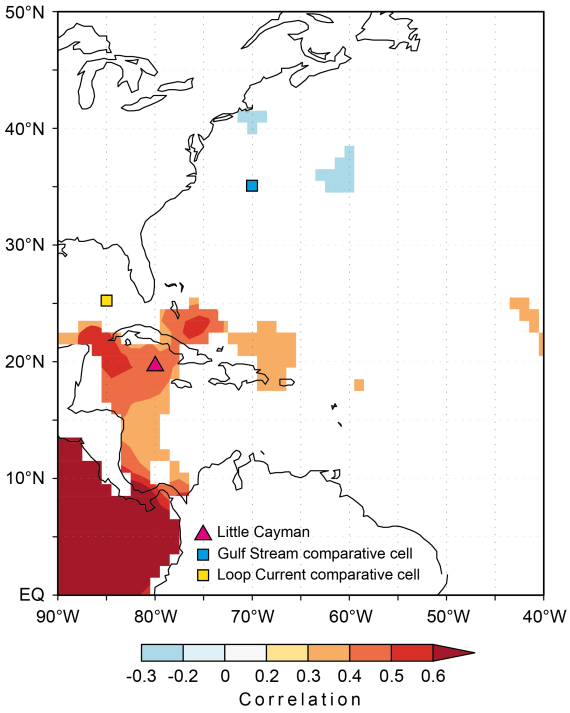

Figure S3-4. Spatial distribution of correlations between annual mean HadISST data (Rayner et al., 2003) and the ONI index. Data cover the period 1970–2000 and were detrended. Note the moderate correlations for the northeast Caribbean while for the Gulf Stream and Loop Current region no or only weak correlations can be observed. ENSO potentially has a measurable impact on local SST and thus coral $\delta^{18}O$ at Little Cayman, while SST in the comparative regions seems to be unaffected. Correlations are significant at the 1% level and were computed and plotted at http://climexp.knmi.nl/.

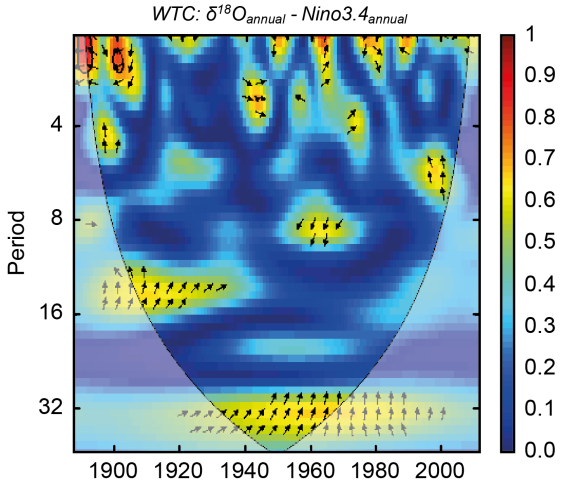

Figure S3-5. Results from a wavelet coherence spectrum between annual coral $\delta^{18}O$ and Nino3.4 index data. The black contour designates the 5% significance level against red noise and the cone of influence where edge effects might distort the picture is shown as a lighter shade. The plots were computed using wavelet coherency software by (Grinsted et al., 2004).

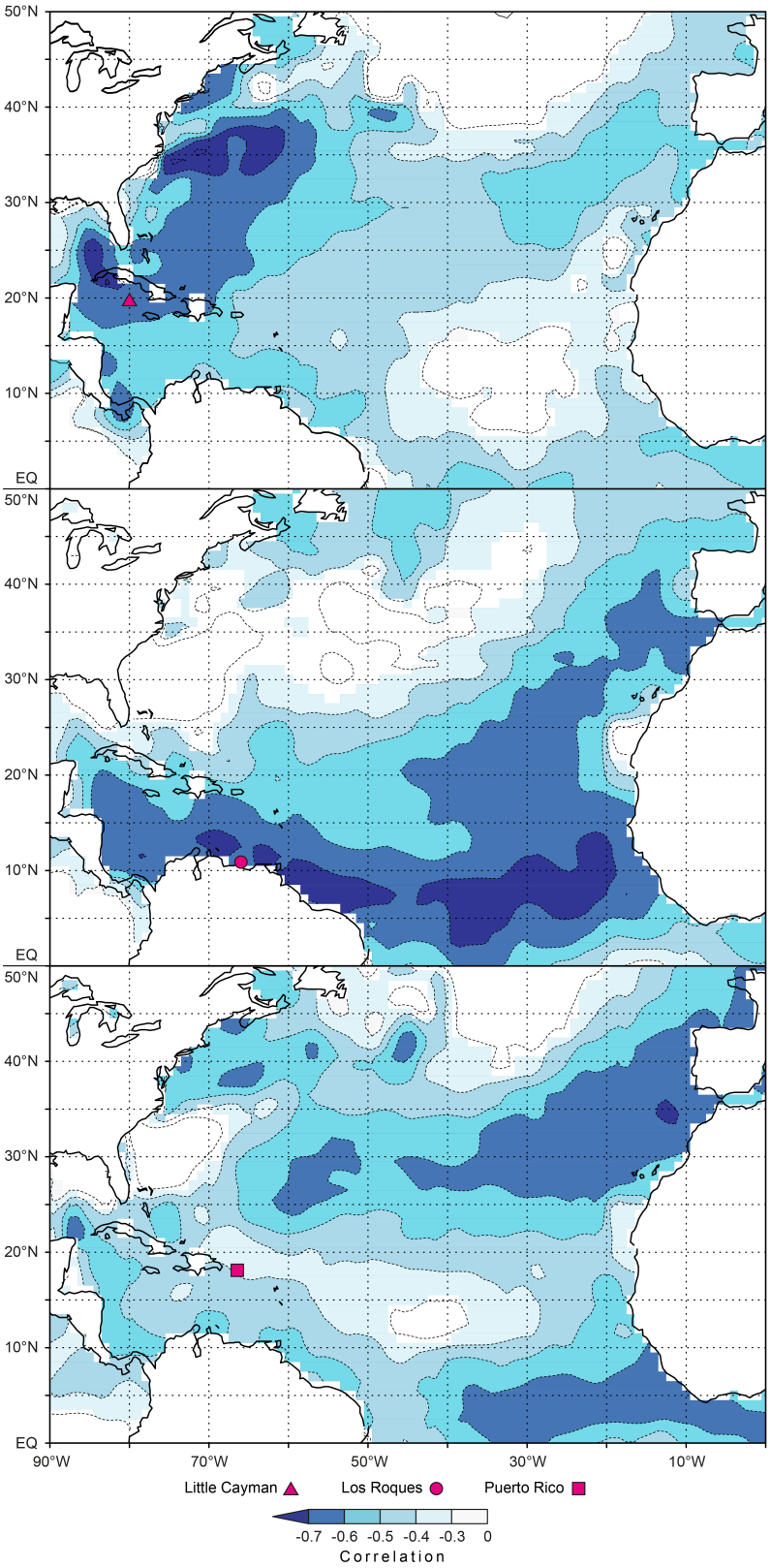

Figure S3-6. Spatial distribution of correlations between annual mean coral $\delta^{18}O$ and HadISST data (Rayner et al., 2003) for Little Cayman, Los Roques (Hetzinger et al., 2008) and Puerto Rico (Kilbourne et al., 2008). Data cover the period 1887–2011 (Little Cayman), 1918–2003 (Los Roques) and 1751–2004 (Puerto Rico) and were detrended. Correlations are significant at the 1% level and were computed and plotted at http://climexp.knmi.nl/.

4. Multidecadal oscillation of Caribbean nitrogen fixation slowdowns during the 20th century

Atsuko Yamazaki[1,2,3], Steffen Hetzinger[2,4], **Jonas von Reumont**[2], Carrie Manfrino[5,6], Urumu Tsunogai[7], Yuji Sano[3], and Tsuyoshi Watanabe[1]

[1]Faculty of Science, Hokkaido University, N10W8, Kita-ku, Sapporo, 060-0810, Japan
[2]GEOMAR Helmholtz-Zentrum für Ozeanforschung Kiel, Wischhofstr. 1-3, 24148 Kiel, Germany
[3]Atmosphere and Ocean Research Institute, The University of Tokyo, 5-1-5, Kashiwanoha, Kashiwa, Chiba, 277-0882, Japan
[4]Institut für Geologie, Universität Hamburg, Bundesstr. 55, 20416 Hamburg, Germany
[5]Central Caribbean Marine Institute, PO Box 1461, Princeton, NJ 08542, USA
[6]Department of Geology and Meteorology, Kean University, 1000 Morris Ave., Union, NJ 07083, USA
[7]Graduate School of Environmental Studies, Nagoya University, Furo, Chikusa-ku, Nagoya, 464-8601, Japan

In preparation for *Nature Geoscience*

Oceanic nitrogen fixation is important for providing new nitrogen in oligotrophic oceans and balances with denitrification in the global nitrogen cycle (Gruber & Sarmiento, 1997). However, no continuous high-resolution data of past nitrogen fixation variability is available. Here, the first centennial-scale record (94-year) of annual nitrogen isotopes in a Caribbean coral reveals changing nitrogen fixation correlating with multidecadal temperature variability in the North Atlantic Ocean. Reconstructed nitrogen fixation also shows a decreasing trend during the 20th century corresponding to the slowdown of the Atlantic Meridional Overturning Circulation, which may be led by global warming (Rahmstorf et al., 2015). Our findings suggest that Atlantic Ocean circulation may drive the century scale variation of nitrogen fixation in the Caribbean Sea. Ongoing trends related to global warming may lead to a reduction in nitrogenous nutrients in the future and an imbalance between carbon and nitrogen.

4.1. Introduction

The available fixed nitrogen is essential for the biological pump removing CO_2 from the atmosphere and sequestering it in the ocean. The North Atlantic Ocean is known as a nitrogen fixation hotspot (Capone et al., 2005). Previous studies discussing historical changes of nitrogen fixation rate in the North Atlantic Ocean have focused on seasonal scale variations based on instrumental observations (Luo et al., 2012) and millennial-scale variations using sediment cores (Straub et al., 2013). However, decadal to centennial scale variability of nitrogen fixation rates is still unknown. In particular, no high-resolution data exist for the 20th century, where climate warming has also influenced nitrogen fixation and global nitrogen cycles (Gruber & Galloway, 2008).

Only recently, nitrogen isotopes in biogenic carbonate skeletons have been used as a proxy for nitrogen fixation in tropical oceans (Straub et al., 2013; Sherwood et al., 2014). For example, nitrogen isotope records in Hawaiian deep sea corals revealed increasing nitrogen fixation since the Little Ice Age in the subtropical Pacific (Sherwood et al., 2014). Reef corals have widely been used as paleoenvironmental proxy archives in oligotrophic oceans (Carricart-Ganivet, 2004; Hetzinger et al., 2006b; Hetzinger et al., 2008; Kilbourne et al., 2008; Saenger et al., 2008; DeLong et al., 2014; von Reumont et al., 2016). We applied newly developed methods for the determination of nitrogen isotopes of organic matter preserved in coral skeletons ($\delta^{15}N_{coral}$) to reconstruct interannual to decadal scale changes in coral nitrogen sources (Yamazaki et al., 2011; Yamazaki et al., 2016). Here, we present a new 94-year record of annual nitrogen isotopes in a modern massive-growing coral from Little Cayman Island, Caribbean Sea. We analyzed a coral core from a live colony of *Diploria strigosa,* which grew in the fore reef at 9 m water depth and had a diameter of 0.8 m.

4.2. Findings and discussion

$\delta^{15}N_{coral}$ varied from about -3 ‰ to 8 ‰ showing strong multidecadal-scale variability, with lower $\delta^{15}N_{coral}$ during the 1920s to 1940s and higher values during the 1950s to 1980s, returning to lower values between 1990 and 2010 (Figure 4-1a). The long-term trend of $\delta^{15}N_{coral}$ gradually increased by about 4 ‰ during the 20th century. $\delta^{15}N_{coral}$ in the modern part of the core is approximately 2 ‰, corresponding to 1.8 ± 0.5 ‰ (1σ, n = 12) of $\delta^{15}N$ in inorganic nitrogen consuming macro algae, suggesting that $\delta^{15}N_{coral}$ in *Diploria strigosa* records $\delta^{15}N$ of inorganic nitrogen in the water column. The $\delta^{15}N_{coral}$ average was 1.9 ± 2.6 (σ) ‰ (n = 139), which is lower than the oceanic average of nitrate $\delta^{15}N$ (~5 ‰) (Sigman et al., 2000), indicating that the coral may consume decomposed products from nitrogen fixation (~0 ‰) in ambient seawater.

On multidecadal scales, reconstructed nitrogen fixation from our coral core suggests enhanced (reduced) fixation with warmer (cooler) SST conditions. Detrended $\delta^{15}N_{coral}$ showed a significant negative correlation with the Atlantic Multidecadal Oscillation (AMO) index (Enfield et al., 2001), a major mode of low-frequency Atlantic SST and climate variability (Figure S4-1; r = -0.71, P << 0.001). The primary nitrogen fixer cyanobacterium *Trichodesmium* is activated at a temperature between 24 and 30 °C (Breitbarth et al., 2007). Modern seasonal SST variation in Little Cayman is within 24 and 32 °C (von Reumont et al., 2016), generally an adequate SST range for the activity of *Trichodesmium*. The low

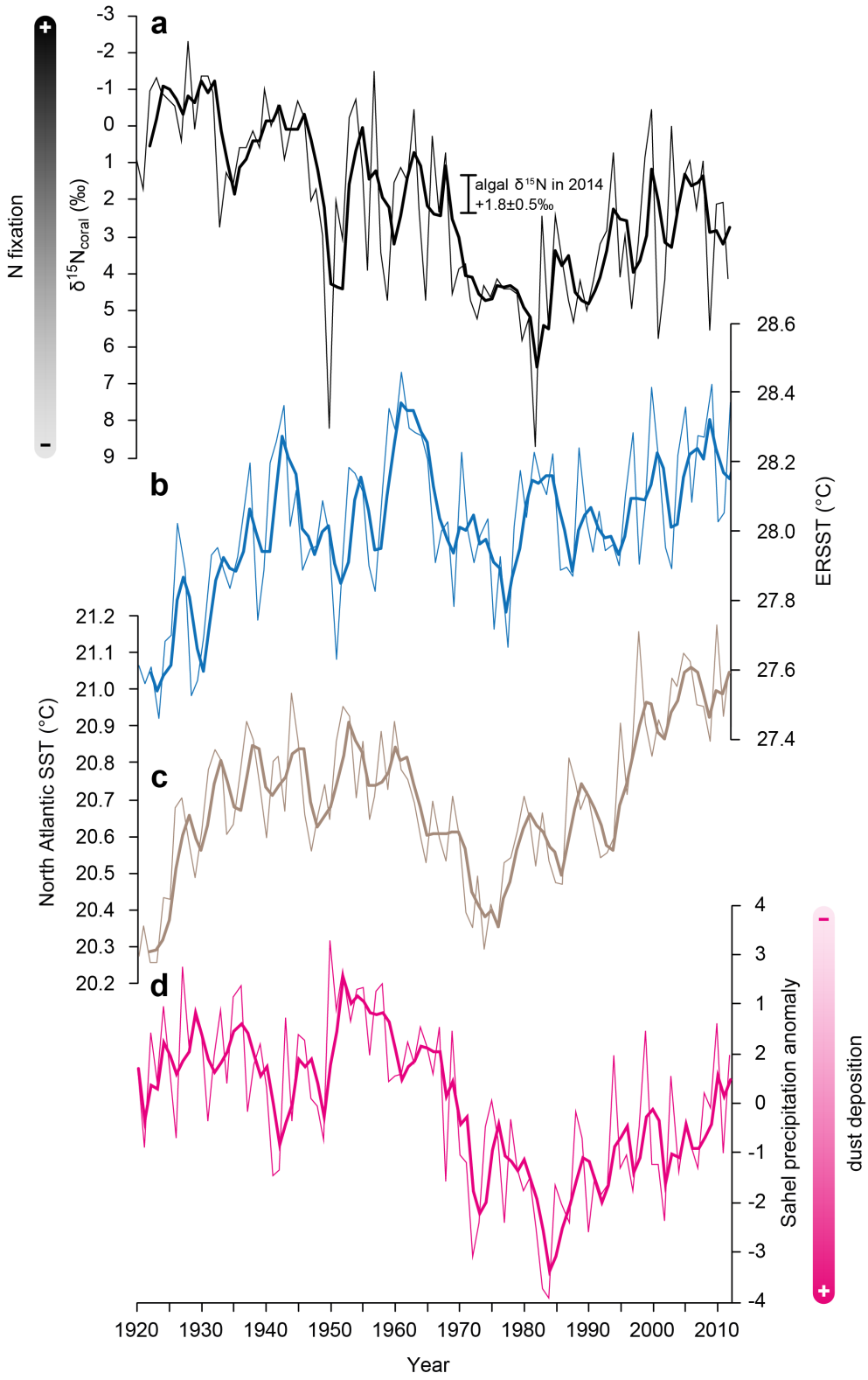

Figure 4-1. 20th century changes in Caribbean $\delta^{15}N_{coral}$. The annual resolution $\delta^{15}N_{coral}$ time series (a) is shown in comparison with ERSST data (Huang et al., 2015; Liu et al., 2015) for the grid box centered on 19.5°N and 79.5°W, including the coral site (b), mean north Atlantic SST (Enfield et al., 2001) (c) and the Sahel precipitation anomaly (Mitchell, 2015) (d). Algal $\delta^{15}N$ (+1.8 ± 0.5 ‰) (scale bar) is shown with $\delta^{15}N_{coral}$ time series (a). Fine lines show annual averages, bold lines show 3-year running means.

correlation between detrended $\delta^{15}N_{coral}$ and detrended ERSST (Huang et al., 2015; Liu et al., 2015) at Little Cayman ($r = -0.14$, $p = 0.20$; Figure S4-1) still raises the question whether multidecadal SST variability within the adequate temperature for *Trichodesmium* over the past 94 years can be a controlling factor of the decadal nitrogen fixation variations.

The distribution of high North Atlantic nitrogen fixation in the present time is explained by water with a lower N/P ratio supplied from the South Atlantic Ocean and higher iron dust deposition from the Sahel region (Moore et al., 2009). Wang et al. (2012) reported that on a multidecadal scale Sahel dust and Atlantic SST inversely covary, i.e., dust deposition decreases while SSTs are increasing and vice versa. However, the high correspondence between Sahel rainfall variability, which negatively corresponds with Sahel dust emissions (Wang et al., 2015), and our coral record suggests increasing nitrogen fixation with reduced dust emissions (Figure 4-1). Thus, our results suggest that iron dust deposition could not explain higher nitrogenfixation rates under higher SST conditions. Another potential cause of decadal nitrogen fixation variations is the changing supply of phosphorus rich water through the South Equatorial Current to the Caribbean Current driven by the Atlantic Meridional Overturning Circulation (AMOC). A recent study based on North Atlantic sea level observations (McCarthy et al., 2015) has provided evidence of the widely hypothesized influence of ocean circulation on the phase changes of the AMO (Figure S4-1).

Although Atlantic nitrogen fixation is enhanced under higher SST conditions on decadal scales, our $\delta^{15}N_{coral}$ record suggests a long-term decreasing trend of Caribbean nitrogen fixation over the 20th century. Decreasing Sahel rainfall during the 20th century has led to an increasing Sahel dust emission (Wang et al., 2012). However, the observed decrease of nitrogen fixation over the past 94 years does not seem to be controlled by iron dust deposition. An ongoing increase in SST with seasonally sustained high temperatures above the thermal optimum for nitrogen fixation (~27 °C) might result in a decrease in *Trichodesmium* (Breitbarth et al., 2007). A decreasing trend of Caribbean nitrogen fixation over the last century could also be explained by changes in ocean current variability. The weakening of AMOC with global warming (Rahmstorf et al., 2015) could lead to decreased Caribbean nitrogen fixation caused by decreasing phosphorus supply from the equatorial Atlantic (Straub et al., 2013).

The North Atlantic Ocean is a major source of fixed nitrogen for the global ocean (Gruber & Sarmiento, 1997; Gruber & Galloway, 2008). Our results suggest that decreasing nitrogen

fixation in the Caribbean Sea leads to an imbalance in the oceans nitrogen budget and that the ocean might have been losing nitrate during the 20th century.

4.3. Acknowledgments

We thank the Central Caribbean Marine Institute for its cooperation and fieldwork support. T. Ohyama and K. Tanaka supported coral and algal nitrogen isotope analysis. The fieldwork was conducted through the financial support of JSPS (KAKEN 26870155). A. Yamazaki was supported by Grants-in-Aid for JSPS research fellows.

4.4. Supporting information

The supporting information provides additional description of the materials and methods used and an additional figure.

4.4.1. Coral sampling and nitrogen isotope analysis.

In July 2012, we drilled a coral core (LC3; d = 3.5 cm) from a 0.8 m high live *Diploria strigosa* coral colony in a water depth of 9 m in the fore reef of Little Cayman, Cayman Islands (19.7° N, 80.06° W). The coral cores were cut into 5 mm thick slabs to observe the annual density bands in X-radiographs. The theca walls of the coral skeletons were cut out from the slab excluding dissepiments. Microsampling was performed at 4-mm intervals along the major growth axis to obtain 30 to 40 mg of coral powder/sample. To remove the extra organic matter in the coral powder, the sampled powder was treated with NaOH (2 mol l^{-1}, 60 °C) for 3 hours and rinsed using Milli-Q water (Yamazaki et al., 2013). Nitrogen isotope analyzes of the dried powder samples were performed based on chemical conversion methods (Yamazaki et al., 2011). The standard deviation of the coral sample measurements was less than 0.2 ‰ (σ).

4.4.2. Age model

The age model was determined by comparing coral density bands and seasonal variation of coral Sr/Ca ratios on the same analytical line (von Reumont et al., 2016). Coral density variations were depicted by grey-scale values of the X-radiographs using ImageJ 1.46 software (W. Rasband, the Research Services Branch, National Institute of Mental Health, Bethesda, Maryland, USA.).

4.4.3. Algal nitrogen isotope analysis

Macro algae specimens, *Dyctyota* sp. and *Halimeda* sp., were collected from 1 to 10 m water depth off the coast of Little Cayman Island including the coral sampling site. Macro algae samples were rinsed with Milli-Q water and dried in a 60 °C oven. 6-mg algae samples were folded in tin capsules. The $\delta^{15}N$ and total nitrogen were measured using an online system of an IsoPrime100 isotope-ratio mass spectrometer coupled to a vario MICRO cube Elemental Analyzer. Isotope compositions were expressed in conventional δ-notation against atmospheric N_2 for nitrogen. The analytical error for $\delta^{15}N$ was estimated to be within 0.15 ‰ (n = 6, σ).

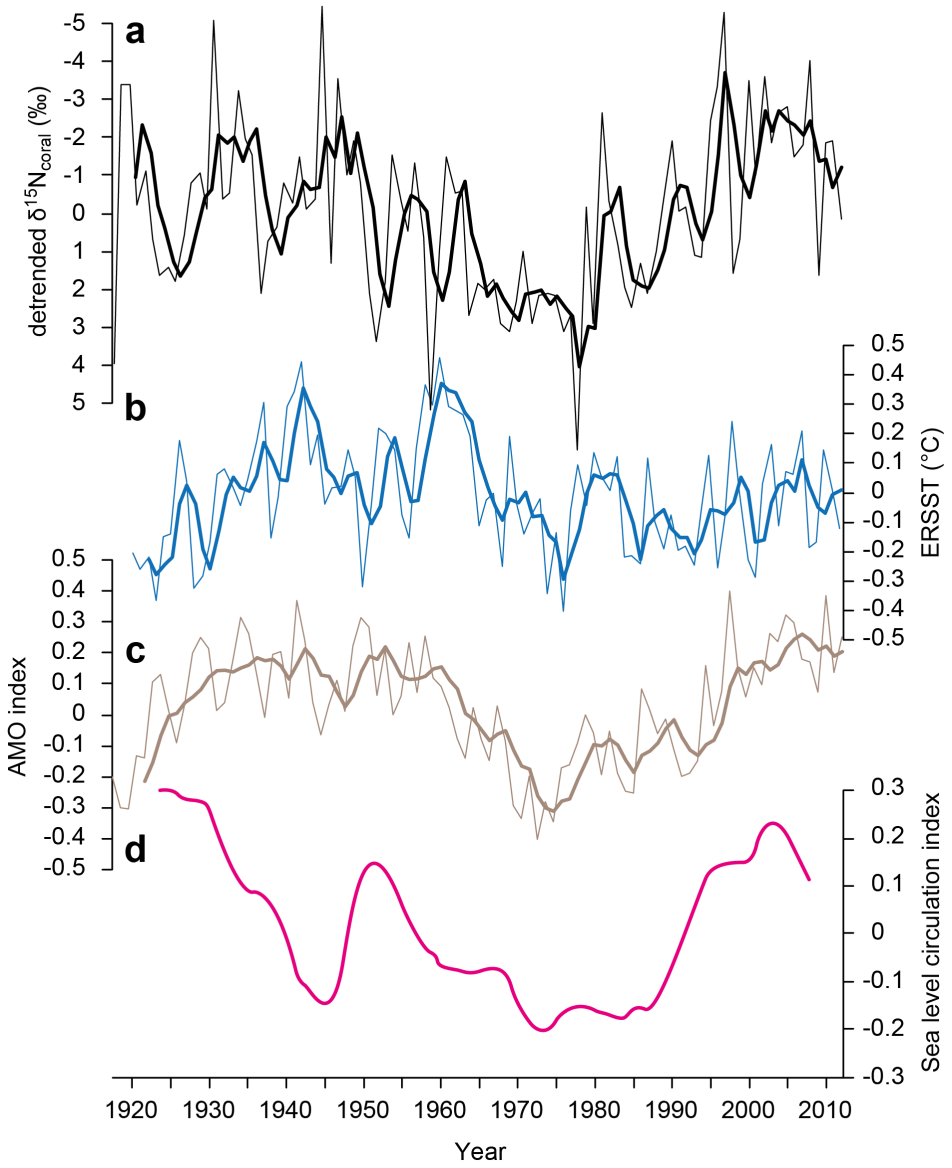

Figure S4-1. Detrended changes in Caribbean $\delta^{15}N_{coral}$. Detrended $\delta^{15}N_{coral}$ time series (a) is shown in comparison with detrended ERSST data (Huang et al., 2015; Liu et al., 2015) for the grid box centered on 19.5°N and 79.5°W, including the coral site (b), AMO index (Enfield et al., 2001) (c) and Sea level circulation index (Wang et al., 2015) (d). (a–c) Fine lines show annual averages, bold lines show 3-year running means.

5. The Eugen Seibold coral mounds offshore western Morocco: oceanographic and bathymetric boundary conditions of a newly discovered cold-water coral province

Silke Glogowski[1], Christian Dullo[1], Peter Feldens[2], Volker Liebetrau[1], **Jonas von Reumont[1]**, Veit Hühnerbach[1], Sebastian Krastel[2], Russell B. Wynn[3] and Sascha Flögel[2]

[1]GEOMAR Helmholtz-Zentrum für Ozeanforschung Kiel, Wischhofstr. 1-3, 24148 Kiel, Germany
[2]IfG, Institute of Geosciences, Christian-Albrechts-University, Otto-Hahn-Platz 1, 24118 Kiel, Germany
[3]National Oceanography Centre, European Way, Southampton SO14 3ZH, United Kingdom

Published in *Geo-Marine Letters*

This study reports a new cold-water coral (CWC) province covering ~410 km² off western Morocco (~31° N) ~40 nautical miles north of the Agadir Canyon system between 678 and 863 m water depth, here named the Eugen Seibold coral mounds. Individual mounds are up to 12 m high with slope angles varying between 3° and 12°. Hydroacoustic data revealed mound axes lengths of 80 to 240 m. Slope angle, mound height, and density of mounds decrease with increasing water depth. The deepest mounds are composed of dead and fragmented *Lophelia pertusa* branches. Living CWCs, mainly *Lophelia pertusa*, were sampled with box cores between 678 and 719 m water depth. Conductivity-temperature-depth (CTD) measurements revealed living CWC colonies to occur within the deeper part of the North Atlantic Central Water (NACW; conservative temperature Θ of 9.78–9.94 °C, absolute salinity SA of about 35.632 g kg^{-1}, and seawater density σ_Θ of 27.31–27.33 kg m^{-3}). Comparable CWC reefs off Mauritania (17° N–18° N) and on the Renard Ridge (35° N) in the Gulf of Cadiz, the latter consisting only of a dead CWC fabric, are also located in the deeper layer of the NACW slightly above the Mediterranean Outflow Water. The new CWC province, with its thin cover of living corals and much larger accumulations of dead thickets and fragmented coral rubble, was successfully discovered by CTD reconnaissance applying seawater density as a potential indicator of CWC occurrences, followed by hydroacoustic mapping. U-Th isotope systematics for macroscopically altered buried Lophelia material (25 cm sediment depth) yielded absolute ages dating back to the late Holocene at least.

Citation: Glogowski, S. Dullo, C., Feldens, P., Liebetrau, V., von Reumont, J., Hühnerbach, V., Krastel, S., Wynn, R. B. and Flögel, S. (2015). The Eugen Seibold coral mounds offshore western Morocco: oceanographic and bathymetric boundary conditions of a newly discovered cold-water coral province. Geo-Marine Letters, 35 (4). 257-269. https://doi.org/10.1007/s00367-015-0405-7.

5.1. Introduction

Cold-water coral (CWC) reefs are widespread along the continental margins of global ocean basins (Roberts et al., 2006b). Since the discovery of spectacular CWC mounds in the Porcupine Seabight (Henriet et al., 1998), many more reef sites have been identified worldwide, predominantly in the North Atlantic. Indeed, the presence of *Lophelia pertusa* as a main frame-builder of CWC reefs is today known from, for example, the Norwegian margin (e.g., Fosså et al., 2002; Freiwald, 2002; Hovland et al., 2012), the Porcupine, Rockall and Hatton banks (e.g., White et al., 2007; Sayago-Gil et al., 2010; Mazzini et al., 2012), the Celtic margin (e.g., Wheeler et al., 2007), the Armorican margin (e.g., Reveillaud et al., 2008), the Cantabrian Sea (e.g., Sánchez et al., 2014), the Iberian margin (e.g., Hernández-Molina et al., 2011; Somoza et al., 2014), the Mediterranean Sea (e.g., Freiwald et al., 2009; Palomino et al., 2011; Taviani et al., 2011; Fink et al., 2012; Gori et al., 2014; Savini et al., 2014), the Gulf of Cadiz (GoC) (e.g., Van Rensbergen et al., 2005; Van Rooij et al., 2011; León et al., 2012), off northern Morocco (southern GoC) (e.g., Foubert et al., 2008), off Mauritania (e.g., Eisele et al., 2011; Eisele et al., 2014), the Angola margin (e.g., Le Guilloux et al., 2009), the Gulf of Mexico (e.g., Brooke & Schroeder, 2007; Hübscher et al., 2010; Hebbeln et al., 2014), and around the Bahamas (e.g., Reed et al., 2006; Correa et al., 2012a; Correa et al., 2012b). Many of these studies explored the impact of various hydrographic factors and nutrient availability (Hovland et al., 2012) on CWC reef growth. In addition, Martorelli et al. (2011) demonstrated the positive influence of topography-enhanced bottom current velocity on coral occurrences. Temperature and salinity are other key factors constraining the distribution of live corals (e.g., Davies et al., 2009; Davies & Guinotte, 2011; Vierod et al., 2014), and indirectly ambient seawater density (e.g., Dullo et al., 2008; Flögel et al., 2014). A new CWC province was discovered off western Morocco during research cruise 32 of R/V Maria S. Merian in October 2013, which mainly targeted the morphology, sedimentary processes and geohazards of giant landslides of the Agadir Canyon system (Krastel et al., 2014). This study explores the recent oceanographic and bathymetric boundary conditions of these CWCs, based on a combination of seafloor bathymetric and acoustic data as well as conductivity-temperature-depth (CTD) data collected from the overlying water masses. One of the cruise aims was to test whether seawater density can be used as a predictive tool to detect living CWC occurrences. The new province is here named the Eugen Seibold coral mounds in honour of the pioneering marine geologist Eugen Seibold (1918–2013).

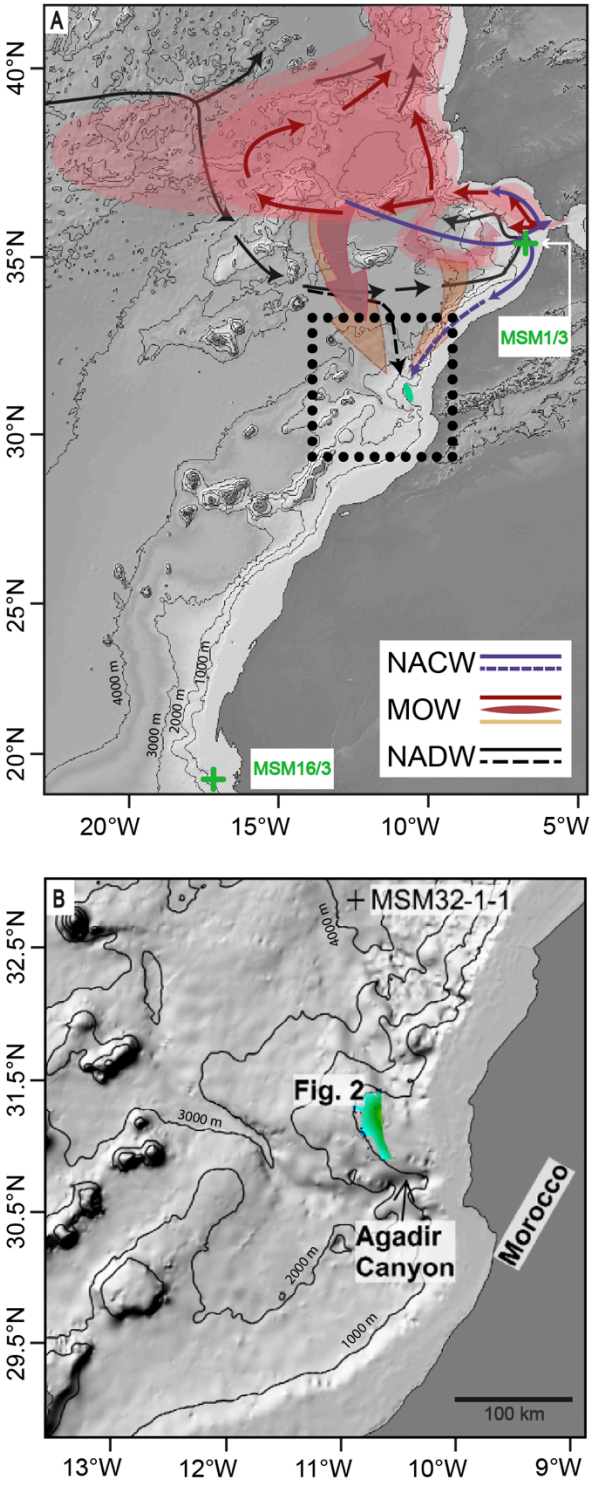

Figure 5-1. Top Map showing the locations of the study area off western Morocco (black box; green dot mound field), and the CTD stations (stars) of earlier cruises off Mauritania (MSM16/3) and in the Gulf of Cadiz (MSM1/3; Table 5-1), with depth contours and water masses. North Atlantic Central Water: solid blue arrows after Vandorpe et al. (2014); dotted blue arrow its continuation, present study. Mediterranean Outflow Water: red area and arrows after Hernández-Molina et al. (2011), including preferred meddy pathways; orange arrows its continuation, CTD data of present study. North Atlantic Deep Water: solid dark grey arrows after Hernández-Molina et al. (2011); dark grey dotted arrow its continuation, present study. Bottom Green Multibeam bathymetry coverage. Note the location of CTD station MSM32-1-1 (see also Figure 5-3 and Table 5-1)

5.2. Physical Settings

This study focuses on the Atlantic Moroccan continental slope off northwest Africa at 32.90°–31.13° N and 10.57°–10.82° W (Figure 5-1). Three investigated sites exhibit the following water masses from the surface to the seafloor. The Central Water (CW) masses comprise Subtropical Underwater (SUW), South Atlantic Central Water (SACW) and North Atlantic Central Water (NACW) (Mittelstaedt, 1991; Van Camp et al., 1991; Morigi et al., 2001; Vandorpe et al., 2014). According to Mittelstaedt (1991) and Arístegui et al. (2009), SACW and predominantly NACW upwell seasonally. The presence of Mediterranean Outflow Water (MOW) below the NACW is associated with a pronounced increase in salinity favouring the formation of a pycnocline, for example, in the GoC (Fusco et al., 2008). Alves et al. (2011) described the MOW off Morocco at 34°N, while Pelegrí et al. (2005) reported this water mass extending as far south as 30.5° N. In the present study area, the deepest part of the water column is formed by the North Atlantic Deep Water (NADW). Unpublished analogue TOPAS (TOpographic PArametric Sonar) sub-bottom profiles kindly supplied by G. Ercilla of the Institute of Marine Sciences (CSIC), Barcelona had revealed the presence of acoustically transparent mounds at more than 750 m water depth ~40 nautical miles north of the upper Agadir Canyon (Figure 5-1), one of the largest submarine canyons worldwide (Wynn et al., 2002) and characterised by tectonic morphologies and giant landslides (Talling et al., 2007; Frenz et al., 2009). Examination of those preliminary data showed that the dimensions and acoustic character of the features were similar to those of known carbonate mounds in the northeast Atlantic (De Mol et al., 2002; Rüggeberg et al., 2011). Subsequent cruises gathered hydrographic data including seawater density, reported to be a predictive tool for coral occurrence in other regions (Foubert et al., 2008; Somoza et al., 2014). Prospective sites were mapped by swath bathymetry and side scan sonar in order to, amongst others, define targets for box coring. Indeed, these confirmed the suspected presence of mostly dead and some living corals in an extensive province of > 400 km^2 (Figure 5-2).

5.3. Material and Methods

5.3.1. Hydrography

Water masses above the coral mounds were investigated by performing 11 CTD casts (Table 5-1) using a Seabird SBE 911-plus underwater unit additionally equipped with two oxygen

sensors and a turbidity sensor (including SBE data processing). CTD data were visualized using Ocean Data View (ODV) software, version 4.5.3 (Schlitzer, 2013). Temperatures and salinities are reported as conservative temperature (Θ, °C) and absolute salinity (SA, g kg^{-1}; TEOS-10, (McDougall & Barker, 2011). T-S plots of temperature against salinity are commonly used to delineate water masses and their geographical distribution as well as dynamics (Tomczak, 1999).

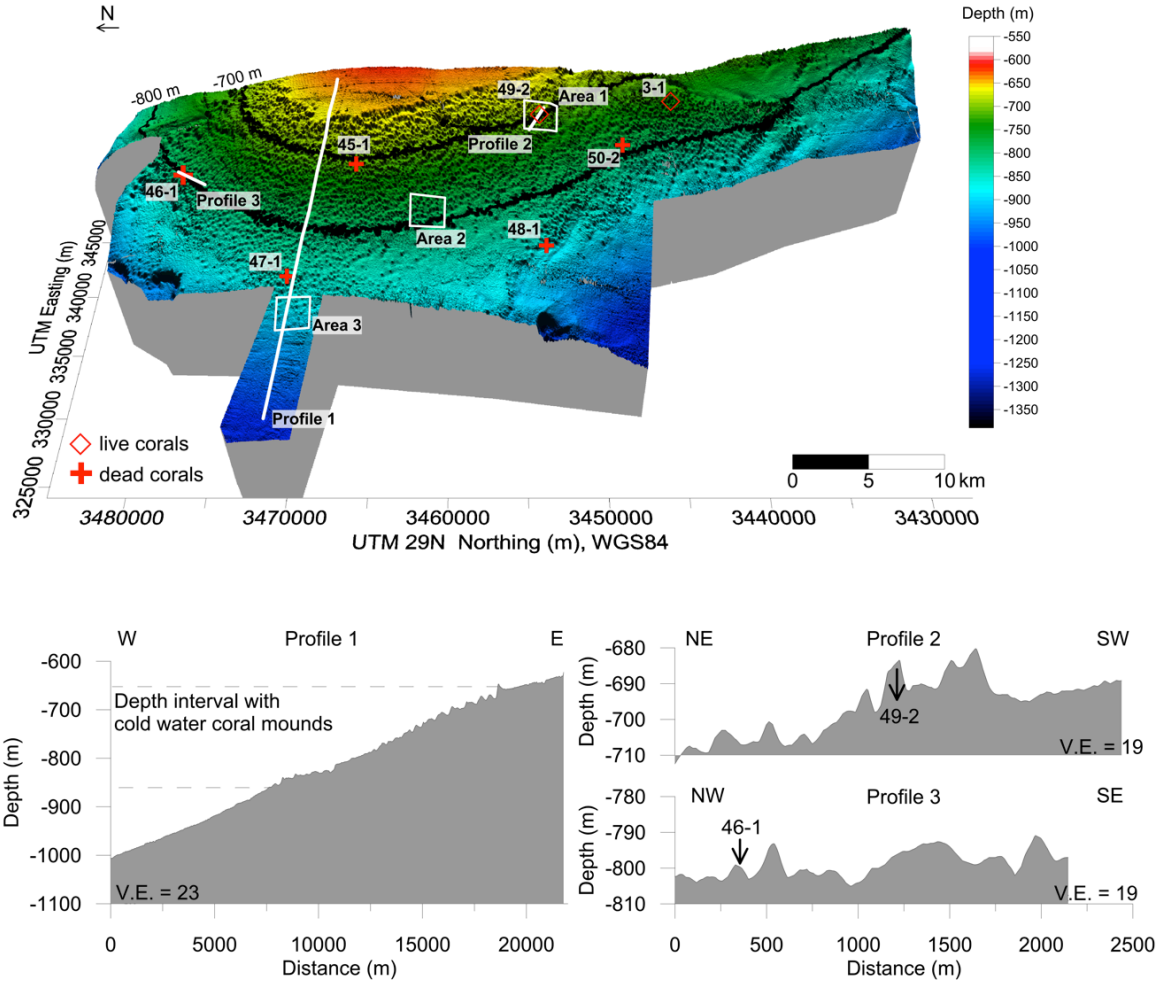

Figure 5-2. Top 3-D perspective view of multibeam bathymetry (lateral pixel resolution 30 m) across the Eugen Seibold coral mounds, and locations of the seven box corer stations (see Table 5-2) with live or dead corals, as well as three areas selected for estimation of coral mound density (Figure 5-4). With the exception of CTD station MSM32-1-1, situated further north beyond the currently known boundaries of the coral mound site (Figure 5-1), the locations of the other ten CTD stations were essentially identical or very close to those of the box corer stations (see Table 5-1). Bottom Bathymetric profile 1 crosses the site from its shallowest to its deepest part, profile 2 incorporates a coral mound with living CWCs, and profile 3 a coral mound with dead corals (box corer stations MSM32-49-2 and 46-1 respectively). V.E. = Vertical Exaggeration.

Table 5-1. CTD stations off Morocco during cruise MSM32 (present study), and off Mauritania (cruise MSM16/3) and in the Gulf of Cadiz (cruise MSM1/3 (for data sources, see main text). T, S, density and oxygen values are given for the deepest sampling locations.

Station Number	Date	Time (UTC)	Bottom Depth[a] (m)	Lat. (°N)	Long. (°W)	*Lophelia pertusa*	Conserv. T (Θ) (°C)	Absolute S (S_A) (g/kg)	Density σ_Θ (kg/m)	Oxygen (ml/l)
Cruise MSM32										
MSM32-41-1	24.10.13	16:09	90	30°18.170	09°47.440	unknown	15.56	36.403	26.78	3.78
MSM32-12-1	09.10.13	13:20	2667	30°42.240	10°59.710	unknown	2.71	35.156	27.88	4.77
MSM32-1-1	01.10.13	13:53	4224	32°54.400	10°49.060	unknown	1.65	35.065	27.88	4.6
MSM32-52-1	26.10.13	09:39	619	31°12.740	10°34.491	unknown	10.6	35.704	27.25	3.35
MSM32-51-2[b,c]	25.10.13	18:37	678	31°12.740	10°37.530	living	9.94	35.632	27.31	3.15
MSM32-45-2[c]	26.10.13	14:37	694	31°18.945	10°40.318	dead	10.31	35.678	27.28	3.28
MSM32-3-2[c]	02.10.13	16:39	704	31°08.055	10°36.248	living	9.78	35.632	27.33	3.14
MSM32-50-3[c]	25.10.13	11:02	763	31°09.784	10°38.236	dead	9.64	35.602	27.33	3.07
MSM32-46-2[c]	26.10.13	16:17	794	31°25.094	10°40.067	dead	9.64	35.621	27.35	3.14
MSM32-47-2[c]	26.10.13	17:55	830	31°21.020	10°44.794	dead	8.99	35.572	27.42	3.08
MSM32-48-2[c]	26.10.13	12:38	857	31°12.470	10°42.850	dead	8.89	35.546	27.41	3.01
Cruises MSM16/3 and MSM1/3										
MSM16/3	27.10.10	20:40	504	19°41.990	17°11.479	living	10.1	35.45	27.15	1.42
MSM1/3-193	28.04.06	13:45	1322	35°39.720	07°19.940	dead	8.8	36.103	27.83	4.3
MSM1/3-268	09.05.06	16:46	612	35°21.340	06°51.029	dead	10.77	35.755	27.24	3.95

[a] CTD stopped approx. 5 m above seafloor. [b] Repeated CTD, first single data. [c] CTD at same locations as box cores

5.3.2. Hydroacoustic data

Multibeam bathymetric data were collected by means of the shipboard Kongsberg Simrad EM122 multibeam echo sound system (MBES) operating with a nominal frequency of 12 kHz. Data were processed by QPS Fledermaus and MBE-system software (Caress & Chayes, 1995), including application of local sound velocity profiles, the creation of a CUBE surface (Calder & Mayer, 2003) with a pixel resolution of 30 m, and manual removal of spikes. Coral mound heights and extensions were evaluated from these data for each of three sites within the mound field (Figure 5-2). Mound heights were measured along N–S oriented depth profiles run parallel to the slope, in each case crossing the highest elevation down to the first break in slope. It should be noted that these values represent conservative approximations. A TOBI (Towed Ocean Bottom Instrument) system, comprising a 30 kHz side scan sonar (Flewellen et al., 1993) and 7 kHz sub-bottom profiler, served to collect a nearly 13 km long side scan sonar line across the south-eastern sector of the coral province. Side scan sonar data were corrected for radiometric and geometric artefacts (Blondel, 2009), and processed to a pixel size of approximately 3 m. The system was towed about 500 m above seafloor, producing a swath width of about 6 km (Murton et al., 1992).

5.3.3. Box cores

Based on hydroacoustic mapping, sites were selected for box coring (50 × 50 cm) to enable ground-truthing of seafloor sediments and potential CWC coverage. Seven box cores were taken (Table 5-2) distributed over the entire study area (Figure 5-2).

Table 5-2. Box corer stations off Morocco during cruise MSM32.

Station Number	Date	Time (UTC)	Depth (m)	Lat. (°N)	Long. (°W)	*Lophelia pertusa*
MSM32-49-2	41572	0.630555556	678	31°12.740	10°37.540	living
MSM32-45-1	41572	0.329861111	701	31°18.945	10°40.318	dead
MSM32-3-1	41549	0.629166667	719	31°08.055	10°36.248	living
MSM32-50-2	41572	0.720833333	788	31°09.784	10°38.236	dead
MSM32-46-1	41572	0.397222222	801	31°25.094	10°40.067	dead
MSM32-47-1	41572	0.458333333	835	31°21.039	10°44.794	dead
MSM32-48-1	41572	0.538194444	863	31°12.470	10°42.850	dead

5.3.4. Geochronology

Box core MSM32-3-1 was selected for a comparison of U-Th absolute ages of exposed surface branches of a living Lophelia reef structure with those of buried branch fragments from the underlying sediment. Measurements were conducted on a multi-collector inductively coupled plasma mass spectrometer (MC-ICP-MS, VG-Axiom), following Fietzke et al. (2005). The required mineralogical pre-investigation was based on X-ray diffractometry (XRD, Philips PW-1820). All analyses were performed using GEOMAR facilities. Sample preparation, laboratory treatment and age determination followed Liebetrau et al. (2010). All uncertainties represent the 2 SE level, and the age data are rounded off to decades. Whole procedure blanks matched typical values of ca. 10 pg for U, 2 pg for ^{232}Th and 0.1 fg for ^{230}Th.

5.4. Results

5.4.1. Hydrography

In October 2013, assessments of regional oceanographic conditions characterising the deep-water MSM32-1-1 site to the north of the study area (4224 m water depth) (Figure 5-1, Figure 5-3 and Table 5-1) revealed an upper surface layer of about 30 m with a mean conservative temperature (Θ) of 23.06 °C, absolute salinity (SA) of 36.917 g kg^{-1}, and oxygen concentration of 4.53 ml l^{-1}. Below, the Central Water (CW) masses comprised Subtropical

Under Water (SUW), South Atlantic Central Water (SACW) and North Atlantic Central Water (NACW). The SUW (31–64 m water depth) had Θ between 23.03 °C and 17.73 °C, SA of 36.914 to 36.526 g kg^{-1}, σ_Θ of 25.23 to 26.38 kg m^{-3}, and oxygen values of 4.51 to 5.09 ml l^{-1}. The SACW (65–94 m) had Θ of 17.69 °C to 16.52 °C, SA of 36.535 to 36.483 g kg^{-1}, σ_Θ of 26.38 to 26.66 kg m^{-3}, and oxygen values of 4.67 to 5.10 ml l^{-1}. The top of the NACW (99–860 m) can be delimited by a strong decrease in Θ (from 16.71 °C to 10.75 °C) and in SA (from 36.512 to 36.072 g kg^{-1}). σ varies between 26.60 and 27.52 kg m^{-3} and oxygen values between 4.56 and 3.65 ml l^{-1}. The deeper part of the NACW can be constrained by a minimum SA range of 35.769 to 35.530 g kg^{-1} between 774 and 904 m water depth. Below the NACW, the Mediterranean Outflow Water (MOW, 863–1252 m) can be identified in terms of small Θ variations in the range 10.77–9.71 °C, and elevated SA of 36.088–36.200 g kg^{-1}. σ_Θ ranges from 27.53 to 27.80 kg m^{-3}, and oxygen values from 3.69 to 3.89 ml l^{-1}. Below the MOW at depths of 1250–4224 m, the North Atlantic Deep Water (NADW) had Θ = 1.65 °C, SA = 35.065 g kg^{-1}, σ_Θ = 27.88 kg m^{-3} and $[O_2]$ = 4.60 ml l^{-1} (Figure 5-3). In the vicinity of two living CWC sites discovered during the cruise – MSM32-3-2 and MSM32-51-2 at 704 and 678 m water depth respectively (see below) – local bottom water masses comprise the deeper part of the NACW. The deeper site at 704 m had Θ = 9.78°C, SA = 35.632 g kg^{-1}, oxygen = 3.14 ml l^{-1}, whereas the shallow site at 678 m had Θ = 9.94 °C, SA = 35.632 g kg^{-1}, oxygen = 3.15 ml l^{-1} (Table 5-1). Conservative temperature and absolute salinity are lower than those of the deep MSM32-1-1 station in 700 m water depth, exhibiting Θ = 10.79 °C, SA = 35.807 g kg^{-1} (Figure 5-3).

5.4.2. Hydroacoustic data

Seafloor bathymetric data (Figure 5-2) reveal that the mapped mound field extends up to 40 km alongslope (north to south) and up to 13 km downslope (east to west), covering an area of about 410 km^2. Cold-water coral mounds occur between 678 and 863 m water depth, immediately downslope of a relatively flat 'plateau' on the upper continental slope (Figure 5-2). Individual mounds have circular to elliptical shapes in planform, and reach maximum heights of up to 12 m in the shallower part of the mound field. However, heights between 4 and 8 m are dominant (Figure 5-2). Lengths of mound axes vary between 80 and 240 m, the longer axis being E–W aligned parallel to the direction of slope inclination. Maximum slope angle (12°) and maximum height (12 m) of individual mounds tend to decrease with increasing water depth (Figure 5-4), as does the density of mounds.

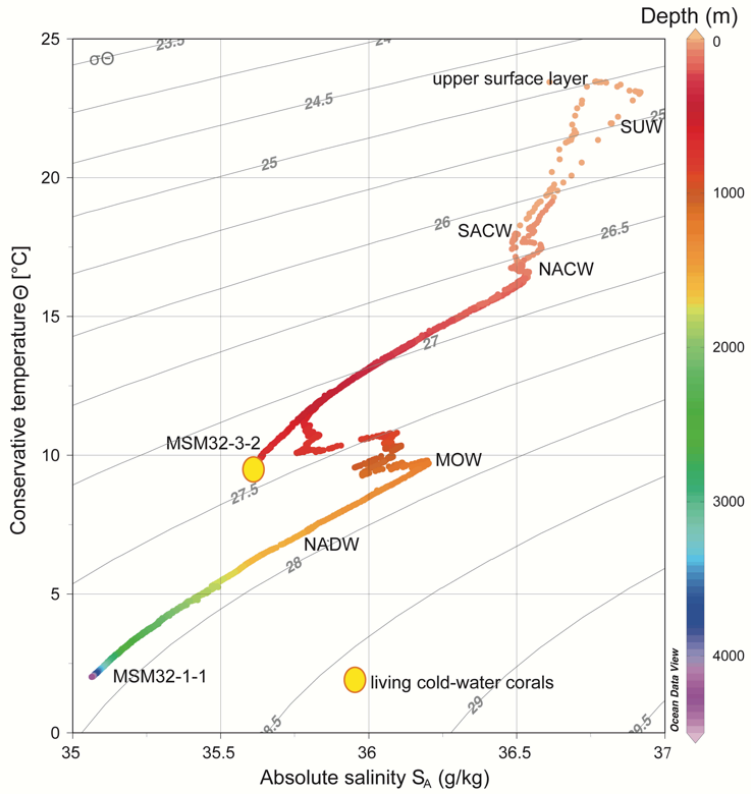

Figure 5-3. T–S plot (Θ = conservative temperature, S_A = absolute salinity) for CTD stations MSM32-1-1 (see Figure 5-1 for location) and MSM32-3-2 (location as for box corer station MSM32-3-1 in Figure 5-2). Water masses comprise (from shallowest to deepest) an upper surface layer, Subtropical Under Water (SUW), South Atlantic Central Water (SACW), North Atlantic Central Water (NACW), Mediterranean Outflow Water (MOW), and North Atlantic Deep Water (NADW). Living CWCs, especially *Lophelia pertusa*, occur in the deeper part of the NACW roughly 150 m above the MOW characterised by still relatively elevated salinities and limited variation in temperature. Isopycnals are calculated with the reference pressure at 0 m (σ_Θ), i.e., sea level.

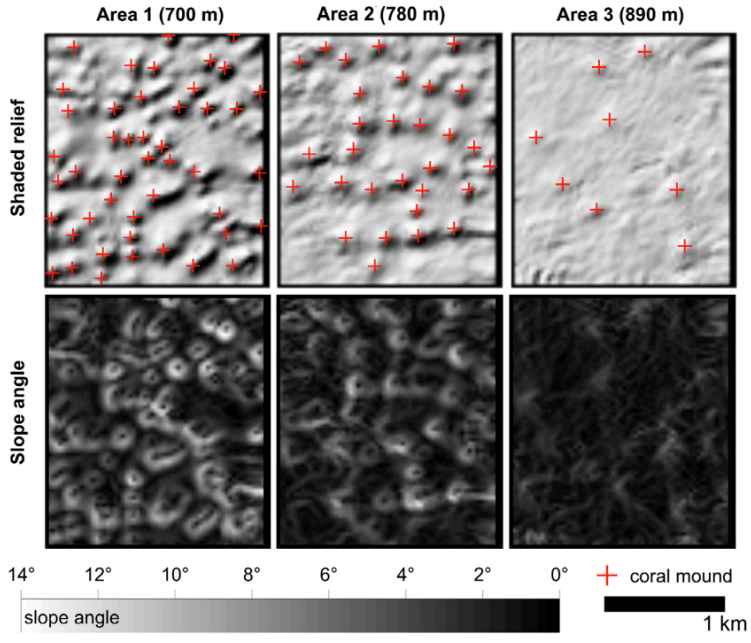

Figure 5-4. Shaded relief (top row) and slope map (bottom row) across selected coral mound areas at three different water depths based on multibeam bathymetry data. Abundance, elevation and slope of coral mounds decrease as water depths increase from area 1 to area 3 (700, 780 and 890 m respectively). See Figure 5-2 for locations of selected areas.

Densities of mounds with slope inclinations larger than approx. 3° were assessed in three areas, each 4 km² in size (Figure 5-2). Mound density varied from 12 mounds/km² (area 1) at about 700 m water depth, to 8 mounds/km² (area 2) at about 790 m water depth, and 2 mounds/km² (area 3) at about 880 m water depth (Figure 5-4 and Figure 5-5). The individual mound-like structures appear as areas of higher backscatter (bright) in TOBI side scan sonar data compared to the lower backscatter of the surrounding seafloor (Figure 5-6). Acoustic shadows (black) are commonly observed on the flanks of the steeper mounds. Shallower settings with more elevated mounds (~700 m water depth) display higher backscatter intensities compared to deeper settings (> 750 m) with less elevated mounds (Figure 5-6).

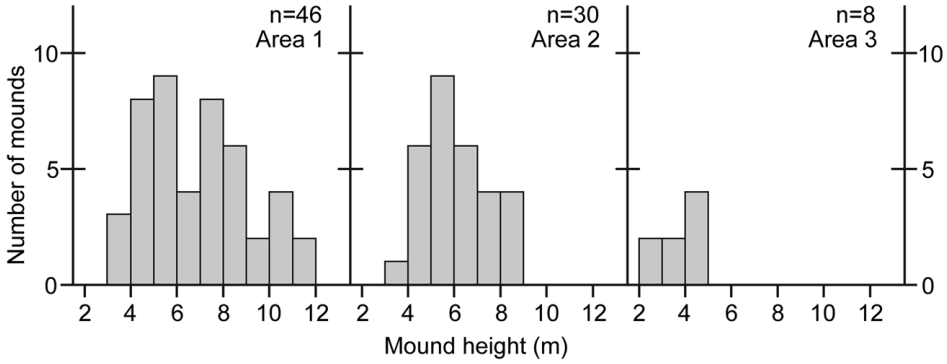

Figure 5-5. Number of mounds with respect to height for the three selected areas (each 4 km²) shown in Figure 5-4. Mound height decreases from shallower depths of area 1, where living corals have been sampled, to deeper depths of area 3. Mean elevation and standard deviation for area 1 = 6.9 ± 2.2 m, area 2 = 6.0 ± 1.4 m, and area 3 = 3.6 ± 1.0 m. Refer to Figure 5-2 for area locations.

5.4.3. Box cores

All seven box cores (see Figure 5-2 and Table 5-2) contained fragments of dead CWCs. The three box cores from the deeper sites (MSM32-46-1, 801 m; MSM32-47-1, 835 m; MSM32-48-1, 863 m) recovered 18–40 cm of a sandy to silty, light and pale brownmud containing dead *Lophelia pertusa* bioclasts of up to 2 cm. Most of the *Lophelia* branches are fragmented down to the size of one polyp. Two shallower box cores (MSM32-45-1, 701 m; MSM32-50-2, 788 m) sampled abundant dead *Lophelia* thickets up to 8 cm long.

These are commonly accompanied by bivalve shells embedded in sandy to silty brown mud, with a maximum recovery of 15 cm. The abundance of bioclasts was more than twice as high in box core MSM32-50-2 and well exposed at the surface, in contrast to all other cores with dead CWC material. Box cores MSM32-49-2 (678 m) and MSM32-3-1 (719 m) contained large specimens of mainly dead but also a few living *Lophelia*. In box core

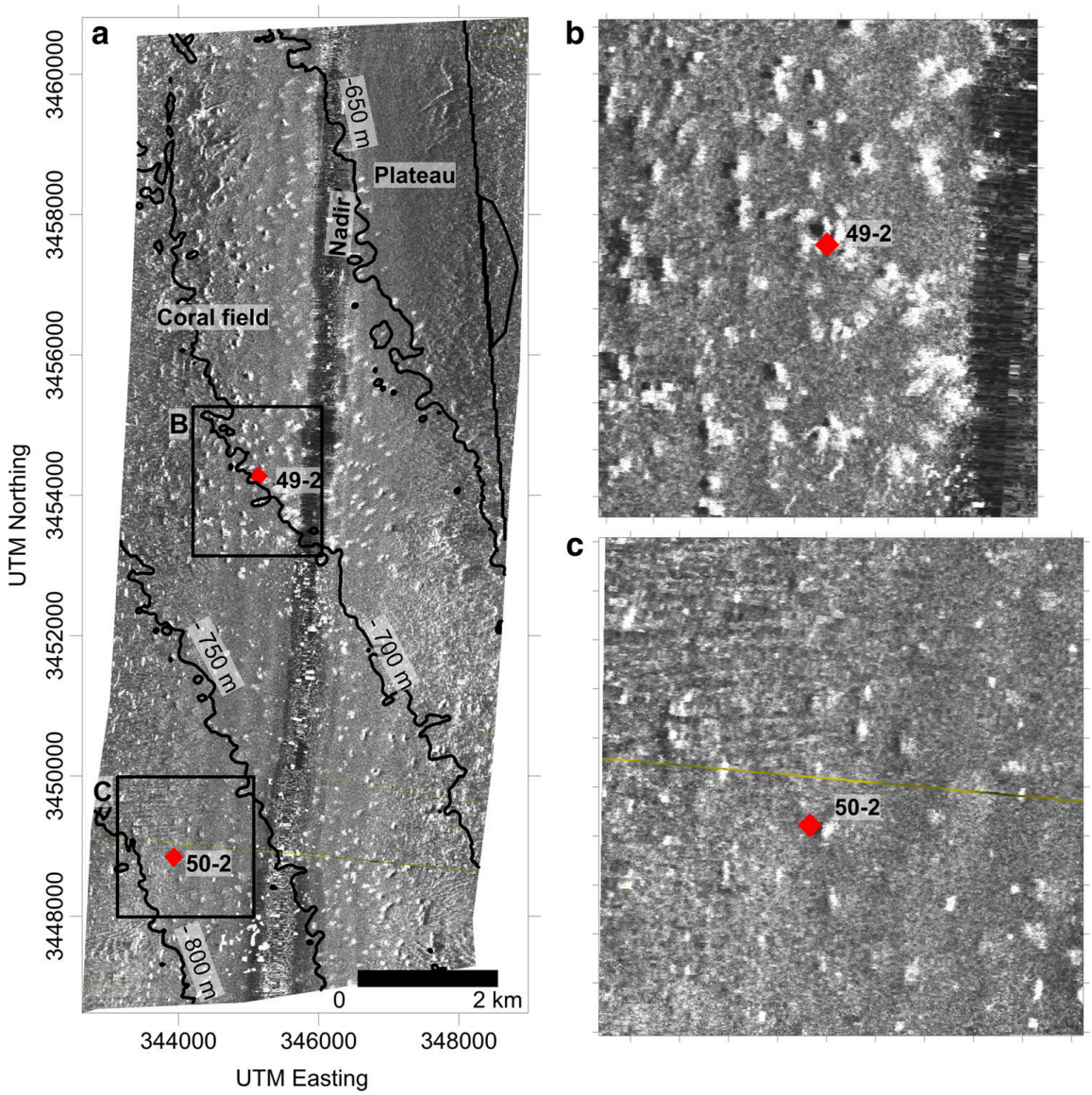

Figure 5-6. Left: TOBI side scan sonar (30 kHz) imagery across the carbonate mound province (swath width = 6 km). Individual coral mounds are recognized by high acoustic backscatter on flanks inclined towards the side scan sonar track, and low backscatter shadows on the lee sides. Right: Higher-resolution imagery in the vicinity of two box corer stations (red stars); top right: MSM32-49-2, with living corals; bottom right: MSM32-50-2, with dead corals. For corresponding locations in study area, see Figure 5-2.

MSM32-3-1, living branches of *Lophelia* exhibited up to 15 consecutive living polyps. Moreover, this box core had a single, live *Madrepora oculata* and *Desmophyllum* sp. specimen (Figure 5-7). The coral framework stood well above the sediment between 10 and 20 cm. Further downcore, coral fragments and bioclasts associated with brown silty to sandy mud were recorded to at least 25 cm (maximum recovery). These shallower core sites are located within area 1 where highest elevations of coral mounds occur (see above). The box core sites deeper than 800 m are located within area 3 where the mounds are less elevated and less abundant (Table 5-2, Figure 5-2, Figure 5-4 and Figure 5-5). These cores recovered only dead CWCs, except for box core MSM32-50-2 (788 m; see above) which also contained

a single living polyp of *Lophelia pertusa*, unlike box core MSM32-3-1 (719 m) earmarked by more profuse live corals. In all box cores *Lophelia pertusa* is by far the dominant CWC species.

Figure 5-7. Photograph showing the contents of the box core recovered from station MSM32-3-1. The large colony of *Lophelia pertusa* (1) exhibits up to 15 consecutive living polyps in one branch. *Madrepora oculata* (2) settled on dead branches of *Lophelia pertusa*, which evidently collapsed prior to settlement as indicated by the different orientation of the polyps of both corals. This is the only living *Madrepora oculata* recovered during the cruise. *Desmophyllum* sp. (3) settled also on dead *Lophelia pertusa* branches. In this box core, the numerous dead corals partly buried in the muddy, bioclast-rich sediment comprise only *Lophelia pertusa*. Among the coral debris, a few bivalves occur. See Figure 5-2 for location of box core station.

5.4.4. Geochronology

U-Th isotope systematics (Table 5-3) were determined for the youngest parts of growing (live) *Lophelia* branches recovered above the sediment surface, and for macroscopically altered material buried at 25 cm sediment depth (maximum penetration depth of box core MSM32-3-1, 719 m water depth). All analysed samples had aragonite contents exceeding 98 %. Based on Liebetrau et al. (2010), and in addition to the common detrital Th correction, the data were normalised in terms of a potentially site-specific initial $^{230}Th/^{234}U$ activity ratio of 0.0005 ± 0.0002, here deduced from three live juvenile branch tops. These integrate only the youngest 2 to 4 mm of sub-recent skeletal growth and are therefore assumed to provide zero age reference values. Their $\delta^{234}U$ signature of 149 ± 2.5 ‰ is in good agreement with the modern seawater reference of 146.8 ± 0.4 ‰ (2 SE) proposed by Andersen et al. (2010). The growth systematics of this reef structure spanning approximately 40 cm (Figure 5-7) enabled the identification of a root-like segment at its base with a

maximum age of 60 ± 20 years before present (BP) and a modern seawater matching initial $\delta^{234}U$ value of 147.3 ± 2.1 ‰. Uth data on two branch fragments from 25 cm sediment depth revealed ages of 1810 ± 30 years BP (initial $\delta^{234}U$ of 144.2 ± 2.2 ‰) and 2680 ± 30 years BP (initial $\delta^{234}U$ of 141.9 ± 2.4 ‰). Inherently, the different degree of morphologically visible alteration implies the former as more reliable than the latter. This is supported by the fact that only the former fragment displays a within error modern seawater matching initial $\delta^{234}U$ value.

Table 5-3. U-Th isotope systematics and age determination of *Lophelia pertusa* from box core MSM32-3-1-1 (719 m water depth), cruise MSM32 off Morocco (uncertainties at 2 SE level).

Lab. code	Ident no.	Descript.	Depth in core (cm)	Aliquot mass (mg)	^{238}U (µg/g)	^{232}Th (ng/g)	$^{230}Th/^{232}Th$	$^{230}Th/^{234}U$[a]	$\partial^{234}U_{(o)}$[b]	$\partial^{234}U_{(t)}$[c]	Age (yr BP)
Juvenile branch tops											
969-14	# 3	juvenile	approx. 15 cm above sedim.	38	4.08 ±0.02	1.036 ±0.011	9.3 ±0.3	*0.00062 ±0.00003*	147.6 ±2.1		0
971-14	# 13			83	3.97 ±0.02	0.464 ±0.003	9.8 ±0.4	*0.00030 ±0.00001*	151.5 ±2.2		0
970-14	# 15			51	3.31 ±0.01	0.509 ±0.004	11.0 ±0.5	*0.00045 ±0.00002*	147.8 ±2.3		0
Average					3.79 ±0.48	0.670 ±0.637	10.0 ±1.0	*0.00046 ±0.00019*	149.0 ±2.5		0
Oldest growth segment of sub-recent reef structure											
968-14	# 4	root	0	109	3.50 ±0.01	1.765 ±0.010	7.6 ±0.2	0.00053 ±0.00019	147.3 ±2.1	147.3 ±2.1	60 ±20
Buried branch fragments of strong or slight macroscopic alteration status											
978-14	# 8	strong alt.	25	127	3.74 ±0.02	0.616 ±0.004	525.4 ±4.7	0.02422 ±0.00026	140.9 ±2.4	141.9 ±2.4	2680 ±30
979-14	# 9	slightly alt.	25	141	3.42 ±0.01	0.288 ±0.002	707.5 ±7.7	0.01647 ±0.00024	143.5 ±2.2	144.2 ±2.2	1810 ±30

[a] *Italics*: $^{230}Th/^{234}U$ activity ratios corrected only for inherited ^{230}Th by application of $^{230}Th/^{232}Th$ activity ratio of 0.75±0.2 (cf. Wedepohl 1995)

[b] (meas. $^{234}U/^{238}U$ act. ratio – 1) × 1000

[c] ($^{234}U/^{238}U$ act. ratio at zero age – 1) × 1000 at time t = U/Th age; measured $^{234}U/^{238}U$ back-calculated for ^{234}U decay since precipitation based on individual U-Th age

5.5. Discussion

Hydrographic measurements above the Eugen Seibold CWC mounds (between 65 and 863 m water depth) revealed that the oceanic water column is controlled mainly by the interaction of SACW and NACW with underlying MOW, which enters the Atlantic Ocean via the Strait of Gibraltar (Figure 5-1 and Figure 5-3). The subsurface SACW flows northwards and typically displays lower salinity, oxygen depletion and nutrient enrichment (Arístegui et al., 2009) relative to the deeper southwardflowing NACW (Mittelstaedt, 1991; Pastor et al., 2008; Vandorpe et al., 2014). The MOW is characterised by a very small temperature gradient, but shows a marked increase in salinity and density between 863 and

904 m water depth (Figure 5-3). These water mass signatures are similar to those documented by Mittelstaedt (1991) and Pelegrí et al. (2005) off northwest Africa (25–35 °N, and Cape Ghir at 30–36 °N). According to Dullo et al. (2008) and Flögel et al. (2014), most of the pristine and profuse live CWC coral reefs along the European continental margin occur at water mass densities of σ_Θ = 27.35-27.65 kg m^{-3}. Living CWCs of the Eugen Seibold province at water depths between 678 and 719 m with density values of about σ_Θ = 27.33 kg m^{-3} correspond to the deeper part of the NACW. Their occurrence is therefore just above the defined density window of Dullo et al. (2008), and about 150 m above the upper limits of the MOW (Figure 5-3 and Figure 5-8) identified at about 863 m water depth. Flögel et al. (2014) differentiated between three types of living CWC assemblages. Category I is characterised by dense horizontal and, most importantly, vertical reef growth, category II by patchy growth with colonies of some square meters, and category III by smaller and commonly more widely scattered isolated colonies. Living CWCs in the present study area

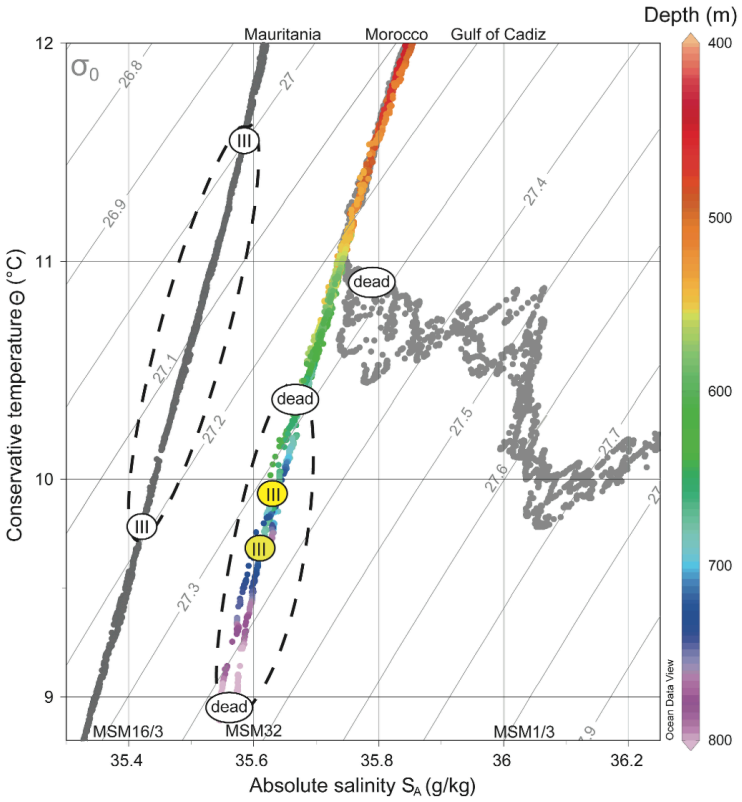

Figure 5-8. Detailed T–S plot (compare Figure 5-3) of water masses bathing living and dead CWCs of the Eugen Seibold coral mounds north of Agadir Canyon (cruise MSM32 of the present study, color), compared with dead CWC sites in the Gulf of Cadiz (cruise MSM1/3, light grey) and living CWC sites off Mauritania (cruise MSM16/3, dark grey). Dashed ellipses Temperature–salinity occurrence range of dead CWCs; yellow, white circles living CWCs, all category III of Flögel et al. (2014). Isopycnals are calculated with the reference pressure at 0 m (σ_Θ), i.e., sea level.

are attributed to category III. This category is further supported by lower oxygen values of 3.14–3.15 ml l^{-1} at the study sites, contrasting with a global mean of around 6 ml l^{-1} for ambient water masses around flourishing CWC reefs (Davies et al., 2008). The classification of three categories in combination with seawater density works well in the Atlantic, but cannot be applied to the Mediterranean due to its higher density and higher alkalinity (Flögel et al., 2014).

Although the information available to date from box cores represents only snapshots of the coral mounds, the general distinction between living mounds clustering around 700 m water depth and dead mounds in deeper waters (Figure 5-2, Figure 5-3 and Figure 5-8) is supported by the acoustic data (Figure 5-4). Contrasting with presumably dead mounds, areas inhabited by living CWCs generally have more elevated (up to 12 m) and more steeply (up to 12°) inclined mounds (Figure 5-4 and Figure 5-5) associated with higher backscatter intensities (Figure 5-6). One might argue that high mounds may result from the higher baffling capacity of CWC fabrics. Less elevated mounds with lower slope inclinations may be a sign of partial burial of dead CWCs, which may explain the reduced occurrence of mounds in such areas. Another mechanism could be that the bathymetrically deeper mounds are already affected by erosion, but this awaits confirmation by additional optical ground-truthing and dating.

A similar situation has been described for CWC mounds off Mauritania, e.g., the Banda Mounds at 17–18° N, which were actively growing from 65 to 57 ka, 45 to 32 ka, and at about 14 ka (Eisele et al., 2011). The Banda Mounds are bathymetrically above the density envelope of Dullo et al. (2008) ($\sigma_\Theta = 27.5 \pm 0.15$ kg m^{-3}), and are also situated within the lower part of the NACW (RV Maria S. Merian cruise MSM16/3 in October 2010, Westphal et al. (2012); see Figure 5-8). Today, these mounds show only a very thin cover of living Lophelia between 415 and 570 m water depth, corresponding to category III of Flögel et al. (2014). The Renard Ridge (35° N) in the Gulf of Cadiz (GoC) is another prominent region of CWC mound occurrence; however, there are no living CWC colonies reported so far (Foubert et al., 2008; Wienberg et al., 2009; Wienberg et al., 2010). These dead CWCs are today found at relatively shallow water depths typified by densities not exceeding $\sigma_\Theta = 27.5 \pm 0.15$ kg m^{-3} (RV Maria S. Merian cruise MSM1/3 of January 2006, Pfannkuche et al. (2006); see Figure 5-8). There is evidence that, over the last 400 ka, these reefs also flourished during glacial times and up to the very early Holocene (Wienberg et al., 2010).

Although Davies and Guinotte (2011) predict a high suitability for CWC growth, especially of *Lophelia pertusa*, between the GoC and Mauritania, to date living CWCs have been found only off Mauritania (17°–18° N) and now off western Morocco (31° N) as small isolated colonies or forming a thin and patchy cover. Vigorous and extensive CWC reef growth apparently occurred only during glacial times in this region, which would explain why the few modern living colonies reported to date do not match bathymetrically with the water mass density values known for CWC reefs belonging to category I of Flögel et al. (2014). The Eugen Seibold coral mounds exhibit a few living colonies (albeit based on limited sampling), and most sampled mound structures consist of a dead fabric.

Dating of a large living coral branch indicated a time span of 60 ± 20 years BP from the base to its living topmost part. The large uncertainty of ± 20 years mainly results from the correction for the initial $^{230}Th/^{234}U$ activity ratio. This implies a mean growth rate of 0.5 to 1 cm a^{-1}. An alternative age estimate is provided by counting the number of polyps in straight succession from the root segment to the juvenile top, which on average could correspond to the number of years according to Freiwald (2002). Resulting in 30 ± 5 polyps (varying with the sub-branch to follow), this approach suggests a slightly younger age. Based on $CaCO_3$ accumulation rates of $8.70 \pm 3.18 \cdot 10^{-3}$% per day (Form & Riebesell, 2012), the maximum mass of 465 g of the dated branch implies a similar value of $9 \pm 2 \cdot 10^{-3}$ % per day in terms of polyp counting age, and $5 \pm 2 \cdot 10^{-3}$ % per day in terms of U-Th age. Deducing in first approximation a local sediment accumulation rate from the most reliable age of the dead fragments (1810 ± 30 years BP) and the observed burial depth results in 14 cm ka^{-1}. This is consistent with the background flux of 12.15 ± 0.6 cm ka^{-1} for the nearby Canary Basin reported by Henderiks et al. (2002).

In their overview of north-eastern Atlantic CWC reefs and climate change, Frank et al. (2011) argue that CWC reefs were growing south of 50° N predominantly during the last glacial periods and the deglacial on the Armorican margin (Reveillaud et al., 2008), the Iberian margin (Hernández-Molina et al., 2011), in the GoC (Wienberg et al., 2009; Wienberg et al., 2010) and the Banda Mounds (Eisele et al., 2011; Eisele et al., 2014), including the Mediterranean (Savini et al., 2014), with the exception of sites in the Alboran Sea still growing until 5 ka (Fink et al., 2012). This would be in contrast with the CWC reef formation north of 50° N being constrained to interglacials, including the late Holocene (Rüggeberg et al., 2007; Frank et al., 2009; Raddatz et al., 2013). The predominantly dead CWC assemblages of the newly discovered Eugen Seibold coral mounds off western

Morocco may support the hypothesis of Frank et al. (2011). However, the initial dataset displays CWC growth since about 2 ka at least. Therefore, interglacial growth periods cannot be excluded in general south of 50° N, as demonstrated also by the discovery of live juvenile corals in the present case. Providing a more comprehensive record of emplacement time intervals for the Eugen Seibold coral mounds requires more detailed archives, notably a drill core through at least one of the major mound structures well identified in this study.

5.6. Conclusions

The newly discovered Eugen Seibold coral mounds off western Morocco extend over more than 410 km^2, associated with known oceanographic settings of CWC occurrences along the north-eastern Atlantic margin. Mounds with living CWCs occur in a bathymetric range between 678 and 719 m characterised by *Lophelia pertusa*, at one site accompanied by a single *Madrepora oculata* excrescent and a single *Desmophyllum* sp. specimen. Most CWCs are represented by dead thickets which are more fragmented in the mounds at deeper water depths (> 710 to 860 m). Shallower mounds are more elevated (12 m) and exhibit higher backscatter in contrast to mounds at deeper sites. Absolute ages of dead coral fragments indicate growth since the late Holocene at least, and imply a sediment accumulation rate of about 14 cm ka^{-1}. These initial geochronological results and the patchy distribution of the cold-water corals suggest recolonization of this area by Lophelia, rather than the continuous evolution of large flourishing reef build-ups. This interpretation for the Eugen Seibold coral mounds awaits confirmation based on additional evidence from optical ground-truthing and dating of longer downcore records.

5.7. Acknowledgments

We acknowledge the superb support by the captain and crew as well as the scientific shipboard party during cruise 32 aboard the RV Maria S. Merian, and the German Science Foundation (DFG) for funding ship time and providing financial support (Du 129/48-1). R.B.W. and the NOC TOBI team were supported by NERC grant NE/J012955/1. We are grateful to Dr. Gemma Ercilla of CSIC, Barcelona for providing analogue TOPAS profiles which enabled us to target the coral mound province. In addition, thanks go to Dr. Steffen Hetzinger for providing data collected during cruise MSM16/3, Anke Bleyer and Bettina Domeyer for their helping hand in preparing the cruise, Jutta Heinze for XRD analyses, Ana Kolevica for clean-lab support (all from GEOMAR), Dr. Jan Fietzke for high performance

level of the Axiom MC-ICP-MS facility, Prof. A. Eisenhauer for unrestricted scientific and infrastructural support, and Prof. Peter Brandt for valuable discussions on water mass structures. Detailed comments provided by two anonymous reviewers, Prof. A. Foubert (Fribourg) and the editors proved useful in improving the paper.

6. Summary, major conclusions and implications

As part of this dissertation, core samples from living colonies of massive growing *Diploria strigosa* corals from Little Cayman, Cayman Islands, were used as archives of past surface ocean conditions based on the geochemistry of the corals' carbonate skeleton. These coral cores allowed for the first time the production of multidecadal to century long proxy time series from the central Caribbean Sea displaying high temporal resolution and extending beyond the period of observational records. The geochemical multi-proxy records were generated from cores that stem from different reef environments, thereby enabling the investigation of both regional- and reef-scale environmental variability. The following paragraphs summarize the major conclusions and implications from the previous chapters

6.1. Reef-scale environment

A study comparing coral Sr/Ca data from massive *Diploria strigosa* corals growing in adjacent but distinct reef environments (fore reef, lagoon) and gridded reanalysis SST data from 1970 to 2012 point to local reef-scale temperature variability, which cannot be resolved by gridded SST data. Specifically, the data show that a calibration of the lagoon Sr/Ca record with gridded SST, although augmented with in-situ observations from NOAA's CREWS station (in operation since 2009) situated in the fore reef zone, would lead to an underestimation of the true temperature range inside the lagoon.

The study also indicates that the two corals responded differently to past warming events. Coral Sr/Ca data from the shallow lagoon successfully record high summer temperatures confirmed by in situ observations (> 33°C). In contrast, Sr/Ca ratios in the deeper fore reef are strongly affected by El Niño related thermal events (high mean Sr/Ca and reduced seasonal amplitude), although seasonal temperature extremes and mean SSTs at this site are reduced compared to the lagoon. The results suggest that *Diploria strigosa* from the fore reef is more susceptible to short-term high temperature events and consequently reacts with stress symptoms. *Diploria strigosa* from the shallow lagoon environment shows a higher level of resilience because it may already be adapted to an environment with rapid thermal fluctuations and higher maximum temperatures. Additionally, the shallow lagoon coral showed decadal variations in Sr/Ca, supposedly related to the modulation of lagoonal temperature through a varying volume of tidal water, forced by the 18.6-year period lunar nodal cycle.

The study shows that reef-scale SST variability can be much larger and site specific than suggested by satellite SST measurements. *Therefore, using coral SST proxy records from different reef zones, combined with in situ observations, will not only improve paleotemperature reconstructions, it will also help conservation programs that are developed to understand, monitor and better manage the complex interactions leading to coral bleaching to identify the environmental conditions that appear to promote coral resilience during thermal events.*

6.2. Regional- to large-scale climate and external climate modes

In a following study, the entire 125-year (1887–2012) record of coral $\delta^{18}O$ and Sr/Ca variations from the fore reef core is described and interpreted, representing the longest continuous seasonal resolution record from a *Diploria strigosa* coral in the Atlantic to date. Both geochemical proxies show decreasing long-term trends, indicating long-term warming. Sr/Ca indicates much stronger regional warming than large-scale grid-SST data, while $\delta^{18}O$ tracks large-scale SST changes in the AWP. The results support the assumptions of previous observational studies, which suggest that Sr/Ca is a better indicator of local changes in temperature, while $\delta^{18}O$ seems to be a better indicator of large-scale/regional scale SST changes. Seawater $\delta^{18}O$ variations ($\Delta\delta^{18}O_{sw\text{-}center}$) are successfully captured by the coral proxy record using paired Sr/Ca and $\delta^{18}O$ measurements. The $\Delta\delta^{18}O_{sw\text{-}center}$ signal shows a high inverse correlation with the AMO until the mid-1970s, then decouples from the AMO signal and shifts to a steadily increasing regime, i.e., precipitation decreases while temperature increases. An overall linear trend towards higher $\Delta\delta^{18}O_{sw\text{-}center}$ also indicates a drying trend over the past century. A continued drying and increase in temperature could have important socioeconomic consequences in the Cayman Islands and in the whole region due to its environmental implications.

The coral $\delta^{18}O$ data show high spatial correlations with SST in the region of the Loop Current and Gulf Stream system. More specifically, the $\delta^{18}O$ data tracks changes in NAO variability on both the decadal and the multidecadal time scales within that region. *Thus, the central Caribbean proxy data generated here contribute new insights into the temporal and spatial nonstationarity of the NAO and can help to specifically investigate its impact on the western Caribbean and the Gulf Stream region. Moreover, these new proxy reconstructions can be compared with model-generated fields of forced (external and internal) and natural variability over the last centuries.* The combined evaluation of the Little Cayman coral $\delta^{18}O$

record and two other records from different Caribbean sites reveals a large total spatial coverage of high correspondence between coral $\delta^{18}O$ and SST variability, comprising principal elements of the North Atlantic subtropical gyre. *This result is a clear demonstration of the potential of proxy data to provide information on SST variability for regions where no instrumental measurements or proxy archives are available as well as to reconstruct the climate system in periods prior to the instrumental record. Thereby the new central Caribbean proxy reconstructions from this thesis help to increase the density and distribution of proxy data over large geographical areas. This is important for gaining more internally consistent and spatially coherent insights into past climatic variability not covered by instrumental data, particularly with regard to model simulations, which tend to underestimate or lack distinct signatures of regional changes related to NAO and ENSO.*

6.3. Caribbean nitrogen fixation

As a secondary objective of the present work, the first centennial-scale record of annual nitrogen isotope data from a Caribbean coral is presented in the context of a short third study. The 94-year record is based on coral material from the fore reef core. *The new finding is that changing nitrogen fixation as interpreted from Caribbean coral nitrogen isotopes is negatively correlating with multidecadal temperature variability in the North Atlantic Ocean throughout the last century, and that Atlantic Ocean circulation may drive the century scale variation of nitrogen fixation in the Caribbean Sea.* A possible controlling factor of nitrogen fixation variations is the changing amount of phosphorus rich water supplied to the Caribbean through the South Equatorial Current. This supply is modulated by AMOC related ocean circulation variability, which also drives the phase changes of the AMO by controlling Atlantic Ocean heat content. However, during the 20th century the $\delta^{15}N_{coral}$ record indicates an overall linear decreasing trend of Caribbean nitrogen fixation. The reason may be increasing average SSTs above the optimum SST for *Trichodesmium* (27 °C) leading to a decrease of this primary nitrogen fixing cyanobacterium. Another possible reason is the global warming related weakening of the AMOC, which has been proposed in some recent studies and could also lead to decreased Caribbean nitrogen fixation caused by decreasing phosphorus supply to the Caribbean through the South Equatorial Current. The North Atlantic Ocean is a major source of fixed nitrogen to the global ocean. *Based these findings it may be speculated that ongoing trends, related to global warming, may lead to a*

reduction in nitrogenous nutrients in the future with an imbalance in the oceans nitrogen budget.

6.4. Cold-water corals

The fourth and final study contributes to the current and incomplete knowledge of the distribution and living conditions of cold and dark dwelling warm water coral relatives and draws attention to the global aspect of scleractinian corals as climate and paleoceanographic archive for surface ocean to deep ocean conditions. The study reports on the newly discovered Eugen Seibold CWC province between 678 and 863 m water depth off western Morocco covering an area of more than 410 km^2. Mounds with living CWCs occur in a bathymetric range between 678 and 719 m and are dominated by *Lophelia pertusa*. The deepest mounds are composed of dead and fragmented *Lophelia pertusa* branches. Shallower mounds are more elevated (12 m) and exhibit higher hydroacoustic backscatter in contrast to mounds at deeper sites. Temperature, salinity and seawater density measurements indicate that living CWC colonies occur within the deeper part of the NACW. U-Th isotope systematics for macroscopically altered buried *Lophelia pertusa* material yielded absolute ages dating back to the late Holocene. These initial geochronological results and the patchy distribution of the cold-water corals suggest recolonization of this area by *Lophelia pertusa*, rather than the continuous evolution of large flourishing reef build-ups.

By providing hydroacoustic data of a newly discovered CWC mound province the study also makes an important contribution to urgently needed high-resolution seafloor mapping data to identify and spatially quantify CWC systems. The global area of living and dead CWCs as well as extensive data of carbonate accumulation rates of CWC ecosystems are necessary to evaluate the contribution of CWC mounds and other CWC factories to the global carbonate budget today and in the past.

7. Future work

The results obtained from this dissertation demonstrate that massive growing *Diploria strigosa* corals from Little Cayman are sensitive recorders of both past local environmental changes and large-scale climate variability beyond the central Caribbean region. The investigations of the two coral records from different reef environments can be regarded as case studies for the development of longer coral records from Little Cayman extending well past industrial times. The sampling of correspondingly large colonies was not possible during the initial campaign due to time constraints. These records could help to reveal the frequency of warming events and their impact (thermal stress) to the local reef further back in time and, on a larger scale, to gain a better understanding of natural (multidecadal) climate variability in the North Atlantic and the underlying mechanisms. Such data may provide the opportunity to assess the susceptibility of different coral species to episodes of temperatures near or above the corals' optimum temperature of growth. The initial analyses on samples from the present thesis confirm for the first time that this approach is feasible. A better knowledge of natural multidecadal variations is of great significance in order to decipher the substructures, and more importantly, the causes of observed long-term trends in Atlantic climate variables (e.g., SST, precipitation), and hence could possibly help to decouple anthropogenic and natural drivers in these records.

Understanding the modern relationships between environmental variability, coral growth parameters (i.e., linear growth, density and calcification) and coral geochemistry provides the basis for the interpretation of fossil coral records from the same region and helps to assess environmental and climate variability in the geological past. Due to their skeletal mesoarchitecture *Diploria strigosa* corals are well suited for this task. Microsampling is confined to the thick and dense theca wall and does not integrate over different skeletal elements and vacated skeleton, thus diminishing concerns regarding diagenetic alteration of fossil samples, which might result in distortion of the climate signals preserved in the coral skeleton (Hendy et al., 2007; Sayani et al., 2011). Thus, future research at Little Cayman should focus on the development of fossil *Diploria strigosa* coral records, which opens up a possibility to investigate surface ocean dynamics (e.g., changes in water temperature, salinity, nutrients) under different boundary conditions such as warm interglacial periods with no anthropogenic interference. Thereby, the obtained proxy-SST calibrations from modern coral specimens play an important role in the development of long-term

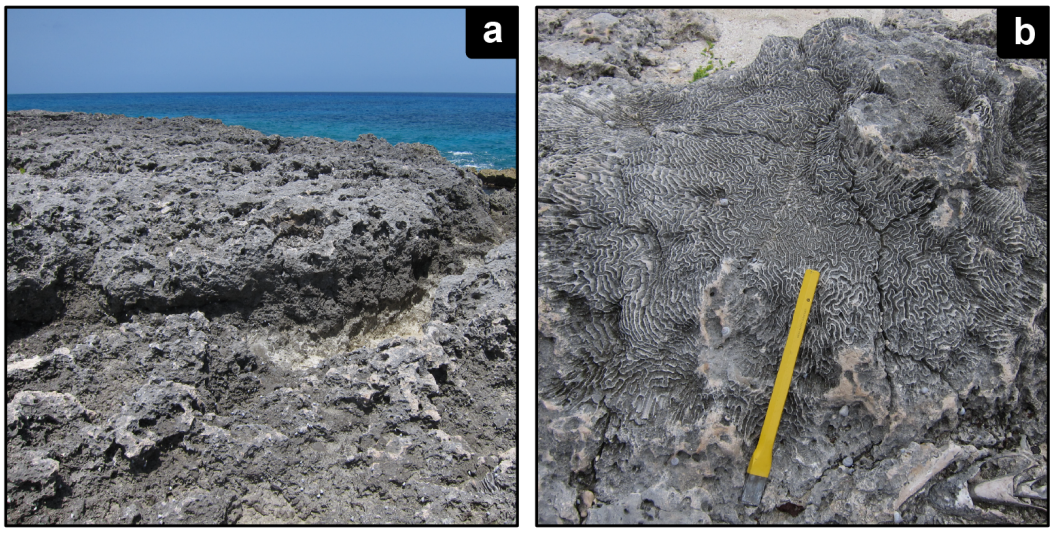

Figure 7-1. Late Pleistocene Ironshore Formation (limestone). (a) Outcrop near Salt Rocks Doc on Little Cayman. (b) Fossil Diploria specimen of the Ironshore Formation (chisel length = 25 cm).

reconstructions of environmental variables. The last interglacial (LIG, Marine Isotope Stage 5e, ~127–117 ka) is the most recent period to have experienced higher than modern seasonality of insolation and remains an important test bed for exploring natural environmental and climate variability during a time of warmer global temperatures as are projected in future-climate-change scenarios (Lunt et al., 2013). The Late Pleistocene Ironshore Formation on Little Cayman (dated at 121 ± 6 ka (Woodroffe et al., 1983)) is a sequence of limestones that was deposited when sea level was about 6 m above present-day sea level (Jones & Hunter, 1990). The Reef Facies of the Ironshore Formation outcrops to form coastal platforms at several places on the island (Figure 7-1). Preliminary data from fossil specimens of *Diploria strigosa* obtained from these platforms show that they can provide decades-long slices of past variability. Recent studies performed on Pleistocene corals from other tropical and subtropical locations were successful in reconstructing climate variability dating back to the LIG (e.g., Winter et al., 2003; Felis et al., 2004; Ayling et al., 2006; Brocas et al., 2016). Fossil corals from Little Cayman potentially yield information on rates and magnitudes of environmental change during the LIG, thus providing critical baseline data for comparison with modern data from the adjacent living coral reef. Mapping and sampling of fossil reef platforms for comparison of coral fauna and associations of the Late Pleistocene with the modern situation could contribute important data to better assess the response of corals to future environmental change. To date, annual resolution proxy data are rarely available from fossil corals from the LIG in the tropical Atlantic (Felis et al., 2015a; Brocas et al., 2016; Brocas et al., 2018) and no data ($\delta^{18}O$, Sr/Ca or $\delta^{15}N$) exists from the central Caribbean from this time period. Coral reefs are facing significant challenges

from climate change and fossil coral data from Little Cayman could assist in developing predictive models of impending threats to local reefs and offer important comparisons for modern reefs in the region and globally. Such information is of high value not only to local conservation efforts and coral reef biologists, but also to the international research community working in the fields of paleoclimatology, paleoceanography, as well as climate modeling.

References

Abram, N. J., Gagan, M. K., Liu, Z., Hantoro, W. S., McCulloch, M. T., & Suwargadi, B. W. (2007). Seasonal characteristics of the Indian Ocean Dipole during the Holocene epoch. *Nature, 445*, doi:10.1038/nature05477.

Adkins, J. F., Boyle, E. A., Curry, W. B., & Lutringer, A. (2003). Stable isotopes in deep-sea corals and a new mechanism for "vital effects". *Geochimica Et Cosmochimica Acta, 67*(6), 1129-1143.

Aharon, P. (1991). Recorders of reef environmental histories: stable isotopes in corals, giant clams, and calcareous algae. *Coral Reefs, 10*, 71-90.

Alibert, C., & McCulloch, M. T. (1997). Strontium/calcium ratios in modern Porites corals from the Great Barrier Reef as a proxy for sea surface temperature: Calibration of the thermometer and monitoring of ENSO. *Paleoceanography, 12*(3), 345-363.

Allan, R. P., & Soden, B. J. (2008). Atmospheric warming and the amplification of precipitation extremes. *SCience, 321*(5895), 1481-1484.

Allemand, D., Tambutté, É., Girard, J.-P., & Jaubert, J. (1998). Organic matrix synthesis in the scleractinian coral Stylophora pistillata: role in biomineralization and potential target of the organotin tributyltin. *Journal of Experimental Biology, 201*(13), 2001-2009.

Allison, N. (1996). Comparative determinations of trace and minor elements in coral aragonite by ion microprobe analysis, with preliminary results from Phuket, southern Thailand. *Geochimica Et Cosmochimica Acta, 60*(18), 3457-3470.

Allison, N., & Finch, A. A. (2004). High-resolution Sr/Ca records in modern *Porites lobata* corals: effects of skeletal extension rate and architecture. *Geochemistry Geophysics Geosystems, 5*(Q05001), doi:10.1029/2004GC000696.

Allison, N., & Finch, A. A. (2007). High temporal resolution Mg/Ca and Ba/Ca records in modern *Porites lobata* corals. *Geochemistry Geophysics Geosystems, 8*(5), doi:10.1029/2006GC001477.

Allison, N., Finch, A. A., Newville, M., & Sutton, S. (2005). Strontium in coral aragonite: 3. Sr coordination and geochemistry in relation to skeletal architecture. *Geochimica Et Cosmochimica Acta*.

Alpert, A. E., Cohen, A. L., Oppo, D. W., DeCarlo, T. M., Gove, J. M., & Young, C. W. (2016). Comparison of equatorial Pacific sea surface temperature variability and trends with Sr/Ca records from multiple corals. *Paleoceanography, 31*(2), 252-265.

Altabet, M. A., Deuser, W. G., Honjo, S., & Stienen, C. (1991). Seasonal and depth-related changes in the source of sinking particles in the North Atlantic. *Nature, 354*(6349), 136.

Alvarez-Garcia, F., Latif, M., & Biastoch, A. (2008). On multidecadal and quasi-decadal North Atlantic variability. *Journal of Climate, 21*(14), 3433-3452.

Alves, J. M. R., Carton, X., & Ambar, I. (2011). Hydrological structure, circulation and water mass transport in the Gulf of Cadiz. *International Journal of Geosciences, 2*(4), 432-456.

Anagnostou, E., Sherrell, R. M., Gagnon, A., LaVigne, M., Field, M. P., & McDonough, W. F. (2011). Seawater nutrient and carbonate ion concentrations recorded as P/Ca, Ba/Ca, and U/Ca in the deep-sea coral Desmophyllum dianthus. *Geochimica Et Cosmochimica Acta, 75*(9), 2529-2543.

Andersen, M., Stirling, C., Zimmermann, B., & Halliday, A. (2010). Precise determination of the open ocean 234U/238U composition. *Geochemistry, Geophysics, Geosystems, 11*(12).

Arístegui, J., Barton, E. D., Álvarez-Salgado, X. A., Santos, A. M. P., Figueiras, F. G., Kifani, S., et al. (2009). Sub-regional ecosystem variability in the Canary Current upwelling. *Progress in Oceanography, 83*(1-4), 33-48.

Asami, R., Felis, T., Deschamps, P., Hanawa, K., Iryu, Y., Bard, E., et al. (2009). Evidence for tropical South Pacific climate change during the Younger Dryas and the Bølling–Allerød from geochemical records of fossil Tahiti corals. *Earth and Planetary Science Letters, 288*(1), 96-107.

Ayling, B. F., McCulloch, M. T., Gagan, M. K., Stirling, C. H., Andersen, M. B., & Blake, S. G. (2006). Sr/Ca and delta O-18 seasonality in a Porites coral from the MIS 9 (339-303 ka) interglacial. *Earth and Planetary Science Letters, 248*(1-2), 462-475.

Beck, J. W., Edwards, L. R., Ito, E., Taylor, F. W., Recy, J., Rougerie, F., et al. (1992a). Sea-surface temperature from coral skeletal strontium/calcium ratios. *SCience, 257*, 644-647.

Beck, J. W., Edwards, R. L., Ito, E., Taylor, F. W., Recy, J., Rougerie, F., et al. (1992b). Sea-Surface Temperature from Coral Skeletal Strontium/Calcium Ratios. *SCience, 257*, 644-647.

Beck, J. W., Récy, J., Taylor, F., Edwards, R. L., & Cabioch, G. (1997). Abrupt changes in early Holocene tropical sea surface temperature derived from coral records. *Nature, 385*, 705-707.

Behrenfeld, M. J., O'Malley, R. T., Siegel, D. A., McClain, C. R., Sarmiento, J. L., Feldman, G. C., et al. (2006). Climate-driven trends in contemporary ocean productivity. *Nature, 444*(7120), 752.

Bender, M. A., Knutson, T. R., Tuleya, R. E., Sirutis, J. J., Vecchi, G. A., Garner, S. T., & Held, I. M. (2010). Modeled Impact of Anthropogenic Warming on the Frequency of Intense Atlantic Hurricanes. *SCience, 327*(5964), 454-458.

Berkelmans, R., & van Oppen, M. J. H. (2006). The role of zooxanthellae in the thermal tolerance of corals: a 'nugget of hope' for coral reefs in an era of climate change. *Proceedings of the Royal Society B: Biological Sciences, 273*(1599), 2305-2312.

Berrisford, P., Dee, D., Poli, P., Brugge, R., Fielding, K., Fuentes, M., et al. (2011). The ERA-Interim archive, version 2.0.

Bigg, G. R., & Rohling, E. J. (2000). An oxygen isotope data set for marine waters. *Journal of Geophysical Research, 105*(C4), 8527-8535.

Blamart, D., Rollion ‐ Bard, C., Meibom, A., Cuif, J. P., Juillet ‐ Leclerc, A., & Dauphin, Y. (2007). Correlation of boron isotopic composition with ultrastructure in the deep ‐ sea coral Lophelia pertusa: Implications for biomineralization and paleo ‐ pH. *Geochemistry, Geophysics, Geosystems, 8*(12).

Blondel, P. (2009). Computer-assisted interpretation. In *The Handbook of Sidescan Sonar* (pp. 249-276). Berlin, Heidelberg: Springer.

Braconnot, P., Harrison, S. P., Kageyama, M., Bartlein, P. J., Masson-Delmotte, V., Abe-Ouchi, A., et al. (2012). Evaluation of climate models using palaeoclimatic data. *Nature Clim. Change, 2*(6), 417-424. 10.1038/nclimate1456.

Breitbarth, E., Oschlies, A., & LaRoche, J. (2007). Physiological constraints on the global distribution of Trichodesmium? effect of temperature on diazotrophy. *Biogeosciences, 4*(1), 53-61.

Brocas, W. M., Felis, T., Gierz, P., Lohmann, G., Werner, M., Obert, J. C., et al. (2018). Last Interglacial Hydroclimate Seasonality Reconstructed From Tropical Atlantic Corals. *Paleoceanography and Paleoclimatology, 33*(2), 198-213.

Brocas, W. M., Felis, T., Obert, J. C., Gierz, P., Lohmann, G., Scholz, D., et al. (2016). Last interglacial temperature seasonality reconstructed from tropical Atlantic corals. *Earth and Planetary Science Letters, 449*, 418-429.

Brooke, S., & Schroeder, W. W. (2007). State of deep coral ecosystems in the Gulf of Mexico region. In E. Lumsden, T. F. Hourigan, A. W. Bruckner, & G. Dorr (Eds.), *The State of Deep Coral Ecosystems of the United States. NOOA Technical Memorandum CRCP-3* (pp. 233-270). Silver Spring, MD.

Brown, B. E. (1997). Coral bleaching: causes and consequences. *Coral Reefs, 16*, S129-S138.

Brown, P. T., Lozier, M. S., Zhang, R., & Li, W. (2016). The necessity of cloud feedback for a basin-scale Atlantic Multidecadal Oscillation. *Geophysical Research Letters, 43*(8), 3955-3963.

Brunt, M., & Davies, J. (2012). *The Cayman Islands: natural history and biogeography* (Vol. 71): Springer Science & Business Media.

Cahyarini, S. Y., Pfeiffer, M., & Dullo, W.-C. (2009). Improving SST reconstructions from coral Sr/Ca records: multiple corals from Tahiti (French Polynesia). *International Journal of Earth Sciences, 98*, 31-40.

Cahyarini, S. Y., Pfeiffer, M., Nurhati, I. S., Aldrian, E., Dullo, W.-C., & Hetzinger, S. (2014). Twentieth century sea surface temperature and salinity variations at Timor inferred from paired coral δ18O and Sr/Ca measurements. *Journal of Geophysical Research: Oceans, 119*(7), 4593-4604.

Cahyarini, S. Y., Pfeiffer, M., Timm, O., Dullo, W.-C., & Garbe-Schönberg, D. (2008). Reconstructing seawater d18O from paired coral d18O and Sr/Ca ratios: Methods, error analysis and problems, with examples from Tahiti (French Polynesia) and Timor (Indonesia). *Geochimica et Cosmochimica Acta, 72*, 2841-2853.

Cairns, S. D. (1984). New records of ahermatypic corals (Scleractinia) from the Hawaiian and Line Islands.

Cairns, S. D., & Stanley, G. D. (1982). Ahermatypic coral banks: living and fossil counterparts.

Calder, B. R., & Mayer, L. A. (2003). Automatic processing of high ‐ rate, high ‐ density multibeam echosounder data. *Geochemistry, Geophysics, Geosystems, 4*(6).

Cane, M. A. (2005). The evolution of El nino, past and future. *Earth and Planetary Science Letters, 230*, 227-240.

Capone, D. G., Burns, J. A., Montoya, J. P., Subramaniam, A., Mahaffey, C., Gunderson, T., et al. (2005). Nitrogen fixation by Trichodesmium spp.: An important source of new nitrogen to the tropical and subtropical North Atlantic Ocean. *Global Biogeochemical Cycles, 19*(2).

Cardinal, D., Hamelin, B., Bard, E., & Pätzold, J. (2001). Sr/Ca, U/Ca and $d^{18}O$ records in recent massive corals from Bermuda: relationships with sea surface temperature. *Chemical Geology, 176*, 213-233.

Caress, D., & Chayes, D. (1995). *New software for processing sidescan data from sidescan-capable multibeam sonars.* Paper presented at the OCEANS'95. MTS/IEEE. Challenges of Our Changing Global Environment. Conference Proceedings.

Carilli, J. E., Norris, R. D., Black, B., Walsh, S. M., & McField, M. (2010). Century-scale records of coral growth rates indicate that local stressors reduce coral thermal tolerance threshold. *Global Change Biology, 16*(4), 1247-1257.

Carricart-Ganivet, J. P. (2004). Sea surface temperature and the growth of the West Atlantic reef-building coral Montastraea annularis. *Journal of Experimental Marine Biology and Ecology, 302*(2), 249-260.

Carton, J. A., Cao, X., Giese, B. S., & da Silva, A. M. (1996). Decadal and interannual SST variability in the tropical Atlantic. *Journal of Physical Oceanography, 26*, 1165-1175.

Case, D. H., Robinson, L. F., Auro, M. E., & Gagnon, A. C. (2010). Environmental and biological controls on Mg and Li in deep-sea scleractinian corals. *Earth and Planetary Science Letters, 300*(3-4), 215-225.

Castillo, K. D., & Helmuth, B. S. T. (2005). Influence of thermal history on the response of Montastraea annularis to short-term temperature exposure. *Marine Biology, 148*(2), 261-270.

Charles, C. D., Cobb, K., Moore, M. D., & Fairbanks, R. G. (2003). Monsoon-tropical ocean interaction in a network of coral records spanning the 20th century. *Marine Geology, 201*(1-3), 207-222.

Charles, C. D., Hunter, D. E., & Fairbanks, R. G. (1997). Interaction between the ENSO and the Asian monsoon in a coral record of tropical climate. *SCience, 277*(5328), 925-928.

Chelliah, M., & Bell, G. D. (2004). Tropical Multidecadal and Interannual Climate Variability in the NCEP-NCAR Reanalysis. *Journal of Climate*.

Chen, X., & Tung, K.-K. (2014). Varying planetary heat sink led to global-warming slowdown and acceleration. *SCience, 345*(6199), 897-903.

Chiang, J. C. H., & Friedman, A. R. (2012). Extratropical Cooling, Interhemispheric Thermal Gradients, and Tropical Climate Change. In R. Jeanloz (Ed.), *Annual Review of Earth and Planetary Sciences, Vol 40* (Vol. 40, pp. 383-412).

Chiang, J. C. H., Kushnir, Y., and Giannini, A. (2002). Deconstructing Atlantic Intertropical Convergence Zone variability: influence of the local cross-equatorial sea surface temperature gradient and remote forcing from the eastern equatorial Pacific. *Journal of Geophysical Research*.

Chollett, I., Muller-Karger, F. E., Heron, S. F., Skirving, W., & Mumby, P. J. (2012). Seasonal and spatial heterogeneity of recent sea surface temperature trends in the Caribbean Sea and southeast Gulf of Mexico. *Marine Pollution Bulletin, 64*(5), 956-965.

Cifuentes, L., Sharp, J., & Fogel, M. L. (1988). Stable carbon and nitrogen isotope biogeochemistry in the Delaware estuary. *Limnology and Oceanography, 33*(5), 1102-1115.

Clarke, H., D'Olivo, J. P., Falter, J., Zinke, J., Lowe, R., & McCulloch, M. (2017). Differential response of corals to regional mass-warming events as evident from skeletal Sr/Ca and Mg/Ca ratios. *Geochemistry, Geophysics, Geosystems, 18*(5), 1794-1809.

Cobb, K. M., Charles, C. D., Cheng, H., & Edwards, R. L. (2003). El Nino/Southern Oscillation and tropical Pacific climate during the last millennium. *Nature, 424*(6946), 271-276.

Cobb, K. M., Charles, C. D., & Hunter, D. E. (2001). A central tropical Pacific coral demonstrates Pacific, Indian, and Atlantic decadal climate connections. *Geophysical Research Letters, 28*(11), 2209-2212.

Coelho, V. R., & Manfrino, C. (2007). Coral community decline at a remote Caribbean island: marine no-take reserves are not enough. *Aquatic Conservation: Marine and Freshwater Ecosystems, 17*(7), 666-685.

Cohen, A. L., & Gaetani, G. A. (2010). Ion Partitioning and the Geochemistry of Coral Skeletons: Solving the Mystery of the vital effect. *EMU Notes in Mineralogy, 11*, 377-397.

Cohen, A. L., Layne, G. D., & Hart, S. R. (2001). Kinetic control of skeletal Sr/Ca in a symbiotic coral: Implications for the paleotemperature proxy. *Paleoceanography, 16*(1), 20-26.

Cohen, A. L., & McConnaughey, T. A. (2003). Geochemical Perspectives on Coral Mineralization. *Reviews in Mineralogy and Geochemistry, 54*, 151-187.

Cohen, A. L., McCorkle, D. C., de Putron, S., Gaetani, G. A., & Rose, K. A. (2009). Morphological and compositional changes in the skeletons of new coral recruits reared in acidified seawater: Insights into the biomineralization response to ocean acidification. *Geochem. Geophys. Geosyst., 10*.

Cohen, A. L., Owens, K. E., Layne, G. D., & Shimizu, N. (2002). The effect of algal symbionts on the accuracy of Sr/Ca paleotemperatures from coral. *SCience, 296*, 331-333.

Cohen, A. L., Smith, S. R., McCartney, M. S., & van Etten, J. (2004). How brain corals record climate: an integration of skeletal structure, growth and chemistry of Diploria labyrinthiformis from Bermuda. *Marine Ecology Progress Series, 271*, 147-158.

Cohen, A. L., & Sohn, R. A. (2004). Tidal modulation of Sr/Ca ratios in a Pacific reef coral. *Geophysical Research Letters, 31*.

Cole, C., Finch, A., Hintz, C., Hintz, K., & Allison, N. (2016). Understanding cold bias: Variable response of skeletal Sr/Ca to seawater pCO(2) in acclimated massive Porites corals. *Scientific Reports, 6*.

Cole, J. E., Dunbar, R. B., McClanahan, T. R., & Muthiga, N. A. (2000). Tropical Pacific Forcing of Decadal SST variability in the Western Indian Ocean over the Past Two Centuries. *SCience, 287*, 617-619.

Cole, J. E., & Fairbanks, R. G. (1990). The southern Oscillation recorded in the ð18O of corals from Tawara atoll. *Paleoceanography, 5*(5), 669-683.

Cole, J. E., Fairbanks, R. G., & Shen, G. T. (1993). Recent variability in the Southern Oscillation: Isotopic results from a Tarawa Atoll coral. *SCience, 260*, 1790-1793.

Coles, S. L. (1975). A comparison of effects of elevated temperature versus temperature fluctuations on reef corals at Kahe Point, Oahu. *Pacific Science, 29*(1), 15-18.

Coles, S. L., & Jokiel, P. L. (1978). Synergistic effects of temperature, salinity and light on the hermatypic coral Montipora verrucosa. *Marine Biology, 49*(3), 187-195.

Colman, J. G., Gordon, D. M., Lane, A. P., Forde, M. J., & Fitzpatrick, J. J. (2005). Carbonate mounds off Mauritania, Northwest Africa: status of deep-water corals and implications for management of fishing and oil exploration activities. In *Cold-water corals and ecosystems* (pp. 417-441): Springer.

Colombo-Pallotta, M. F., Rodríguez-Román, A., & Iglesias-Prieto, R. (2010). Calcification in bleached and unbleached Montastraea faveolata: evaluating the role of oxygen and glycerol. *Coral Reefs, 29*(4), 899-907. journal article.

Comas-Bru, L., & McDermott, F. (2014). Impacts of the EA and SCA patterns on the European twentieth century NAO–winter climate relationship. *Quarterly Journal of the Royal Meteorological Society, 140*(679), 354-363.

Correa, T. B., Eberli, G. P., Grasmueck, M., Reed, J. K., & Correa, A. M. (2012a). Genesis and morphology of cold-water coral ridges in a unidirectional current regime. *Marine Geology, 326*, 14-27.

Correa, T. B., Grasmueck, M., Eberli, G. P., Reed, J. K., Verwer, K., & Purkis, S. (2012b). Variability of cold‐water coral mounds in a high sediment input and tidal current regime, Straits of Florida. *Sedimentology, 59*(4), 1278-1304.

Corrège, T., Gagan, M. K., Beck, J. W., Burr, G. S., Cabioch, G., & Le Cornec, F. (2004). Interdecadal variation in the extent of South Pacific tropical waters during the Younger Dryas event. *Nature, 428*, 927-929.

Craig, H., & Gordon, L. I. (1965). Deuterium and oxygen 18 variations in the ocean and the marine atmosphere. In E. Tongiorgi (Ed.), *Stable Isotopes in Oceanographic studies and Paleotemperatures* (pp. 9-130). Pisa: CNR.

Cross, T. S., & Cross, B. W. (1983). U, Sr, and Mg in Holocene and Pleistocene corals A. palmata and M. annularis. *Journal of Sedimentary Research, 53*(2), 587-594.

Crowley, T. J., Quinn, T. M., & Hyde, W. T. (1999). Validation of coral temperature calibrations. *Paleoceanography, 14*(5), 605-615.

Crueger, T., Kuhnert, H., Pätzold, J., & Zorita, E. (2006). Calibrations of Bermuda corals against large-scale sea surface temperature and sea level pressure pattern time series and implications for climate reconstructions. *Journal of Geophysical Research Atmospheres, 111*(23).

Curtis, S., & Hastenrath, S. (1995). Forcing of anomalous sea surface temperature evolution in the tropical Atlantic during Pacific warm events. *Journal of Geophysical Research, 100*, 15835-15847.

Czaja, A. (2004). Why is the Tropical Atlantic SST Variability Stronger in Boreal Spring? *Journal of Climate, 17*, 3017-3025.

Czaja, A., van der Vaart, P., & Marshall, J. (2002). A Diagnostic Study of the Role of Remote Forcing in Tropical Atlantic Variability. *Journal of Climate, 15*, 3280-3290.

Dai, A., Trenberth, K. E., & Qian, T. T. (2004). A global dataset of Palmer Drought Severity Index for 1870-2002: Relationship with soil moisture and effects of surface warming. *Journal of Hydrometeorology, 5*(6), 1117-1130.

Davies, A. J., Duineveld, G. C., Lavaleye, M. S., Bergman, M. J., van Haren, H., & Roberts, J. M. (2009). Downwelling and deep‐water bottom currents as food supply

mechanisms to the cold‐water coral Lophelia pertusa (Scleractinia) at the Mingulay Reef Complex. *Limnology and Oceanography, 54*(2), 620-629.

Davies, A. J., & Guinotte, J. M. (2011). Global habitat suitability for framework-forming cold-water corals. *PLoS ONE, 6*(4), e18483.

Davies, A. J., Wisshak, M., Orr, J. C., & Roberts, J. M. (2008). Predicting suitable habitat for the cold-water coral Lophelia pertusa (Scleractinia). *Deep Sea Research Part I: Oceanographic Research Papers, 55*(8), 1048-1062.

De Deckker, P. (2004). On the celestite-secreting Acantharia and their effect on seawater strontium to calcium ratios. *Hydrobiologia, 517*(1), 1-13. journal article.

De Mol, B., Van Rensbergen, P., Pillen, S., Van Herreweghe, K., Van Rooij, D., McDonnell, A., et al. (2002). Large deep-water coral banks in the Porcupine Basin, southwest of Ireland. *Marine Geology, 188*(1-2), 193-231.

de Villiers, S. (1999). Sewater strontium and Sr/Ca variability in the Atlantic and Pacific oceans. *Earth and Planetary Science Letters, 171*, 623-634.

de Villiers, S., Greaves, M., & Elderfield, H. (2002). An intensity ratio calibration method for the accurate determination of Mg/Ca and Sr/Ca of marine carbonates by ICP-AES. *Geochemistry Geophysics Geosystems, 3*, 2001GC000169.

de Villiers, S., Nelson, B. K., & Chivas, A. R. (1995). Biological Controls on Coral Sr/Ca and d18O Reconstructions of Sea Surface Temperature. *SCience, 269*, 1247-1249.

de Villiers, S., Shen, G. T., & Nelson, B. K. (1994). The Sr/Ca-temperature relationship in coralline aragonite: Influence of variability in $(Sr/Ca)_{seawater}$ and skeletal growth parameters. *Geochimica Et Cosmochimica Acta, 58*, 197-208.

DeCarlo, T. M., Gaetani, G. A., Holcomb, M., & Cohen, A. L. (2015). Experimental determination of factors controlling U/Ca of aragonite precipitated from seawater: Implications for interpreting coral skeleton. *Geochimica Et Cosmochimica Acta, 162*, 151-165.

Delaygue, G., Jouzel, J., & Dutay, J.-C. (2000). Oxygen 18-salinity relationship simulated by an oceanic general circulation model. *Earth and Planetary Science Letters, 178*, 113-123.

DeLong, K. L., Flannery, J. A., Maupin, C. R., Poore, R. Z., & Quinn, T. M. (2011). A coral Sr/Ca calibration and replication study of two massive corals from the Gulf of Mexico. *Palaeogeography, Palaeoclimatology, Palaeoecology, 307*(1-4), 117-128. doi: 10.1016/j.palaeo.2011.05.005.

DeLong, K. L., Flannery, J. A., Poore, R. Z., Quinn, T. M., Maupin, C. R., Lin, K., & Shen, C. C. (2014). A reconstruction of sea surface temperature variability in the southeastern Gulf of Mexico from 1734 to 2008 CE using cross-dated Sr/Ca records from the coral Siderastrea siderea. *Paleoceanography, 29*(5), 403-422.

DeLong, K. L., Quinn, T. M., Shen, C. C., & Lin, K. (2010). A snapshot of climate variability at Tahiti at 9.5 ka using a fossil coral from IODP Expedition 310. *Geochemistry, Geophysics, Geosystems, 11*(6).

DeLong, K. L., Quinn, T. M., & Taylor, F. W. (2007). Reconstructing twentieth-century sea surface temperature variability in the southwest Pacific: A replication study using multiple coral Sr/Ca records from New Caledonia. *Paleoceanography, 22*(4), PA4212.

DeLong, K. L., Quinn, T. M., Taylor, F. W., Lin, K., & Shen, C.-C. (2012). Sea surface temperature variability in the southwest tropical Pacific since AD 1649. *Nature Clim. Change, 2*(11), 799-804. 10.1038/nclimate1583.

Delworth, T. L., & Mann, M. E. (2000). Observed and simulated multidecadal variability in the Northern Hemisphere. *Climate Dynamics, 16*, 661-676.

Deng, W.-f., Wei, G.-j., Li, X.-h., Yu, K.-f., Zhao, J.-x., Sun, W.-d., & Liu, Y. (2009). Paleoprecipitation record from coral Sr/Ca and δ18O during the mid Holocene in the northern South China Sea. *The Holocene, 19*(6), 811-821.

Deser, C., Alexander, M. A., Xie, S.-P., & Phillips, A. S. (2010). Sea Surface Temperature Variability: Patterns and Mechanisms. *Annual Review of Marine Science, 2*(1), 115-143.

Deser, C., & Blackmon, M. L. (1993). Surface Climate Variations over the North-Atlantic Ocean during Winter - 1900-1989. *Journal of Climate, 6*(9), 1743-1753.

Dickson, R., & McCave, I. (1986). Nepheloid layers on the continental slope west of Porcupine Bank. *Deep Sea Research Part A. Oceanographic Research Papers, 33*(6), 791-818.

Dodds, L., Roberts, J., Taylor, A., & Marubini, F. (2007). Metabolic tolerance of the cold-water coral Lophelia pertusa (Scleractinia) to temperature and dissolved oxygen change. *Journal of Experimental Marine Biology and Ecology, 349*(2), 205-214.

Dodge, R. E., & Vaisnys, J. R. (1975). Hermatypic coral growth banding as environmental recorder. *Nature, 258*(5537), 706-708. 10.1038/258706a0.

Dommenget, D., & Latif, M. (2000). Interannual to decadal variability in the tropical Atlantic. *Journal of Climate, 13*(4), 777-792.

Dong, B., & Sutton, R. T. (2005). Mechanism of interdecadal thermohaline circulation variability in a coupled ocean–atmosphere GCM. *Journal of Climate, 18*(8), 1117-1135.

Donner, S. D., Rickbeil, G. J. M., & Heron, S. F. (2017). A new, high-resolution global mass coral bleaching database. *PLoS ONE, 12*(4).

Doodson, A. T. (1928). The Analysis of Tidal Observations. *Philosophical Transactions of the Royal Society of London. Series A, Containing Papers of a Mathematical or Physical Character, 227*, 223-279.

Dorschel, B., Hebbeln, D., Foubert, A., White, M., & Wheeler, A. (2007). Hydrodynamics and cold-water coral facies distribution related to recent sedimentary processes at Galway Mound west of Ireland. *Marine Geology, 244*(1-4), 184-195.

Dorschel, B., Hebbeln, D., Rüggeberg, A., Dullo, W.-C., & Freiwald, A. (2005). Growth and erosion of a cold-water coral covered carbonate mound in the Northeast Atlantic during the Late Pleistocene and Holocene. *Earth and Planetary Science Letters, 233*(1), 33-44.

Drake, J. L., Mass, T., Haramaty, L., Zelzion, E., Bhattacharya, D., & Falkowski, P. G. (2013). Proteomic analysis of skeletal organic matrix from the stony coral Stylophora pistillata. *Proceedings of the National Academy of Sciences*, 201301419.

Dullo, W.-C., Flögel, S., & Rüggeberg, A. (2008). Cold-water coral growth in relation to the hydrography of the Celtic and Nordic European continental margin. *Marine Ecology Progress Series, 371*, 165-176.

Dunbar, R. B., & Wellington, G. M. (1981). Stable isotopes in a branching coral monitor seasonal temperature variation. *Nature, 293*, 453-455.

Dunbar, R. B., Wellington, G. M., Colgan, M. W., & Glynn, P. W. (1994). Eastern Pacific sea surface temperature since 1600 A. D.: The $d^{18}O$ record of climate variability in Galápagos corals. *Paleoceanography, 9*(2), 291-315.

Eakin, C. M., Lough, J. M., & Heron, S. F. (2009). Climate Variability and Change: Monitoring Data and Evidence for Increased Coral Bleaching Stress. In M. J. H. van Oppen & J. M. Lough (Eds.), *Coral Bleaching: Patterns, Processes, Causes and Consequences* (pp. 41-67). Berlin, Heidelberg: Springer Berlin Heidelberg.

Eakin, C. M., Morgan, J. A., Heron, S. F., Smith, T. B., Liu, G., Alvarez-Filip, L., et al. (2010). Caribbean Corals in Crisis: Record Thermal Stress, Bleaching, and Mortality in 2005. *PLoS ONE, 5*(11), e13969.

Edmunds, P. J., & Gates, R. D. (2008). Acclimatization in tropical reef corals. *Marine Ecology Progress Series, 361*, 307-310.

Eisele, M., Frank, N., Wienberg, C., Hebbeln, D., Correa, M. L., Douville, E., & Freiwald, A. (2011). Productivity controlled cold-water coral growth periods during the last glacial off Mauritania. *Marine Geology, 280*(1), 143-149.

Eisele, M., Frank, N., Wienberg, C., Titschack, J., Mienis, F., Beuck, L., et al. (2014). Sedimentation patterns on a cold-water coral mound off Mauritania. *Deep Sea Research Part II: Topical Studies in Oceanography, 99*, 307-315.

Eisele, M., Hebbeln, D., & Wienberg, C. (2008). Growth history of a cold-water coral covered carbonate mound—Galway Mound, Porcupine Seabight, NE-Atlantic. *Marine Geology, 253*(3), 160-169.

Emery, K., & Milliman, J. (1980). Shallow-water limestones from slope off Grand Cayman Island. *The Journal of Geology, 88*(4), 483-488.

Emiliani, C., Hudson, J. H., Shinn, E. A., & George, R. Y. (1978). Oxygen and Carbon Isotopic Growth Record in a Reef Coral from the Florida Keys and a Deep-Sea Coral from Blake Plateau. *SCience, 202*, 627-629.

Enfield, D. B., & Alfaro, E. J. (1999). The Dependence of Caribbean Rainfall on the Interaction of the Tropical Atlantic and Pacific Oceans. *Journal of Climate, 12*, 2093-2103.

Enfield, D. B., & Cid-Serrano, L. (2010). Secular and multidecadal warmings in the North Atlantic and their relationships with major hurricane activity. *International Journal of Climatology, 30*(2), 174-184.

Enfield, D. B., Lee, S.-K., & Wang, C. (2006). How are large western hemisphere warm pools formed? *Progress in Oceanography, 70*(2), 346-365.

Enfield, D. B., & Mayer, D. A. (1997). Tropical Atlantic sea surface temperature variability and its relation to El Nino-Southern Oscillation. *Journal of Geophysical Research, 102*(C1), 929-945.

Enfield, D. B., Mestas-Nunez, A. M., & Trimble, P. J. (2001). The Atlantic multidecadal oscillation and its relation to rainfall and river flows in the continental U.S. *Geophysical Research Letters, 28*(10), 2077-2080.

Epstein, S., Buchsbaum, R., Lowenstamm, H. A., & Orey, H. C. (1953). Revised carbonate-water isotopic temperature scale. *Geological Society of AMerica Bulletin, 64*, 1315-1326.

Erez, J. (1978). Vital effect on stable-isotope composition seen in foraminifera and coral skeletons. *Nature, 273*(5659), 199.

Evans, M. N., Fairbanks, R. G., & Rubenstone, J. L. (1999). The thermal oceanographic signal of El Nino reconstructed from a Kiritimati Island coral. *Journal of Geophysical Research, 104*, 13409-13421.

Fadlallah, Y. H. (1983). Sexual reproduction, development and larval biology in scleractinian corals. *Coral Reefs, 2*(3), 129-150.

Falkowski, P. G., Barber, R. T., & Smetacek, V. (1998). Biogeochemical controls and feedbacks on ocean primary production. *SCience, 281*(5374), 200-206.

Fallon, S., McCulloch, M. T., & Alibert, C. (2003). Examining water temperature proxis in *Porites* corals from the Great Barrier Reef: a cross-shelf comparison. *Coral Reefs, 22*, 389-404.

Farrell, J., Pedersen, T., Calvert, S., & Nielsen, B. (1995). Glacialá¤-interglacial changes in nutrient utilization in the equatorial Pacific Ocean. *Nature, 377*(6549), 514.

Farrow, D. E., & Patterson, J. C. (1993). On the response of a reservoir sidearm to diurnal heating and cooling. *Journal of Fluid Mechanics, 246*, 143-161.

Felis, T., Giry, C., Scholz, D., Lohmann, G., Pfeiffer, M., Pätzold, J., et al. (2015a). Tropical Atlantic temperature seasonality at the end of the last interglacial. *Nat Commun, 6*. Article.

Felis, T., Giry, C., Scholz, D., Lohmann, G., Pfeiffer, M., Pätzold, J., et al. (2015b). Tropical Atlantic temperature seasonality at the end of the last interglacial. *Nature Communications, 6*, 6159. Article.

Felis, T., Lohmann, G., Kuhnert, H., Lorenz, S. J., Scholz, D., Pätzold, J., et al. (2004). Increased seasonality in Middle East temperatures during the last interglacial period. *Nature, 429*, 164-168.

Felis, T., Pätzold, J., & Loya, Y. (2003). Mean oxygen-isotope signatures in Porites spp. corals: inter-colony variability and correction for extension-rate effects. *Coral Reefs, 22*(4), 328-336.

Felis, T., Pätzold, J., Loya, Y., Fine, M., Nawar, A. H., & Wefer, G. (2000). A coral oxygen isotope record from the northern Red Sea documenting NAO, ENSO, and North Pacific teleconnections on Middle East climate variability since the year 1750. *Paleoceanography, 15*(6), 679-694.

Felis, T., Suzuki, A., Kuhnert, H., Dima, M., Lohmann, G., & Kawahata, H. (2009). Subtropical coral reveals abrupt early-twentieth-century freshening in the western North Pacific Ocean. *Geology, 37*(6), doi:10.1130/G25581A.25581.

Ferrier-Pages, C., Boisson, F., Allemand, D., & Tambutte, E. (2002). Kinematics of strontium uptake in the scleractinian coral Stylophora pistillata. *Marine Ecology Progress Series, 245*, 93-100.

Fietzke, J., Liebetrau, V., Eisenhauer, A., & Dullo, C. (2005). Determination of uranium isotope ratios by multi-static MIC-ICP-MS: method and implementation for precise U-and Th-series isotope measurements. *Journal of Analytical Atomic Spectrometry, 20*(5), 395-401.

Fink, H. G., Wienberg, C., Hebbeln, D., McGregor, H. V., Schmiedl, G., Taviani, M., & Freiwald, A. (2012). Oxygen control on Holocene cold-water coral development in the eastern Mediterranean Sea. *Deep Sea Research Part I: Oceanographic Research Papers, 62*, 89-96.

Flewellen, C., Millard, N., & Rouse, I. (1993). TOBI, a vehicle for deep ocean survey. *Electronics & communication engineering journal, 5*(2), 85-93.

Flögel, S., Dullo, W.-C., Pfannkuche, O., Kiriakoulakis, K., & Rüggeberg, A. (2014). Geochemical and physical constraints for the occurrence of living cold-water corals. *Deep Sea Research Part II: Topical Studies in Oceanography, 99*, 19-26.

Form, A. U., & Riebesell, U. (2012). Acclimation to ocean acidification during long ‐ term CO2 exposure in the cold ‐ water coral Lophelia pertusa. *Global Change Biology, 18*(3), 843-853.

Fosså, J. H., Lindberg, B., Christensen, O., Lundälv, T., Svellingen, I., Mortensen, P. B., & Alvsvåg, J. (2005). Mapping of Lophelia reefs in Norway: experiences and survey methods. In *Cold-water corals and ecosystems* (pp. 359-391): Springer.

Fosså, J. H., Mortensen, P., & Furevik, D. M. (2002). The deep-water coral Lophelia pertusa in Norwegian waters: distribution and fishery impacts. *Hydrobiologia, 471*(1-3), 1-12.

Foubert, A., Depreiter, D., Beck, T., Maignien, L., Pannemans, B., Frank, N., et al. (2008). Carbonate mounds in a mud volcano province off north-west Morocco: key to processes and controls. *Marine Geology, 248*(1-2), 74-96.

Frank, N., Freiwald, A., Correa, M. L., Wienberg, C., Eisele, M., Hebbeln, D., et al. (2011). Northeastern Atlantic cold-water coral reefs and climate. *Geology, 39*(8), 743-746.

Frank, N., Ricard, E., Lutringer-Paquet, A., van der Land, C., Colin, C., Blamart, D., et al. (2009). The Holocene occurrence of cold water corals in the NE Atlantic: implications for coral carbonate mound evolution. *Marine Geology, 266*(1-4), 129-142.

Fratantoni, D. M. (2001). North Atlantic surface circulation during the 1990`s observed with satellite-tracked drifters. *Journal of Geophysical Research*.

Frederiksen, R., Jensen, A., & Westerberg, H. (1992). The distribution of the scleractinian coral Lophelia pertusa around the Faroe Islands and the relation to internal tidal mixing. *Sarsia, 77*(2), 157-171.

Freiwald, A. (2002). Reef-forming cold-water corals. In *Ocean margin systems* (pp. 365-385): Springer.

Freiwald, A., Beuck, L., Rüggeberg, A., Taviani, M., & Hebbeln, D. (2009). The white coral community in the central Mediterranean Sea revealed by ROV surveys. *Oceanography, 22*(1), 58-74.

Freiwald, A., Fossa, J. H., Grehan, A., Koslow, T., & Roberts, J. M. (2004). Cold water coral reefs: out of sight-no longer out of mind.

Frenz, M., Wynn, R. B., Georgiopoulou, A., Bender, V. B., Hough, G., Masson, D. G., et al. (2009). Provenance and pathways of late Quaternary turbidites in the deep-water Agadir Basin, northwest African margin. *International Journal of Earth Sciences, 98*(4), 721-733.

Fusco, G., Artale, V., Cotroneo, Y., & Sannino, G. (2008). Thermohaline variability of Mediterranean Water in the Gulf of Cadiz, 1948–1999. *Deep Sea Research Part I: Oceanographic Research Papers, 55*(12), 1624-1638.

Gabitov, R. I., & Watson, E. B. (2006). Partitioning of strontium between calcite and fluid. *Geochemistry, Geophysics, Geosystems, 7*(11).

Gagan, M. K., Ayliffe, L. K., Beck, J. W., Cole, J. E., Druffel, E. R. M., Dunbar, R. B., & Schrag, D. P. (2000). New views of tropical paleoclimates from corals. *Quaternary Science Reviews, 19*, 45-64.

Gagan, M. K., Ayliffe, L. K., Hopley, D., Cali, J. A., Mortimer, G. E., Chappell, J., et al. (1998). Temperature and surface-ocean water balance of the mid-Holocene tropical western Pacific. *SCience, 279*, 1014-1018.

Gagan, M. K., Chivas, A. R., & Isdale, P. J. (1994). High-resolution isotopic records from corals using ocean temperature and mass-spawning chronometers. *Earth and Planetary Science Letters, 121*, 549-558.

Gagan, M. K., Dunbar, G. B., & Suzuki, A. (2012). The effect of skeletal mass accumulation in Porites on coral Sr/Ca and d18O paleothermometry. *Paleoceanography, 27*(1), PA1203.

Gagnon, A. C., Adkins, J. F., Erez, J., Eiler, J. M., & Guan, Y. (2013). Sr/Ca sensitivity to aragonite saturation state in cultured subsamples from a single colony of coral: Mechanism of biomineralization during ocean acidification. *Geochimica Et Cosmochimica Acta, 105*, 240-254.

Gagnon, A. C., Adkins, J. F., Fernandez, D. P., & Robinson, L. F. (2007). Sr/Ca and Mg/Ca vital effects correlated with skeletal architecture in a scleractinian deep-sea coral and the role of Rayleigh fractionation. *Earth and Planetary Science Letters, 261*(1-2), 280-295.

Gardner, T. A., Coté, I. M., Gill, J. A., Grant, A., & Watkinson, A. R. (2003). Long-Term Region-Wide Declines in Caribbean Corals. *SCience, 301*, 958-960.

Gates, R. D., & Edmunds, P. J. (1999). The Physiological Mechanisms of Acclimatization in Tropical Reef Corals. *American Zoologist, 39*(1), 30-43.

Genin, A., Dayton, P. K., Lonsdale, P. F., & Spiess, F. N. (1986). Corals on seamount peaks provide evidence of current acceleration over deep-sea topography. *Nature, 322*(6074), 59.

George, S. E., & Saunders, M. A. (2001). North Atlantic Oscillation impact on tropical north Atlantic winter atmospheric variability. *Geophysical Research Letters, 28*(6), 1015-1018.

Ghiold, J., & Smith, S. (1990). Bleaching and recovery of deep-water, reef dwelling invertebrates in the Cayman Islands. *British West Indies Caribbean Journal of Science, 26*, 52-61.

Giannini, A., Cane, M. A., & Kushnir, Y. (2001a). Interdecadal changes in the ENSO teleconnection to the Caribbean region and the North Atlantic Oscillation. *Journal of Climate, 14*, 2867-2879.

Giannini, A., Chiang, J. C. H., Cane, M. A., Kushnir, Y., & Seager, R. (2001b). The ENSO teleconnection to the tropical Atlantic Ocean: Contributions of the remote and local

SSTs to rainfall variability in the tropical Americas. *Journal of Climate, 14*, 4530-4544.

Giannini, A., Kushnir, Y., & Cane, M. A. (2000). Interannual Variability of Caribbean Rainfall, ENSO, and the Atlantic Ocean. *Journal of Climate, 13*, 297-311.

Giry, C., Felis, T., Kölling, M., & Scheffers, S. (2010). Geochemistry and skeletal structure of Diploria strigosa, implications for coral-based climate reconstruction. *Palaeogeography, Palaeoclimatology, Palaeoecology, 298*(3-4), 378-387. doi: DOI: 10.1016/j.palaeo.2010.10.022.

Giry, C., Felis, T., Kölling, M., Scholz, D., Wei, W., Lohmann, G., & Scheffers, S. (2012). Mid- to late Holocene changes in tropical Atlantic temperature seasonality and interannual to multidecadal variability documented in southern Caribbean corals. *Earth and Planetary Science Letters, 331–332*(0), 187-200.

Gleeson, M. W., & Strong, A. (1995). Applying MCSST to coral-reef bleaching. *Advances in Space Research, 16*, 151-154.

Glynn, P. W. (1993). Coral reef bleaching: ecological perspectives. *Coral Reefs, 12*(1), 1-17.

Goldenberg, S. B., Landsea, C. W., Mestas-Nunez, A. M., & Gray, W. M. (2001). The recent increase in Atlantic hurricane activity: Causes and implications. *SCience, 293*, 474-479.

Goodkin, N. F., Hughen, K. A., & Cohen, A. L. (2007). A multicoral calibration method to approximate a universal equation relating Sr/Ca and growth rate to sea surface temperature. *Paleoceanography, 22*(PA1214), doi:10.1029/2006PA001312.

Goodkin, N. F., Hughen, K. A., Cohen, A. L., & Smith, S. R. (2005). Record of Little Ice Age sea surface temperatures at Bermuda using a growth-dependent calibration of coral Sr/Ca. *Paleoceanography, 20*(PA4016), doi:10.1029/2005PA001140.

Goodkin, N. F., Hughen, K. A., Doney, S. C., & Curry, W. B. (2008). Increased multidecadal variability of the North Atlantic Oscillation since 1781. *Nature Geosci, 1*(12), 844-848. 10.1038/ngeo352.

Gordon, A. L. (1967). Circulation of the Caribbean Sea. *Journal of Geophysical Research, 72*, 6207-6223.

Goreau, T., & Hayes, R. (1994). Coral bleaching and ocean hot-spots. *Ambio, 23*, 176-180.

Gori, A., Grover, R., Orejas, C., Sikorski, S., & Ferrier-Pagès, C. (2014). Uptake of dissolved free amino acids by four cold-water coral species from the Mediterranean Sea. *Deep Sea Research Part II: Topical Studies in Oceanography, 99*, 42-50.

Grasmueck, M., Eberli, G. P., Viggiano, D. A., Correa, T., Rathwell, G., & Luo, J. (2006). Autonomous underwater vehicle (AUV) mapping reveals coral mound distribution, morphology, and oceanography in deep water of the Straits of Florida. *Geophysical Research Letters, 33*(23).

Gray, W. M. (1984). Atlantic seasonal hurricane frequency. Part 1: El Nino and 30 mb quasi-biennial oscillation influences. *Monthly Weather Review, 112*, 1649-1668.

Grinsted, A., Moore, J. C., & Jevrejeva, S. (2004). Application of the cross wavelet transform and wavelet coherence to geophysical time series. *Nonlinear Processes in Geophysics, 11*(5-6), 561-566.

Grove, C., Nagtegaal, R., Zinke, J., Scheufen, T., Koster, B., Kasper, S., et al. (2010). River runoff reconstructions from novel spectral luminescence scanning of massive coral skeletons. *Coral Reefs, 29*(3), 579-591.

Gruber, N., & Galloway, J. N. (2008). An Earth-system perspective of the global nitrogen cycle. *Nature, 451*(7176), 293.

Gruber, N., & Sarmiento, J. L. (1997). Global patterns of marine nitrogen fixation and denitrification. *Global Biogeochemical Cycles, 11*(2), 235-266.

Guan, B., & Nigam, S. (2009). Analysis of Atlantic SST Variability Factoring Interbasin Links and the Secular Trend: Clarified Structure of the Atlantic Multidecadal Oscillation. *Journal of Climate, 22*(15), 4228-4240.

Gunn, J., & Watts, D. (1982). On the currents and water masses north of the Antilles/Bahamas arc [Netherlands Antilles]. *Journal of Marine Research*.

Harris, I. C., & Jones, P. D. (2017). CRU TS3.25: Climatic Research Unit (CRU) Time-Series (TS) Version 3.25 of High-Resolution Gridded Data of Month-by-month Variation in Climate (Jan. 1901- Dec. 2016). *Centre for Environmental Data Analysis, University of East Anglia Climatic Research Unit*.

Hastenrath, S. (1976). Variations in low-latitude circulation and extreme climatic events in the tropical Americas. *Journal of the Atmospheric Sciences, 33*, 202-215.

Hastenrath, S. (1984). Interannual variability and annual cycle: Mechanisms of circulation and climate in the tropical Atlantic sector. *Monthly Weather Review, 112*, 1097-1107.

Hathorne, E. C., Gagnon, A., Felis, T., Adkins, J., Asami, R., Boer, W., et al. (2013). Interlaboratory study for coral Sr/Ca and other element/Ca ratio measurements. *Geochemistry, Geophysics, Geosystems, 14*(9), 3730-3750.

Hayashi, E., Suzuki, A., Nakamura, T., Iwase, A., Ishimura, T., Iguchi, A., et al. (2013). Growth-rate influences on coral climate proxies tested by a multiple colony culture experiment. *Earth and Planetary Science Letters, 362*, 198-206.

Haylock, M. R., Jones, P. D., Allan, R. J., & Ansell, T. J. (2007). Decadal changes in 1870-2004 Northern Hemisphere winter sea level pressure variability and its relationship with surface temperature. *Journal of Geophysical Research-Atmospheres, 112*(D11).

Hebbeln, D., Bender, M., Gaide, S., Wintersteller, P., & Wienberg, C. (2017). *Thousands of Late Quaternary carbonate mounds along the Moroccan continental margin*. GeoBremen 2017, Joint Meeting of DGGV and DMG: The System Earth and its Materials - from Seafloor to Summit. Abstract. Bremen, Germany.

Hebbeln, D., Van Rooij, D., & Wienberg, C. (2016). Good neighbours shaped by vigorous currents: cold-water coral mounds and contourites in the North Atlantic. *Marine Geology, 378*, 171-185.

Hebbeln, D., Wienberg, C., Wintersteller, P., Freiwald, A., Becker, M., Beuck, L., et al. (2014). Environmental forcing of the Campeche cold-water coral province, southern Gulf of Mexico. *Biogeosciences (BG), 11*, 1799-1815.

Helmle, K. P., Dodge, R. E., & Ketcham, R. A. (2002). Skeletal architecture and density banding in Diploria strigosa by X-ray computed tomography. *Proceedings 9th International Coral Reef Symposium*.

Henderiks, J., Freudenthal, T., Meggers, H., Nave, S., Abrantes, F., Bollmann, J., & Thierstein, H. R. (2002). Glacial–interglacial variability of particle accumulation in the Canary Basin: a time-slice approach. *Deep Sea Research Part II: Topical Studies in Oceanography, 49*(17), 3675-3705.

Hendy, E., Gagan, M. K., Alibert, C. A., McCulloch, M. T., Lough, J. M., & Isdale, P. J. (2002). Abrupt Decrease in Tropical Pacific Sea Surface Salinity at End of Little Ice Age. *SCience, 295*, 1511-1514.

Hendy, E. J., Gagan, M. K., Lough, J. M., McCulloch, M., & deMenocal, P. B. (2007). Impact of skeletal dissolution and secondary aragonite on trace element and isotopic climate proxies in Porites corals. *Paleoceanography, 22*(4).

Henriet, J., De Mol, B., Pillen, S., Vanneste, M., Van Rooij, D., Versteeg, W., et al. (1998). Gas hydrate crystals may help build reefs. *Nature, 391*(6668), 648.

Henry, L.-A., Frank, N., Hebbeln, D., Wienberg, C., Robinson, L., van de Flierdt, T., et al. (2014). Global ocean conveyor lowers extinction risk in the deep sea. *Deep Sea Research Part I: Oceanographic Research Papers, 88*, 8-16.

Hernandez-Guerra, A., & Joyce, T. M. (2000). Water Masses and Circulation in the Surface Layers of the Caribbean at 66°W. *Geophysical Research Letters*.

Hernández-Molina, F. J., Serra, N., Stow, D. A., Llave, E., Ercilla, G., & Van Rooij, D. (2011). Along-slope oceanographic processes and sedimentary products around the Iberian margin. *Geo-Marine Letters, 31*(5-6), 315-341.

Hetzinger, S., Halfar, J., Mecking, J. V., Keenlyside, N. S., Kronz, A., Steneck, R. S., et al. (2012). Marine proxy evidence linking decadal North Pacific and Atlantic climate. *Climate Dynamics*.

Hetzinger, S., Pfeiffer, M., Dullo, W.-C., Garbe-Schönberg, D., & Halfar, J. (2010a). Rapid 20th century warming in the Caribbean and impact of remote forcing on climate in the northern tropical Atlantic as recorded in a Guadeloupe coral. *Palaeogeography, Palaeoclimatology, Palaeoecology, 296*(1-2), 111-124. doi: DOI: 10.1016/j.palaeo.2010.06.019.

Hetzinger, S., Pfeiffer, M., Dullo, W.-C., Garbe-Schönberg, D., & Halfar, J. (2010b). Rapid 20th century warming in the Caribbean and impact of remote forcing on climate in

the northern tropical Atlantic as recorded in a Guadeloupe coral. *Palaeogeography, Palaeoclimatology, Palaeoecology, 296*(1–2), 111-124.

Hetzinger, S., Pfeiffer, M., Dullo, W.-C., Keenlyside, N. S., Latif, M., & Zinke, J. (2008). Caribbean coral tracks Atlantic Multidecadal Oscillation and past hurricane activity. *Geology, 36*(1), 11-14.

Hetzinger, S., Pfeiffer, M., Dullo, W.-C., Ruprecht, E., & Garbe-Schönberg, D. (2006a). Sr/Ca and $d^{18}O$ in a fast-growing *Diploria strigosa* coral: Evaluation of a new climate archive for the tropical Atlantic. *Geochemistry Geophysics Geosystems, 7*(10), doi:10.1029/2006GC001347.

Hetzinger, S., Pfeiffer, M., Dullo, W.-C., Ruprecht, E., & Garbe-Schönberg, D. (2006b). Sr/Ca and δ18O in a fast-growing Diploria strigosa coral: Evaluation of a new climate archive for the tropical Atlantic. *Geochemistry, Geophysics, Geosystems, 7*(10), Q10002.

Hetzinger, S., Pfeiffer, M., Dullo, W. C., Zinke, J., & Garbe-Schönberg, D. (2016). A change in coral extension rates and stable isotopes after El Niño-induced coral bleaching and regional stress events. *Scientific Reports, 6*, 32879. Article.

Hirabayashi, S., Yokoyama, Y., Suzuki, A., Kawakubo, Y., Miyairi, Y., Okai, T., & Nojima, S. (2013). Coral growth-rate insensitive Sr/Ca as a robust temperature recorder at the extreme latitudinal limits of Porites. *Geochemical Journal, 47*(3), e1-e5.

Hodson, D. L. R., Robson, J. I., & Sutton, R. T. (2014). An Anatomy of the Cooling of the North Atlantic Ocean in the 1960s and 1970s. *Journal of Climate, 27*(21), 8229-8243.

Hoegh-Guldberg, O. (1999). Climate change, coral bleaching and the future of the world's coral reefs. *Marine and freshwater research, 50*(8), 839-866.

Hoerling, M. P., Hurrell, J. W., & Xu, T. (2001). Tropical origins for recent North Atlantic climate change. *SCience, 292*, doi:10.1126/science.1058582.

Hogg, N. G., & Johns, W. E. (1995). Western boundary currents. *Reviews of Geophysics Supplement, U.S. National Report to IUGG 1991-1994*, 1311-1344.

Hovland, M., Jensen, S., & Indreiten, T. (2012). Unit pockmarks associated with Lophelia coral reefs off mid-Norway: more evidence of control by 'fertilizing'bottom currents. *Geo-Marine Letters, 32*(5-6), 545-554.

Hu, Q., & Feng, S. (2008). Variation of the North American summer monsoon regimes and the Atlantic multidecadal oscillation. *Journal of Climate, 21*(11), 2371-2383.

Huang, B., Banzon, V. F., Freeman, E., Lawrimore, J., Liu, W., Peterson, T. C., et al. (2015). Extended reconstructed sea surface temperature version 4 (ERSST. v4). Part I: upgrades and intercomparisons. *Journal of Climate, 28*(3), 911-930.

Huang, B. H., Schopf, P. F., & Shukla, J. (2004). Intrinsic ocean-atmosphere variability of the tropical Atlantic Ocean. *Journal of Climate, 17*, 2058-2077.

Hübscher, C., Dullo, C., Flögel, S., Titschack, J., & Schönfeld, J. (2010). Contourite drift evolution and related coral growth in the eastern Gulf of Mexico and its gateways. *International Journal of Earth Sciences, 99*(1), 191-206.

Hughes, T. P., Anderson, K. D., Connolly, S. R., Heron, S. F., Kerry, J. T., Lough, J. M., et al. (2018). Spatial and temporal patterns of mass bleaching of corals in the Anthropocene. *SCience, 359*(6371), 80-+.

Hughes, T. P., Baird, A. H., Bellwood, D. R., Card, M., Conolly, S. R., Folke, C., et al. (2003). Climate change, human impacts, and the resilience of coral reefs. *SCience, 301*, 929-933.

Hurrell, J. W. (1995). Decadal trends in the North Atlantic Oscillation: regional temperatures and precipitation. *SCience, 269*, 676-679.

Hurrell, J. W., Kushnir, Y., Ottersen, G., & Visbeck, M. (2003a). *The North Atlantic Oscillation - Climatic Significance and Environmental Impact* (Vol. 134). Washington, DC: American Geophysical Union.

Hurrell, J. W., Kushnir, Y., Ottersen, G., & Visbeck, M. (2003b). An Overview of the North Atlantic Oscillation. In J. W. Hurrell, Y. Kushnir, G. Ottersen, & M. Visbeck (Eds.), *The North Atlantic Oscillation - Climatic Significance and Environmental Impact* (pp. 1-35). Washington, DC: American Geophysical Union.

Hurrell, J. W., & van Loon, H. (1997). Decadal variations in climate associated with the North Atlantic Oscillation. *Climatic Change, 36*, 310-326.

Hurrell, J. W., Visbeck, M., Busalacchi, A., Clarke, R. A., Delworth, T. L., Dickson, R. R., et al. (2006). Atlantic climate variability and predictability: A CLIVAR perspective. *Journal of Climate, 19*(20), 5100-5121.

Huston, M. (1985). Variation in coral growth rates with depth at Discovery Bay, Jamaica. *Coral Reefs, 4*(1), 19-25.

Ingalls, A. E., Lee, C., & Druffel, E. R. (2003). Preservation of organic matter in mound-forming coral skeletons. *Geochimica Et Cosmochimica Acta, 67*(15), 2827-2841.

Inoue, M., Nohara, M., Okai, T., Suzuki, A., & Kawahata, H. (2004). Concentrations of Trace Elements in Carbonate Reference Materials Coral JCp-1 and Giant Clam JCt-1 by Inductively Coupled Plasma-Mass Spectrometry. *Geostandards and Geoanalytical Research, 28*(3), 411-416.

Inoue, M., Suwa, R., Suzuki, A., Sakai, K., & Kawahata, H. (2011). Effects of seawater pH on growth and skeletal U/Ca ratios of Acropora digitifera coral polyps. *Geophysical Research Letters, 38*(12).

Ip, Y. K., & Lim, A. L. L. (1991). Short Communication: Are Calcium and Strontium Transported by the Same Mechanism in the Hermatypic Coral Galaxea Fascicularis? *Journal of Experimental Biology, 159*(1), 507-513.

IPCC. (2013). *Climate Change 2013: The Physical Science Basis. Contribution of Working Group I to the Fifth Assessment Report of the Intergovernmental Panel on Climate Change*. Cambridge, United Kingdom and New York, NY, USA: Cambridge University Press.

Johns, W. E., Townsend, T. L., Fratantoni, D. M., & Wilson, W. D. (2002). On the Atlantic inflow to the Caribbean Sea. *Deep-Sea Research Part I-Oceanographic Research Papers, 49*(2), 211-243.

Jones, B. (1994). Geology of the Cayman Islands. In *The Cayman Islands* (pp. 13-49): Springer.

Jones, B., & Hunter, I. G. (1990). Pleistocene paleogeography and sea levels on the Cayman Islands, British West Indies. *Coral Reefs, 9*(2), 81-91.

Jones, P. D., Jonsson, T., & Wheeler, D. (1997). Extension to the North Atlantic Oscillation using early instrumental pressure observations from Gibraltar and South-West Iceland. *International Journal of Climatology, 17*, 1433-1450.

Jones, P. D., Osborn, T. J., & Briffa, K. R. (2001). The evolution of climate over the last millennium. *SCience, 292*, 662-667.

Juillet-Leclerc, A., & Reynaud, S. (2010). Light effects on the isotopic fractionation of skeletal oxygen and carbon in the cultured zooxanthellate coral, Acropora: implications for coral-growth rates. *Biogeosciences, 7*(3), 893-906.

Juillet-Leclerc, A., & Schmidt, G. A. (2001). A calibration of the oxygen isotope paleothermometer of coral aragonite from Porites. *Geophysical Research Letters, 28*(21), 4135-4138.

Kalnay, E., Kanamitsu, M., Kistler, R., Collins, W., Deaven, D., Gandin, L., et al. (1996). The NCEP/NCAR 40-Year Reanalysis Project. *Bulletin of the American Meteorological Society, 77*(3), 437-471.

Kano, A., Ferdelman, T. G., Williams, T., Henriet, J.-P., Ishikawa, T., Kawagoe, N., et al. (2007). Age constraints on the origin and growth history of a deep-water coral mound in the northeast Atlantic drilled during Integrated Ocean Drilling Program Expedition 307. *Geology, 35*(11), 1051-1054.

Kaplan, A., Cane, M. A., Kushnir, Y., Clement, A., Blumenthal, M., & Rajagopalan, B. (1998). Analyses of global sea surface temperature 1856-1991. *Journal of Geophysical Research, 103*, 18,567-518,589.

Kavvada, A., Ruiz-Barradas, A., & Nigam, S. (2013). AMO's structure and climate footprint in observations and IPCC AR5 climate simulations. *Climate Dynamics, 41*(5-6), 1345-1364.

Keenlyside, N. S., Latif, M., Jungclaus, J., Kornblueh, L., & Roeckner, E. (2008). Advancing decadal-scale climate prediction in the North Atlantic sector. *Nature, 453*, doi:10.1038/nature06921.

Kerr, R. A. (2000). A North Atlantic Climate Pacemaker for the Centuries. *SCience, 288*(5473), 1984-1985.

Kilbourne, K. H., Quinn, T. M., Taylor, F. W., Delcroix, T., & Gouriou, Y. (2004). El Nino-Southern Oscillation-related salinity variations recorded in the skeletal geochemistry of a Porites coral from Espiritu Santo, Vanuatu. *Paleoceanography, 19*(PA4002), doi:10.1029/2004PA001033.

Kilbourne, K. H., Quinn, T. M., Webb, R., Guilderson, T., Nyberg, J., & Winter, A. (2008). Paleoclimate proxy perspective on Caribbean climate since the year 1751: Evidence of cooler temperatures and multidecadal variability. *Paleoceanography, 23*(3), doi:10.1029/2008PA001598.

Kilbourne, K. H., Quinn, T. M., Webb, R., Guilderson, T., Nyberg, J., & Winter, A. (2010). Coral windows onto seasonal climate variability in the northern Caribbean since 1479. *Geochem. Geophys. Geosyst., 11*(10), Q10006.

Kinder, T. H., Heburn, G. W., & Green, A. W. (1985). Some aspects of the Caribbean circulation. *Marine Geology, 68*, 25-52.

Kjerfve, B. (1981). Tides of the Caribbean Sea. *Journal of Geophysical Research: Oceans, 86*(C5), 4243-4247.

Knight, J. R., Allan, R. J., Folland, C. K., Vellinga, M., & Mann, M. E. (2005). A signature of persistent natural thermohaline circulation cycles in observed climate. *Geophysical Research Letters, 32*(L20708), doi:10.1029/2005GL024233.

Knight, J. R., Folland, C. K., & Scaife, A. A. (2006). Climate impacts of the Atlantic Multidecadal Oscillation. *Geophysical Research Letters, 33*(L17706), doi:10.1029/2006GL026242.

Knudsen, M. F., Seidenkrantz, M.-S., Jacobsen, B. H., & Kuijpers, A. (2011). Tracking the Atlantic Multidecadal Oscillation through the last 8,000 years. *Nat Commun, 2*, 178. 10.1038/ncomms1186.

Krastel, S., Böttner, C., Cartigny, M., Feldens, P., Fu, L., Glogowski, S., et al. (2014). Morphology, processes and geohazards of giant landslides in and around Agadir Canyon, northwest Africa-Cruise MSM32-September 25-October 30, 2013-Bremen (Germany)-Cádiz (Spain).

Kuffner, I. B., Jokiel, P. L., Rodgers, K. u. S., Andersson, A. J., & Mackenzie, F. T. (2012). An apparent "vital effect" of calcification rate on the Sr/Ca temperature proxy in the reef coral Montipora capitata. *Geochemistry, Geophysics, Geosystems, 13*(8).

Kuhnert, H., Crüger, T., & Pätzold, J. (2005). NAO signature in a Bermuda coral Sr/Ca record. *Geochemistry Geophysics Geosystems, 6*(4), doi:10.1029/2004GC000786.

Kushnir, Y. (1994). Interdecadal Variations in North Atlantic Sea Surface Temperature and Associated Atmospheric Conditions. *Journal of Climate, 7*(1), 141-157.

Kushnir, Y., Robinson, W. A., Chang, P., & Robertson, A. W. (2006). The physical basis for predicting Atlantic sector seasonal-to-interannual climate variability. *Journal of Climate, 19*(23), 5949-5970.

Küttel, M., Xoplaki, E., Gallego, D., Luterbacher, J., García-Herrera, R., Allan, R., et al. (2010). The importance of ship log data: reconstructing North Atlantic, European and Mediterranean sea level pressure fields back to 1750. *Climate Dynamics, 34*(7), 1115-1128. journal article.

Latif, M. (2001a). Tropical Pacific / Atlantic Ocean Interactions at Multi-Decadal Time Scales. *Geophysical Research Letters, 28*(3), 539-542.

Latif, M. (2001b). Tropical Pacific/Atlantic Ocean interactions at multi-decadal time scales. *Geophysical Research Letters, 28*(3), 539-542.

Latif, M., Boening, C., Willebrand, J., Biastoch, A., Dengg, J., Keenlyside, N., et al. (2006a). Is the Thermohaline Circulation Changing? *Journal of Climate, 19*, 4631-4637.

Latif, M., Collins, M., Pohlmann, H., & Keenlyside, N. S. (2006b). A Review of Predictability Studies of Atlantic Sector Climate on Decadal Time Scales. *Journal of Climate, 19*(23), 5971-5987.

Latif, M., & Keenlyside, N. S. (2011). A perspective on decadal climate variability and predictability. *Deep Sea Research Part II: Topical Studies in Oceanography, 58*(17–18), 1880-1894.

Latif, M., Roeckner, E., Mikolajewicz, U., & Voss, R. (2000). Tropical Stabilization of the Thermohaline Circulation in a Greenhouse Warming Simulation. *Journal of Climate, 13*, 1809-1813.

LaVigne, M., Field, M. P., Anagnostou, E., Grottoli, A. G., Wellington, G. M., & Sherrell, R. M. (2008). Skeletal P/Ca tracks upwelling in Gulf of Panama coral: Evidence for a new seawater phosphate proxy. *Geophysical Research Letters, 35*(5).

Le Guilloux, E., Olu, K., Bourillet, J.-F., Savoye, B., Iglésias, S., & Sibuet, M. (2009). First observations of deep-sea coral reefs along the Angola margin. *Deep Sea Research Part II: Topical Studies in Oceanography, 56*(23), 2394-2403.

Lea, D., Shen, G. T., & Boyle, E. A. (1989). Coralline barium records temporal variability in equatorial Pacific upwelling. *Nature, 340*, 373-376.

Leder, J. J., Swart, P. K., Szmant, A. M., & Dodge, R. E. (1996). The origin of variations in the isotopic record of scleractinian corals .1. Oxygen. *Geochimica Et Cosmochimica Acta, 60*(15), 2857-2870.

Lee, T. N., Johns, W. E., Zantopp, R. J., & Fillenbaum, E. R. (1996). Moored observations of western boundary current variability and thermohaline circulation at 26.5 in the subtropical North Atlantic. *Journal of Physical Oceanography, 26*(6), 962-983.

León, R., Somoza, L., Medialdea, T., Vázquez, J. T., González, F. J., López-González, N., et al. (2012). New discoveries of mud volcanoes on the Moroccan Atlantic continental

margin (Gulf of Cádiz): morpho-structural characterization. *Geo-Marine Letters, 32*(5-6), 473-488.

Levitus, S., Antonov, J. I., Boyer, T. P., & Stephens, C. (2000). Warming of the world ocean. *SCience, 287*(5461), 2225-2229.

Liebetrau, V., Eisenhauer, A., & Linke, P. (2010). Cold seep carbonates and associated cold-water corals at the Hikurangi Margin, New Zealand: new insights into fluid pathways, growth structures and geochronology. *Marine Geology, 272*(1-4), 307-318.

Lindberg, B., & Mienert, J. (2005). Postglacial carbonate production by cold-water corals on the Norwegian Shelf and their role in the global carbonate budget. *Geology, 33*(7), 537-540.

Linsley, B., Messier, R., & Dunbar, R. (1999). Assessing between-colony oxygen isotope variability in the coral Porites lobata at Clipperton Atoll. *Coral Reefs, 18*(1), 13-27.

Linsley, B. K., Dunbar, R. B., Wellington, G. M., & Mucciarone, D. A. (1994). A coral based reconstruction of Intertropical Convergence Zone variability over Central America since 1707. *Journal of Geophysical Research, 99*(C5), 9977-9994.

Linsley, B. K., Kaplan, A., Gouriou, Y., Salinger, J., deMenocal, P. B., Wellington, G. M., & Howe, S. S. (2006). Tracking the extent of the South Pacific Convergence Zone since the early 1600s. *Geochemistry Geophysics Geosystems, 7*(Q05003), doi:10.1029/2005GC001115.

Linsley, B. K., Wellington, G. M., & Schrag, D. P. (2000). Decadal sea surface temperature variability in the subtropical South Pacific from 1726 to 1997 A.D. *SCience, 290*, 1145-1148.

Linsley, B. K., Wellington, G. M., Schrag, D. P., Ren, L., Salinger, M. J., & Tudhope, A. W. (2004). Geochemical evidence from corals for changes in the amplitude and spatial pattern of South Pacific interdecadal climate variability over the last 300 years. *Climate Dynamics, 22*, 1-11.

Liu, W., Huang, B., Thorne, P. W., Banzon, V. F., Zhang, H.-M., Freeman, E., et al. (2015). Extended reconstructed sea surface temperature version 4 (ERSST. v4): Part II. Parametric and structural uncertainty estimations. *Journal of Climate, 28*(3), 931-951.

Liu, Y. Y., Lee, S. K., Muhling, B. A., Lamkin, J. T., & Enfield, D. B. (2012). Significant reduction of the Loop Current in the 21st century and its impact on the Gulf of Mexico. *Journal of Geophysical Research-Oceans, 117*.

Loder, J. W., & Garrett, C. (1978). The 18.6-year cycle of sea surface temperature in shallow seas due to variations in tidal mixing. *Journal of Geophysical Research: Oceans, 83*(C4), 1967-1970.

Loram, J. E., Trapido-Rosenthal, H. G., & Douglas, A. E. (2007). Functional significance of genetically different symbiotic algae Symbiodinium in a coral reef symbiosis. *Molecular Ecology, 16*(22), 4849-4857.

Lough, J. M. (2004). A strategy to improve the contribution of coral data to high-resolution paleoclimatology. *Palaeogeography, Palaeoclimatology, Palaeoecology, 204*(1–2), 115-143.

Lough, J. M. (2011). Great Barrier Reef coral luminescence reveals rainfall variability over northeastern Australia since the 17th century. *Paleoceanography, 26*(2), PA2201.

Lough, J. M., & Cooper, T. F. (2011). New insights from coral growth band studies in an era of rapid environmental change. *Earth-Science Reviews, 108*(3–4), 170-184.

Lund, D. C., Lynch-Stieglitz, J., & Curry, W. B. (2006). Gulf Stream density structure and transport during the past millennium. *Nature, 444*(7119), 601-604. 10.1038/nature05277.

Luo, Y., Doney, S., Anderson, L., Benavides, M., Berman-Frank, I., Bode, A., et al. (2012). Database of Diazotrophs in Global Ocean: Abundance, Biomass, and Nitrogen Fixation Rates. *Earth System Science Data, 4*(1).

Manabe, S., & Stouffer, R. J. (1999). The role of thermohaline circulation in climate. *Tellus B, 51*(1), 91-109.

Mangini, A., Godoy, J., Godoy, M., Kowsmann, R., Santos, G., Ruckelshausen, M., et al. (2010). Deep sea corals off Brazil verify a poorly ventilated Southern Pacific Ocean during H2, H1 and the Younger Dryas. *Earth and Planetary Science Letters, 293*(3-4), 269-276.

Marion, G. S., Dunbar, R. B., Mucciarone, D. A., Kremer, J. N., Lansing, J. S., & Arthawiguna, A. (2005). Coral skeletal δ15N reveals isotopic traces of an agricultural revolution. *Marine Pollution Bulletin, 50*(9), 931-944.

Marshall, J. F., Kushnir, Y., Battisti, D., Chang, P., Czaja, A., Dickson, R., et al. (2001). North Atlantic climate variability: phenomena, impacts and mechanisms. *International Journal of Climatology, 21*, 1863-1898.

Marshall, J. F., & McCulloch, M. T. (2002). An assessment of the Sr/Ca ratio in shallow water hermatypic corals as a proxy for sea surface temperature. *Geochimica Et Cosmochimica Acta, 66*(18), 3263-3280.

Martorelli, E., Petroni, G., & Chiocci, F. L. (2011). Contourites offshore Pantelleria Island (Sicily Channel, Mediterranean Sea): depositional, erosional and biogenic elements. *Geo-Marine Letters, 31*(5-6), 481-493.

Matson, E. G. (2011). Core Plugs. In D. Hopley (Ed.), *Encyclopedia of Modern Coral Reefs: Structure, Form and Process* (pp. 294-296). Dordrecht: Springer Netherlands.

Maupin, C. R., Quinn, T. M., & Halley, R. B. (2008). Extracting a climate signal from the skeletal geochemistry of the Caribbean coral Siderastrea siderea. *Geochem. Geophys. Geosyst., 9*(12), Q12012.

Mazzini, A., Akhmetzhanov, A., Monteys, X., & Ivanov, M. (2012). The Porcupine Bank Canyon coral mounds: oceanographic and topographic steering of deep-water

carbonate mound development and associated phosphatic deposition. *Geo-Marine Letters, 32*(3), 205-225.

McCabe, R. M., Estrade, P., Middleton, J. H., Melville, W. K., Roughan, M., & Lenain, L. (2010). Temperature variability in a shallow, tidally isolated coral reef lagoon. *Journal of Geophysical Research: Oceans, 115*(C12), C12011.

McCarthy, G. D., Haigh, I. D., Hirschi, J. J. M., Grist, J. P., & Smeed, D. A. (2015). Ocean impact on decadal Atlantic climate variability revealed by sea-level observations. *Nature, 521*, 508.

McConnaughey, T. (1989a). ^{13}C and ^{18}O isotopic disequilibrium in biological carbonates: I. Patterns. *Geochimica Et Cosmochimica Acta, 53*(1), 151-162.

McConnaughey, T. (1989b). ^{13}C and ^{18}O isotopic disequilibrium in biological carbonates: II. In Vitro simulation of kinetic isotope effects. *Geochimica Et Cosmochimica Acta, 53*, 163-171.

McCrea, J. M. (1950). On the isotopic chemistry of carbonates and a paleotemperature scale. *Journal of Chemical Physics, 18*, 849-857.

McCulloch, M. T., Alibert, C., Sinclair, D., Mortimer, G., & L., K. (1997). *Trace-element systematics in Porites coral: High-resolution proxies of sea-surface temperature.* Paper presented at the V. M. Goldschmidt Conference, Prog. & Abstr., Tucson.

McCulloch, M. T., Gagan, M. K., Mortimer, G. E., Chivas, A. R., & Isdale, P. J. (1994). A high-resolution Sr/Ca and d^{18}O coral record from the Great Barrier Reef, Australia, and the 1982-1983 El Nino. *Geochimica Et Cosmochimica Acta, 58*(12), 2747-2754.

McDougall, T. J., & Barker, P. M. (2011). Getting started with TEOS-10 and the Gibbs Seawater (GSW) oceanographic toolbox. *SCOR/IAPSO WG, 127*, 1-28.

McGregor, H. V., & Gagan, M. K. (2004). Western Pacific coral d18O records of anomalous Holocene variability in the El Nino-Southern Oscillation. *Geophysical Research Letters, 31*(L11204), doi:10.1029/2004GL019972.

Meibom, A., Stage, M., Wooden, J., Constantz, B. R., Dunbar, R. B., Owen, A., et al. (2003). Monthly Strontium/Calcium oscillations in coral aragonite: Biological effects limiting the precision of the paleotemperature proxy. *Geophysical Research Letters, 30*(7), 1418.

Messing, C. G., Reed, J. K., Brooke, S. D., & Ross, S. W. (2008). Deep-water coral reefs of the United States. In *Coral Reefs of the USA* (pp. 767-791): Springer.

Middlebrook, R., Hoegh-Guldberg, O., & Leggat, W. (2008). The effect of thermal history on the susceptibility of reef-building corals to thermal stress. *Journal of Experimental Biology, 211*(7), 1050-1056.

Mienis, F., Van Weering, T., De Haas, H., De Stigter, H., Huvenne, V., & Wheeler, A. (2006). Carbonate mound development at the SW Rockall Trough margin based on high resolution TOBI and seismic recording. *Marine Geology, 233*(1-4), 1-19.

Milliman, J., & Droxler, A. (1996). Neritic and pelagic carbonate sedimentation in the marine environment: ignorance is not bliss. *Geologische Rundschau, 85*(3), 496-504.

Milliman, J. D. (1993). Production and accumulation of calcium carbonate in the ocean: budget of a nonsteady state. *Global Biogeochemical Cycles, 7*(4), 927-957.

Mitchell, J. F. B., Wilson, C. A., & Cunnington, W. M. (1987). On CO2 climate sensitivity and model dependence of results. *Quarterly Journal of the Royal Meteorological Society, 113*, 293-322.

Mitchell, T. (2015). Sahel precipitation index. *Joint Institute for the Study of the Atmosphere and Ocean, Univ. of Washington, Seattle, doi, 10*, H5MW2F2Q.

Mitsuguchi, T., Dang, P. X., Kitagawa, H., Uchida, T., & Shibata, Y. (2008). Coral Sr/Ca and Mg/Ca records in Con Dao Island off the Mekong Delta: assessment of their potential for monitoring ENSO and East Asian monsoon. *Global and Planetary Change, 63*(4), 341-352.

Mitsuguchi, T., Matsumato, E., Abe, O., Uchida, T., & Isdale, P. J. (1996). Mg/Ca thermometry in coral skeletons. *SCience, 274*, 961-963.

Mittelstaedt, E. (1991). The ocean boundary along the northwest African coast: Circulation and oceanographic properties at the sea surface. *Progress in Oceanography, 26*(4), 307-355.

Molinari, R. L., Spillane, M., Brooks, I., Atwood, D., & Duckett, C. (1981). Surface currents in the Caribbean Sea as deduced from Lagrangian observations. *Journal of Geophysical Research: Oceans, 86*(C7), 6537-6542.

Monismith, S. G., Genin, A., Reidenbach, M. A., Yahel, G., & Koseff, J. R. (2006). Thermally Driven Exchanges between a Coral Reef and the Adjoining Ocean. *Journal of Physical Oceanography, 36*(7), 1332-1347.

Montagna, P., McCulloch, M., Douville, E., Correa, M. L., Trotter, J., Rodolfo-Metalpa, R., et al. (2014). Li/Mg systematics in scleractinian corals: Calibration of the thermometer. *Geochimica Et Cosmochimica Acta, 132*, 288-310.

Montagna, P., McCulloch, M., Mazzoli, C., Silenzi, S., & Odorico, R. (2007). The non-tropical coral *Cladocora caespitosa* as the new cliamte archive for the Mediterranean: high-resolution (~weekly) trace element systematics. *Quaternary Science Reviews, 26*, 441-462.

Montagna, P., McCulloch, M., Taviani, M., Remia, A., & Rouse, G. (2005). High-resolution trace and minor element compositions in deep-water scleractinian corals (Desmophyllum dianthus) from the Mediterranean Sea and the Great Australian Bight. In *Cold-Water Corals and Ecosystems* (pp. 1109-1126): Springer.

Moore, C. M., Mills, M. M., Achterberg, E. P., Geider, R. J., LaRoche, J., Lucas, M. I., et al. (2009). Large-scale distribution of Atlantic nitrogen fixation controlled by iron availability. *Nature Geoscience, 2*(12), 867.

Morigi, C., Jorissen, F., Gervais, A., Guichard, S., & Borsetti, A. (2001). Benthic foraminiferal faunas in surface sediments off NW Africa: relationship with organic flux to the ocean floor. *Journal of Foraminiferal Research, 31*(4), 350-368.

Morrison, J. M., & Nowlin, W. D. (1982). General distribution of water masses within the eastern Caribbean Sea during the winter 1972 and fall of 1973. *Journal of Geophysical Research, 87*, 4207-4229.

Moses, C. S., Swart, P. K., & Dodge, R. E. (2006). Calibration of stable oxygen isotopes in Siderastrea radians (Cnidaria:Scleractinia): Implications for slow-growing corals. *Geochemistry Geophysics Geosystems, 7*(9), doi:10.1029/2005GC001196.

Moura, A. D., & Shukla, J. (1981). On the dynamics of droughts in Northeast Brazil - observations, theory and numerical experiments with a general circulation model. *Journal of Atmospheric Science, 38*, 2653-2675.

Murton, B. J., Rouse, I. P., Millard, N. W., & Flewellen, C. G. (1992). Multisensor, deep - towed instrument explores ocean floor. *Eos, Transactions American Geophysical Union, 73*(20), 225-228.

Muscatine, L., Goiran, C., Land, L., Jaubert, J., Cuif, J.-P., & Allemand, D. (2005). Stable isotopes (δ13C and δ15N) of organic matrix from coral skeleton. *Proceedings of the National Academy of Sciences, 102*(5), 1525-1530.

National Oceanic and Atmospheric Administration (NOAA). (2018). Coral Bleaching During & Since the 2014-2017 Global Coral Bleaching Event Status and an Appeal for Observations. Retrieved from https://coralreefwatch.noaa.gov/satellite/analyses_guidance_global_coral_bleaching_2014-17_status.php

Newton, C. R., Mullins, H. T., Gardulski, A. F., Hine, A. C., & Dix, G. R. (1987). Coral mounds on the west Florida slope: unanswered questions regarding the development of deep-water banks. *PALAIOS*, 359-367.

Nyberg, J., Malmgren, B. A., Winter, A., Jury, M. R., Kilbourne, K. H., & Quinn, T. M. (2007). Low Atlantic hurricane activity in the 1970s and 1980s compared to the past 270 years. *Nature, 447*, doi:10.1038/nature05895.

O'Reilly, C. H., Huber, M., Woollings, T., & Zanna, L. (2016). The signature of low - frequency oceanic forcing in the Atlantic Multidecadal Oscillation. *Geophysical Research Letters, 43*(6), 2810-2818.

Oliver, J. K., Berkelmans, R., & Eakin, C. M. (2009). Coral Bleaching in Space and Time. In M. J. H. van Oppen & J. M. Lough (Eds.), *Coral Bleaching: Patterns, Processes, Causes and Consequences* (pp. 21-39). Berlin, Heidelberg: Springer Berlin Heidelberg.

Oliver, T. A., & Palumbi, S. R. (2011). Do fluctuating temperature environments elevate coral thermal tolerance? *Coral Reefs, 30*(2), 429-440.

Oomori, T., Kaneshima, K., Nakamura, Y., & Kitano, Y. (1982). Seasonal variation of minor elements in coral skeletons. *Galaxea, 1*, 77–86.

Ourbak, T., Correge, T., Malaize, B., Le Cornec, F., Charlier, K., & Peypouquet, J. P. (2006). ENSO and interdecadal climate variability over the last century documented by geochemical records of two coral cores from the South West Pacific. *Advances in Geosciences, 6*, 23-27.

Ourbak, T., Delong, K., Correge, T., Malaize, B., Kilbourne, K., Caquineau, S., & Hollander, D. (2008). *The significance of geochemical proxies in corals, does size (age) matter* (Vol. 1): Nova Southeastern University National Coral Reef Institute.

Paillard, D., Labeyrie, L., & Yiou, P. (1996). Macintosh program performs time-series analysis. *Eos Transactions AGU, 77*, 379.

Palomino, D., Vázquez, J.-T., Ercilla, G., Alonso, B., López-González, N., & Díaz-del-Río, V. (2011). Interaction between seabed morphology and water masses around the seamounts on the Motril Marginal Plateau (Alboran Sea, Western Mediterranean). *Geo-Marine Letters, 31*(5-6), 465-479.

Pandolfi, J. M., Bradbury, R. H., Sala, E., Hughes, T. P., Bjorndal, K. A., Cooke, R. G., et al. (2003). Global Trajectories of the Long-Term Decline of Coral Reef Ecosystems. *SCience, 301*, 955-958.

Pandolfi, J. M., Connolly, S. R., Marshall, D. J., & Cohen, A. L. (2011). Projecting Coral Reef Futures Under Global Warming and Ocean Acidification. *SCience, 333*(6041), 418-422.

Parker, D., Folland, C., Scaife, A., Knight, J., Colman, A., Baines, P., & Dong, B. (2007). Decadal to multidecadal variability and the climate change background. *J. Geophys. Res., 112*(D18), D18115.

Pastor, M. V., Pelegrí, J. L., Hernández-Guerra, A., Font, J., Salat, J., & Emelianov, M. (2008). Water and nutrient fluxes off Northwest Africa. *Continental Shelf Research, 28*(7), 915-936.

Pelegrí, J., Marrero-Díaz, A., Ratsimandresy, A., Antoranz, A., Cisneros-Aguirre, J., Gordo, C., et al. (2005). Hydrographic cruises off northwest Africa: the Canary Current and the Cape Ghir region. *Journal of Marine Systems, 54*(1-4), 39-63.

Peterson, L. C., Overpeck, J. T., Kipp, N. G., & Imbrie, J. (1991). A high-resolution late Quaternary upwelling record from the anoxic Cariaco Basin, Venezuela. *Paleoceanography, 6*, 99-119.

Pfannkuche, O., Bannert, B., Cragg, B., Domeyer, B., Flögel, S., Gürs, K., et al. (2006). *Cruise Report Maria S. Merian 1/3, 12. April - 19. Mai 2006*. Retrieved from http://www.senckenberg.de/files/content/forschung/abteilung/meeresforschung/meeresgeologie/expeditionen/msm1_3_final_report-olafsteil.pdf:

Pfeiffer, M., Dullo, W.-C., Zinke, J., & Garbe-Schönberg, D. (2009). Three monthly coral Sr/Ca records from the Chagos Archipelago covering the period of 1950–1995 A.D.: reproducibility and implications for quantitative reconstructions of sea surface temperature variations. *International Journal of Earth Sciences, 98*, 53-66.

Pfeiffer, M., & Dullo, W. C. (2006). Monsoon-induced cooling of the western equatorial Indian Ocean as recorded in coral oxygen isotope records from the Seychelles covering the period of 1840–1994AD. *Quaternary Science Review, 25*, 993-1009.

Pfeiffer, M., Dullo, W. C., & Eisenhauer, A. (2004a). Variability of the Intertropical Convergence Zone recorded in coral isotopic records from the central Indian Ocean (Chagos Archipelago). *Quaternary Research, 61*, 245-255.

Pfeiffer, M., Timm, O., Dullo, W., & Garbe-Schöneberg, D. (2006a). Paired coral Sr/Ca and $d^{18}O$ records from the Chagos Archipelago: Late twentieth century warming affects rainfall variability in the tropical Indian Ocean. *Geology, 34*(12), 1069-1072.

Pfeiffer, M., Timm, O., Dullo, W.-C., & Podlech, S. (2004b). Oceanic forcing of interannual and multidecadal climate variability in the southwestern Indian Ocean: Evidence from a 160 year coral isotopic record (La Reunion, 55°E, 21°S). *Paleoceanography, 19*, PA4006, doi:4010.1029/2003PA000964.

Pfeiffer, M., Timm, O., & Dullo, W. C. (2006b). *Sr/Ca and oxygen isotope records of modern Porites corals from the tropical Indian Ocean: 20th century warming affects rainfall variability*. Paper presented at the AGU Ocean Sciences, Honolulu.

Pfeiffer, M., Timm, O., Dullo, W. C., & Podlech, S. (2004c). Oceanic forcing of interannal and multidecadal climate variability in the southwestern Indian Ocean: Evidence from a 160 year coral isotopic record (La Réunion, 55°E, 21°S). *Paleoceanography, 19*.

Pfeiffer, M., Zinke, J., Dullo, W.-C., Garbe-Schönberg, D., Latif, M., & Weber, M. (2017). Indian Ocean corals reveal crucial role of World War II bias for twentieth century warming estimates. *Scientific Reports, 7*(1), 14434.

Philander, S. G. H. (1990). *El Niño, La Niña, and the Southern Oscillation*. San Diego, California: Academic Press.

Pozo-Vazquez, D., Esteban-Parra, M. J., Rodrigo, F. S., & Castro-Diez, Y. (2001). A study of NAO variability and its possible non-linear influences on European surface temperature. *Climate Dynamics, 17*(9), 701-715.

Qu, X., Hall, A., Klein, S. A., & Caldwell, P. M. (2014). On the spread of changes in marine low cloud cover in climate model simulations of the 21st century. *Climate Dynamics, 42*(9-10), 2603-2626.

Quinn, T. M., Crowley, T. J., Taylor, F. W., Henin, C., Joannot, P., & Join, Y. (1998). A multicentury stable isotope record from a New Caledonia coral: Interannual and decadal sea surface temperature variability in the southwest Pacific since 1657 AD. *Paleoceanography, 13*(4), 412-426.

Quinn, T. M., & Sampson, D. E. (2002). A multiproxy approach to reconstructing sea surface conditions using coral skeleton geochemistry. *Paleoceanography, 17*(4), 1062.

Quinn, T. M., & Taylor, F. W. (2006). SST artifacts in coral proxy records produced by early marine diagenesis in a modern coral from Rabaul, Papua New Guinea. *Geophysical Research Letters, 33*(L04601), doi:10.1029/2005GL024972.

Quinn, T. M., Taylor, F. W., & Crowley, T. J. (2006). Coral-based climate variability in the Western Pacific Warm Pool since 1867. *Journal of Geophysical Research, 111*(C11006), doi:10.1029/2005JC003243.

Raddatz, J., Liebetrau, V., Rüggeberg, A., Hathorne, E., Krabbenhöft, A., Eisenhauer, A., et al. (2013). Stable Sr-isotope, Sr/Ca, Mg/Ca, Li/Ca and Mg/Li ratios in the scleractinian cold-water coral Lophelia pertusa. *Chemical Geology, 352*, 143-152.

Raddatz, J., Liebetrau, V., Trotter, J., Rüggeberg, A., Flögel, S., Dullo, W. C., et al. (2016). Environmental constraints on Holocene cold‐water coral reef growth off Norway: Insights from a multiproxy approach. *Paleoceanography, 31*(10), 1350-1367.

Raddatz, J., Rüggeberg, A., Liebetrau, V., Foubert, A., Hathorne, E. C., Fietzke, J., et al. (2014). Environmental boundary conditions of cold-water coral mound growth over the last 3 million years in the Porcupine Seabight, Northeast Atlantic. *Deep Sea Research Part II: Topical Studies in Oceanography, 99*, 227-236.

Rahmstorf, S., Box, J. E., Feulner, G., Mann, M. E., Robinson, A., Rutherford, S., & Schaffernicht, E. J. (2015). Exceptional twentieth-century slowdown in Atlantic Ocean overturning circulation. *Nature climate change, 5*(5), 475.

Raible, C. C., Lehner, F., Gonzalez-Rouco, J. F., & Fernandez-Donado, L. (2014). Changing correlation structures of the Northern Hemisphere atmospheric circulation from 1000 to 2100 AD. *Climate of the Past, 10*(2), 537-550.

Raible, C. C., Luksch, U., Fraedrich, K., & Voss, R. (2001). North Atlantic decadal regimes in a coupled GCM simulation. *Climate Dynamics, 18*(3-4), 321-330.

Raible, C. C., Stocker, T. F., Yoshimori, M., Renold, M., Beyerle, U., Casty, C., & Luterbacher, J. (2005). Northern hemispheric trends of pressure indices and atmospheric circulation patterns in observations, reconstructions, and coupled GCM simulations. *Journal of Climate, 18*(19), 3968-3982.

Rapp, H., & Sneli, J. (1999). *Lophelia pertusa–myths and realities–poster*. Paper presented at the Proceedings of the 2nd Nordic Marine Oceanographes Conference, Hirtshals, Denmark.

Ray, R. D. (2007). Decadal Climate Variability: Is There a Tidal Connection? *Journal of Climate, 20*(14), 3542-3560.

Rayner, N. A., Parker, D. E., Horton, E. B., Folland, C. K., Alexander, L. V., Rowell, D. P., et al. (2003). Global analyses of sea surface temperature, sea ice, and night marine air temperature since the late nineteenth century. *J. Geophys. Res., 108*(D14), 4407.

Reed, J. K., Weaver, D. C., & Pomponi, S. A. (2006). Habitat and fauna of deep-water Lophelia pertusa coral reefs off the southeastern US: Blake Plateau, Straits of Florida, and Gulf of Mexico. *Bulletin of Marine Science, 78*(2), 343-375.

Ren, L., Linsley, B. K., Wellington, G. M., Schrag, D., & Hoegh-Guldberg, O. (2002). Deconvolving the $d^{18}O$ seawater component from subseasonal coral $d^{18}O$ and Sr/Ca at Rarotonga in the southwestern subtropical Pacific for the period 1726 to 1997. *Geochimica Et Cosmochimica Acta, 67*(9), 1609-1621.

Reveillaud, J., Freiwald, A., Van Rooij, D., Le Guilloux, E., Altuna, A., Foubert, A., et al. (2008). The distribution of scleractinian corals in the Bay of Biscay, NE Atlantic. *Facies, 54*(3), 317-331.

Reyes, J., Santodomingo, N., Gracia, A., Borrero-Pérez, G., Navas, G., Mejía-Ladino, L. M., et al. (2005). Southern Caribbean azooxanthellate coral communities off Colombia. In *Cold-water corals and Ecosystems* (pp. 309-330): Springer.

Reynaud, S., Ferrier-Pages, C., Meibom, A., Mostefaoui, S., Mortlock, R., Fairbanks, R., & Allemand, D. (2007). Light and temperature effects on Sr/Ca and Mg/Ca ratios in the scleractinian coral Acropora sp. *Geochimica Et Cosmochimica Acta, 71*(2), 354-362.

Rice, A., Billett, D., Thurston, M., & Lampitt, R. (1991). The Institute of Oceanographic Sciences biology programme in the Porcupine Seabight: background and general introduction. *Journal of the Marine Biological Association of the United Kingdom, 71*(2), 281-310.

Richardson, P. L. (2005). Caribbean current and eddies as observed by surface drifters. *Deep Sea Research II*.

Richardson, P. L., & McKee, T. K. (1984). Average Seasonal Variation of the Atlantic Equatorial Currents from Historical Ship Drifts. *Journal of Physical Oceanography, 14*, 1226-1238.

Roberts, H. H., Murray, S. P., & Suhayda, J. N. (1975). Physical processes in fringing reef systems. *Journal of Marine Research, 33*(2), 233-260.

Roberts, J., Harvey, S., Lamont, P., Gage, J., & Humphery, J. (2000). Seabed photography, environmental assessment and evidence for deep-water trawling on the continental margin west of the Hebrides. *Hydrobiologia, 441*(1), 173-183.

Roberts, J. M., Wheeler, A., Freiwald, A., & Cairns, S. (2009). *Cold-water corals: the biology and geology of deep-sea coral habitats*: Cambridge University Press.

Roberts, J. M., Wheeler, A. J., & Freiwald, A. (2006a). Reefs of the deep: The biology and geology of cold-water coral ecosystems. *SCience, 312*, 543-547.

Roberts, J. M., Wheeler, A. J., & Freiwald, A. (2006b). Reefs of the deep: the biology and geology of cold-water coral ecosystems. *SCience, 312*(5773), 543-547.

Rodwell, M. J., Rowell, D. P., & Folland, C. K. (1999). Oceanic forcing of the wintertime North Atlantic Oscillation and European climate. *Nature, 398*, 320-323.

Roemmich, D. (1981). Circulation in the Caribbean Sea: A well-resolved inverse problem. *Journal of Geophysical Research, 81*, 7993-8005.

Rogers, J. C., & Van Loon, H. (1979). The Seesaw in Winter Temperatures between Greenland and Northern Europe. Part II: Some Oceanic and Atmospheric Effects in Middle and High Latitudes. *Monthly Weather Review, 107*(5), 509-519.

Rosenheim, B. E., Swart, P. K., Thorrold, S. R., Eisenhauer, A., & Willenz, P. (2005). Salinity change in the subtropical Atlantic: Secular increase and teleconnections to the North Atlantic Oscillation. *Geophysical Research Letters, 32*(2).

Rosenheim, B. E., Swart, P. K., Thorrold, S. R., Willenz, P., Berry, L., & Latkoczy, C. (2004). High-resolution Sr/Ca records in sclerosponges calibrated to temperature in situ. *Geology, 32*(2), 145-148.

Rüggeberg, A., Dorschel, B., Dullo, W.-C., & Hebbeln, D. (2005). Sedimentary patterns in the vicinity of a carbonate mound in the Hovland Mound Province, northern Porcupine Seabight. In *Cold-water Corals and Ecosystems* (pp. 87-112): Springer.

Rüggeberg, A., Dullo, C., Dorschel, B., & Hebbeln, D. (2007). Environmental changes and growth history of a cold-water carbonate mound (Propeller Mound, Porcupine Seabight). *International Journal of Earth Sciences, 96*(1), 57-72.

Rüggeberg, A., Fietzke, J., Liebetrau, V., Eisenhauer, A., Dullo, W.-C., & Freiwald, A. (2008). Stable strontium isotopes (δ88/86Sr) in cold-water corals—a new proxy for reconstruction of intermediate ocean water temperatures. *Earth and Planetary Science Letters, 269*(3-4), 570-575.

Rüggeberg, A., Flögel, S., Dullo, W.-C., Hissmann, K., & Freiwald, A. (2011). Water mass characteristics and sill dynamics in a subpolar cold-water coral reef setting at Stjernsund, northern Norway. *Marine Geology, 282*(1-2), 5-12.

Ruggeberg, A., Flogel, S., Dullo, W. C., Raddatz, J., & Liebetrau, V. (2016). Paleoseawater density reconstruction and its implication for cold-water coral carbonate mounds in the northeast Atlantic through time. *Paleoceanography, 31*(3), 365-379.

Ruiz-Barradas, A., Carton, J. A., & Nigam, S. (2003). Role of the Atmosphere in Climate Variability of the Tropical Atlanic. *Journal of Climate, 16*, 2052-2065.

Saenger, C., Cohen, A. L., Oppo, D. W., Halley, R. B., & Carilli, J. E. (2009). Surface-temperature trends and variability in the low-latitude North Atlantic since 1552. *Nature Geoscience, 2*(7), 492-495.

Saenger, C., Cohen, A. L., Oppo, D. W., & Hubbard, D. (2008). Interpreting sea surface temperature from strontium/calcium ratios in Montastrea corals: Link with growth rate and implications for proxy reconstructions. *Paleoceanography, 23*(3), PA3102.

Sagar, N., Hetzinger, S., Pfeiffer, M., Masood Ahmad, S., Dullo, W.-C., & Garbe-Schönberg, D. (2016). High-resolution Sr/Ca ratios in a Porites lutea coral from Lakshadweep Archipelago, southeast Arabian Sea: An example from a region experiencing steady rise in the reef temperature. *Journal of Geophysical Research: Oceans, 121*(1), 252-266.

Sakai, S., Kano, A., & Abe, K. (2009). Origin, glacial-interglacial responses, and controlling factors of a cold-water coral mound in NE Atlantic. *Paleoceanography, 24*.

Sánchez, F., González-Pola, C., Druet, M., García-Alegre, A., Acosta, J., Cristobo, J., et al. (2014). Habitat characterization of deep-water coral reefs in La Gaviera canyon (Avilés Canyon System, Cantabrian Sea). *Deep Sea Research Part II: Topical Studies in Oceanography, 106*, 118-140.

Saravanan, R., & Chang, P. (2000). Interaction between tropical Atlantic variability and El Nino-Southern Oscillation. *Journal of Climate, 13*, 2177-2194.

Sato, O. T., & Rossby, T. (1995). Seasonal and low frequency variations in dynamic height anomaly and transport of the Gulf Stream. *Deep Sea Research Part I, 42*, 149-164.

Savini, A., Vertino, A., Marchese, F., Beuck, L., & Freiwald, A. (2014). Mapping cold-water coral habitats at different scales within the Northern Ionian Sea (Central Mediterranean): an assessment of coral coverage and associated vulnerability. *PLoS ONE, 9*(1), e87108.

Sayago-Gil, M., Long, D., Hitchen, K., Díaz-del-Río, V., Fernández-Salas, L. M., & Durán-Muñoz, P. (2010). Evidence for current-controlled morphology along the western slope of Hatton Bank (Rockall Plateau, NE Atlantic Ocean). *Geo-Marine Letters, 30*(2), 99-111.

Sayani, H. R., Cobb, K. M., Cohen, A. L., Elliott, W. C., Nurhati, I. S., Dunbar, R. B., et al. (2011). Effects of diagenesis on paleoclimate reconstructions from modern and young fossil corals. *Geochimica Et Cosmochimica Acta, 75*(21), 6361-6373. doi: 10.1016/j.gca.2011.08.026.

Scheltema, R. S. (1971). Larval dispersal as a means of genetic exchange between geographically separated populations of shallow-water benthic marine gastropods. *The biological bulletin, 140*(2), 284-322.

Schlesinger, M. E., & Ramankutty, N. (1994). An oscillation in the global climate system of period 65-70 years. *Nature, 367*(6465), 723-726.

Schlitzer, R. (2013). Ocean Data View. Retrieved from http://odv.awi.de

Schmidt, G. A. (1999). Error analysis of paleosalinity calculations. *Paleoceanography, 14*(3), 422-429.

Schmitz, W. J., Luyten, J. R., & Schmitt, R. W. (1993). On the Florida Current T/S envelope. *Bulletin of Marine Science, 53*, 1048-1065.

Schmitz, W. J., & McCartney, M. S. (1993). On the North Atlantic circulation. *Rev. Geophys., 31*, 29-49.

Schmitz, W. J., & Richardson, P. L. (1991). On the Sources of the Florida Current. *Deep-Sea Research Part a-Oceanographic Research Papers, 38*, S379-S409.

Schneider, R. R., Schulz, H. D., & Hensen, C. (2006). Marine carbonates: their formation and destruction. In *Marine geochemistry* (pp. 311-337): Springer.

Schrag, D. P. (1999). Rapid analysis of high-precision Sr/Ca ratios in corals and other marine carbonates. *Paleoceanography, 14*, 97-102.

Scott, R. B., Holland, C. L., & Quinn, T. M. (2010). Multidecadal Trends in Instrumental SST and Coral Proxy Sr/Ca Records. *Journal of Climate, 23*(5), 1017-1033.

Shaffrey, L., & Sutton, R. (2006). Bjerknes compensation and the decadal variability of the energy transports in a coupled climate model. *Journal of Climate, 19*(7), 1167-1181.

Shannon, R. D. (1976). Revised effective ionic radii and systematic studies of interatomic distances in halides and chalcogenides. *Acta crystallographica section A: crystal physics, diffraction, theoretical and general crystallography, 32*(5), 751-767.

Shen, C., Wang, W.-C., Gong, W., & Hao, Z. (2006). A Pacific Decadal Oscillation record since 1470 AD reconstructed from proxy data of summer rainfall over eastern China. *Geophysical Research Letters, 33*.

Shen, C.-C., Lee, T., Chen, C.-Y., Wang, C.-H., Dai, C.-F., & Li, L.-A. (1996a). The calibration of D[Sr/Ca]versus sea surface temperature relationship for Porites corals. *Geochimica Et Cosmochimica Acta, 60*(20), 3849-3858.

Shen, C. C., Lee, T., Chen, C. Y., Wang, C. H., Dai, C. F., & Li, L. A. (1996b). The calibration of D[Sr/Ca] versus sea surface temperature relationship for Porites corals. *Geochimica Et Cosmochimica Acta, 60*(20), 3849-3858.

Sherwood, O. A., Guilderson, T. P., Batista, F. C., Schiff, J. T., & McCarthy, M. D. (2014). Increasing subtropical North Pacific Ocean nitrogen fixation since the Little Ice Age. *Nature, 505*(7481), 78.

Shirai, K., Kusakabe, M., Nakai, S., Ishii, T., Watanabe, T., Hiyagon, H., & Sano, Y. (2005). Deep-sea coral geochemistry: Implication for the vital effect. *Chemical Geology, 224*, 212-222.

Sigman, D., Altabet, M., McCorkle, D., Francois, R., & Fischer, G. (2000). The δ15N of nitrate in the Southern Ocean: Nitrogen cycling and circulation in the ocean interior. *Journal of Geophysical Research: Oceans, 105*(C8), 19599-19614.

Sinclair, D. J. (1999). *High Spatial-resolution Analysis of Trace Elements in Corals Using Laser Ablation ICP-MS*. Canberra: Australlian National University 1999.

Sinclair, D. J., Williams, B., & Risk, M. (2006). A biological origin for climate signals in corals-Trace element "vital effects" are ubiquitious in Scleractinian coral skeletons. *Geophysical Research Letters, 33*(L17707), doi:10.1029/2006GL027183.

Smith, J. E., Schwarcz, H. P., Risk, M. J., McCONNAUGHEY, T. A., & Keller, N. (2000). Paleotemperatures from deep-sea corals: overcoming 'vital effects'. *PALAIOS, 15*(1), 25-32.

Smith, J. M., Quinn, T. M., Helmle, K. P., & Halley, R. B. (2006). Reproducibility of geochemical and climatic signals in the Atlantic coral *Montastrea faveolata*. *Paleoceanography, 21*(PA1010), doi:10.1029/2005PA001187.

Smith, N. P., & Kierspe, G. H. (1981). Local energy exchanges in a shallow, coastal lagoon: Winter conditions. *Estuarine, Coastal and Shelf Science, 13*(2), 159-167.

Smith, S. V., Buddemeier, R. W., Redalje, R. C., & Houck, J. E. (1979). Strontium-calcium thermometry in coral skeletons. *SCience, 204*, 404-407.

Smith, S. V., & Mackenzie, F. T. (2016). The role of CaCO 3 reactions in the contemporary oceanic CO 2 cycle. *Aquatic geochemistry, 22*(2), 153-175.

Smith, T. M., & Reynolds, R. W. (2003). Extended reconstruction of global sea surface temperatures based on COADS data (1854-1997). *Journal of Climate, 16*, 1495-1510.

Somoza, L., Ercilla, G., Urgorri, V., León, R., Medialdea, T., Paredes, M., et al. (2014). Detection and mapping of cold-water coral mounds and living Lophelia reefs in the Galicia Bank, Atlantic NW Iberia margin. *Marine Geology, 349*, 73-90.

Stephans, C. L., Quinn, T. M., Taylor, F. W., & Correge, T. (2004). Assessing the reproducibility of coral-based climate records. *Geophysical Research Letters, 31*(L18210), doi:10.1029/2004GL020343.

Stoddart, D. R. (1980). Geology and Geomorphology of Little Cayman. Geography and Ecology of Little Cayman.

Stoll, H. M., & Schrag, D. P. (1998). Effects of Quaternary sea level cycles on strontium in seawater. *Geochimica Et Cosmochimica Acta, 62*(7), 1107-1118.

Straub, M., Sigman, D. M., Ren, H., Martínez-García, A., Meckler, A. N., Hain, M. P., & Haug, G. H. (2013). Changes in North Atlantic nitrogen fixation controlled by ocean circulation. *Nature, 501*(7466), 200.

Sumida, P. Y. G., Yoshinaga, M. Y., Madureira, L. A. S.-P., & Hovland, M. (2004). Seabed pockmarks associated with deepwater corals off SE Brazilian continental slope, Santos Basin. *Marine Geology, 207*(1-4), 159-167.

Sun, D., Gagan, M.K.,. (2005). Seasonal and interannual variability of the Mid-Holocene East Asian monsoon in coral d18O records from the South China Sea. *Earth and Planetary Science Letters*.

Sutton, R. T., & Dong, B. (2012). Atlantic Ocean influence on a shift in European climate in the 1990s. *Nature Geoscience, 5*(11), 788.

Sutton, R. T., & Hodson, D. L. R. (2003). Influence of the ocean on North Atlantic climate variability 1871-1999. *Journal of Climate, 16*, 3296-3313.

Sutton, R. T., & Hodson, D. L. R. (2005). Atlantic Ocean forcing of North American and European summer climate. *SCience, 309*, 115-118.

Sutton, R. T., Jewson, S. P., & Rowell, D. P. (2000). The Elements of Climate Variability in the Tropical Atlantic Region. *Journal of Climate, 13*, 3261-3284.

Suzuki, A., Hibino, K., Iwase, A., & Kawahata, H. (2005). Intercolony variability of skeletal oxygen and carbon isotope signatures of cultured *Porites* corals: Temperature-controlled experiments. *Geochimica Et Cosmochimica Acta, 69*(18), 4453-4462.

Svendsen, L., Hetzinger, S., Keenlyside, N., & Gao, Y. (2014). Marine-based multiproxy reconstruction of Atlantic multidecadal variability. *Geophysical Research Letters, 41*(4), 1295-1300.

Swart, P. K. (1983). Carbon and Oxygen isotope fractionation in scleractinian corals: a review. *Earth-Science Reviews, 19*, 51-80.

Swart, P. K., Elderfield, H., & Greaves, M. J. (2002). A high-resolution calibration of Sr/Ca thermometry using the Caribbean coral Montastraea annularis. *Geochemistry Geophysics Geosystems, 3*(11), 1-11.

Swart, P. K., Leder, J. J., Szmant, A. M., & Dodge, R. E. (1996). The origin of variations in the isotopic record of scleractinian corals: II. Carbon. *Geochimica Et Cosmochimica Acta, 60*(15), 2871-2885.

Swart, P. K., & Szmant, A., ... (2005). The isotopic composition of respired carbon dioxide in scleractinian corals: Implications for cycling of organic carbon in corals. *Geochimica Et Cosmochimica Acta*.

Talling, P., Wynn, R., Masson, D., Frenz, M., Cronin, B., Schiebel, R., et al. (2007). Onset of submarine debris flow deposition far from original giant landslide. *Nature, 450*(7169), 541.

Tanaka, K., Holcomb, M., Takahashi, A., Kurihara, H., Asami, R., Shinjo, R., et al. (2015). Response of Acropora digitifera to ocean acidification: constraints from δ 11 B, Sr, Mg, and Ba compositions of aragonitic skeletons cultured under variable seawater pH. *Coral Reefs, 34*(4), 1139-1149.

Tang, B. H., & Neelin, J. D. (2004). ENSO influence on Atlantic hurricanes via tropospheric warming. *Geophysical Research Letters, 31*(L24204), doi:10.1029/2005GL021072.

Taviani, M., Angeletti, L., Antolini, B., Ceregato, A., Froglia, C., Lopez Correa, M., et al. (2011). Geo-biology of Mediterranean deep-water coral ecosystems. *Marine Research at CNR, 6*, 705-719.

Taviani, M., Freiwald, A., & Zibrowius, H. (2005a). Deep coral growth in the Mediterranean Sea: an overview. In *Cold-water corals and ecosystems* (pp. 137-156): Springer.

Taviani, M., Remia, A., Corselli, C., Freiwald, A., Malinverno, E., Mastrototaro, F., et al. (2005b). First geo-marine survey of living cold-water Lophelia reefs in the Ionian Sea (Mediterranean basin). *Facies, 50*(3-4), 409-417.

Taylor, A. M., Enfield, D. B., & Chen, A. A. (2002). Influence of the tropical Atlantic versus the tropical Pacific on Caribbean rainfall. *Journal of Geophysical Research, 107*(C9), doi:10.1029/2001JC001097.

Thiem, Ø., Ravagnan, E., Fosså, J. H., & Berntsen, J. (2006). Food supply mechanisms for cold-water corals along a continental shelf edge. *Journal of Marine Systems, 60*(3-4), 207-219.

Tierney, J. E., Abram, N. J., Anchukaitis, K. J., Evans, M. N., Giry, C., Kilbourne, K. H., et al. (2015). Tropical sea surface temperatures for the past four centuries reconstructed from coral archives. *Paleoceanography, 30*(3), 226-252. Article.

Titschack, J., Baum, D., De Pol‐Holz, R., Lopez Correa, M., Forster, N., Flögel, S., et al. (2015). Aggradation and carbonate accumulation of Holocene Norwegian cold‐water coral reefs. *Sedimentology, 62*(7), 1873-1898.

Titschack, J., Thierens, M., Dorschel, B., Schulbert, C., Freiwald, A., Kano, A., et al. (2009). Carbonate budget of a cold-water coral mound (Challenger Mound, IODP Exp. 307). *Marine Geology, 259*(1-4), 36-46.

Tomczak, M. (1999). Some historical, theoretical and applied aspects of quantitative water mass analysis. *Journal of Marine Research, 57*(2), 275-303.

Trenberth, K. E. (1997). The Definition of El Nino. *Bulletin of the American Meteorological Society, 78*(12), 2771-2777.

Trenberth, K. E. (2011). Changes in precipitation with climate change. *Climate Research, 47*(1-2), 123-138.

Trenberth, K. E., Dai, A., Rasmussen, R. M., & Parsons, D. B. (2003). The changing character of precipitation. *Bulletin of the American Meteorological Society, 84*(9), 1205-1217.

Trenberth, K. E., Jones, P. D., Ambenje, P., Bojariu, R., Easterling, D., Klein Tank, A., et al. (2007). *Observations: Surface and Atmospheric Climate Change*. Cambridge, United Kingdom and New York, NY, USA: Cambridge University Press.

Trenberth, K. E., & Shea, D. J. (2006). Atlantic hurricanes and natural variability in 2005. *Geophysical Research Letters, 33*(L12704), doi:10.1029/2006GL026894.

Tudhope, A. W., Chilcott, C. P., McCulloch, M., Cook, E. R., Chappell, J., Ellam, R. M., et al. (2001). Variability in the El Nino-Southern oscillation through a glacial-interglacial cycle. *SCience, 291*, 1511-1517.

Tudhope, A. W., Shimmield, G. B., Chilcott, C. P., Jebb, M., Fallick, A. E., & Dalgleish, A. N. (1995). Recent changes in climate in the far western equatorial Pacific and their relationship to the Southern Oscillation; oxygen isotope records from massive corals, Papua New Guinea. *Earth and Planetary Science Letters, 136*(575-590).

Uchida, A., Nishizawa, M., Shirai, K., Iijima, H., Kayanne, H., Takahata, N., & Sano, Y. (2008). High sensitivity measurements of nitrogen isotopic ratios in coral skeletons

from Palau, western Pacific: Temporal resolution and seasonal variation of nitrogen sources. *Geochemical Journal, 42*(3), 255-262.

UNEP-WCMC. (2009). Cold-water coral. United Nations Environment Programme - World Conservation Monitoring Centre. http://bure.unep-wcmc.org/marine/coldcoral/viewer.htm.

Urey, H. C., Lowenstam, H. A., Epstein, S., & McKinney, C. R. (1951). Measurement of paleotemperatures and temperatures of the Upper Cretaceous of England, Denmark and the southeastern United States. *Geological Society of AMerica Bulletin, 62*(4), 399-416.

Van Camp, L., Nykjaer, L., Mittelstaedt, E., & Schlittenhardt, P. (1991). Upwelling and boundary circulation off Northwest Africa as depicted by infrared and visible satellite observations. *Progress in Oceanography, 26*(4), 357-402.

Van de Flierdt, T., Robinson, L. F., & Adkins, J. F. (2010). Deep-sea coral aragonite as a recorder for the neodymium isotopic composition of seawater. *Geochimica Et Cosmochimica Acta, 74*(21), 6014-6032.

van Hooidonk, R., & Huber, M. (2009). Quantifying the quality of coral bleaching predictions. *Coral Reefs, 28*(3), 579-587.

van Hooidonk, R. J., Manzello, D. P., Moye, J., Brandt, M. E., Hendee, J. C., McCoy, C., & Manfrino, C. (2012). Coral bleaching at Little Cayman, Cayman Islands 2009. *Estuarine, Coastal and Shelf Science, 106*(0), 80-84.

van Loon, H., & Rogers, J. C. (1978). The Seesaw in Winter Temperatures between Greenland and Northern Europe. Part I: General Description. *Monthly Weather Review, 106*, 296-310.

van Oldenborgh, G. J., te Raa, L. A., Dijkstra, H. A., & Philip, S. Y. (2009). Frequency- or amplitude-dependent effects of the Atlantic meridional overturning on the tropical Pacific Ocean. *Ocean Sci., 5*(3), 293-301.

Van Rensbergen, P., Depreiter, D., Pannemans, B., & Henriet, J. P. (2005). Seafloor expression of sediment extrusion and intrusion at the El Arraiche mud volcano field, Gulf of Cadiz. *Journal of Geophysical Research: Earth Surface, 110*(F2).

Van Rooij, D., Blamart, D., De Mol, L., Mienis, F., Pirlet, H., Wehrmann, L., et al. (2011). Cold-water coral mounds on the Pen Duick Escarpment, Gulf of Cadiz: The MiCROSYSTEMS project approach. *Marine Geology, 282*(1), 102-117.

Vandorpe, T., Van Rooij, D., & De Haas, H. (2014). Stratigraphy and paleoceanography of a topography-controlled contourite drift in the Pen Duick area, southern Gulf of Cádiz. *Marine Geology, 349*, 136-151.

Vásquez-Bedoya, L. F., Cohen, A. L., Oppo, D. W., & Blanchon, P. (2012). Corals record persistent multidecadal SST variability in the Atlantic Warm Pool since 1775 AD. *Paleoceanography, 27*(3), PA3231.

Vecsei, A. (2004). A new estimate of global reefal carbonate production including the fore-reefs. *Global and Planetary Change, 43*, 1-18.

Vellinga, M., & Wu, P. (2004a). Low-Latitude Freshwater Influence on Centennial Variability of the Atlantic Thermohaline Circulation. *Journal of Climate, 17*, 4498-4511.

Vellinga, M., & Wu, P. L. (2004b). Low-latitude freshwater influence on centennial variability of the Atlantic thermohaline circulation. *Journal of Climate, 17*(23), 4498-4511.

Veron, J., Hoegh-Guldberg, O., Lenton, T., Lough, J., Obura, D., Pearce-Kelly, P., et al. (2009). The coral reef crisis: The critical importance of< 350 ppm CO2. *Marine Pollution Bulletin, 58*(10), 1428-1436.

Veron, J. E. N. (1995). *Corals in Space and Time, the Biogeography and Evolution of the Scleractinia*. Cornell: Cornell University Press.

Veron, J. E. N. (2000). *Corals of the World* (Vol. 1). Townsville: Australian Institute of Marine Science.

Viana, A., Faugères, J., Kowsmann, R., Lima, J., Caddah, L., & Rizzo, J. (1998). Hydrology, morphology and sedimentology of the Campos continental margin, offshore Brazil. *Sedimentary Geology, 115*(1-4), 133-157.

Vicente-Serrano, S. M., & Lopez-Moreno, J. I. (2008). Nonstationary influence of the North Atlantic Oscillation on European precipitation. *Journal of Geophysical Research-Atmospheres, 113*(D20).

Vierod, A. D., Guinotte, J. M., & Davies, A. J. (2014). Predicting the distribution of vulnerable marine ecosystems in the deep sea using presence-background models. *Deep Sea Research Part II: Topical Studies in Oceanography, 99*, 6-18.

Visbeck, M. (2002). The ocean's role in Atlantic climate variability. *SCience, 297*, 2223-2224.

Visbeck, M., Hurrell, J. W., Polvani, L., & Cullen, H. M. (2001). The North Atlantic Oscillation: Past, present, and future. *Proceedings of the National Academy of Sciences, 98*(23), 12876-12877.

von Reumont, J., Hetzinger, S., Garbe-Schönberg, D., Manfrino, C., & Dullo, W. C. (2016). Impact of warming events on reef-scale temperature variability as captured in two Little Cayman coral Sr/Ca records. *Geochemistry, Geophysics, Geosystems, 17*(3), 846-857.

Voss, J. D., & Richardson, L. L. (2006). Nutrient enrichment enhances black band disease progression in corals. *Coral Reefs, 25*(4), 569-576.

Wada, E., & Hattori, A. (1976). Natural abundance of 15N in particulate organic matter in the North Pacific Ocean. *Geochimica Et Cosmochimica Acta, 40*(2), 249-251.

Walker, G., & Bliss, E. (1932). World weather V. *Memoirs of the Royal Meteorological Society, 4*(36), 53-84.

Walter, K., & Graf, H. F. (2002). On the changing nature of the regional connection between the North Atlantic Oscillation and sea surface temperature. *Journal of Geophysical Research-Atmospheres, 107*(D17).

Wanamaker, A. D., Hetzinger, S., & Halfar, J. (2011). Reconstructing mid- to high-latitude marine climate and ocean variability using bivalves, coralline algae, and marine sediment cores from the Northern Hemisphere. *Palaeogeography, Palaeoclimatology, Palaeoecology, 302*(1-2), 1-9. doi:10.1016/j.palaeo.2010.12.024.

Wang, C., Dong, S., Evan, A. T., Foltz, G. R., & Lee, S.-K. (2012). Multidecadal Covariability of North Atlantic Sea Surface Temperature, African Dust, Sahel Rainfall, and Atlantic Hurricanes. *Journal of Climate, 25*(15), 5404-5415.

Wang, C., & Enfield, D. B. (2001). The tropical western hemisphere warm pool. *Geophysical Research Letters, 28*, 1635-1638.

Wang, C., Enfield, D. B., Lee, S.-k., & Landsea, C. W. (2006). Influences of the Atlantic Warm Pool on Western Hemisphere Summer Rainfall and Atlantic Hurricanes. *Journal of Climate, 19*(12), 3011-3028.

Wang, C., Lee, S.-k., & Enfield, D. B. (2007). Impact of the Atlantic Warm Pool on the Summer Climate of the Western Hemisphere. *Journal of Climate, 20*(20), 5021-5040.

Wang, C., Lee, S.-K., & Enfield, D. B. (2008a). Atlantic Warm Pool acting as a link between Atlantic Multidecadal Oscillation and Atlantic tropical cyclone activity. *Geochem. Geophys. Geosyst., 9*(5), Q05V03.

Wang, C., Lee, S.-K., & Enfield, D. B. (2008b). Climate Response to Anomalously Large and Small Atlantic Warm Pools during the Summer. *Journal of Climate, 21*(11), 2437-2450.

Wang, W., Evan, A. T., Flamant, C., & Lavaysse, C. (2015). On the decadal scale correlation between African dust and Sahel rainfall: The role of Saharan heat low–forced winds. *Science advances, 1*(9), e1500646.

Warner, M. E., Fitt, W. K., & Schmidt, G. W. (1996). The effects of elevated temperature on the photosynthetic efficiency of zooxanthellae in hospite from four different species of reef coral: a novel approach. *Plant, Cell & Environment, 19*(3), 291-299.

Watanabe, T., Minagawa, M., Oba, T., & Winter, A. (2001). Pretreatment of coral aragonite for Mg and Sr analysis: Implications for coral thermometers. *Geochemical Journal, 35*, 265-269. Journal.

Watanabe, T., Winter, A., Oba, T., Anzai, R., & Ishioroshi, T. (2002). Evaluation of the fidelity of isotope records as an environmental proxy in the coral Montastrea. *Coral Reefs, 21*, 169-178.

Watson, E. B. (1996). Surface enrichment and trace-element uptake during crystal growth. *Geochimica Et Cosmochimica Acta, 60*(24), 5013-5020.

Weber, J. N. (1973). Incorporation of strontium into reef coral skeletal carbonate. *Geochimica Et Cosmochimica Acta, 37*, 2173-2190.

Weber, J. N., & Woodhead, P. M. (1970). Carbon and oxygen isotope fractionation in the skeletal carbonate of reef-building corals. *Chemical Geology, 6*, 93-117.

Weber, J. N., & Woodhead, P. M. J. (1972). Temperature dependance of oxygen-18 concentration in reef coral carbonates. *Journal of Geophysical Research, 77*(3), 463-473.

Weil, E., & Vargas, W. L. (2010). Comparative aspects of sexual reproduction in the Caribbean coral genus Diploria (Scleractinia: Faviidae). *Marine Biology, 157*(2), 413-426.

Weis, V. M. (2010). The susceptibility and resilience of corals to thermal stress: adaptation, acclimatization or both? *Molecular Ecology, 19*(8), 1515-1517.

Wellington, G. M., & Dunbar, R. B. (1995). Stable isotopic signature of El Niño-Southern Oscillation events in eastern tropical Pacific reef corals. *Coral Reefs, 14*, 5-25.

Wellington, G. M., Dunbar, R. B., & Merlen, G. (1996). Calibration of stable oxygen isotope signatures in Galapagos corals. *Paleoceanography, 11*(4), 467-480.

Wellington, G. M., & Glynn, P. W. (2007). Responses of Coral Reefs to El Niñno-Southern Oscillation Sea-Warming Events. In R. B. Aronson (Ed.), *Geological Approaches to Coral Reef Ecology* (pp. 342-385). New York, NY: Springer New York.

Westphal, H., Beuck, L., Braun, S., Freiwald, A., Hanebuth, T., Hetzinger, S., et al. (2012). Phaeton - Report - Paleoceanographic and paleo-climatic record on the Mauritanian Shelf Cruise No. MSM16-3, Oct 13 - Nov 20, 2010, Bremerhaven (Germany) - Mindelo (Cap Verde). In *Maria S. Merian - Berichte* (pp. 1-53).

Wheeler, A. J., Beyer, A., Freiwald, A., De Haas, H., Huvenne, V., Kozachenko, M., et al. (2007). Morphology and environment of cold-water coral carbonate mounds on the NW European margin. *International Journal of Earth Sciences, 96*(1), 37-56.

White, M., Roberts, J. M., & van Weering, T. (2007). Do bottom-intensified diurnal tidal currents shape the alignment of carbonate mounds in the NE Atlantic? *Geo-Marine Letters, 27*(6), 391.

Wienberg, C., Frank, N., Mertens, K. N., Stuut, J.-B., Marchant, M., Fietzke, J., et al. (2010). Glacial cold-water coral growth in the Gulf of Cádiz: Implications of increased palaeo-productivity. *Earth and Planetary Science Letters, 298*(3), 405-416.

Wienberg, C., Hebbeln, D., Fink, H. G., Mienis, F., Dorschel, B., Vertino, A., et al. (2009). Scleractinian cold-water corals in the Gulf of Cádiz—first clues about their spatial and temporal distribution. *Deep Sea Research Part I: Oceanographic Research Papers, 56*(10), 1873-1893.

Winter, A., Ishioroshi, H., Watanabe, T., Oba, T., & Christy, J. (2000). Caribbean sea surface temperatures: two-to-three degrees cooler than present during the Little Ice Age. *Geophysical Research Letters, 27*(20), 3365-3368.

Winter, A., Paul, A., Nyberg, J., Oba, T., Lundberg, J., Schrag, D., & Taggart, B. (2003). Orbital control of low-latitude seasonality during the Eemian. *Geophysical Research Letters, 30*(4), doi:10.1029/2002GL016275.

Woodroffe, C. (1988). Vertical movement of isolated oceanic islands at plate margins: evidence from emergent reefs in Tonga (Pacific Ocean), Cayman Islands (Caribbean Sea) and Christmas Island (Indian Ocean). *Zeitschrift für Geomorphologie, Suppl, 69*, 17-39.

Woodroffe, C. D., Stoddart, D. R., Harmon, R. S., & Spencer, T. (1983). Coastal Morphology and Late Quaternary History, Cayman Islands, West Indies. *Quaternary Research, 19*(1), 64-84.

Woollings, T., Franzke, C., Hodson, D. L. R., Dong, B., Barnes, E. A., Raible, C. C., & Pinto, J. G. (2015). Contrasting interannual and multidecadal NAO variability. *Climate Dynamics, 45*(1), 539-556. journal article.

Wüst, G. (1964). *Stratification and circulation in the Antillean-Caribbean Basins*. Palisades, NY: Columbia University Press.

Wynn, R. B., Weaver, P. P., Masson, D. G., & Stow, D. A. (2002). Turbidite depositional architecture across three interconnected deep‐water basins on the north‐west African margin. *Sedimentology, 49*(4), 669-695.

Xie, S.-P., & Carton, J. A. (2004). Tropical Atlantic variability: Patterns, mechanisms, and impacts. In C. Wang, S.-P. Xie, & J. A. Carton (Eds.), *Earth Climate: The Ocean-Atmosphere Interaction, Geophys. Monogr. Ser.* (Vol. 147, pp. 121-142). Washington , D. C.: AGU.

Xie, S.-P., & Tanimoto, Y. (1998). A pan-Atlantic decadal climate oscillation. *Geophysical Research Letters, 25*(12), 2185-2188.

Xu, Y.-Y., Pearson, S., & Halimeda Kilbourne, K. (2015). Assessing coral Sr/Ca–SST calibration techniques using the species Diploria strigosa. *Palaeogeography, Palaeoclimatology, Palaeoecology, 440*, 353-362.

Yamazaki, A., Watanabe, T., Takahata, N., Sano, Y., & Tsunogai, U. (2013). Nitrogen isotopes in intra-crystal coralline aragonites. *Chemical Geology, 351*, 276-280.

Yamazaki, A., Watanabe, T., & Tsunogai, U. (2011). Nitrogen isotopes of organic nitrogen in reef coral skeletons as a proxy of tropical nutrient dynamics. *Geophysical Research Letters, 38*(19).

Yamazaki, A., Watanabe, T., Tsunogai, U., Iwase, F., & Yamano, H. (2016). A 150‐year variation of the Kuroshio transport inferred from coral nitrogen isotope signature. *Paleoceanography and Paleoclimatology, 31*(6), 838-846.

Yuan, T., Oreopoulos, L., Zelinka, M., Yu, H., Norris, J. R., Chin, M., et al. (2016). Positive low cloud and dust feedbacks amplify tropical North Atlantic Multidecadal Oscillation. *Geophysical Research Letters, 43*(3), 1349-1356.

Zhang, R., & Delworth, T. L. (2006). Impact of Atlantic multidecadal oscillations on India/Sahel rainfall and Atlantic hurricanes. *Geophysical Research Letters, 33*(L17712), doi:10.1029/2006GL026267.

Zhang, Z., Falter, J., Lowe, R., Ivey, G., & McCulloch, M. (2013). Atmospheric forcing intensifies the effects of regional ocean warming on reef-scale temperature anomalies during a coral bleaching event. *Journal of Geophysical Research: Oceans, 118*(9), 4600-4616.

Zibrowius, H. (1980). Les Scléractiniaires de la Méditerranée et de l'Atlantique nord-oriental. *Mémoires de l'Institut océanographique, Monaco*.

Zibrowius, H. E. (1973). *Revision of Some Serpulidae (Annelida: Polychaeta) from Abyssal Depths in Atlantic and Pacific, Collected by the" Challenger" and Prince of Monaco Expeditions*: British Museum (Natural History).

Zinke, J., Dullo, W.-C., Heiss, G. A., & Eisenhauer, A. (2004). ENSO and Indian Ocean subtropical dipole variability is recorded in a coral record off southwest Madagascar for the period 1659 to 1995. *Earth and Planetary Science Letters, 228*, 177-194.

Zinke, J., Loveday, B. R., Reason, C. J. C., Dullo, W. C., & Kroon, D. (2014). Madagascar corals track sea surface temperature variability in the Agulhas Current core region over the past 334 years. *4*, 4393. Article.

Zinke, J., Pfeiffer, M., Timm, O., Dullo, W. C., Kroon, D., & Thomassin, B. A. (2008). Mayotte coral reveals hydrological changes in the western Indian Ocean between 1881 and 1994. *Geophys. Res. Lett., 35*(23), L23707.

Zweng, M. M., Reagan, J. R., Antonov, J. I., Locarnini, R. A., Mishonov, A. V., Boyer, T. P., et al. (2013). World ocean atlas 2013. Volume 2, Salinity.

Appendix

Table A1: Trace element and oxygen isotope data together with age model for *Diploria strigosa* coral core LC3 from the fore reef of Little Cayman. Table continues on the following pages.

LC3			Age Model		Linear interpolation				Monthly Resampling		
Sample ID	Sr/Ca (mmol/mol)	δ18O (‰)	Sample ID	Time Pointer (year.month)	Sample ID	Sr/Ca (mmol/mol)	δ18O (‰)	Age (year.month)	Sr/Ca (mmol/mol)	δ18O (‰)	Age (year.month)
1	8.878	-4.372	6	2011.67	1350	9.006	-3.777	1887.04	9.006	-3.777	1887.04
2	8.900	-4.288	12	2011.12	1349	9.036	-3.936	1887.13	9.036	-3.935	1887.13
3	8.886	-4.035	18	2010.71	1348	9.021	-3.743	1887.21	9.021	-3.744	1887.21
4	8.919	-4.005	21	2010.11	1347	9.031	-3.848	1887.29	9.031	-3.848	1887.29
5	8.826	-4.621	25	2009.71	1346	9.009	-3.951	1887.37	9.009	-3.952	1887.38
6	8.872	-4.242	33	2009.15	1345	8.979	-4.177	1887.46	8.979	-4.177	1887.46
7	8.827	-4.809	34	2008.72	1344	8.976	-4.223	1887.54	8.976	-4.223	1887.54
8	8.859	-4.818	41	2008.11	1343	8.952	-4.227	1887.62	8.952	-4.226	1887.63
9	8.877	-4.444	48	2007.71	1342	8.939	-3.897	1887.71	8.939	-3.897	1887.71
10	8.931	-4.469	53	2007.15	1341	8.979	-3.837	1887.79	8.979	-3.837	1887.79
11	8.937	-4.312	60	2006.72	1340	9.001	-3.877	1887.87	9.001	-3.877	1887.88
12	8.973	-3.932	61	2006.65	1339	9.019	-3.787	1887.96	9.019	-3.789	1887.96
13	8.926	-4.140	66	2006.13	1338	9.023	-4.043	1888.04	9.023	-4.043	1888.04
14	8.944	-4.199	72	2005.71	1337	9.030	-3.836	1888.13	9.030	-3.837	1888.13
15	8.989	-4.241	77	2005.12	1336	9.026	-3.971	1888.20	9.023	-3.990	1888.21
16	8.902	-4.334	81	2004.71	1335	9.008	-4.101	1888.27	9.005	-4.069	1888.29
17	8.967	-4.078	85	2004.12	1334	8.996	-3.990	1888.34	8.979	-4.038	1888.38
18	8.898	-4.419	88	2003.70	1333	8.957	-4.101	1888.42	8.966	-4.179	1888.46
19	8.923	-4.345	95	2003.14	1332	8.973	-4.235	1888.49	8.964	-4.207	1888.54
20	8.968	-4.017	99	2002.70	1331	8.961	-4.197	1888.56	8.931	-4.253	1888.63
21	9.043	-4.289	104	2002.14	1330	8.926	-4.262	1888.64	8.927	-3.967	1888.71
22	8.886	-4.242	109	2001.69	1329	8.927	-3.968	1888.71	8.975	-3.874	1888.79
23	8.961	-4.326	115	2001.12	1328	8.977	-3.884	1888.78	8.977	-3.841	1888.88
24	8.845	-4.646	118	2000.70	1327	8.967	-3.833	1888.85	9.001	-3.858	1888.96
25	8.882	-4.571	122	2000.14	1326	8.991	-3.852	1888.92	9.014	-3.900	1889.04
26	8.845	-4.386	127	1999.74	1325	9.007	-3.862	1888.99	9.033	-3.919	1889.13
27	8.869	-4.868	132	1999.12	1324	9.016	-3.910	1889.06	9.024	-4.129	1889.21
28	8.929	-4.208	136	1998.65	1323	9.033	-3.918	1889.13	9.004	-4.123	1889.29
29	8.907	-4.179	147	1998.12	1322	9.020	-4.213	1889.24	8.983	-4.003	1889.38
30	8.918	-4.087	153	1997.70	1321	8.984	-4.005	1889.36	8.979	-3.991	1889.46
31	8.910	-4.214	159	1997.13	1320	8.978	-3.989	1889.47	8.974	-4.105	1889.54
32	8.900	-4.063	163	1996.71	1319	8.971	-4.189	1889.59	8.954	-4.157	1889.63
33	8.998	-4.252	169	1996.14	1318	8.914	-4.080	1889.71	8.914	-4.081	1889.71
34	8.844	-4.269	172	1995.69	1317	8.937	-4.189	1889.78	8.935	-4.169	1889.79
35	8.889	-4.233	175	1995.15	1316	8.926	-4.088	1889.85	8.929	-4.037	1889.88
36	8.898	-4.274	186	1993.71	1315	8.934	-3.963	1889.92	8.948	-3.845	1889.96
37	8.922	-4.225	197	1992.69	1314	8.957	-3.768	1889.99	8.985	-3.910	1890.04
38	8.898	-4.262	201	1992.13	1313	8.992	-3.946	1890.06	9.023	-4.041	1890.13
39	8.897	-3.867	205	1991.70	1312	9.023	-4.041	1890.13	9.023	-3.940	1890.21
40	8.896	-4.129	210	1991.10	1311	9.023	-3.940	1890.21	9.012	-3.916	1890.29
41	8.921	-3.989	214	1990.71	1310	9.012	-3.916	1890.29	8.999	-4.028	1890.38
42	8.885	-4.094	223	1989.76	1309	8.999	-4.027	1890.37	8.996	-4.163	1890.46
43	8.899	-4.115	224	1989.65	1308	8.996	-4.162	1890.46	8.949	-4.313	1890.54
44	8.894	-4.084	231	1988.71	1307	8.949	-4.313	1890.54	8.943	-4.311	1890.63
45	8.882	-4.316	235	1988.16	1306	8.943	-4.311	1890.62	8.919	-4.379	1890.71
46	8.903	-4.354	240	1987.75	1305	8.919	-4.379	1890.71	8.936	-4.055	1890.79
47	8.868	-4.296	241	1987.65	1304	8.927	-4.345	1890.75	8.987	-3.935	1890.88
48	8.846	-4.357	246	1987.10	1303	8.938	-3.986	1890.80	8.956	-4.084	1890.96
49	8.873	-4.389	251	1986.70	1302	8.941	-3.964	1890.85	9.010	-4.213	1891.04
50	8.897	-4.331	259	1985.67	1301	9.016	-3.917	1890.89	9.100	-4.021	1891.13
51	8.917	-4.232	263	1985.15	1300	8.945	-4.148	1890.94	9.063	-4.055	1891.21
52	8.931	-4.125	268	1984.67	1299	8.973	-3.990	1890.99	9.041	-4.097	1891.29
53	8.916	-4.183	273	1984.15	1298	9.007	-4.271	1891.03	9.026	-4.167	1891.38
54	8.912	-4.272	282	1983.10	1297	9.020	-3.998	1891.08	9.008	-4.313	1891.46
55	8.887	-4.286	286	1982.72	1296	9.100	-4.021	1891.13	8.977	-4.366	1891.54
56	8.861	-4.339	295	1981.71	1295	9.049	-4.068	1891.24	8.936	-4.359	1891.63
57	8.851	-4.386	303	1980.75	1294	9.030	-4.136	1891.36	8.886	-4.301	1891.71
58	8.839	-4.382	304	1980.66	1293	9.005	-4.342	1891.47	8.928	-4.145	1891.79
59	8.869	-4.570	312	1979.71	1292	8.956	-4.383	1891.59	8.963	-4.017	1891.88
60	8.835	-4.539	318	1978.68	1291	8.886	-4.302	1891.71	8.964	-4.079	1891.96
61	8.834	-4.629	322	1978.11	1290	8.928	-4.147	1891.79	8.957	-3.964	1892.04
62	8.851	-4.486	334	1976.75	1289	8.963	-4.017	1891.87	8.969	-4.002	1892.13
63	8.870	-4.444	342	1975.71	1288	8.964	-4.080	1891.96	8.961	-3.975	1892.21
64	8.855	-4.096	350	1974.70	1287	8.957	-3.964	1892.04	8.951	-3.980	1892.29
65	8.895	-4.087	356	1974.15	1286	8.969	-4.002	1892.13	8.934	-4.078	1892.38
66	8.905	-4.032	359	1973.71	1285	8.955	-3.955	1892.27	8.929	-4.128	1892.46
67	8.888	-4.175	371	1972.71	1284	8.925	-4.127	1892.42	8.937	-4.131	1892.54
68	8.857	-4.349	379	1972.14	1283	8.939	-4.132	1892.56	8.930	-4.186	1892.63
69	8.812	-4.421	385	1971.72	1282	8.920	-4.251	1892.70	8.929	-4.208	1892.71
70	8.837	-4.441	398	1970.69	1281	8.966	-4.037	1892.74	8.987	-4.132	1892.79

LC3			Age Model		Linear interpolation				Monthly Resampling		
Sample ID	Sr/Ca (mmol/mol)	$\delta^{18}O$ (‰)	Sample ID	Time Pointer (year.month)	Sample ID	Sr/Ca (mmol/mol)	$\delta^{18}O$ (‰)	Age (year.month)	Sr/Ca (mmol/mol)	$\delta^{18}O$ (‰)	Age (year.month)
71	8.821	-4.450	403	1970.12	1280	8.992	-4.118	1892.79	8.954	-3.984	1892.88
72	8.807	-4.566	408	1969.67	1279	8.962	-4.203	1892.83	8.977	-3.828	1892.96
73	8.852	-4.321	412	1969.13	1278	8.956	-3.988	1892.87	8.972	-3.984	1893.04
74	8.847	-4.152	416	1968.69	1277	8.941	-3.952	1892.91	9.006	-3.916	1893.13
75	8.890	-4.191	421	1968.14	1276	8.975	-3.826	1892.96	8.976	-4.012	1893.21
76	8.909	-4.024	426	1967.70	1275	8.996	-3.851	1893.00	8.971	-4.175	1893.29
77	8.922	-4.040	431	1967.13	1274	8.971	-3.991	1893.04	8.966	-4.021	1893.38
78	8.888	-4.070	437	1966.69	1273	8.999	-3.846	1893.08	8.945	-4.251	1893.46
79	8.843	-4.016	440	1966.15	1272	9.006	-3.916	1893.13	8.936	-4.273	1893.54
80	8.859	-4.080	445	1965.71	1271	8.979	-3.971	1893.19	8.939	-4.083	1893.63
81	8.830	-4.397	451	1965.13	1270	8.968	-4.114	1893.25	8.929	-4.014	1893.71
82	8.847	-4.193	454	1964.70	1269	8.973	-4.219	1893.32	8.954	-4.037	1893.79
83	8.860	-4.196	461	1964.13	1268	8.965	-3.990	1893.38	8.970	-3.928	1893.88
84	8.876	-4.072	466	1963.70	1267	8.947	-4.237	1893.45	8.996	-3.904	1893.96
85	8.900	-4.032	476	1962.66	1266	8.931	-4.330	1893.51	9.011	-3.883	1894.04
86	8.894	-3.962	480	1962.14	1265	8.943	-4.200	1893.58	9.044	-3.846	1894.13
87	8.867	-4.100	485	1961.70	1264	8.937	-4.040	1893.64	9.028	-3.920	1894.21
88	8.840	-4.281	491	1961.13	1263	8.929	-4.013	1893.71	9.001	-3.980	1894.29
89	8.854	-3.471	494	1960.71	1262	8.952	-4.082	1893.78	9.013	-4.065	1894.38
90	8.863	-4.420	504	1959.69	1261	8.963	-3.858	1893.85	8.991	-4.297	1894.46
91	8.879	-4.410	510	1959.11	1260	8.981	-4.031	1893.92	8.956	-4.379	1894.54
92	8.888	-3.657	513	1958.71	1259	9.006	-3.820	1893.99	8.950	-4.383	1894.63
93	8.896	-4.261	517	1958.12	1258	9.012	-3.899	1894.06	8.926	-4.409	1894.71
94	8.882	-4.173	524	1957.71	1257	9.044	-3.846	1894.13	8.950	-4.072	1894.79
95	8.904	-4.334	525	1957.65	1256	9.028	-3.920	1894.21	8.943	-4.051	1894.88
96	8.895	-4.145	534	1957.12	1255	9.001	-3.980	1894.29	8.958	-3.865	1894.96
97	8.887	-4.166	539	1956.71	1254	9.013	-4.064	1894.37	9.017	-3.972	1895.04
98	8.848	-4.421	540	1956.13	1253	8.991	-4.296	1894.46	9.046	-3.870	1895.13
99	8.833	-4.534	546	1955.76	1252	8.956	-4.379	1894.54	9.024	-3.771	1895.21
100	8.849	-4.391	547	1955.69	1251	8.950	-4.383	1894.62	9.000	-3.941	1895.29
101	8.874	-4.364	553	1955.15	1250	8.926	-4.412	1894.71	8.966	-4.185	1895.38
102	8.905	-4.430	557	1954.71	1249	8.950	-4.072	1894.79	8.952	-4.338	1895.46
103	8.942	-4.477	566	1953.71	1248	8.943	-4.052	1894.87	8.999	-4.140	1895.54
104	8.903	-4.164	569	1953.11	1247	8.958	-3.864	1894.96	8.946	-4.158	1895.63
105	8.924	-4.222	573	1952.71	1246	9.017	-3.972	1895.04	8.914	-4.408	1895.71
106	8.931	-4.073	579	1952.11	1245	9.046	-3.870	1895.13	8.938	-4.235	1895.79
107	8.872	-4.229	584	1951.67	1244	9.024	-3.770	1895.21	8.956	-4.341	1895.88
108	8.823	-4.397	588	1951.13	1243	9.000	-3.941	1895.29	8.958	-4.157	1895.96
109	8.843	-4.426	594	1950.71	1242	8.966	-4.184	1895.37	8.968	-3.944	1896.04
110	8.832	-4.363	599	1950.16	1241	8.952	-4.340	1895.46	9.006	-3.812	1896.13
111	8.842	-4.322	603	1949.70	1240	8.999	-4.140	1895.54	8.979	-3.871	1896.21
112	8.900	-4.094	607	1949.12	1239	8.946	-4.157	1895.62	8.943	-3.961	1896.29
113	8.914	-4.009	612	1948.71	1238	8.914	-4.409	1895.71	8.995	-3.875	1896.38
114	8.938	-4.069	619	1948.13	1237	8.929	-4.309	1895.76	8.981	-3.961	1896.46
115	8.940	-4.015	626	1947.69	1236	8.944	-4.188	1895.81	8.986	-4.108	1896.54
116	8.897	-4.139	633	1947.12	1235	8.951	-4.412	1895.86	8.964	-4.147	1896.63
117	8.882	-4.117	638	1946.74	1234	8.974	-4.078	1895.92	8.946	-4.199	1896.71
118	8.869	-4.294	639	1946.65	1233	8.954	-4.177	1895.97	8.966	-4.186	1896.79
119	8.868	-4.217	644	1946.11	1232	8.957	-3.994	1896.02	8.970	-4.115	1896.88
120	8.950	-4.137	649	1945.70	1231	8.985	-3.871	1896.07	8.973	-4.045	1896.96
121	8.966	-4.047	656	1945.13	1230	9.006	-3.812	1896.13	9.007	-3.950	1897.04
122	8.975	-4.069	663	1944.69	1229	8.980	-3.869	1896.21	9.039	-3.750	1897.13
123	8.939	-3.954	667	1944.11	1228	8.941	-3.965	1896.29	8.999	-3.922	1897.21
124	8.949	-3.966	672	1943.69	1227	8.996	-3.870	1896.37	8.987	-3.819	1897.29
125	8.907	-4.033	680	1943.12	1226	8.980	-3.948	1896.45	9.001	-4.033	1897.38
126	8.873	-4.204	687	1942.71	1225	8.988	-4.104	1896.53	9.044	-3.852	1897.46
127	8.901	-4.401	694	1942.10	1224	8.967	-4.140	1896.62	9.006	-4.145	1897.54
128	8.895	-4.371	701	1941.75	1223	8.943	-4.203	1896.70	8.998	-4.149	1897.63
129	8.864	-4.569	702	1941.70	1222	8.962	-4.181	1896.77	8.976	-4.058	1897.71
130	8.922	-4.151	705	1941.14	1221	8.973	-4.196	1896.84	8.980	-4.137	1897.79
131	8.948	-4.1	711	1940.71	1220	8.966	-4.034	1896.91	8.984	-4.221	1897.88
132	8.960	-3.914	715	1940.14	1219	8.977	-4.050	1896.98	8.997	-4.224	1897.96
133	8.944	-3.814	721	1939.70	1218	9.013	-3.930	1897.05	9.023	-4.109	1898.04
134	8.916	-3.803	726	1939.12	1217	9.039	-3.749	1897.13	9.048	-3.994	1898.13
135	8.923	-3.931	730	1938.70	1216	8.999	-3.923	1897.21	9.000	-4.129	1898.21
136	8.890	-4.001	743	1937.14	1215	8.987	-3.819	1897.29	8.990	-4.022	1898.29
137	8.906	-4.22	748	1936.72	1214	9.001	-4.035	1897.38	8.974	-3.954	1898.38
138	8.955	-4.402	755	1936.13	1213	9.044	-3.851	1897.46	8.969	-3.976	1898.46
139	8.932	-4.295	758	1935.71	1212	9.006	-4.149	1897.54	8.975	-4.018	1898.54
140	8.943	-4.188	764	1935.12	1211	8.998	-4.149	1897.63	8.969	-4.184	1898.63
141	8.968	-4.125	769	1934.70	1210	8.975	-4.055	1897.71	8.935	-4.260	1898.71
142	8.956	-3.835	774	1934.15	1209	8.987	-4.271	1897.92	8.968	-4.055	1898.79
143	8.941	-4.029	778	1933.70	1208	9.049	-3.990	1898.13	9.001	-3.850	1898.88
144	8.961	-3.988	784	1933.12	1207	9.003	-4.128	1898.19	9.027	-3.778	1898.96
145	8.958	-4.054	787	1932.73	1206	8.991	-4.131	1898.26	9.046	-3.840	1899.04
146	8.959	-4.167	793	1932.13	1205	8.990	-3.928	1898.32	9.066	-3.902	1899.13
147	8.968	-4.28	798	1931.68	1204	8.971	-3.959	1898.39	9.031	-3.974	1899.21
148	8.974	-4.274	801	1931.13	1203	8.972	-3.972	1898.45	8.996	-4.045	1899.29
149	8.940	-4.399	810	1930.75	1202	8.950	-4.002	1898.51	8.980	-4.128	1899.38

LC3			Age Model		Linear interpolation				Monthly Resampling		
Sample ID	Sr/Ca (mmol/mol)	$\delta^{18}O$ (‰)	Sample ID	Time Pointer (year.month)	Sample ID	Sr/Ca (mmol/mol)	$\delta^{18}O$ (‰)	Age (year.month)	Sr/Ca (mmol/mol)	$\delta^{18}O$ (‰)	Age (year.month)
150	8.944	-4.007	811	1930.71	1201	9.009	-4.041	1898.58	8.971	-4.217	1899.46
151	8.977	-4.023	819	1930.13	1200	8.953	-4.242	1898.64	8.963	-4.275	1899.54
152	8.985	-4.052	824	1929.76	1199	8.935	-4.262	1898.71	8.955	-4.271	1899.63
153	8.914	-4.161	825	1929.67	1198	9.017	-3.747	1898.92	8.947	-4.266	1899.71
154	8.946	-4.333	830	1929.14	1197	9.066	-3.902	1899.13	8.965	-4.177	1899.79
155	8.922	-4.282	836	1928.71	1196	8.985	-4.068	1899.32	8.963	-4.100	1899.88
156	8.977	-4.506	842	1928.14	1195	8.966	-4.276	1899.51	8.971	-4.134	1899.96
157	8.932	-4.347	847	1927.68	1194	8.947	-4.267	1899.71	8.972	-4.030	1900.04
158	8.961	-4.127	857	1926.68	1193	8.967	-4.170	1899.80	8.981	-4.016	1900.13
159	8.979	-3.958	861	1926.13	1192	8.962	-4.087	1899.89	8.980	-4.033	1900.21
160	8.943	-4.172	864	1925.70	1191	8.974	-4.149	1899.98	8.982	-4.080	1900.29
161	8.922	-3.88	867	1925.11	1190	8.971	-3.971	1900.07	9.000	-4.069	1900.38
162	8.894	-4.512	871	1924.71	1189	8.988	-4.047	1900.16	9.015	-3.918	1900.46
163	8.847	-4.574	877	1924.12	1188	8.972	-4.019	1900.25	9.025	-4.052	1900.54
164	8.867	-4.648	881	1923.69	1187	8.996	-4.162	1900.34	8.985	-4.324	1900.63
165	8.944	-4.475	886	1923.14	1186	9.009	-3.892	1900.44	8.965	-4.231	1900.71
166	8.898	-4.357	893	1922.70	1185	9.033	-3.992	1900.53	8.989	-4.275	1900.79
167	8.904	-4.166	898	1922.14	1184	8.987	-4.333	1900.62	9.037	-4.220	1900.88
168	8.925	-4.039	904	1921.72	1183	8.965	-4.231	1900.71	9.019	-4.230	1900.96
169	8.953	-4.099	909	1921.13	1182	8.991	-4.225	1900.76	9.043	-3.997	1901.04
170	8.928	-3.939	915	1920.69	1181	8.988	-4.307	1900.81	9.090	-3.817	1901.13
171	8.846	-4.174	919	1920.13	1180	9.046	-4.209	1900.86	9.054	-3.895	1901.21
172	8.863	-4.367	926	1919.71	1179	9.001	-4.260	1900.92	9.061	-3.836	1901.29
173	8.852	-4.441	930	1919.11	1178	9.023	-4.222	1900.97	9.057	-3.891	1901.38
174	8.866	-4.234	936	1918.71	1177	9.028	-4.214	1901.02	9.011	-4.033	1901.46
175	8.920	-4.092	943	1918.15	1176	9.065	-3.676	1901.07	9.024	-4.049	1901.54
176	8.912	-4.225	949	1917.72	1175	9.090	-3.817	1901.13	8.989	-3.992	1901.63
177	8.911	-4.218	954	1916.71	1174	9.054	-3.903	1901.20	8.978	-4.013	1901.71
178	8.916	-4.132	958	1916.13	1173	9.055	-3.837	1901.28	8.985	-3.980	1901.79
179	8.895	-4.111	964	1915.70	1172	9.081	-3.834	1901.35	9.006	-3.992	1901.88
180	8.919	-4.342	970	1915.13	1171	9.005	-4.012	1901.43	8.985	-4.024	1901.96
181	8.912	-4.236	974	1914.72	1170	9.019	-4.062	1901.50	9.004	-4.066	1902.04
182	8.938	-4.083	980	1914.12	1169	9.029	-4.038	1901.58	8.991	-4.092	1902.13
183	8.957	-4.012	988	1913.71	1168	8.966	-3.965	1901.65	8.990	-4.069	1902.21
184	8.963	-3.969	989	1913.65	1167	8.982	-4.030	1901.73	8.981	-4.093	1902.29
185	8.934	-4.236	997	1913.16	1166	8.985	-3.971	1901.80	8.979	-3.987	1902.38
186	8.884	-4.060	1004	1912.70	1165	9.007	-3.993	1901.88	8.982	-4.063	1902.46
187	8.925	-4.272	1012	1912.15	1164	8.984	-4.022	1901.95	8.976	-4.122	1902.54
188	8.954	-4.484	1020	1911.71	1163	9.007	-4.057	1902.03	8.979	-4.036	1902.63
189	8.923	-4.382	1021	1911.65	1162	8.988	-4.114	1902.10	8.944	-4.233	1902.71
190	8.914	-4.252	1029	1911.15	1161	8.999	-4.032	1902.18	9.003	-4.111	1902.79
191	8.952	-4.338	1036	1910.71	1160	8.976	-4.131	1902.26	9.009	-3.918	1902.88
192	8.950	-4.139	1045	1910.13	1159	8.986	-4.051	1902.33	8.992	-3.963	1902.96
193	8.940	-4.189	1053	1909.71	1158	8.974	-3.943	1902.41	8.973	-4.042	1903.04
194	8.908	-4.294	1061	1909.14	1157	8.986	-4.116	1902.48	9.000	-3.881	1903.13
195	8.887	-4.358	1067	1908.71	1156	8.974	-4.123	1902.56	8.995	-3.912	1903.21
196	8.892	-4.407	1068	1908.65	1155	8.980	-4.026	1902.63	8.975	-3.981	1903.29
197	8.895	-4.519	1076	1908.15	1154	8.943	-4.234	1902.71	9.011	-3.949	1903.38
198	8.864	-4.518	1083	1907.71	1153	8.994	-4.170	1902.77	9.000	-4.046	1903.46
199	8.911	-4.224	1088	1907.13	1152	9.024	-3.967	1902.84	8.982	-4.163	1903.54
200	8.928	-4.384	1094	1906.71	1151	8.998	-3.881	1902.90	8.972	-4.217	1903.63
201	8.987	-4.273	1103	1906.13	1150	8.991	-3.977	1902.97	8.954	-4.168	1903.71
202	8.955	-4.111	1112	1905.75	1149	8.969	-4.069	1903.03	8.975	-4.013	1903.79
203	8.931	-4.295	1113	1905.71	1148	9.000	-3.875	1903.10	8.981	-4.290	1903.88
204	8.869	-4.435	1114	1905.66	1147	8.999	-3.897	1903.19	9.014	-4.077	1903.96
205	8.889	-4.468	1124	1905.13	1146	8.974	-3.984	1903.29	9.039	-3.922	1904.04
206	8.870	-4.528	1128	1904.71	1145	9.021	-3.939	1903.40	9.018	-3.903	1904.13
207	8.882	-4.682	1136	1904.14	1144	8.985	-4.121	1903.50	9.015	-3.984	1904.21
208	8.915	-4.373	1142	1903.71	1143	8.977	-4.228	1903.60	9.032	-3.832	1904.29
209	8.922	-4.189	1154	1902.71	1142	8.954	-4.170	1903.71	9.019	-3.831	1904.38
210	8.924	-4.288	1162	1902.10	1141	8.977	-3.942	1903.78	9.029	-3.860	1904.46
211	8.911	-4.327	1167	1901.73	1140	8.968	-4.337	1903.85	9.053	-3.939	1904.54
212	8.887	-4.283	1168	1901.65	1139	9.005	-4.200	1903.92	9.040	-3.857	1904.63
213	8.866	-4.567	1175	1901.13	1138	9.023	-3.959	1903.99	9.003	-4.086	1904.71
214	8.854	-4.621	1183	1900.71	1137	9.047	-3.904	1904.07	9.017	-4.040	1904.79
215	8.871	-4.520	1194	1899.71	1136	9.013	-3.903	1904.14	9.015	-4.025	1904.88
216	8.908	-4.440	1197	1899.13	1135	9.015	-3.985	1904.21	9.028	-3.915	1904.96
217	8.932	-4.192	1199	1898.71	1134	9.036	-3.827	1904.28	9.057	-3.749	1905.04
218	8.945	-4.269	1208	1898.13	1133	9.012	-3.852	1904.35	9.075	-3.720	1905.13
219	8.980	-4.093	1210	1897.71	1132	9.032	-3.792	1904.42	9.026	-3.840	1905.21
220	8.912	-4.136	1217	1897.13	1131	9.026	-3.926	1904.49	9.033	-3.881	1905.29
221	8.868	-4.254	1223	1896.70	1130	9.066	-3.945	1904.57	9.026	-3.950	1905.38
222	8.861	-4.535	1230	1896.13	1129	9.035	-3.840	1904.64	9.016	-3.999	1905.46
223	8.854	-4.404	1238	1895.71	1128	9.003	-4.086	1904.71	8.973	-4.116	1905.54
224	8.841	-4.574	1245	1895.13	1127	9.020	-4.029	1904.81	8.967	-4.167	1905.63
225	8.865	-4.482	1250	1894.71	1126	9.011	-4.022	1904.92	8.937	-4.122	1905.71
226	8.880	-4.364	1257	1894.13	1125	9.052	-3.756	1905.02	8.945	-3.857	1905.79
227	8.892	-4.332	1263	1893.71	1124	9.075	-3.720	1905.13	8.991	-4.036	1905.88
228	8.913	-4.378	1272	1893.13	1123	9.018	-3.795	1905.18	8.994	-3.835	1905.96

LC3			Age Model		Linear interpolation				Monthly Resampling		
Sample ID	Sr/Ca (mmol/mol)	$\delta^{18}O$ (‰)	Sample ID	Time Pointer (year.month)	Sample ID	Sr/Ca (mmol/mol)	$\delta^{18}O$ (‰)	Age (year.month)	Sr/Ca (mmol/mol)	$\delta^{18}O$ (‰)	Age (year.month)
229	8.893	-4.136	1281	1892.74	1122	9.032	-3.873	1905.23	8.997	-3.939	1906.04
230	8.871	-4.387	1282	1892.70	1121	9.045	-3.875	1905.28	9.035	-3.863	1906.13
231	8.851	-4.376	1286	1892.13	1120	8.964	-3.917	1905.34	9.009	-3.989	1906.21
232	8.862	-4.315	1291	1891.71	1119	9.050	-3.962	1905.39	8.994	-4.037	1906.29
233	8.871	-4.517	1296	1891.13	1118	9.025	-3.994	1905.44	8.991	-4.225	1906.38
234	8.896	-4.227	1304	1890.75	1117	8.996	-4.011	1905.50	8.961	-4.158	1906.46
235	8.934	-4.055	1305	1890.71	1116	8.970	-4.132	1905.55	8.961	-4.014	1906.54
236	8.919	-4.080	1312	1890.13	1115	8.945	-4.274	1905.60	8.952	-3.981	1906.63
237	8.925	-4.282	1318	1889.71	1114	8.996	-4.030	1905.66	8.909	-3.982	1906.71
238	8.891	-4.304	1323	1889.13	1113	8.937	-4.124	1905.71	8.983	-3.932	1906.79
239	8.874	-4.268	1329	1888.71	1112	8.964	-4.001	1905.75	9.015	-3.920	1906.88
240	8.840	-4.616	1337	1888.13	1111	8.945	-3.853	1905.79	9.034	-4.014	1906.96
241	8.844	-4.607	1342	1887.71	1110	8.972	-4.033	1905.83	9.046	-4.038	1907.04
242	8.878	-4.462	1349	1887.13	1109	8.991	-4.037	1905.87	9.050	-4.030	1907.13
243	8.880	-4.261			1108	9.011	-3.895	1905.92	9.028	-3.987	1907.21
244	8.940	-4.327			1107	8.994	-3.836	1905.96	9.019	-3.958	1907.29
245	8.945	-4.126			1106	9.038	-3.783	1906.00	9.014	-3.920	1907.38
246	8.923	-4.262			1105	8.997	-3.939	1906.04	8.997	-3.807	1907.46
247	8.912	-4.187			1104	9.025	-3.948	1906.08	8.997	-3.880	1907.54
248	8.873	-4.537			1103	9.035	-3.862	1906.13	8.992	-3.951	1907.63
249	8.842	-4.274			1102	9.011	-4.023	1906.19	8.974	-3.951	1907.71
250	8.921	-4.481			1101	9.003	-3.906	1906.25	9.003	-3.800	1907.79
251	8.859	-4.451			1100	8.987	-4.132	1906.32	9.024	-3.629	1907.88
252	8.878	-4.329			1099	8.992	-4.239	1906.38	9.012	-4.030	1907.96
253	8.900	-4.189			1098	8.962	-4.169	1906.45	8.993	-3.914	1908.04
254	8.983	-4.022			1097	8.953	-4.098	1906.51	8.964	-3.819	1908.13
255	8.944	-3.846			1096	8.971	-3.907	1906.58	9.010	-3.948	1908.21
256	8.935	-3.953			1095	8.945	-4.009	1906.64	9.000	-4.169	1908.29
257	8.925	-4.016			1094	8.908	-3.982	1906.71	8.986	-4.107	1908.38
258	8.911	-4.202			1093	8.979	-3.947	1906.78	8.976	-3.961	1908.46
259	8.937	-4.182			1092	9.000	-3.872	1906.85	8.968	-4.104	1908.54
260	8.889	-4.508			1091	9.037	-3.991	1906.92	8.991	-4.142	1908.63
261	8.899	-4.385			1090	9.032	-4.029	1906.99	8.918	-4.175	1908.71
262	8.936	-4.228			1089	9.049	-4.040	1907.06	8.951	-4.152	1908.79
263	8.966	-4.181			1088	9.050	-4.030	1907.13	8.946	-4.071	1908.88
264	8.960	-4.146			1087	9.019	-3.970	1907.24	8.943	-4.013	1908.96
265	8.936	-4.161			1086	9.018	-3.943	1907.36	8.962	-4.056	1909.04
266	8.878	-4.183			1085	8.994	-3.785	1907.47	8.980	-4.054	1909.13
267	8.860	-4.087			1084	8.999	-3.950	1907.59	8.955	-4.053	1909.21
268	8.880	-4.474			1083	8.974	-3.952	1907.71	9.002	-4.060	1909.29
269	8.866	-4.181			1082	8.994	-3.830	1907.77	8.990	-4.065	1909.38
270	8.873	-4.509			1081	9.019	-3.741	1907.83	8.947	-4.158	1909.46
271	8.915	-4.228			1080	9.027	-3.574	1907.90	8.930	-4.227	1909.54
272	8.935	-4.004			1079	9.012	-4.031	1907.96	8.941	-4.230	1909.63
273	8.936	-4.199			1078	8.985	-3.936	1908.02	8.878	-4.283	1909.71
274	8.899	-4.332			1077	9.008	-3.870	1908.08	8.944	-4.173	1909.79
275	8.881	-4.178			1076	8.943	-3.794	1908.15	8.934	-4.052	1909.88
276	8.898	-4.510			1075	9.010	-3.946	1908.21	8.921	-4.038	1909.96
277	8.875	-4.510			1074	9.000	-4.122	1908.27	8.969	-3.850	1910.04
278	8.871	-4.431			1073	8.999	-4.261	1908.33	8.984	-3.669	1910.13
279	8.900	-4.378			1072	8.980	-4.032	1908.40	8.968	-3.914	1910.21
280	8.921	-4.267			1071	8.976	-3.960	1908.46	8.975	-3.927	1910.29
281	8.939	-4.255			1070	8.977	-4.015	1908.52	8.959	-3.942	1910.38
282	8.936	-4.262			1069	8.952	-4.277	1908.58	8.960	-4.017	1910.46
283	8.885	-4.338			1068	9.010	-4.076	1908.65	8.947	-4.215	1910.54
284	8.865	-4.309			1067	8.918	-4.175	1908.71	8.910	-4.354	1910.63
285	8.864	-4.312			1066	8.952	-4.160	1908.78	8.875	-4.368	1910.71
286	8.847	-4.484			1065	8.947	-4.113	1908.85	8.897	-4.391	1910.79
287	8.841	-4.699			1064	8.943	-3.990	1908.92	8.965	-4.263	1910.88
288	8.859	-4.391			1063	8.942	-4.036	1908.99	8.920	-4.105	1910.96
289	8.925	-4.353			1062	8.973	-4.067	1909.07	8.933	-4.029	1911.04
290	8.945	-4.230			1061	8.982	-4.051	1909.14	8.937	-3.914	1911.13
291	8.950	-3.966			1060	8.955	-4.053	1909.21	8.941	-4.027	1911.21
292	8.903	-4.180			1059	9.002	-4.059	1909.28	8.948	-3.986	1911.29
293	8.878	-4.291			1058	9.001	-4.067	1909.35	9.008	-4.010	1911.38
294	8.852	-4.416			1057	8.966	-4.059	1909.43	8.939	-4.238	1911.46
295	8.832	-4.797			1056	8.925	-4.271	1909.50	8.903	-4.162	1911.54
296	8.863	-4.509			1055	8.933	-4.201	1909.57	8.891	-4.317	1911.63
297	8.893	-4.471			1054	8.943	-4.238	1909.64	8.871	-4.299	1911.71
298	8.924	-4.242			1053	8.875	-4.285	1909.71	8.922	-4.116	1911.79
299	9.020	-4.152			1052	8.950	-4.155	1909.76	8.965	-3.996	1911.88
300	8.938	-4.359			1051	8.938	-4.189	1909.82	8.985	-3.849	1911.96
301	8.899	-4.525			1050	8.937	-4.049	1909.87	9.000	-3.867	1912.04
302	8.869	-4.545			1049	8.915	-4.071	1909.92	9.026	-3.781	1912.13
303	8.855	-4.504			1048	8.923	-4.024	1909.97	9.009	-4.069	1912.21
304	8.842	-4.332			1047	8.978	-3.898	1910.03	8.965	-3.954	1912.29
305	8.952	-4.270			1046	8.948	-3.739	1910.08	8.954	-4.145	1912.38
306	8.935	-4.284			1045	8.989	-3.659	1910.13	8.930	-4.205	1912.46
307	8.928	-4.224			1044	8.966	-3.913	1910.20	8.913	-4.237	1912.54

LC3			Age Model		Linear interpolation				Monthly Resampling		
Sample ID	Sr/Ca (mmol/mol)	$\delta^{18}O$ (‰)	Sample ID	Time Pointer (year.month)	Sample ID	Sr/Ca (mmol/mol)	$\delta^{18}O$ (‰)	Age (year.month)	Sr/Ca (mmol/mol)	$\delta^{18}O$ (‰)	Age (year.month)
308	8.911	-4.179			1043	8.976	-3.917	1910.26	8.899	-4.259	1912.63
309	8.839	-4.300			1042	8.975	-3.937	1910.32	8.894	-4.008	1912.71
310	8.857	-4.378			1041	8.955	-3.943	1910.39	8.933	-3.921	1912.79
311	8.835	-4.361			1040	8.961	-4.007	1910.45	8.969	-3.884	1912.88
312	8.834	-4.384			1039	8.949	-4.106	1910.52	8.978	-3.824	1912.96
313	8.888	-4.349			1038	8.944	-4.375	1910.58	8.986	-3.924	1913.04
314	8.923	-4.283			1037	8.896	-4.345	1910.64	9.004	-4.076	1913.13
315	8.928	-4.103			1036	8.875	-4.368	1910.71	8.984	-4.083	1913.21
316	8.912	-4.218			1035	8.906	-4.362	1910.77	8.932	-4.178	1913.29
317	8.876	-3.862			1034	8.880	-4.449	1910.83	8.965	-4.268	1913.38
318	8.847	-4.181			1033	9.007	-4.170	1910.90	8.924	-4.178	1913.46
319	8.884	-4.479			1032	8.919	-4.105	1910.96	8.949	-4.474	1913.54
320	8.905	-4.425			1031	8.934	-4.097	1911.02	8.942	-4.300	1913.63
321	8.932	-4.372			1030	8.932	-3.883	1911.08	8.885	-4.248	1913.71
322	8.937	-4.163			1029	8.940	-3.930	1911.15	8.939	-4.155	1913.79
323	8.888	-4.288			1028	8.941	-4.029	1911.21	8.971	-4.189	1913.88
324	8.856	-4.404			1027	8.922	-3.962	1911.27	8.991	-3.949	1913.96
325	8.881	-4.521			1026	9.006	-4.043	1911.34	8.955	-3.924	1914.04
326	8.884	-4.466			1025	9.009	-3.991	1911.40	9.008	-4.152	1914.13
327	8.923	-3.880			1024	8.936	-4.248	1911.46	9.015	-4.316	1914.21
328	8.932	-4.167			1023	8.908	-4.131	1911.52	8.961	-4.202	1914.29
329	8.963	-4.028			1022	8.889	-4.241	1911.59	8.962	-4.331	1914.38
330	8.943	-4.058			1021	8.893	-4.366	1911.65	8.946	-4.349	1914.46
331	8.892	-4.237			1020	8.870	-4.295	1911.71	8.922	-4.279	1914.54
332	8.900	-4.304			1019	8.925	-4.172	1911.77	8.927	-4.262	1914.63
333	8.890	-4.323			1018	8.919	-4.047	1911.82	8.920	-4.007	1914.71
334	8.878	-4.071			1017	8.967	-3.994	1911.88	8.922	-4.009	1914.79
335	8.901	-4.341			1016	8.986	-3.893	1911.93	8.952	-4.015	1914.88
336	8.941	-4.252			1015	8.984	-3.802	1911.99	8.983	-3.984	1914.96
337	8.931	-4.164			1014	9.000	-3.870	1912.04	8.993	-3.921	1915.04
338	8.911	-4.257			1013	8.988	-3.722	1912.10	9.001	-3.866	1915.13
339	8.930	-4.271			1012	9.060	-3.834	1912.15	8.959	-3.982	1915.21
340	8.893	-4.284			1011	8.998	-4.120	1912.22	8.982	-3.997	1915.29
341	8.914	-4.329			1010	8.965	-3.949	1912.29	8.993	-4.058	1915.38
342	8.879	-4.373			1009	8.959	-4.132	1912.36	8.973	-4.118	1915.46
343	8.882	-4.452			1008	8.939	-4.189	1912.43	8.960	-4.118	1915.54
344	8.891	-4.531			1007	8.919	-4.225	1912.50	8.963	-4.109	1915.63
345	8.984	-4.442			1006	8.910	-4.244	1912.57	8.924	-4.165	1915.71
346	8.982	-4.352			1005	8.897	-4.262	1912.64	8.958	-4.135	1915.79
347	8.975	-4.186			1004	8.893	-4.016	1912.70	8.928	-4.064	1915.88
348	8.914	-4.289			1003	8.912	-3.875	1912.77	8.939	-3.926	1915.96
349	8.854	-4.416			1002	8.974	-4.012	1912.84	8.964	-3.942	1916.04
350	8.898	-4.525			1001	8.966	-3.801	1912.90	9.015	-3.875	1916.13
351	8.874	-4.644			1000	8.980	-3.827	1912.97	8.993	-3.853	1916.21
352	8.859	-4.500			999	8.981	-3.903	1913.03	8.973	-3.828	1916.29
353	8.886	-4.364			998	9.013	-4.041	1913.10	8.988	-3.753	1916.38
354	8.925	-4.170			997	8.992	-4.121	1913.16	8.990	-3.769	1916.46
355	8.928	-4.113			996	8.982	-4.072	1913.22	8.979	-3.879	1916.54
356	8.934	-4.065			995	8.922	-4.153	1913.28	8.967	-3.984	1916.63
357	8.929	-4.197			994	8.992	-4.322	1913.34	8.955	-4.085	1916.71
358	8.888	-4.288			993	8.938	-4.217	1913.41	8.966	-4.086	1916.79
359	8.877	-4.313			992	8.922	-4.172	1913.47	8.980	-4.089	1916.88
360	8.898	-4.605			991	8.945	-4.510	1913.53	9.006	-4.098	1916.96
361	8.897	-4.425			990	8.964	-4.351	1913.59	9.024	-4.060	1917.04
362	8.901	-4.268			989	8.926	-4.265	1913.65	9.035	-3.961	1917.13
363	8.928	-4.414			988	8.883	-4.247	1913.71	9.035	-3.900	1917.21
364	8.912	-4.222			987	8.935	-4.101	1913.76	9.011	-3.936	1917.29
365	8.948	-4.173			986	8.941	-4.192	1913.81	8.986	-3.973	1917.38
366	8.938	-4.076			985	8.966	-4.236	1913.86	8.962	-4.008	1917.46
367	8.952	-4.150			984	8.988	-4.026	1913.92	8.947	-4.019	1917.54
368	8.937	-4.053			983	8.991	-3.936	1913.97	8.932	-4.031	1917.63
369	8.916	-4.167			982	8.934	-3.938	1914.02	8.918	-4.042	1917.71
370	8.897	-4.272			981	8.977	-3.910	1914.07	8.966	-4.020	1917.79
371	8.885	-4.588			980	9.007	-4.139	1914.12	8.964	-3.446	1917.88
372	8.908	-4.481			979	9.016	-4.317	1914.21	8.977	-3.672	1917.96
373	8.925	-4.576			978	8.949	-4.177	1914.31	9.017	-3.790	1918.04
374	8.926	-4.183			977	8.969	-4.415	1914.41	9.030	-3.629	1918.13
375	8.930	-4.249			976	8.919	-4.273	1914.51	9.020	-3.916	1918.21
376	8.957	-4.095			975	8.928	-4.294	1914.62	8.977	-4.067	1918.29
377	8.948	-4.116			974	8.919	-3.982	1914.72	8.958	-4.071	1918.38
378	8.934	-4.201			973	8.923	-4.020	1914.82	8.968	-4.043	1918.46
379	8.928	-4.108			972	8.978	-4.010	1914.93	8.944	-4.330	1918.54
380	8.956	-4.179			971	8.992	-3.929	1915.03	9.011	-4.242	1918.63
381	8.917	-4.357			970	9.002	-3.861	1915.13	8.918	-4.121	1918.71
382	8.912	-4.420			969	8.948	-4.011	1915.23	8.966	-3.896	1918.79
383	8.892	-4.564			968	8.997	-3.990	1915.32	8.996	-3.824	1918.88
384	8.875	-4.461			967	8.990	-4.109	1915.42	8.982	-3.817	1918.96
385	8.848	-4.434			966	8.953	-4.129	1915.51	9.000	-3.816	1919.04
386	8.861	-4.400			965	8.975	-4.095	1915.61	9.012	-3.669	1919.13

LC3			Age Model		Linear interpolation				Monthly Resampling		
Sample ID	Sr/Ca (mmol/mol)	$\delta^{18}O$ (‰)	Sample ID	Time Pointer (year.month)	Sample ID	Sr/Ca (mmol/mol)	$\delta^{18}O$ (‰)	Age (year.month)	Sr/Ca (mmol/mol)	$\delta^{18}O$ (‰)	Age (year.month)
387	8.892	-4.349			964	8.918	-4.165	1915.70	9.003	-3.866	1919.21
388	8.874	-4.284			963	8.970	-4.163	1915.77	8.993	-3.996	1919.29
389	8.912	-4.229			962	8.927	-4.061	1915.84	8.981	-4.068	1919.38
390	8.965	-4.191			961	8.930	-4.068	1915.92	8.973	-4.072	1919.46
391	8.975	-3.968			960	8.945	-3.829	1915.99	8.967	-4.047	1919.54
392	8.966	-4.206			959	8.970	-3.979	1916.06	8.937	-4.062	1919.63
393	8.988	-3.999			958	9.020	-3.864	1916.13	8.901	-4.085	1919.71
394	8.951	-4.258			957	8.970	-3.844	1916.27	8.921	-4.268	1919.79
395	9.015	-4.240			956	8.995	-3.715	1916.42	8.943	-3.994	1919.88
396	9.072	-3.701			955	8.976	-3.905	1916.56	8.967	-3.987	1919.96
397	8.873	-4.635			954	8.955	-4.085	1916.71	8.946	-4.089	1920.04
398	8.851	-4.523			953	8.974	-4.087	1916.86	8.995	-3.972	1920.13
399	8.866	-4.673			952	9.020	-4.103	1917.01	8.960	-4.056	1920.21
400	8.871	-4.519			951	9.042	-3.890	1917.19	8.924	-4.161	1920.29
401	8.937	-4.323			950	8.962	-4.008	1917.46	8.905	-4.258	1920.38
402	8.947	-3.940			949	8.916	-4.043	1917.72	8.891	-4.285	1920.46
403	8.961	-3.844			948	8.966	-4.046	1917.79	8.880	-4.268	1920.54
404	8.944	-4.118			947	8.964	-3.419	1917.86	8.885	-4.176	1920.63
405	8.928	-4.074			946	8.963	-3.555	1917.93	8.884	-4.061	1920.71
406	8.908	-4.420			945	9.000	-3.866	1918.00	8.904	-3.909	1920.79
407	8.867	-4.539			944	9.031	-3.725	1918.07	8.966	-3.848	1920.88
408	8.860	-4.457			943	9.030	-3.588	1918.15	8.987	-3.885	1920.96
409	8.920	-4.428			942	9.017	-4.014	1918.23	9.008	-3.902	1921.04
410	8.953	-4.216			941	8.967	-4.080	1918.31	9.023	-3.836	1921.13
411	8.959	-4.001			940	8.956	-4.069	1918.39	8.995	-3.970	1921.21
412	9.002	-3.851			939	8.970	-4.039	1918.47	8.971	-4.066	1921.29
413	8.971	-4.053			938	8.942	-4.354	1918.55	8.957	-4.106	1921.38
414	8.905	-4.184			937	9.013	-4.238	1918.63	8.969	-4.126	1921.46
415	8.910	-4.381			936	8.918	-4.123	1918.71	8.953	-4.212	1921.54
416	8.864	-4.553			935	8.959	-3.891	1918.77	8.931	-4.322	1921.63
417	8.898	-4.355			934	8.987	-3.910	1918.84	8.925	-4.426	1921.71
418	8.939	-4.325			933	9.004	-3.742	1918.91	8.947	-4.276	1921.79
419	8.969	-4.132			932	8.975	-3.840	1918.97	8.973	-4.015	1921.88
420	8.982	-3.941			931	9.000	-3.819	1919.04	8.997	-4.222	1921.96
421	9.012	-3.971			930	9.014	-3.628	1919.11	8.978	-4.080	1922.04
422	9.001	-4.019			929	8.999	-3.957	1919.25	9.033	-3.936	1922.13
423	8.935	-4.147			928	8.977	-4.090	1919.40	9.009	-4.045	1922.21
424	8.901	-4.449			927	8.966	-4.043	1919.56	8.979	-4.149	1922.29
425	8.892	-4.646			926	8.901	-4.085	1919.71	8.966	-4.172	1922.38
426	8.881	-4.437			925	8.928	-4.361	1919.77	8.957	-4.140	1922.46
427	8.920	-4.578			924	8.905	-4.057	1919.83	8.930	-4.279	1922.54
428	8.931	-4.233			923	8.959	-3.967	1919.89	8.910	-4.368	1922.63
429	8.982	-4.429			922	8.971	-3.979	1919.95	8.903	-4.391	1922.71
430	8.976	-3.932			921	8.934	-4.053	1920.01	8.927	-4.317	1922.79
431	9.006	-4.060			920	8.957	-4.124	1920.07	8.957	-3.920	1922.88
432	8.967	-4.012			919	8.999	-3.956	1920.13	8.956	-3.822	1922.96
433	8.964	-4.197			918	8.929	-4.134	1920.27	8.990	-3.848	1923.04
434	8.942	-4.104			917	8.898	-4.296	1920.41	9.012	-3.902	1923.13
435	8.933	-4.424			916	8.879	-4.267	1920.55	8.987	-4.121	1923.21
436	8.887	-4.307			915	8.889	-4.106	1920.69	8.970	-4.314	1923.29
437	8.873	-4.315			914	8.873	-3.946	1920.77	8.970	-4.439	1923.38
438	8.914	-3.932			913	8.963	-3.840	1920.84	8.970	-4.540	1923.46
439	8.948	-4.078			912	8.968	-3.856	1920.91	8.968	-4.504	1923.54
440	8.958	-3.901			911	8.997	-3.900	1920.98	8.954	-4.386	1923.63
441	8.951	-4.177			910	9.010	-3.902	1921.06	8.944	-4.225	1923.71
442	8.939	-4.281			909	9.024	-3.830	1921.13	9.003	-4.115	1923.79
443	8.928	-4.468			908	8.980	-4.044	1921.25	8.981	-4.192	1923.88
444	8.901	-4.472			907	8.956	-4.104	1921.37	8.972	-4.143	1923.96
445	8.884	-4.567			906	8.973	-4.132	1921.48	8.989	-4.027	1924.04
446	8.888	-4.493			905	8.933	-4.291	1921.60	9.030	-3.997	1924.13
447	8.900	-4.641			904	8.924	-4.436	1921.72	8.981	-4.240	1924.21
448	8.918	-4.388			903	8.946	-4.306	1921.79	9.000	-4.294	1924.29
449	8.946	-4.249			902	8.968	-3.892	1921.86	8.978	-4.380	1924.38
450	8.932	-4.206			901	8.986	-4.360	1921.93	8.955	-4.428	1924.46
451	8.967	-4.240			900	9.010	-4.056	1922.00	8.956	-4.418	1924.54
452	8.909	-4.403			899	8.961	-4.093	1922.07	8.955	-4.433	1924.63
453	8.896	-4.403			898	9.050	-3.899	1922.14	8.946	-4.411	1924.71
454	8.867	-4.477			897	8.985	-4.133	1922.25	8.959	-4.270	1924.79
455	8.872	-4.493			896	8.968	-4.177	1922.36	8.953	-4.277	1924.88
456	8.880	-4.719			895	8.955	-4.135	1922.47	8.964	-4.186	1924.96
457	8.881	-4.467			894	8.915	-4.367	1922.58	8.994	-4.137	1925.04
458	8.903	-4.262			893	8.902	-4.370	1922.70	9.020	-4.212	1925.13
459	8.938	-4.387			892	8.909	-4.480	1922.76	9.016	-4.105	1925.21
460	8.945	-4.286			891	8.946	-4.148	1922.82	9.012	-3.998	1925.29
461	8.973	-4.293			890	8.959	-3.878	1922.88	9.007	-4.076	1925.38
462	8.945	-4.165			889	8.949	-3.832	1922.95	9.002	-4.153	1925.46
463	8.932	-4.250			888	8.985	-3.783	1923.01	8.982	-4.214	1925.54
464	8.915	-4.641			887	8.993	-3.899	1923.07	8.950	-4.262	1925.63
465	8.891	-4.530			886	9.016	-3.903	1923.14	8.926	-4.315	1925.71

LC3			Age Model		Linear interpolation				Monthly Resampling		
Sample ID	Sr/Ca (mmol/mol)	$\delta^{18}O$ (‰)	Sample ID	Time Pointer (year.month)	Sample ID	Sr/Ca (mmol/mol)	$\delta^{18}O$ (‰)	Age (year.month)	Sr/Ca (mmol/mol)	$\delta^{18}O$ (‰)	Age (year.month)
466	8.886	-4.249			885	8.970	-4.246	1923.25	8.949	-4.397	1925.79
467	8.933	-4.260			884	8.970	-4.422	1923.36	8.964	-4.409	1925.88
468	8.911	-4.406			883	8.970	-4.556	1923.47	8.968	-4.322	1925.96
469	8.946	-4.296			882	8.967	-4.474	1923.58	8.988	-4.262	1926.04
470	8.982	-4.046			881	8.934	-4.244	1923.69	9.015	-4.214	1926.13
471	9.010	-4.149			880	9.010	-4.102	1923.80	9.001	-4.279	1926.21
472	9.012	-4.056			879	8.968	-4.234	1923.91	8.989	-4.309	1926.29
473	8.965	-4.209			878	8.976	-4.039	1924.02	8.988	-4.259	1926.38
474	8.918	-4.547			877	9.031	-3.990	1924.12	8.977	-4.208	1926.46
475	8.874	-4.540			876	8.973	-4.279	1924.22	8.962	-4.158	1926.54
476	8.874	-4.477			875	9.010	-4.300	1924.32	8.959	-4.105	1926.63
477	8.882	-4.598			874	8.955	-4.440	1924.38	8.961	-4.039	1926.71
478	8.896	-4.498			873	8.950	-4.411	1924.42	8.973	-3.948	1926.79
479	8.961	-4.330			872	8.956	-4.436	1924.61	8.960	-3.948	1926.88
480	8.951	-4.168			871	8.946	-4.411	1924.71	8.995	-3.847	1926.96
481	8.962	-4.323			870	8.962	-4.243	1924.81	9.025	-3.706	1927.04
482	8.927	-4.344			869	8.949	-4.293	1924.91	9.037	-3.644	1927.13
483	8.899	-4.504			868	8.979	-4.083	1925.01	9.035	-3.700	1927.21
484	8.900	-4.664			867	9.021	-4.210	1925.11	9.032	-3.819	1927.29
485	8.860	-4.754			866	9.012	-3.998	1925.29	9.017	-4.062	1927.38
486	8.890	-4.708			865	9.000	-4.187	1925.49	9.000	-4.151	1927.46
487	8.891	-4.833			864	8.923	-4.303	1925.70	8.965	-4.217	1927.54
488	8.944	-4.535			863	8.963	-4.445	1925.84	8.939	-4.256	1927.63
489	8.942	-4.380			862	8.969	-4.296	1925.98	8.931	-4.249	1927.71
490	8.970	-4.273			861	9.016	-4.213	1926.13	8.941	-4.158	1927.79
491	8.996	-4.327			860	8.990	-4.325	1926.27	8.974	-3.963	1927.88
492	8.925	-4.396			859	8.987	-4.241	1926.41	9.023	-3.823	1927.96
493	8.906	-4.663			858	8.961	-4.156	1926.54	9.030	-3.785	1928.04
494	8.892	-4.571			857	8.957	-4.067	1926.68	9.046	-4.003	1928.13
495	8.976	-4.475			856	8.974	-3.948	1926.79	9.030	-4.021	1928.21
496	8.910	-4.759			855	8.958	-3.948	1926.89	9.015	-4.165	1928.29
497	8.901	-4.801			854	9.009	-3.809	1926.99	9.020	-4.163	1928.38
498	8.944	-4.581			853	9.037	-3.627	1927.08	9.004	-4.105	1928.46
499	8.975	-4.569			852	9.036	-3.669	1927.18	8.965	-4.152	1928.54
500	8.994	-4.391			851	9.033	-3.793	1927.28	8.961	-4.205	1928.63
501	8.994	-4.542			850	9.016	-4.084	1927.38	8.920	-4.256	1928.71
502	8.958	-4.412			849	8.995	-4.172	1927.48	8.986	-4.122	1928.79
503	8.893	-4.620			848	8.946	-4.246	1927.58	8.989	-3.974	1928.88
504	8.808	-4.362			847	8.930	-4.268	1927.68	9.001	-3.845	1928.96
505	8.851	-4.472			846	8.934	-4.204	1927.77	9.032	-3.817	1929.04
506	8.862	-4.548			845	8.967	-3.985	1927.86	9.034	-3.922	1929.13
507	8.904	-4.438			844	9.023	-3.825	1927.95	9.039	-3.971	1929.21
508	8.930	-4.396			843	9.030	-3.784	1928.04	9.027	-4.058	1929.29
509	8.954	-4.037			842	9.048	-4.029	1928.14	9.006	-4.141	1929.38
510	8.960	-3.976			841	9.025	-4.019	1928.23	9.000	-4.133	1929.46
511	8.954	-4.196			840	9.010	-4.246	1928.33	9.000	-4.088	1929.54
512	8.869	-4.177			839	9.029	-4.085	1928.42	8.987	-4.186	1929.63
513	8.871	-4.282			838	8.964	-4.136	1928.52	8.980	-4.277	1929.71
514	8.873	-4.568			837	8.968	-4.197	1928.61	8.991	-4.154	1929.79
515	8.894	-4.477			836	8.919	-4.257	1928.71	9.007	-4.100	1929.88
516	8.944	-4.335			835	8.987	-4.154	1928.78	9.009	-3.877	1929.96
517	8.975	-4.213			834	8.983	-3.980	1928.85	9.036	-3.881	1930.04
518	8.950	-4.093			833	8.998	-3.963	1928.92	9.049	-3.924	1930.13
519	8.946	-4.241			832	9.004	-3.749	1928.99	8.998	-3.861	1930.21
520	8.922	-4.215			831	9.043	-3.842	1929.06	9.025	-3.831	1930.29
521	8.894	-4.344			830	9.032	-3.937	1929.14	8.982	-3.965	1930.38
522	8.864	-4.377			829	9.043	-3.988	1929.24	8.958	-4.084	1930.46
523	8.868	-4.643			828	9.008	-4.144	1929.35	8.969	-4.168	1930.54
524	8.851	-4.462			827	9.000	-4.133	1929.46	8.963	-4.185	1930.63
525	8.907	-4.273			826	9.000	-4.076	1929.57	8.919	-4.203	1930.71
526	8.928	-4.326			825	8.977	-4.271	1929.67	8.968	-3.851	1930.79
527	8.926	-4.269			824	8.984	-4.284	1929.76	8.977	-3.765	1930.88
528	8.940	-4.296			823	8.999	-4.017	1929.83	9.038	-4.089	1930.96
529	8.928	-4.279			822	9.012	-4.160	1929.91	9.019	-4.072	1931.04
530	8.915	-4.393			821	9.008	-3.743	1929.98	9.054	-4.134	1931.13
531	8.941	-4.390			820	9.044	-3.918	1930.06	9.025	-4.167	1931.21
532	8.994	-4.034			819	9.050	-3.925	1930.13	8.996	-4.201	1931.29
533	9.043	-4.167			818	8.997	-3.864	1930.21	8.985	-4.264	1931.38
534	9.064	-4.113			817	9.034	-3.795	1930.28	8.980	-4.335	1931.46
535	9.038	-4.105			816	8.989	-3.979	1930.35	8.967	-4.359	1931.54
536	9.030	-3.917			815	8.793	-3.938	1930.42	8.950	-4.346	1931.63
537	9.052	-4.018			814	8.948	-4.225	1930.49	8.946	-4.308	1931.71
538	9.054	-4.112			813	8.979	-4.140	1930.57	8.962	-4.205	1931.79
539	8.989	-3.959			812	8.960	-4.194	1930.64	8.945	-4.036	1931.88
540	9.088	-4.694			811	8.918	-4.203	1930.71	8.959	-3.917	1931.96
541	9.086	-3.984			810	8.988	-4.077	1930.75	8.999	-3.910	1932.04
542	9.051	-3.743			809	8.968	-3.845	1930.79	9.036	-4.085	1932.13
543	9.034	-3.622			808	8.984	-3.823	1930.83	9.029	-4.104	1932.21
544	9.057	-3.741			807	8.977	-3.764	1930.88	9.001	-4.290	1932.29

LC3			Age Model		Linear interpolation				Monthly Resampling		
Sample ID	Sr/Ca (mmol/mol)	$\delta^{18}O$ (‰)	Sample ID	Time Pointer (year.month)	Sample ID	Sr/Ca (mmol/mol)	$\delta^{18}O$ (‰)	Age (year.month)	Sr/Ca (mmol/mol)	$\delta^{18}O$ (‰)	Age (year.month)
545	8.982	-3.688			806	9.016	-3.809	1930.92	8.985	-4.293	1932.38
546	9.048	-3.613			805	9.038	-4.091	1930.96	8.973	-4.205	1932.46
547	8.947	-4.122			804	9.041	-3.875	1931.00	8.949	-4.245	1932.54
548	8.966	-4.327			803	9.019	-4.072	1931.04	8.937	-4.283	1932.63
549	8.978	-4.314			802	9.033	-4.154	1931.08	8.921	-4.306	1932.71
550	9.016	-3.570			801	9.054	-4.134	1931.13	8.943	-4.289	1932.79
551	9.017	-3.786			800	8.990	-4.208	1931.31	8.971	-4.228	1932.88
552	8.997	-3.656			799	8.977	-4.366	1931.49	8.992	-4.034	1932.96
553	9.040	-4.128			798	8.938	-4.338	1931.68	9.009	-3.972	1933.04
554	8.999	-4.154			797	8.965	-4.234	1931.78	9.022	-3.985	1933.13
555	8.951	-4.418			796	8.944	-4.050	1931.87	9.014	-3.852	1933.21
556	8.929	-4.531			795	8.957	-3.917	1931.95	9.011	-3.946	1933.29
557	8.926	-4.376			794	8.999	-3.910	1932.04	9.002	-4.034	1933.38
558	8.993	-4.252			793	9.038	-4.097	1932.13	8.974	-4.172	1933.46
559	8.973	-4.086			792	9.027	-4.106	1932.23	8.947	-4.276	1933.54
560	8.997	-4.148			791	8.986	-4.392	1932.33	8.940	-4.231	1933.63
561	9.000	-4.173			790	8.983	-4.189	1932.43	8.928	-4.138	1933.71
562	8.984	-4.165			789	8.952	-4.237	1932.52	8.950	-4.199	1933.79
563	8.962	-4.078			788	8.937	-4.282	1932.62	8.969	-4.054	1933.88
564	8.935	-4.361			787	8.918	-4.311	1932.73	8.982	-3.985	1933.96
565	8.918	-4.555			786	8.967	-4.268	1932.86	8.991	-4.105	1934.04
566	8.908	-4.537			785	9.000	-3.961	1932.99	9.013	-4.065	1934.13
567	8.935	-4.304			784	9.022	-3.989	1933.12	9.000	-4.027	1934.21
568	8.666	-4.380			783	9.013	-3.835	1933.22	8.979	-3.992	1934.29
569	8.982	-4.032			782	9.010	-3.983	1933.32	8.964	-3.986	1934.38
570	8.968	-4.201			781	8.997	-4.065	1933.41	8.965	-4.221	1934.46
571	8.919	-4.299			780	8.949	-4.287	1933.51	8.975	-4.235	1934.54
572	8.946	-4.402			779	8.944	-4.255	1933.61	8.956	-4.220	1934.63
573	8.918	-4.530			778	8.926	-4.134	1933.70	8.907	-4.248	1934.71
574	8.899	-4.483			777	8.956	-4.214	1933.81	8.950	-4.225	1934.79
575	8.967	-4.045			776	8.979	-3.929	1933.92	8.956	-4.152	1934.88
576	8.907	-4.703			775	8.989	-4.108	1934.03	8.996	-4.201	1934.96
577	8.962	-4.544			774	9.018	-4.055	1934.15	8.998	-4.079	1935.04
578	8.975	-4.251			773	8.986	-4.006	1934.26	9.032	-3.974	1935.13
579	8.977	-4.288			772	8.964	-3.962	1934.37	9.012	-3.978	1935.21
580	8.950	-4.313			771	8.965	-4.276	1934.48	8.978	-4.074	1935.29
581	8.949	-4.194			770	8.982	-4.205	1934.59	9.010	-4.171	1935.38
582	8.908	-4.413			769	8.902	-4.250	1934.70	8.999	-4.261	1935.46
583	8.892	-4.375			768	8.950	-4.231	1934.79	8.954	-4.393	1935.54
584	8.888	-4.645			767	8.953	-4.147	1934.87	8.934	-4.524	1935.63
585	8.905	-4.431			766	8.996	-4.209	1934.95	8.899	-4.407	1935.71
586	8.951	-4.334			765	8.996	-4.087	1935.04	8.916	-4.409	1935.79
587	8.970	-4.348			764	9.033	-3.974	1935.12	8.938	-4.316	1935.88
588	8.983	-4.456			763	9.010	-3.978	1935.22	8.971	-4.040	1935.96
589	8.948	-4.313			762	8.968	-4.102	1935.31	8.994	-3.940	1936.04
590	8.945	-4.333			761	9.035	-4.213	1935.41	9.012	-3.935	1936.13
591	8.908	-4.432			760	8.960	-4.313	1935.51	8.999	-4.078	1936.21
592	8.891	-4.573			759	8.942	-4.550	1935.61	8.983	-4.127	1936.29
593	8.886	-4.717			758	8.899	-4.407	1935.71	8.961	-4.261	1936.38
594	8.868	-4.663			757	8.927	-4.410	1935.85	8.943	-4.148	1936.46
595	8.913	-4.507			756	8.983	-3.943	1935.99	8.917	-4.278	1936.54
596	8.949	-4.423			755	9.013	-3.935	1936.13	8.897	-4.354	1936.63
597	8.961	-4.242			754	8.998	-4.091	1936.22	8.888	-4.315	1936.71
598	8.982	-4.127			753	8.982	-4.131	1936.30	8.967	-4.101	1936.79
599	8.987	-4.028			752	8.959	-4.276	1936.38	8.992	-4.005	1936.88
600	8.984	-4.161			751	8.941	-4.134	1936.47	9.022	-3.952	1936.96
601	8.953	-4.393			750	8.914	-4.295	1936.55	9.043	-3.890	1937.04
602	8.949	-4.558			749	8.895	-4.362	1936.63	9.057	-3.942	1937.13
603	8.933	-4.660			748	8.887	-4.308	1936.72	9.050	-4.091	1937.21
604	8.941	-4.516			747	8.978	-4.070	1936.80	9.032	-4.198	1937.29
605	8.985	-4.371			746	8.994	-3.995	1936.89	9.005	-4.148	1937.38
606	9.023	-4.320			745	9.026	-3.945	1936.97	8.986	-4.156	1937.46
607	9.037	-4.028			744	9.046	-3.881	1937.05	8.963	-4.174	1937.54
608	9.020	-4.098			743	9.060	-3.958	1937.14	8.927	-4.182	1937.63
609	9.008	-4.109			742	9.040	-4.213	1937.27	8.923	-4.296	1937.71
610	8.990	-4.030			741	9.000	-4.138	1937.39	8.927	-4.261	1937.79
611	8.980	-4.173			740	8.974	-4.171	1937.52	8.934	-3.998	1937.88
612	8.934	-4.266			739	8.921	-4.183	1937.64	8.970	-4.146	1937.96
613	8.964	-4.532			738	8.925	-4.377	1937.76	9.009	-4.046	1938.04
614	8.971	-4.572			737	8.932	-3.990	1937.87	9.034	-3.914	1938.13
615	8.936	-4.538			736	8.981	-4.191	1937.98	9.032	-3.927	1938.21
616	8.966	-4.416			735	9.035	-3.909	1938.10	9.021	-4.052	1938.29
617	8.962	-4.281			734	9.032	-3.928	1938.22	9.008	-4.071	1938.38
618	8.993	-4.139			733	9.014	-4.127	1938.34	8.994	-3.946	1938.46
619	9.004	-4.226			732	8.994	-3.944	1938.46	8.987	-4.095	1938.54
620	8.990	-4.173			731	8.983	-4.168	1938.58	8.952	-4.278	1938.63
621	8.975	-4.217			730	8.896	-4.476	1938.70	8.897	-4.467	1938.71
622	8.964	-4.339			729	8.912	-4.313	1938.81	8.910	-4.338	1938.79
623	8.930	-4.450			728	8.952	-4.155	1938.91	8.938	-4.211	1938.88

LC3			Age Model		Linear interpolation				Monthly Resampling		
Sample ID	Sr/Ca (mmol/mol)	$\delta^{18}O$ (‰)	Sample ID	Time Pointer (year.month)	Sample ID	Sr/Ca (mmol/mol)	$\delta^{18}O$ (‰)	Age (year.month)	Sr/Ca (mmol/mol)	$\delta^{18}O$ (‰)	Age (year.month)
624	8.905	-4.444			727	9.001	-3.902	1939.02	8.974	-4.041	1938.96
625	8.910	-4.440			726	9.044	-3.982	1939.12	9.012	-3.922	1939.04
626	8.890	-4.438			725	9.024	-3.964	1939.23	9.043	-3.981	1939.13
627	8.901	-4.534			724	8.980	-3.965	1939.35	9.029	-3.968	1939.21
628	8.915	-4.418			723	8.992	-4.248	1939.47	9.002	-3.964	1939.29
629	8.948	-4.292			722	8.935	-4.374	1939.58	8.983	-4.027	1939.38
630	8.964	-3.997			721	8.930	-4.416	1939.70	8.991	-4.232	1939.46
631	8.940	-4.327			720	8.960	-4.440	1939.77	8.954	-4.332	1939.54
632	8.958	-4.220			719	8.972	-4.326	1939.84	8.933	-4.390	1939.63
633	8.970	-4.141			718	8.983	-4.238	1939.92	8.935	-4.420	1939.71
634	8.964	-4.196			717	9.000	-4.088	1939.99	8.963	-4.407	1939.79
635	8.937	-4.281			716	8.963	-4.003	1940.06	8.977	-4.289	1939.88
636	8.920	-4.366			715	9.044	-4.076	1940.14	8.992	-4.154	1939.96
637	8.921	-4.553			714	9.002	-3.975	1940.28	8.974	-4.029	1940.04
638	8.907	-4.504			713	8.957	-4.113	1940.43	9.030	-4.064	1940.13
639	8.908	-4.506			712	8.978	-4.124	1940.57	9.024	-4.027	1940.21
640	8.947	-4.600			711	8.960	-4.186	1940.71	8.999	-3.984	1940.29
641	8.944	-4.464			710	8.980	-4.048	1940.78	8.973	-4.063	1940.38
642	8.964	-4.388			709	8.973	-4.006	1940.85	8.962	-4.115	1940.46
643	8.974	-4.233			708	8.971	-3.971	1940.92	8.974	-4.122	1940.54
644	9.012	-4.072			707	9.007	-4.030	1940.99	8.971	-4.148	1940.63
645	8.948	-4.148			706	9.017	-3.985	1941.06	8.961	-4.184	1940.71
646	8.945	-4.362			705	9.029	-3.931	1941.14	8.979	-4.043	1940.79
647	8.937	-4.262			704	9.000	-4.206	1941.33	8.972	-3.995	1940.88
648	8.931	-4.501			703	8.930	-4.227	1941.52	8.989	-4.001	1940.96
649	8.888	-4.434			702	8.923	-4.134	1941.70	9.014	-3.999	1941.04
650	8.893	-4.461			701	8.965	-4.127	1941.75	9.026	-3.943	1941.13
651	8.928	-4.500			700	8.958	-4.373	1941.80	9.019	-4.028	1941.21
652	8.955	-4.444			699	8.965	-4.156	1941.85	9.006	-4.150	1941.29
653	8.956	-4.390			698	8.977	-4.260	1941.90	8.983	-4.211	1941.38
654	8.963	-4.302			697	8.989	-4.109	1941.95	8.952	-4.220	1941.46
655	8.973	-4.292			696	9.008	-4.035	1942.00	8.929	-4.215	1941.54
656	9.003	-4.205			695	9.012	-3.843	1942.05	8.926	-4.173	1941.63
657	8.975	-4.139			694	9.041	-4.088	1942.10	8.928	-4.133	1941.71
658	8.977	-4.055			693	9.036	-4.128	1942.18	8.959	-4.324	1941.79
659	8.954	-3.985			692	8.977	-4.032	1942.27	8.971	-4.205	1941.88
660	8.942	-4.251			691	8.989	-4.064	1942.36	8.991	-4.099	1941.96
661	8.949	-4.378			690	8.986	-4.214	1942.45	9.011	-3.881	1942.04
662	8.949	-4.500			689	8.957	-4.579	1942.54	9.040	-4.100	1942.13
663	8.927	-4.506			688	8.982	-4.312	1942.62	9.017	-4.098	1942.21
664	8.964	-4.394			687	8.929	-4.555	1942.71	8.980	-4.040	1942.29
665	8.993	-4.226			686	8.966	-4.275	1942.77	8.988	-4.093	1942.38
666	9.009	-4.119			685	8.940	-4.297	1942.83	8.982	-4.262	1942.46
667	9.040	-4.154			684	8.949	-4.323	1942.89	8.959	-4.558	1942.54
668	8.996	-4.194			683	8.963	-4.227	1942.95	8.981	-4.316	1942.63
669	9.006	-4.085			682	8.995	-4.221	1943.00	8.931	-4.543	1942.71
670	9.014	-4.096			681	9.013	-4.099	1943.06	8.957	-4.283	1942.79
671	8.981	-4.117			680	9.040	-4.295	1943.12	8.947	-4.318	1942.88
672	8.953	-4.209			679	9.012	-4.230	1943.19	8.970	-4.226	1942.96
673	8.978	-4.221			678	8.995	-4.410	1943.26	9.007	-4.139	1943.04
674	8.989	-4.453			677	8.967	-4.432	1943.33	9.038	-4.289	1943.13
675	8.984	-4.389			676	8.977	-4.396	1943.41	9.008	-4.277	1943.21
676	8.977	-4.396			675	8.984	-4.389	1943.48	8.983	-4.419	1943.29
677	8.967	-4.432			674	8.989	-4.453	1943.55	8.973	-4.411	1943.38
678	8.995	-4.410			673	8.978	-4.221	1943.62	8.982	-4.391	1943.46
679	9.012	-4.230			672	8.953	-4.209	1943.69	8.989	-4.447	1943.54
680	9.040	-4.295			671	8.981	-4.117	1943.77	8.976	-4.220	1943.63
681	9.013	-4.099			670	9.014	-4.096	1943.86	8.959	-4.190	1943.71
682	8.995	-4.221			669	9.006	-4.085	1943.94	8.988	-4.113	1943.79
683	8.963	-4.227			668	8.996	-4.194	1944.03	9.012	-4.094	1943.88
684	8.949	-4.323			667	9.040	-4.154	1944.11	9.004	-4.107	1943.96
685	8.940	-4.297			666	9.009	-4.119	1944.25	9.005	-4.186	1944.04
686	8.966	-4.275			665	8.993	-4.226	1944.40	9.037	-4.150	1944.13
687	8.929	-4.555			664	8.964	-4.394	1944.54	9.018	-4.129	1944.21
688	8.982	-4.312			663	8.927	-4.506	1944.69	9.004	-4.150	1944.29
689	8.957	-4.579			662	8.949	-4.500	1944.76	8.995	-4.211	1944.38
690	8.986	-4.214			661	8.949	-4.378	1944.82	8.980	-4.300	1944.46
691	8.989	-4.064			660	8.942	-4.251	1944.88	8.964	-4.396	1944.54
692	8.977	-4.032			659	8.954	-3.985	1944.95	8.942	-4.460	1944.63
693	9.036	-4.128			658	8.977	-4.055	1945.01	8.934	-4.504	1944.71
694	9.041	-4.088			657	8.975	-4.139	1945.07	8.949	-4.442	1944.79
695	9.012	-3.843			656	9.003	-4.205	1945.13	8.943	-4.271	1944.88
696	9.008	-4.035			655	8.973	-4.292	1945.21	8.959	-4.000	1944.96
697	8.989	-4.109			654	8.963	-4.302	1945.29	8.976	-4.103	1945.04
698	8.977	-4.260			653	8.956	-4.390	1945.38	9.001	-4.201	1945.13
699	8.965	-4.156			652	8.955	-4.444	1945.46	8.974	-4.290	1945.21
700	8.958	-4.373			651	8.928	-4.500	1945.54	8.963	-4.302	1945.29
701	8.965	-4.127			650	8.893	-4.461	1945.62	8.956	-4.389	1945.38
702	8.923	-4.134			649	8.888	-4.434	1945.70	8.955	-4.444	1945.46

LC3			Age Model		Linear interpolation				Monthly Resampling		
Sample ID	Sr/Ca (mmol/mol)	$\delta^{18}O$ (‰)	Sample ID	Time Pointer (year.month)	Sample ID	Sr/Ca (mmol/mol)	$\delta^{18}O$ (‰)	Age (year.month)	Sr/Ca (mmol/mol)	$\delta^{18}O$ (‰)	Age (year.month)
703	8.930	-4.227			648	8.931	-4.501	1945.79	8.927	-4.499	1945.54
704	9.000	-4.206			647	8.937	-4.262	1945.87	8.893	-4.460	1945.63
705	9.029	-3.931			646	8.945	-4.362	1945.95	8.890	-4.438	1945.71
706	9.017	-3.985			645	8.948	-4.148	1946.03	8.931	-4.480	1945.79
707	9.007	-4.030			644	9.012	-4.072	1946.11	8.938	-4.274	1945.88
708	8.971	-3.971			643	8.974	-4.233	1946.21	8.945	-4.331	1945.96
709	8.973	-4.006			642	8.964	-4.388	1946.32	8.959	-4.135	1946.04
710	8.980	-4.048			641	8.944	-4.464	1946.43	9.006	-4.097	1946.13
711	8.960	-4.186			640	8.947	-4.600	1946.54	8.976	-4.223	1946.21
712	8.978	-4.124			639	8.908	-4.506	1946.65	8.967	-4.344	1946.29
713	8.957	-4.113			638	8.907	-4.504	1946.74	8.954	-4.425	1946.38
714	9.002	-3.975			637	8.921	-4.553	1946.82	8.945	-4.499	1946.46
715	9.044	-4.076			636	8.920	-4.366	1946.89	8.946	-4.597	1946.54
716	8.963	-4.003			635	8.937	-4.281	1946.97	8.916	-4.525	1946.63
717	9.000	-4.088			634	8.964	-4.196	1947.04	8.907	-4.505	1946.71
718	8.983	-4.238			633	8.970	-4.141	1947.12	8.916	-4.537	1946.79
719	8.972	-4.326			632	8.958	-4.220	1947.20	8.920	-4.408	1946.88
720	8.960	-4.440			631	8.940	-4.327	1947.28	8.935	-4.290	1946.96
721	8.930	-4.416			630	8.964	-3.997	1947.36	8.964	-4.195	1947.04
722	8.935	-4.374			629	8.948	-4.292	1947.45	8.969	-4.150	1947.13
723	8.992	-4.248			628	8.915	-4.418	1947.53	8.956	-4.235	1947.21
724	8.980	-3.965			627	8.901	-4.534	1947.61	8.943	-4.279	1947.29
725	9.024	-3.964			626	8.890	-4.438	1947.69	8.962	-4.041	1947.38
726	9.044	-3.982			625	8.910	-4.440	1947.76	8.943	-4.313	1947.46
727	9.001	-3.902			624	8.905	-4.444	1947.82	8.913	-4.438	1947.54
728	8.952	-4.155			623	8.930	-4.450	1947.88	8.899	-4.516	1947.63
729	8.912	-4.313			622	8.964	-4.339	1947.95	8.895	-4.438	1947.71
730	8.896	-4.476			621	8.975	-4.217	1948.01	8.907	-4.442	1947.79
731	8.983	-4.168			620	8.990	-4.173	1948.07	8.927	-4.449	1947.88
732	8.994	-3.944			619	9.004	-4.226	1948.13	8.966	-4.314	1947.96
733	9.014	-4.127			618	8.993	-4.139	1948.22	8.983	-4.193	1948.04
734	9.032	-3.928			617	8.962	-4.281	1948.30	9.002	-4.219	1948.13
735	9.035	-3.909			616	8.966	-4.416	1948.38	8.994	-4.147	1948.21
736	8.981	-4.191			615	8.936	-4.538	1948.46	8.965	-4.269	1948.29
737	8.932	-3.990			614	8.971	-4.572	1948.55	8.966	-4.407	1948.38
738	8.925	-4.377			613	8.964	-4.532	1948.63	8.938	-4.532	1948.46
739	8.921	-4.183			612	8.934	-4.266	1948.71	8.970	-4.571	1948.54
740	8.974	-4.171			611	8.980	-4.173	1948.79	8.964	-4.533	1948.63
741	9.000	-4.138			610	8.990	-4.030	1948.87	8.934	-4.270	1948.71
742	9.040	-4.213			609	9.008	-4.109	1948.96	8.980	-4.173	1948.79
743	9.060	-3.958			608	9.020	-4.098	1949.04	8.990	-4.031	1948.88
744	9.046	-3.881			607	9.037	-4.028	1949.12	9.008	-4.109	1948.96
745	9.026	-3.945			606	9.023	-4.320	1949.26	9.021	-4.095	1949.04
746	8.994	-3.995			605	8.985	-4.371	1949.41	9.037	-4.037	1949.13
747	8.978	-4.070			604	8.941	-4.516	1949.55	9.028	-4.211	1949.21
748	8.887	-4.308			603	8.933	-4.660	1949.70	9.015	-4.331	1949.29
749	8.895	-4.362			602	8.949	-4.558	1949.82	8.993	-4.360	1949.38
750	8.914	-4.295			601	8.953	-4.393	1949.93	8.970	-4.421	1949.46
751	8.941	-4.134			600	8.984	-4.161	1950.04	8.945	-4.503	1949.54
752	8.959	-4.276			599	8.987	-4.028	1950.16	8.937	-4.585	1949.63
753	8.982	-4.131			598	8.982	-4.127	1950.27	8.934	-4.653	1949.71
754	8.998	-4.091			597	8.961	-4.242	1950.38	8.946	-4.579	1949.79
755	9.013	-3.935			596	8.949	-4.423	1950.49	8.951	-4.471	1949.88
756	8.983	-3.943			595	8.913	-4.507	1950.60	8.961	-4.333	1949.96
757	8.927	-4.410			594	8.868	-4.663	1950.71	8.984	-4.163	1950.04
758	8.899	-4.407			593	8.886	-4.717	1950.78	8.986	-4.064	1950.13
759	8.942	-4.550			592	8.891	-4.573	1950.85	8.985	-4.075	1950.21
760	8.960	-4.313			591	8.908	-4.432	1950.92	8.977	-4.153	1950.29
761	9.035	-4.213			590	8.945	-4.333	1950.99	8.961	-4.239	1950.38
762	8.968	-4.102			589	8.948	-4.313	1951.06	8.952	-4.375	1950.46
763	9.010	-3.978			588	8.983	-4.456	1951.13	8.932	-4.464	1950.54
764	9.033	-3.974			587	8.970	-4.348	1951.26	8.902	-4.544	1950.63
765	8.996	-4.087			586	8.951	-4.334	1951.40	8.868	-4.661	1950.71
766	8.996	-4.209			585	8.905	-4.431	1951.53	8.887	-4.696	1950.79
767	8.953	-4.147			584	8.888	-4.645	1951.67	8.897	-4.524	1950.88
768	8.950	-4.231			583	8.892	-4.375	1951.77	8.928	-4.378	1950.96
769	8.902	-4.250			582	8.908	-4.413	1951.85	8.947	-4.318	1951.04
770	8.982	-4.205			581	8.949	-4.194	1951.94	8.981	-4.448	1951.13
771	8.965	-4.276			580	8.950	-4.313	1952.02	8.975	-4.392	1951.21
772	8.964	-3.962			579	8.977	-4.288	1952.11	8.966	-4.345	1951.29
773	8.986	-4.006			578	8.975	-4.251	1952.20	8.954	-4.336	1951.38
774	9.018	-4.055			577	8.962	-4.544	1952.31	8.931	-4.377	1951.46
775	8.989	-4.108			576	8.907	-4.703	1952.41	8.904	-4.444	1951.54
776	8.979	-3.929			575	8.967	-4.045	1952.51	8.894	-4.575	1951.63
777	8.956	-4.214			574	8.899	-4.483	1952.61	8.890	-4.537	1951.71
778	8.926	-4.134			573	8.918	-4.530	1952.71	8.897	-4.386	1951.79
779	8.944	-4.255			572	8.946	-4.402	1952.81	8.919	-4.352	1951.88
780	8.949	-4.287			571	8.919	-4.299	1952.91	8.949	-4.226	1951.96
781	8.997	-4.065			570	8.968	-4.201	1953.01	8.957	-4.307	1952.04

LC3			Age Model		Linear interpolation				Monthly Resampling		
Sample ID	Sr/Ca (mmol/mol)	$\delta^{18}O$ (‰)	Sample ID	Time Pointer (year.month)	Sample ID	Sr/Ca (mmol/mol)	$\delta^{18}O$ (‰)	Age (year.month)	Sr/Ca (mmol/mol)	$\delta^{18}O$ (‰)	Age (year.month)
782	9.010	-3.983			569	8.982	-4.032	1953.11	8.977	-4.280	1952.13
783	9.013	-3.835			568	8.666	-4.380	1953.21	8.974	-4.265	1952.21
784	9.022	-3.989			567	8.935	-4.304	1953.51	8.964	-4.506	1952.29
785	9.000	-3.961			566	8.908	-4.537	1953.71	8.924	-4.655	1952.38
786	8.967	-4.268			565	8.918	-4.555	1953.79	8.939	-4.356	1952.46
787	8.918	-4.311			564	8.935	-4.361	1953.86	8.943	-4.201	1952.54
788	8.937	-4.282			563	8.962	-4.078	1953.94	8.902	-4.492	1952.63
789	8.952	-4.237			562	8.984	-4.165	1954.02	8.918	-4.529	1952.71
790	8.983	-4.189			561	9.000	-4.173	1954.09	8.941	-4.422	1952.79
791	8.986	-4.392			560	8.997	-4.148	1954.20	8.928	-4.333	1952.88
792	9.027	-4.106			559	8.973	-4.086	1954.37	8.943	-4.251	1952.96
793	9.038	-4.097			558	8.993	-4.252	1954.54	8.973	-4.147	1953.04
794	8.999	-3.910			557	8.926	-4.376	1954.71	8.980	-4.059	1953.13
795	8.957	-3.917			556	8.929	-4.531	1954.82	8.970	-4.207	1953.21
796	8.944	-4.050			555	8.951	-4.418	1954.93	8.961	-4.355	1953.29
797	8.965	-4.234			554	8.999	-4.154	1955.04	8.951	-4.354	1953.38
798	8.938	-4.338			553	9.040	-4.128	1955.15	8.941	-4.323	1953.46
799	8.977	-4.366			552	8.997	-3.656	1955.24	8.930	-4.343	1953.54
800	8.990	-4.208			551	9.017	-3.786	1955.33	8.919	-4.440	1953.63
801	9.054	-4.134			550	9.016	-3.570	1955.42	8.908	-4.537	1953.71
802	9.033	-4.154			549	8.978	-4.314	1955.51	8.919	-4.540	1953.79
803	9.019	-4.072			548	8.966	-4.327	1955.61	8.939	-4.315	1953.88
804	9.041	-3.875			547	8.947	-4.122	1955.69	8.968	-4.100	1953.96
805	9.038	-4.091			546	9.048	-3.613	1955.76	8.989	-4.168	1954.04
806	9.016	-3.809			545	8.982	-3.688	1955.82	8.999	-4.166	1954.13
807	8.977	-3.764			544	9.057	-3.741	1955.88	8.996	-4.146	1954.21
808	8.984	-3.823			543	9.034	-3.622	1955.94	8.984	-4.115	1954.29
809	8.968	-3.845			542	9.051	-3.743	1956.00	8.974	-4.090	1954.38
810	8.988	-4.077			541	9.086	-3.984	1956.06	8.983	-4.173	1954.46
811	8.918	-4.203			540	9.088	-4.694	1956.13	8.991	-4.255	1954.54
812	8.960	-4.194			539	8.989	-3.959	1956.71	8.958	-4.317	1954.63
813	8.979	-4.140			538	9.054	-4.112	1956.79	8.926	-4.381	1954.71
814	8.948	-4.225			537	9.052	-4.018	1956.87	8.928	-4.492	1954.79
815	8.793	-3.938			536	9.030	-3.917	1956.95	8.940	-4.476	1954.88
816	8.989	-3.979			535	9.038	-4.105	1957.04	8.963	-4.355	1954.96
817	9.034	-3.795			534	9.064	-4.113	1957.12	8.999	-4.156	1955.04
818	8.997	-3.864			533	9.043	-4.167	1957.18	9.030	-4.134	1955.13
819	9.050	-3.925			532	8.994	-4.034	1957.24	9.013	-3.834	1955.21
820	9.044	-3.918			531	8.941	-4.390	1957.30	9.008	-3.727	1955.29
821	9.008	-3.743			530	8.915	-4.393	1957.35	9.017	-3.686	1955.38
822	9.012	-4.160			529	8.928	-4.279	1957.41	9.001	-3.853	1955.46
823	8.999	-4.017			528	8.940	-4.296	1957.47	8.974	-4.318	1955.54
824	8.984	-4.284			527	8.926	-4.269	1957.53	8.962	-4.280	1955.63
825	8.977	-4.271			526	8.928	-4.326	1957.59	8.971	-4.002	1955.71
826	9.000	-4.076			525	8.907	-4.273	1957.65	9.009	-3.657	1955.79
827	9.000	-4.133			524	8.851	-4.462	1957.71	9.053	-3.738	1955.88
828	9.008	-4.144			523	8.868	-4.643	1957.76	9.039	-3.658	1955.96
829	9.043	-3.988			522	8.864	-4.377	1957.82	9.074	-3.901	1956.04
830	9.032	-3.937			521	8.894	-4.344	1957.88	9.088	-4.694	1956.13
831	9.043	-3.842			520	8.922	-4.215	1957.94	9.074	-4.589	1956.21
832	9.004	-3.749			519	8.946	-4.241	1958.00	9.060	-4.483	1956.29
833	8.998	-3.963			518	8.950	-4.093	1958.06	9.045	-4.378	1956.38
834	8.983	-3.980			517	8.975	-4.213	1958.12	9.031	-4.273	1956.46
835	8.987	-4.154			516	8.944	-4.335	1958.26	9.017	-4.168	1956.54
836	8.919	-4.257			515	8.894	-4.477	1958.41	9.003	-4.063	1956.63
837	8.968	-4.197			514	8.873	-4.568	1958.56	8.990	-3.960	1956.71
838	8.964	-4.136			513	8.871	-4.282	1958.71	9.054	-4.110	1956.79
839	9.029	-4.085			512	8.869	-4.177	1958.84	9.051	-4.014	1956.88
840	9.010	-4.246			511	8.954	-4.196	1958.98	9.031	-3.930	1956.96
841	9.025	-4.019			510	8.960	-3.976	1959.11	9.040	-4.106	1957.04
842	9.048	-4.029			509	8.954	-4.037	1959.21	9.061	-4.120	1957.13
843	9.030	-3.784			508	8.930	-4.396	1959.31	9.019	-4.101	1957.21
844	9.023	-3.825			507	8.904	-4.438	1959.40	8.945	-4.360	1957.29
845	8.967	-3.985			506	8.862	-4.548	1959.50	8.920	-4.353	1957.38
846	8.934	-4.204			505	8.851	-4.472	1959.59	8.937	-4.292	1957.46
847	8.930	-4.268			504	8.808	-4.362	1959.69	8.926	-4.281	1957.54
848	8.946	-4.246			503	8.893	-4.620	1959.81	8.915	-4.293	1957.63
849	8.995	-4.172			502	8.958	-4.412	1959.94	8.852	-4.470	1957.71
850	9.016	-4.084			501	8.994	-4.542	1960.06	8.866	-4.517	1957.79
851	9.033	-3.793			500	8.994	-4.391	1960.17	8.890	-4.348	1957.88
852	9.036	-3.669			499	8.975	-4.569	1960.26	8.929	-4.223	1957.96
853	9.037	-3.627			498	8.944	-4.581	1960.35	8.949	-4.136	1958.04
854	9.009	-3.809			497	8.901	-4.801	1960.44	8.973	-4.219	1958.13
855	8.958	-3.948			496	8.910	-4.759	1960.53	8.956	-4.289	1958.21
856	8.974	-3.948			495	8.976	-4.475	1960.62	8.934	-4.363	1958.29
857	8.957	-4.067			494	8.892	-4.571	1960.71	8.906	-4.442	1958.38
858	8.961	-4.156			493	8.906	-4.663	1960.85	8.887	-4.505	1958.46
859	8.987	-4.241			492	8.925	-4.396	1960.99	8.876	-4.556	1958.54
860	8.990	-4.325			491	8.996	-4.327	1961.13	8.872	-4.446	1958.63

LC3			Age Model		Linear interpolation				Monthly Resampling		
Sample ID	Sr/Ca (mmol/mol)	$\delta^{18}O$ (‰)	Sample ID	Time Pointer (year.month)	Sample ID	Sr/Ca (mmol/mol)	$\delta^{18}O$ (‰)	Age (year.month)	Sr/Ca (mmol/mol)	$\delta^{18}O$ (‰)	Age (year.month)
861	9.016	-4.213			490	8.970	-4.273	1961.23	8.871	-4.286	1958.71
862	8.969	-4.296			489	8.942	-4.380	1961.32	8.870	-4.219	1958.79
863	8.963	-4.445			488	8.944	-4.535	1961.42	8.888	-4.181	1958.88
864	8.923	-4.303			487	8.891	-4.833	1961.51	8.941	-4.193	1958.96
865	9.000	-4.187			486	8.890	-4.708	1961.61	8.957	-4.093	1959.04
866	9.012	-3.998			485	8.860	-4.754	1961.70	8.959	-3.983	1959.13
867	9.021	-4.210			484	8.900	-4.664	1961.79	8.954	-4.034	1959.21
868	8.979	-4.083			483	8.899	-4.504	1961.87	8.934	-4.336	1959.29
869	8.949	-4.293			482	8.927	-4.344	1961.96	8.912	-4.426	1959.38
870	8.962	-4.243			481	8.962	-4.323	1962.05	8.879	-4.502	1959.46
871	8.946	-4.411			480	8.951	-4.168	1962.14	8.857	-4.513	1959.54
872	8.956	-4.436			479	8.961	-4.330	1962.27	8.837	-4.435	1959.63
873	8.950	-4.411			478	8.896	-4.498	1962.40	8.821	-4.401	1959.71
874	8.955	-4.440			477	8.882	-4.598	1962.53	8.878	-4.576	1959.79
875	9.010	-4.300			476	8.874	-4.477	1962.66	8.926	-4.515	1959.88
876	8.973	-4.279			475	8.874	-4.540	1962.77	8.964	-4.435	1959.96
877	9.031	-3.990			474	8.918	-4.547	1962.87	8.989	-4.523	1960.04
878	8.976	-4.039			473	8.965	-4.209	1962.97	8.994	-4.450	1960.13
879	8.968	-4.234			472	9.012	-4.056	1963.07	8.985	-4.473	1960.21
880	9.010	-4.102			471	9.010	-4.149	1963.17	8.963	-4.574	1960.29
881	8.934	-4.244			470	8.982	-4.046	1963.28	8.931	-4.650	1960.38
882	8.967	-4.474			469	8.946	-4.296	1963.39	8.903	-4.791	1960.46
883	8.970	-4.556			468	8.911	-4.406	1963.49	8.921	-4.715	1960.54
884	8.970	-4.422			467	8.933	-4.260	1963.60	8.969	-4.483	1960.63
885	8.970	-4.246			466	8.886	-4.249	1963.70	8.892	-4.571	1960.71
886	9.016	-3.903			465	8.891	-4.530	1963.79	8.900	-4.625	1960.79
887	8.993	-3.899			464	8.915	-4.641	1963.87	8.909	-4.615	1960.88
888	8.985	-3.783			463	8.932	-4.250	1963.96	8.921	-4.459	1960.96
889	8.949	-3.832			462	8.945	-4.165	1964.04	8.950	-4.372	1961.04
890	8.959	-3.878			461	8.973	-4.293	1964.13	8.992	-4.331	1961.13
891	8.946	-4.148			460	8.945	-4.286	1964.21	8.975	-4.284	1961.21
892	8.909	-4.480			459	8.938	-4.387	1964.29	8.951	-4.345	1961.29
893	8.902	-4.370			458	8.903	-4.262	1964.37	8.943	-4.466	1961.38
894	8.915	-4.367			457	8.881	-4.467	1964.46	8.921	-4.667	1961.46
895	8.955	-4.135			456	8.880	-4.719	1964.54	8.891	-4.792	1961.54
896	8.968	-4.177			455	8.872	-4.493	1964.62	8.884	-4.717	1961.63
897	8.985	-4.133			454	8.867	-4.477	1964.70	8.864	-4.745	1961.71
898	9.050	-3.899			453	8.896	-4.403	1964.85	8.900	-4.655	1961.79
899	8.961	-4.093			452	8.909	-4.403	1964.99	8.899	-4.502	1961.88
900	9.010	-4.056			451	8.967	-4.240	1965.13	8.926	-4.348	1961.96
901	8.986	-4.360			450	8.932	-4.206	1965.23	8.960	-4.324	1962.04
902	8.968	-3.892			449	8.946	-4.249	1965.32	8.953	-4.194	1962.13
903	8.946	-4.306			448	8.918	-4.388	1965.42	8.956	-4.252	1962.21
904	8.924	-4.436			447	8.900	-4.641	1965.52	8.951	-4.357	1962.29
905	8.933	-4.291			446	8.888	-4.493	1965.61	8.909	-4.465	1962.38
906	8.973	-4.132			445	8.884	-4.567	1965.71	8.890	-4.542	1962.46
907	8.956	-4.104			444	8.901	-4.472	1965.80	8.881	-4.588	1962.54
908	8.980	-4.044			443	8.928	-4.468	1965.88	8.876	-4.510	1962.63
909	9.024	-3.830			442	8.939	-4.281	1965.97	8.874	-4.505	1962.71
910	9.010	-3.902			441	8.951	-4.177	1966.05	8.884	-4.542	1962.79
911	8.997	-3.900			440	8.958	-3.901	1966.15	8.921	-4.529	1962.88
912	8.968	-3.856			439	8.948	-4.078	1966.33	8.959	-4.250	1962.96
913	8.963	-3.840			438	8.914	-3.932	1966.51	8.998	-4.100	1963.04
914	8.873	-3.946			437	8.873	-4.315	1966.69	9.011	-4.105	1963.13
915	8.889	-4.106			436	8.887	-4.307	1966.77	9.001	-4.115	1963.21
916	8.879	-4.267			435	8.933	-4.424	1966.84	8.978	-4.074	1963.29
917	8.898	-4.296			434	8.942	-4.104	1966.91	8.950	-4.271	1963.38
918	8.929	-4.134			433	8.964	-4.197	1966.99	8.922	-4.371	1963.46
919	8.999	-3.956			432	8.967	-4.012	1967.06	8.921	-4.336	1963.54
920	8.957	-4.124			431	9.006	-4.060	1967.13	8.921	-4.257	1963.63
921	8.934	-4.053			430	8.976	-3.932	1967.25	8.886	-4.268	1963.71
922	8.971	-3.979			429	8.982	-4.429	1967.36	8.892	-4.534	1963.79
923	8.959	-3.967			428	8.931	-4.233	1967.47	8.915	-4.635	1963.88
924	8.905	-4.057			427	8.920	-4.578	1967.59	8.932	-4.252	1963.96
925	8.928	-4.361			426	8.881	-4.437	1967.70	8.945	-4.166	1964.04
926	8.901	-4.085			425	8.892	-4.646	1967.79	8.972	-4.289	1964.13
927	8.966	-4.043			424	8.901	-4.449	1967.88	8.945	-4.286	1964.21
928	8.977	-4.090			423	8.935	-4.147	1967.97	8.938	-4.387	1964.29
929	8.999	-3.957			422	9.001	-4.019	1968.05	8.903	-4.265	1964.38
930	9.014	-3.628			421	9.012	-3.971	1968.14	8.881	-4.478	1964.46
931	9.000	-3.819			420	8.982	-3.941	1968.25	8.880	-4.705	1964.54
932	8.975	-3.840			419	8.969	-4.132	1968.36	8.872	-4.492	1964.63
933	9.004	-3.742			418	8.939	-4.325	1968.47	8.868	-4.474	1964.71
934	8.987	-3.910			417	8.898	-4.355	1968.58	8.885	-4.431	1964.79
935	8.959	-3.891			416	8.864	-4.553	1968.69	8.899	-4.403	1964.88
936	8.918	-4.123			415	8.910	-4.381	1968.80	8.906	-4.403	1964.96
937	9.013	-4.238			414	8.905	-4.184	1968.91	8.931	-4.341	1965.04
938	8.942	-4.354			413	8.971	-4.053	1969.02	8.965	-4.246	1965.13
939	8.970	-4.039			412	9.002	-3.851	1969.13	8.939	-4.213	1965.21

LC3			Age Model		Linear interpolation				Monthly Resampling		
Sample ID	Sr/Ca (mmol/mol)	$\delta^{18}O$ (‰)	Sample ID	Time Pointer (year.month)	Sample ID	Sr/Ca (mmol/mol)	$\delta^{18}O$ (‰)	Age (year.month)	Sr/Ca (mmol/mol)	$\delta^{18}O$ (‰)	Age (year.month)
940	8.956	-4.069			411	8.959	-4.001	1969.27	8.941	-4.234	1965.29
941	8.967	-4.080			410	8.953	-4.216	1969.40	8.931	-4.322	1965.38
942	9.017	-4.014			409	8.920	-4.428	1969.53	8.911	-4.487	1965.46
943	9.030	-3.588			408	8.860	-4.457	1969.67	8.897	-4.603	1965.54
944	9.031	-3.725			407	8.867	-4.539	1969.77	8.888	-4.502	1965.63
945	9.000	-3.866			406	8.908	-4.420	1969.86	8.884	-4.566	1965.71
946	8.963	-3.555			405	8.928	-4.074	1969.95	8.900	-4.476	1965.79
947	8.964	-3.419			404	8.944	-4.118	1970.03	8.926	-4.468	1965.88
948	8.966	-4.046			403	8.961	-3.844	1970.12	8.938	-4.299	1965.96
949	8.916	-4.043			402	8.947	-3.940	1970.23	8.950	-4.190	1966.04
950	8.962	-4.008			401	8.937	-4.323	1970.35	8.956	-3.977	1966.13
951	9.042	-3.890			400	8.871	-4.519	1970.46	8.955	-3.956	1966.21
952	9.020	-4.103			399	8.866	-4.673	1970.57	8.950	-4.038	1966.29
953	8.974	-4.087			398	8.851	-4.523	1970.69	8.940	-4.044	1966.38
954	8.955	-4.085			397	8.873	-4.635	1970.77	8.924	-3.977	1966.46
955	8.976	-3.905			396	9.072	-3.701	1970.85	8.908	-3.992	1966.54
956	8.995	-3.715			395	9.015	-4.240	1970.93	8.889	-4.169	1966.63
957	8.970	-3.844			394	8.951	-4.258	1971.01	8.876	-4.313	1966.71
958	9.020	-3.864			393	8.988	-3.999	1971.09	8.902	-4.344	1966.79
959	8.970	-3.979			392	8.966	-4.206	1971.17	8.937	-4.276	1966.88
960	8.945	-3.829			391	8.975	-3.968	1971.25	8.955	-4.161	1966.96
961	8.930	-4.068			390	8.965	-4.191	1971.33	8.966	-4.058	1967.04
962	8.927	-4.061			389	8.912	-4.229	1971.40	9.002	-4.056	1967.13
963	8.970	-4.163			388	8.874	-4.284	1971.48	8.986	-3.973	1967.21
964	8.918	-4.165			387	8.892	-4.349	1971.56	8.978	-4.135	1967.29
965	8.975	-4.095			386	8.861	-4.400	1971.64	8.975	-4.403	1967.38
966	8.953	-4.129			385	8.848	-4.434	1971.72	8.938	-4.261	1967.46
967	8.990	-4.109			384	8.875	-4.461	1971.79	8.925	-4.436	1967.54
968	8.997	-3.990			383	8.892	-4.564	1971.86	8.908	-4.533	1967.63
969	8.948	-4.011			382	8.912	-4.420	1971.93	8.882	-4.448	1967.71
970	9.002	-3.861			381	8.917	-4.357	1972.00	8.892	-4.646	1967.79
971	8.992	-3.929			380	8.956	-4.179	1972.07	8.901	-4.457	1967.88
972	8.978	-4.010			379	8.928	-4.108	1972.14	8.932	-4.172	1967.96
973	8.923	-4.020			378	8.934	-4.201	1972.21	8.992	-4.035	1968.04
974	8.919	-3.982			377	8.948	-4.116	1972.28	9.010	-3.980	1968.13
975	8.928	-4.294			376	8.957	-4.095	1972.36	8.994	-3.953	1968.21
976	8.919	-4.273			375	8.930	-4.249	1972.43	8.977	-4.012	1968.29
977	8.969	-4.415			374	8.926	-4.183	1972.50	8.965	-4.157	1968.38
978	8.949	-4.177			373	8.925	-4.576	1972.57	8.943	-4.302	1968.46
979	9.016	-4.317			372	8.908	-4.481	1972.64	8.913	-4.344	1968.54
980	9.007	-4.139			371	8.885	-4.588	1972.71	8.885	-4.433	1968.63
981	8.977	-3.910			370	8.897	-4.272	1972.81	8.871	-4.527	1968.71
982	8.934	-3.938			369	8.916	-4.167	1972.90	8.906	-4.397	1968.79
983	8.991	-3.936			368	8.937	-4.053	1973.00	8.907	-4.250	1968.88
984	8.988	-4.026			367	8.952	-4.150	1973.10	8.933	-4.129	1968.96
985	8.966	-4.236			366	8.938	-4.076	1973.18	8.976	-4.018	1969.04
986	8.941	-4.192			365	8.948	-4.173	1973.25	9.000	-3.865	1969.13
987	8.935	-4.101			364	8.912	-4.222	1973.33	8.978	-3.936	1969.21
988	8.883	-4.247			363	8.928	-4.414	1973.40	8.958	-4.043	1969.29
989	8.926	-4.265			362	8.901	-4.268	1973.48	8.954	-4.176	1969.38
990	8.964	-4.351			361	8.897	-4.425	1973.56	8.938	-4.310	1969.46
991	8.945	-4.510			360	8.898	-4.605	1973.63	8.916	-4.430	1969.54
992	8.922	-4.172			359	8.877	-4.313	1973.71	8.879	-4.448	1969.63
993	8.938	-4.217			358	8.888	-4.288	1973.86	8.863	-4.490	1969.71
994	8.992	-4.322			357	8.929	-4.197	1974.01	8.877	-4.509	1969.79
995	8.922	-4.153			356	8.934	-4.065	1974.15	8.912	-4.351	1969.88
996	8.982	-4.072			355	8.928	-4.113	1974.24	8.930	-4.081	1969.96
997	8.992	-4.121			354	8.925	-4.170	1974.33	8.946	-4.090	1970.04
998	9.013	-4.041			353	8.886	-4.364	1974.42	8.960	-3.849	1970.13
999	8.981	-3.903			352	8.859	-4.500	1974.52	8.950	-3.919	1970.21
1000	8.980	-3.827			351	8.874	-4.644	1974.61	8.942	-4.138	1970.29
1001	8.966	-3.801			350	8.898	-4.525	1974.70	8.921	-4.372	1970.38
1002	8.974	-4.012			349	8.854	-4.416	1974.79	8.872	-4.515	1970.46
1003	8.912	-3.875			348	8.914	-4.289	1974.88	8.867	-4.628	1970.54
1004	8.893	-4.016			347	8.975	-4.186	1974.98	8.859	-4.607	1970.63
1005	8.897	-4.262			346	8.982	-4.352	1975.07	8.856	-4.550	1970.71
1006	8.910	-4.244			345	8.984	-4.442	1975.18	8.926	-4.387	1970.79
1007	8.919	-4.225			344	8.891	-4.531	1975.35	9.054	-3.874	1970.88
1008	8.939	-4.189			343	8.882	-4.452	1975.53	8.991	-4.247	1970.96
1009	8.959	-4.132			342	8.879	-4.373	1975.71	8.967	-4.150	1971.04
1010	8.965	-3.949			341	8.914	-4.329	1975.78	8.978	-4.097	1971.13
1011	8.998	-4.120			340	8.893	-4.284	1975.85	8.971	-4.080	1971.21
1012	9.060	-3.834			339	8.930	-4.271	1975.92	8.969	-4.098	1971.29
1013	8.988	-3.722			338	8.911	-4.257	1975.99	8.931	-4.215	1971.38
1014	9.000	-3.870			337	8.931	-4.164	1976.06	8.886	-4.267	1971.46
1015	8.984	-3.802			336	8.941	-4.252	1976.17	8.887	-4.332	1971.54
1016	8.986	-3.893			335	8.901	-4.341	1976.46	8.867	-4.389	1971.63
1017	8.967	-3.994			334	8.878	-4.071	1976.75	8.850	-4.429	1971.71
1018	8.919	-4.047			333	8.890	-4.323	1976.84	8.875	-4.462	1971.79

LC3			Age Model		Linear interpolation				Monthly Resampling		
Sample ID	Sr/Ca (mmol/mol)	$\delta^{18}O$ (‰)	Sample ID	Time Pointer (year.month)	Sample ID	Sr/Ca (mmol/mol)	$\delta^{18}O$ (‰)	Age (year.month)	Sr/Ca (mmol/mol)	$\delta^{18}O$ (‰)	Age (year.month)
1019	8.925	-4.172			332	8.900	-4.304	1976.91	8.896	-4.535	1971.88
1020	8.870	-4.295			331	8.892	-4.237	1976.97	8.914	-4.396	1971.96
1021	8.893	-4.366			330	8.943	-4.058	1977.03	8.939	-4.257	1972.04
1022	8.889	-4.241			329	8.963	-4.028	1977.10	8.935	-4.126	1972.13
1023	8.908	-4.131			328	8.932	-4.167	1977.21	8.934	-4.194	1972.21
1024	8.936	-4.248			327	8.923	-3.880	1977.31	8.949	-4.114	1972.29
1025	9.009	-3.991			326	8.884	-4.466	1977.42	8.949	-4.139	1972.38
1026	9.006	-4.043			325	8.881	-4.521	1977.53	8.928	-4.218	1972.46
1027	8.922	-3.962			324	8.856	-4.405	1977.64	8.925	-4.438	1972.54
1028	8.941	-4.029			323	8.888	-4.288	1977.88	8.911	-4.497	1972.63
1029	8.940	-3.930			322	8.937	-4.163	1978.11	8.885	-4.586	1972.71
1030	8.932	-3.883			321	8.932	-4.372	1978.27	8.895	-4.314	1972.79
1031	8.934	-4.097			320	8.905	-4.425	1978.41	8.911	-4.197	1972.88
1032	8.919	-4.105			319	8.884	-4.479	1978.55	8.928	-4.102	1972.96
1033	9.007	-4.170			318	8.847	-4.181	1978.68	8.943	-4.095	1973.04
1034	8.880	-4.449			317	8.876	-3.862	1978.85	8.947	-4.124	1973.13
1035	8.906	-4.362			316	8.912	-4.218	1979.01	8.942	-4.116	1973.21
1036	8.875	-4.368			315	8.928	-4.103	1979.18	8.929	-4.198	1973.29
1037	8.896	-4.345			314	8.923	-4.283	1979.36	8.922	-4.339	1973.38
1038	8.944	-4.375			313	8.888	-4.349	1979.53	8.909	-4.310	1973.46
1039	8.949	-4.106			312	8.834	-4.384	1979.71	8.898	-4.396	1973.54
1040	8.961	-4.007			311	8.835	-4.361	1979.77	8.898	-4.589	1973.63
1041	8.955	-3.943			310	8.857	-4.378	1979.83	8.877	-4.313	1973.71
1042	8.975	-3.937			309	8.839	-4.300	1979.89	8.883	-4.299	1973.79
1043	8.976	-3.917			308	8.911	-4.179	1979.95	8.892	-4.278	1973.88
1044	8.966	-3.913			307	8.928	-4.224	1980.01	8.915	-4.228	1973.96
1045	8.989	-3.659			306	8.935	-4.284	1980.07	8.930	-4.167	1974.04
1046	8.948	-3.739			305	8.952	-4.270	1980.20	8.933	-4.087	1974.13
1047	8.978	-3.898			304	8.842	-4.332	1980.66	8.930	-4.097	1974.21
1048	8.923	-4.024			303	8.855	-4.504	1980.75	8.926	-4.145	1974.29
1049	8.915	-4.071			302	8.869	-4.545	1980.83	8.907	-4.261	1974.38
1050	8.937	-4.049			301	8.899	-4.525	1980.90	8.876	-4.415	1974.46
1051	8.938	-4.189			300	8.938	-4.359	1980.98	8.863	-4.541	1974.54
1052	8.950	-4.155			299	9.020	-4.152	1981.05	8.879	-4.622	1974.63
1053	8.875	-4.285			298	8.924	-4.242	1981.22	8.894	-4.515	1974.71
1054	8.943	-4.238			297	8.893	-4.471	1981.38	8.854	-4.416	1974.79
1055	8.933	-4.201			296	8.863	-4.509	1981.55	8.908	-4.301	1974.88
1056	8.925	-4.271			295	8.832	-4.797	1981.71	8.963	-4.205	1974.96
1057	8.966	-4.059			294	8.852	-4.416	1981.79	8.980	-4.305	1975.04
1058	9.001	-4.067			293	8.878	-4.291	1981.88	8.983	-4.388	1975.13
1059	9.002	-4.059			292	8.903	-4.180	1981.96	8.967	-4.440	1975.21
1060	8.955	-4.053			291	8.950	-3.966	1982.05	8.923	-4.493	1975.29
1061	8.982	-4.051			290	8.945	-4.230	1982.19	8.890	-4.521	1975.38
1062	8.973	-4.067			289	8.925	-4.353	1982.33	8.886	-4.484	1975.46
1063	8.942	-4.036			288	8.859	-4.391	1982.48	8.882	-4.447	1975.54
1064	8.943	-3.990			287	8.841	-4.699	1982.62	8.880	-4.410	1975.63
1065	8.947	-4.113			286	8.847	-4.484	1982.72	8.879	-4.373	1975.71
1066	8.952	-4.160			285	8.864	-4.312	1982.82	8.910	-4.321	1975.79
1067	8.918	-4.175			284	8.865	-4.309	1982.91	8.906	-4.279	1975.88
1068	9.010	-4.076			283	8.885	-4.338	1983.00	8.920	-4.264	1975.96
1069	8.952	-4.277			282	8.936	-4.262	1983.10	8.925	-4.266	1976.04
1070	8.977	-4.015			281	8.939	-4.255	1983.19	8.937	-4.281	1976.13
1071	8.976	-3.960			280	8.921	-4.267	1983.28	8.935	-4.296	1976.21
1072	8.980	-4.032			279	8.900	-4.378	1983.37	8.924	-4.311	1976.29
1073	8.999	-4.261			278	8.871	-4.431	1983.46	8.912	-4.326	1976.38
1074	9.000	-4.122			277	8.875	-4.510	1983.55	8.901	-4.339	1976.46
1075	9.010	-3.946			276	8.898	-4.510	1983.64	8.894	-4.262	1976.54
1076	8.943	-3.794			275	8.881	-4.178	1983.81	8.888	-4.185	1976.63
1077	9.008	-3.870			274	8.899	-4.332	1983.98	8.881	-4.107	1976.71
1078	8.985	-3.936			273	8.936	-4.199	1984.15	8.883	-4.187	1976.79
1079	9.012	-4.031			272	8.935	-4.004	1984.27	8.895	-4.314	1976.88
1080	9.027	-3.574			271	8.915	-4.228	1984.37	8.893	-4.249	1976.96
1081	9.019	-3.741			270	8.873	-4.509	1984.47	8.946	-4.054	1977.04
1082	8.994	-3.830			269	8.866	-4.181	1984.57	8.955	-4.065	1977.13
1083	8.974	-3.952			268	8.880	-4.474	1984.67	8.932	-4.157	1977.21
1084	8.999	-3.950			267	8.860	-4.087	1984.77	8.925	-3.940	1977.29
1085	8.994	-3.785			266	8.878	-4.183	1984.86	8.901	-4.204	1977.38
1086	9.018	-3.943			265	8.936	-4.161	1984.96	8.883	-4.483	1977.46
1087	9.019	-3.970			264	8.960	-4.146	1985.05	8.879	-4.516	1977.54
1088	9.050	-4.030			263	8.966	-4.181	1985.15	8.860	-4.459	1977.63
1089	9.049	-4.040			262	8.936	-4.228	1985.28	8.865	-4.402	1977.71
1090	9.032	-4.029			261	8.899	-4.385	1985.41	8.877	-4.345	1977.79
1091	9.037	-3.991			260	8.889	-4.508	1985.54	8.888	-4.288	1977.88
1092	9.000	-3.872			259	8.937	-4.182	1985.67	8.906	-4.243	1977.96
1093	8.979	-3.947			258	8.911	-4.202	1985.77	8.923	-4.198	1978.04
1094	8.908	-3.982			257	8.925	-4.016	1985.87	8.936	-4.186	1978.13
1095	8.945	-4.009			256	8.935	-3.953	1985.97	8.934	-4.292	1978.21
1096	8.971	-3.907			255	8.944	-3.846	1986.07	8.928	-4.380	1978.29
1097	8.953	-4.098			254	8.983	-4.022	1986.17	8.912	-4.412	1978.38

LC3			Age Model		Linear interpolation				Monthly Resampling		
Sample ID	Sr/Ca (mmol/mol)	$\delta^{18}O$ (‰)	Sample ID	Time Pointer (year.month)	Sample ID	Sr/Ca (mmol/mol)	$\delta^{18}O$ (‰)	Age (year.month)	Sr/Ca (mmol/mol)	$\delta^{18}O$ (‰)	Age (year.month)
1098	8.962	-4.169			253	8.900	-4.189	1986.35	8.897	-4.445	1978.46
1099	8.992	-4.239			252	8.878	-4.329	1986.52	8.885	-4.477	1978.54
1100	8.987	-4.132			251	8.859	-4.451	1986.70	8.863	-4.306	1978.63
1101	9.003	-3.906			250	8.921	-4.481	1986.78	8.852	-4.131	1978.71
1102	9.011	-4.023			249	8.842	-4.274	1986.86	8.866	-3.970	1978.79
1103	9.035	-3.862			248	8.873	-4.537	1986.94	8.882	-3.921	1978.88
1104	9.025	-3.948			247	8.912	-4.187	1987.02	8.900	-4.099	1978.96
1105	8.997	-3.939			246	8.923	-4.262	1987.10	8.915	-4.199	1979.04
1106	9.038	-3.783			245	8.945	-4.126	1987.18	8.923	-4.141	1979.13
1107	8.994	-3.836			244	8.940	-4.327	1987.30	8.927	-4.132	1979.21
1108	9.011	-3.895			243	8.880	-4.261	1987.42	8.925	-4.218	1979.29
1109	8.991	-4.037			242	8.878	-4.462	1987.53	8.919	-4.291	1979.38
1110	8.972	-4.033			241	8.844	-4.607	1987.65	8.902	-4.322	1979.46
1111	8.945	-3.853			240	8.840	-4.616	1987.75	8.885	-4.351	1979.54
1112	8.964	-4.001			239	8.874	-4.268	1987.83	8.859	-4.368	1979.63
1113	8.937	-4.124			238	8.891	-4.304	1987.91	8.834	-4.384	1979.71
1114	8.996	-4.030			237	8.925	-4.282	1987.99	8.843	-4.368	1979.79
1115	8.945	-4.274			236	8.919	-4.080	1988.07	8.843	-4.319	1979.88
1116	8.970	-4.132			235	8.934	-4.055	1988.16	8.913	-4.185	1979.96
1117	8.996	-4.011			234	8.896	-4.227	1988.29	8.932	-4.254	1980.04
1118	9.025	-3.994			233	8.871	-4.517	1988.43	8.942	-4.278	1980.13
1119	9.050	-3.962			232	8.862	-4.315	1988.57	8.949	-4.272	1980.21
1120	8.964	-3.917			231	8.851	-4.376	1988.71	8.929	-4.283	1980.29
1121	9.045	-3.875			230	8.871	-4.387	1988.88	8.910	-4.294	1980.38
1122	9.032	-3.873			229	8.893	-4.136	1989.06	8.890	-4.305	1980.46
1123	9.018	-3.795			228	8.913	-4.378	1989.22	8.870	-4.316	1980.54
1124	9.075	-3.720			227	8.892	-4.332	1989.33	8.850	-4.327	1980.63
1125	9.052	-3.756			226	8.880	-4.364	1989.44	8.849	-4.420	1980.71
1126	9.011	-4.022			225	8.865	-4.482	1989.54	8.862	-4.525	1980.79
1127	9.020	-4.029			224	8.841	-4.574	1989.65	8.888	-4.533	1980.88
1128	9.003	-4.086			223	8.854	-4.404	1989.76	8.928	-4.402	1980.96
1129	9.035	-3.840			222	8.861	-4.535	1989.86	9.007	-4.185	1981.04
1130	9.066	-3.945			221	8.868	-4.254	1989.97	8.978	-4.191	1981.13
1131	9.026	-3.926			220	8.912	-4.136	1990.08	8.930	-4.237	1981.21
1132	9.032	-3.792			219	8.980	-4.093	1990.18	8.910	-4.345	1981.29
1133	9.012	-3.852			218	8.945	-4.269	1990.29	8.894	-4.462	1981.38
1134	9.036	-3.827			217	8.932	-4.192	1990.39	8.879	-4.489	1981.46
1135	9.015	-3.985			216	8.908	-4.440	1990.50	8.864	-4.508	1981.54
1136	9.013	-3.903			215	8.871	-4.520	1990.60	8.848	-4.651	1981.63
1137	9.047	-3.904			214	8.854	-4.621	1990.71	8.832	-4.790	1981.71
1138	9.023	-3.959			213	8.866	-4.567	1990.81	8.852	-4.416	1981.79
1139	9.005	-4.200			212	8.887	-4.283	1990.91	8.878	-4.292	1981.88
1140	8.968	-4.337			211	8.911	-4.327	1991.00	8.902	-4.183	1981.96
1141	8.977	-3.942			210	8.924	-4.288	1991.10	8.948	-3.976	1982.04
1142	8.954	-4.170			209	8.922	-4.189	1991.22	8.947	-4.112	1982.13
1143	8.977	-4.228			208	8.915	-4.373	1991.34	8.942	-4.247	1982.21
1144	8.985	-4.121			207	8.882	-4.682	1991.46	8.931	-4.319	1982.29
1145	9.021	-3.939			206	8.870	-4.528	1991.58	8.905	-4.364	1982.38
1146	8.974	-3.984			205	8.889	-4.468	1991.70	8.867	-4.386	1982.46
1147	8.999	-3.897			204	8.869	-4.435	1991.81	8.851	-4.533	1982.54
1148	9.000	-3.875			203	8.931	-4.295	1991.91	8.841	-4.686	1982.63
1149	8.969	-4.069			202	8.955	-4.111	1992.02	8.846	-4.515	1982.71
1150	8.991	-3.977			201	8.987	-4.273	1992.13	8.859	-4.360	1982.79
1151	8.998	-3.881			200	8.928	-4.384	1992.27	8.865	-4.310	1982.88
1152	9.024	-3.967			199	8.911	-4.224	1992.41	8.875	-4.324	1982.96
1153	8.994	-4.170			198	8.864	-4.518	1992.55	8.905	-4.308	1983.04
1154	8.943	-4.234			197	8.895	-4.519	1992.69	8.937	-4.260	1983.13
1155	8.980	-4.026			196	8.892	-4.407	1992.78	8.935	-4.258	1983.21
1156	8.974	-4.123			195	8.887	-4.358	1992.88	8.918	-4.283	1983.29
1157	8.986	-4.116			194	8.908	-4.294	1992.97	8.898	-4.382	1983.38
1158	8.974	-3.943			193	8.940	-4.189	1993.07	8.871	-4.432	1983.46
1159	8.986	-4.051			192	8.950	-4.139	1993.16	8.875	-4.506	1983.54
1160	8.976	-4.131			191	8.952	-4.338	1993.26	8.894	-4.510	1983.63
1161	8.999	-4.032			190	8.914	-4.252	1993.35	8.891	-4.382	1983.71
1162	8.988	-4.114			189	8.923	-4.382	1993.44	8.883	-4.219	1983.79
1163	9.007	-4.057			188	8.954	-4.484	1993.53	8.888	-4.234	1983.88
1164	8.984	-4.022			187	8.925	-4.272	1993.62	8.896	-4.310	1983.96
1165	9.007	-3.993			186	8.884	-4.060	1993.71	8.912	-4.286	1984.04
1166	8.985	-3.971			185	8.934	-4.236	1993.90	8.930	-4.221	1984.13
1167	8.982	-4.030			184	8.963	-3.969	1994.10	8.936	-4.106	1984.21
1168	8.966	-3.965			183	8.957	-4.012	1994.21	8.931	-4.053	1984.29
1169	9.029	-4.038			182	8.938	-4.083	1994.32	8.913	-4.240	1984.38
1170	9.019	-4.062			181	8.912	-4.236	1994.42	8.879	-4.470	1984.46
1171	9.005	-4.012			180	8.919	-4.342	1994.53	8.868	-4.285	1984.54
1172	9.081	-3.834			179	8.895	-4.111	1994.63	8.873	-4.331	1984.63
1173	9.055	-3.837			178	8.916	-4.132	1994.76	8.873	-4.331	1984.71
1174	9.054	-3.903			177	8.911	-4.218	1994.89	8.865	-4.112	1984.79
1175	9.090	-3.817			176	8.912	-4.225	1995.02	8.886	-4.180	1984.88
1176	9.065	-3.676			175	8.920	-4.092	1995.15	8.937	-4.161	1984.96

LC3			Age Model		Linear interpolation				Monthly Resampling		
Sample ID	Sr/Ca (mmol/mol)	$\delta^{18}O$ (‰)	Sample ID	Time Pointer (year.month)	Sample ID	Sr/Ca (mmol/mol)	$\delta^{18}O$ (‰)	Age (year.month)	Sr/Ca (mmol/mol)	$\delta^{18}O$ (‰)	Age (year.month)
1177	9.028	-4.214			174	8.866	-4.234	1995.33	8.958	-4.147	1985.04
1178	9.023	-4.222			173	8.852	-4.441	1995.51	8.965	-4.173	1985.13
1179	9.001	-4.260			172	8.863	-4.367	1995.69	8.952	-4.203	1985.21
1180	9.046	-4.209			171	8.846	-4.174	1995.84	8.932	-4.244	1985.29
1181	8.988	-4.307			170	8.928	-3.939	1995.99	8.909	-4.344	1985.38
1182	8.991	-4.225			169	8.953	-4.099	1996.14	8.895	-4.432	1985.46
1183	8.965	-4.231			168	8.925	-4.039	1996.23	8.890	-4.503	1985.54
1184	8.987	-4.333			167	8.904	-4.166	1996.33	8.920	-4.294	1985.63
1185	9.033	-3.992			166	8.898	-4.357	1996.42	8.927	-4.190	1985.71
1186	9.009	-3.892			165	8.944	-4.475	1996.52	8.914	-4.165	1985.79
1187	8.996	-4.162			164	8.867	-4.648	1996.61	8.925	-4.014	1985.88
1188	8.972	-4.019			163	8.847	-4.574	1996.71	8.934	-3.962	1985.96
1189	8.988	-4.047			162	8.894	-4.512	1996.81	8.941	-3.879	1986.04
1190	8.971	-3.971			161	8.922	-3.880	1996.92	8.964	-3.938	1986.13
1191	8.974	-4.149			160	8.943	-4.172	1997.02	8.966	-4.056	1986.21
1192	8.962	-4.087			159	8.979	-3.958	1997.13	8.927	-4.135	1986.29
1193	8.967	-4.170			158	8.961	-4.127	1997.23	8.897	-4.210	1986.38
1194	8.947	-4.267			157	8.932	-4.347	1997.32	8.886	-4.276	1986.46
1195	8.966	-4.276			156	8.977	-4.506	1997.42	8.876	-4.341	1986.54
1196	8.985	-4.068			155	8.922	-4.282	1997.51	8.867	-4.399	1986.63
1197	9.066	-3.902			154	8.946	-4.333	1997.61	8.866	-4.454	1986.71
1198	9.017	-3.747			153	8.914	-4.161	1997.70	8.909	-4.450	1986.79
1199	8.935	-4.262			152	8.985	-4.052	1997.77	8.848	-4.325	1986.88
1200	8.953	-4.242			151	8.977	-4.023	1997.84	8.882	-4.451	1986.96
1201	9.009	-4.041			150	8.944	-4.007	1997.91	8.915	-4.209	1987.04
1202	8.950	-4.002			149	8.940	-4.399	1997.98	8.930	-4.217	1987.13
1203	8.972	-3.972			148	8.974	-4.274	1998.05	8.944	-4.177	1987.21
1204	8.971	-3.959			147	8.968	-4.280	1998.12	8.940	-4.318	1987.29
1205	8.990	-3.928			146	8.959	-4.167	1998.19	8.900	-4.283	1987.38
1206	8.991	-4.131			145	8.958	-4.054	1998.23	8.879	-4.335	1987.46
1207	9.003	-4.128			144	8.961	-3.988	1998.28	8.876	-4.473	1987.54
1208	9.049	-3.990			143	8.941	-4.029	1998.32	8.852	-4.575	1987.63
1209	8.987	-4.271			142	8.956	-3.835	1998.37	8.842	-4.612	1987.71
1210	8.975	-4.055			141	8.968	-4.125	1998.41	8.858	-4.431	1987.79
1211	8.998	-4.149			140	8.943	-4.188	1998.46	8.883	-4.288	1987.88
1212	9.006	-4.149			139	8.932	-4.295	1998.50	8.911	-4.291	1987.96
1213	9.044	-3.851			138	8.955	-4.402	1998.55	8.921	-4.161	1988.04
1214	9.001	-4.035			137	8.906	-4.220	1998.59	8.928	-4.064	1988.13
1215	8.987	-3.819			136	8.890	-4.001	1998.65	8.919	-4.122	1988.21
1216	8.999	-3.923			135	8.923	-3.931	1998.77	8.896	-4.227	1988.29
1217	9.039	-3.749			134	8.916	-3.803	1998.89	8.881	-4.401	1988.38
1218	9.013	-3.930			133	8.944	-3.814	1999.00	8.869	-4.477	1988.46
1219	8.977	-4.050			132	8.960	-3.914	1999.12	8.864	-4.355	1988.54
1220	8.966	-4.034			131	8.948	-4.100	1999.25	8.858	-4.340	1988.63
1221	8.973	-4.196			130	8.922	-4.151	1999.38	8.851	-4.376	1988.71
1222	8.962	-4.181			129	8.864	-4.569	1999.51	8.861	-4.381	1988.79
1223	8.943	-4.203			128	8.895	-4.371	1999.64	8.870	-4.387	1988.88
1224	8.967	-4.140			127	8.901	-4.401	1999.74	8.880	-4.278	1988.96
1225	8.988	-4.104			126	8.873	-4.204	1999.82	8.891	-4.159	1989.04
1226	8.980	-3.948			125	8.907	-4.033	1999.90	8.901	-4.235	1989.13
1227	8.996	-3.870			124	8.949	-3.966	1999.98	8.911	-4.358	1989.21
1228	8.941	-3.965			123	8.939	-3.954	2000.06	8.899	-4.348	1989.29
1229	8.980	-3.869			122	8.975	-4.069	2000.14	8.887	-4.346	1989.38
1230	9.006	-3.812			121	8.966	-4.047	2000.28	8.877	-4.390	1989.46
1231	8.985	-3.871			120	8.950	-4.137	2000.42	8.865	-4.482	1989.54
1232	8.957	-3.994			119	8.868	-4.217	2000.56	8.846	-4.554	1989.63
1233	8.954	-4.177			118	8.869	-4.294	2000.70	8.848	-4.478	1989.71
1234	8.974	-4.078			117	8.882	-4.117	2000.84	8.856	-4.449	1989.79
1235	8.951	-4.412			116	8.897	-4.139	2000.98	8.862	-4.500	1989.88
1236	8.944	-4.188			115	8.940	-4.015	2001.12	8.867	-4.279	1989.96
1237	8.929	-4.309			114	8.938	-4.069	2001.22	8.898	-4.172	1990.04
1238	8.914	-4.409			113	8.914	-4.009	2001.31	8.944	-4.116	1990.13
1239	8.946	-4.157			112	8.900	-4.094	2001.41	8.971	-4.138	1990.21
1240	8.999	-4.140			111	8.842	-4.322	2001.50	8.944	-4.265	1990.29
1241	8.952	-4.340			110	8.832	-4.363	2001.60	8.934	-4.204	1990.38
1242	8.966	-4.184			109	8.843	-4.426	2001.69	8.917	-4.348	1990.46
1243	9.000	-3.941			108	8.823	-4.397	2001.78	8.892	-4.474	1990.54
1244	9.024	-3.770			107	8.872	-4.229	2001.87	8.867	-4.541	1990.63
1245	9.046	-3.870			106	8.931	-4.073	2001.96	8.854	-4.621	1990.71
1246	9.017	-3.972			105	8.924	-4.222	2002.05	8.864	-4.575	1990.79
1247	8.958	-3.864			104	8.903	-4.164	2002.14	8.880	-4.371	1990.88
1248	8.943	-4.052			103	8.942	-4.477	2002.26	8.900	-4.306	1990.96
1249	8.950	-4.072			102	8.905	-4.430	2002.37	8.916	-4.312	1991.04
1250	8.926	-4.412			101	8.874	-4.364	2002.48	8.924	-4.270	1991.13
1251	8.950	-4.383			100	8.849	-4.391	2002.59	8.922	-4.199	1991.21
1252	8.956	-4.379			99	8.833	-4.534	2002.70	8.918	-4.298	1991.29
1253	8.991	-4.296			98	8.848	-4.421	2002.81	8.906	-4.458	1991.38
1254	9.013	-4.064			97	8.887	-4.166	2002.92	8.883	-4.671	1991.46
1255	9.001	-3.980			96	8.895	-4.145	2003.04	8.874	-4.581	1991.54

LC3			Age Model		Linear interpolation				Monthly Resampling		
Sample ID	Sr/Ca (mmol/mol)	$\delta^{18}O$ (‰)	Sample ID	Time Pointer (year.month)	Sample ID	Sr/Ca (mmol/mol)	$\delta^{18}O$ (‰)	Age (year.month)	Sr/Ca (mmol/mol)	$\delta^{18}O$ (‰)	Age (year.month)
1256	9.028	-3.920			95	8.904	-4.334	2003.14	8.877	-4.507	1991.63
1257	9.044	-3.846			94	8.882	-4.173	2003.22	8.888	-4.466	1991.71
1258	9.012	-3.899			93	8.896	-4.261	2003.30	8.872	-4.440	1991.79
1259	9.006	-3.820			92	8.888	-3.657	2003.38	8.908	-4.347	1991.88
1260	8.981	-4.031			91	8.879	-4.410	2003.46	8.941	-4.217	1991.96
1261	8.963	-3.858			90	8.863	-4.420	2003.54	8.962	-4.146	1992.04
1262	8.952	-4.082			89	8.854	-3.471	2003.62	8.987	-4.272	1992.13
1263	8.929	-4.013			88	8.840	-4.281	2003.70	8.952	-4.339	1992.21
1264	8.937	-4.040			87	8.867	-4.100	2003.84	8.925	-4.354	1992.29
1265	8.943	-4.200			86	8.894	-3.962	2003.98	8.915	-4.259	1992.38
1266	8.931	-4.330			85	8.900	-4.032	2004.12	8.893	-4.335	1992.46
1267	8.947	-4.237			84	8.876	-4.072	2004.27	8.865	-4.510	1992.54
1268	8.965	-3.990			83	8.860	-4.196	2004.42	8.881	-4.519	1992.63
1269	8.973	-4.219			82	8.847	-4.193	2004.56	8.894	-4.492	1992.71
1270	8.968	-4.114			81	8.830	-4.397	2004.71	8.891	-4.401	1992.79
1271	8.979	-3.971			80	8.859	-4.080	2004.81	8.887	-4.359	1992.88
1272	9.006	-3.916			79	8.843	-4.016	2004.92	8.905	-4.303	1992.96
1273	8.999	-3.846			78	8.888	-4.070	2005.02	8.932	-4.217	1993.04
1274	8.971	-3.991			77	8.922	-4.040	2005.12	8.946	-4.158	1993.13
1275	8.996	-3.851			76	8.909	-4.024	2005.24	8.951	-4.239	1993.21
1276	8.975	-3.826			75	8.890	-4.191	2005.36	8.937	-4.303	1993.29
1277	8.941	-3.952			74	8.847	-4.152	2005.47	8.917	-4.293	1993.38
1278	8.956	-3.988			73	8.852	-4.321	2005.59	8.930	-4.405	1993.46
1279	8.962	-4.203			72	8.807	-4.566	2005.71	8.950	-4.454	1993.54
1280	8.992	-4.118			71	8.821	-4.450	2005.78	8.923	-4.260	1993.63
1281	8.966	-4.037			70	8.837	-4.441	2005.85	8.885	-4.068	1993.71
1282	8.920	-4.251			69	8.812	-4.421	2005.92	8.905	-4.134	1993.79
1283	8.939	-4.132			68	8.857	-4.349	2005.99	8.927	-4.211	1993.88
1284	8.925	-4.127			67	8.888	-4.175	2006.06	8.942	-4.159	1993.96
1285	8.955	-3.955			66	8.905	-4.032	2006.13	8.955	-4.043	1994.04
1286	8.969	-4.002			65	8.895	-4.087	2006.23	8.961	-3.980	1994.13
1287	8.957	-3.964			64	8.855	-4.096	2006.34	8.957	-4.011	1994.21
1288	8.964	-4.080			63	8.870	-4.444	2006.44	8.942	-4.067	1994.29
1289	8.963	-4.017			62	8.851	-4.486	2006.54	8.923	-4.169	1994.38
1290	8.928	-4.147			61	8.834	-4.629	2006.65	8.914	-4.273	1994.46
1291	8.886	-4.302			60	8.835	-4.539	2006.72	8.916	-4.309	1994.54
1292	8.956	-4.383			59	8.869	-4.570	2006.78	8.897	-4.128	1994.63
1293	9.005	-4.342			58	8.839	-4.382	2006.84	8.907	-4.123	1994.71
1294	9.030	-4.136			57	8.851	-4.386	2006.90	8.915	-4.152	1994.79
1295	9.049	-4.068			56	8.861	-4.339	2006.96	8.912	-4.208	1994.88
1296	9.100	-4.021			55	8.887	-4.286	2007.03	8.912	-4.222	1994.96
1297	9.020	-3.998			54	8.912	-4.272	2007.09	8.913	-4.203	1995.04
1298	9.007	-4.271			53	8.916	-4.183	2007.15	8.918	-4.121	1995.13
1299	8.973	-3.990			52	8.931	-4.125	2007.21	8.904	-4.134	1995.21
1300	8.945	-4.148			51	8.917	-4.232	2007.33	8.879	-4.200	1995.29
1301	9.016	-3.917			50	8.897	-4.331	2007.46	8.863	-4.281	1995.38
1302	8.941	-3.964			49	8.873	-4.389	2007.58	8.856	-4.377	1995.46
1303	8.938	-3.986			48	8.846	-4.357	2007.71	8.854	-4.429	1995.54
1304	8.927	-4.345			47	8.868	-4.296	2007.77	8.859	-4.395	1995.63
1305	8.919	-4.379			46	8.903	-4.354	2007.82	8.861	-4.348	1995.71
1306	8.943	-4.311			45	8.882	-4.316	2007.88	8.852	-4.241	1995.79
1307	8.949	-4.313			44	8.894	-4.084	2007.94	8.863	-4.125	1995.88
1308	8.996	-4.162			43	8.899	-4.115	2007.99	8.909	-3.994	1995.96
1309	8.999	-4.027			42	8.885	-4.094	2008.05	8.936	-3.992	1996.04
1310	9.012	-3.916			41	8.921	-3.989	2008.11	8.951	-4.084	1996.13
1311	9.023	-3.940			40	8.896	-4.129	2008.19	8.932	-4.055	1996.21
1312	9.023	-4.041			39	8.897	-3.867	2008.28	8.912	-4.119	1996.29
1313	8.992	-3.946			38	8.898	-4.262	2008.36	8.901	-4.263	1996.38
1314	8.957	-3.768			37	8.922	-4.225	2008.44	8.916	-4.403	1996.46
1315	8.934	-3.963			36	8.898	-4.274	2008.53	8.923	-4.522	1996.54
1316	8.926	-4.088			35	8.889	-4.233	2008.61	8.864	-4.637	1996.63
1317	8.937	-4.189			34	8.844	-4.269	2008.72	8.849	-4.572	1996.71
1318	8.914	-4.080			33	8.998	-4.252	2009.15	8.885	-4.523	1996.79
1319	8.971	-4.189			32	8.900	-4.063	2009.22	8.911	-4.132	1996.88
1320	8.978	-3.989			31	8.910	-4.214	2009.29	8.930	-3.991	1996.96
1321	8.984	-4.005			30	8.918	-4.087	2009.36	8.949	-4.138	1997.04
1322	9.020	-4.213			29	8.907	-4.179	2009.43	8.977	-3.969	1997.13
1323	9.033	-3.918			28	8.929	-4.208	2009.50	8.964	-4.096	1997.21
1324	9.016	-3.910			27	8.869	-4.868	2009.57	8.941	-4.278	1997.29
1325	9.007	-3.862			26	8.845	-4.386	2009.64	8.957	-4.436	1997.38
1326	8.991	-3.852			25	8.882	-4.571	2009.71	8.953	-4.408	1997.46
1327	8.967	-3.833			24	8.845	-4.646	2009.81	8.929	-4.298	1997.54
1328	8.977	-3.884			23	8.961	-4.326	2009.91	8.940	-4.302	1997.63
1329	8.927	-3.968			22	8.886	-4.242	2010.01	8.920	-4.152	1997.71
1330	8.926	-4.262			21	9.043	-4.289	2010.11	8.983	-4.045	1997.79
1331	8.961	-4.197			20	8.968	-4.017	2010.31	8.962	-4.016	1997.88
1332	8.973	-4.235			19	8.923	-4.345	2010.51	8.941	-4.257	1997.96
1333	8.957	-4.101			18	8.898	-4.419	2010.71	8.968	-4.295	1998.04
1334	8.996	-3.990			17	8.967	-4.078	2010.78	8.968	-4.277	1998.13

LC3			Age Model		Linear interpolation				Monthly Resampling		
Sample ID	Sr/Ca (mmol/mol)	$\delta^{18}O$ (‰)	Sample ID	Time Pointer (year.month)	Sample ID	Sr/Ca (mmol/mol)	$\delta^{18}O$ (‰)	Age (year.month)	Sr/Ca (mmol/mol)	$\delta^{18}O$ (‰)	Age (year.month)
1335	9.008	-4.101			16	8.902	-4.334	2010.85	8.959	-4.103	1998.21
1336	9.026	-3.971			15	8.989	-4.241	2010.91	8.954	-4.002	1998.29
1337	9.030	-3.836			14	8.944	-4.199	2010.98	8.958	-3.889	1998.38
1338	9.023	-4.043			13	8.926	-4.140	2011.05	8.943	-4.192	1998.46
1339	9.019	-3.787			12	8.973	-3.932	2011.12	8.952	-4.390	1998.54
1340	9.001	-3.877			11	8.937	-4.312	2011.21	8.897	-4.098	1998.63
1341	8.979	-3.837			10	8.931	-4.469	2011.30	8.906	-3.967	1998.71
1342	8.939	-3.897			9	8.877	-4.444	2011.39	8.922	-3.907	1998.79
1343	8.952	-4.227			8	8.859	-4.818	2011.49	8.917	-3.816	1998.88
1344	8.976	-4.223			7	8.827	-4.809	2011.58	8.933	-3.810	1998.96
1345	8.979	-4.177			6	8.872	-4.242	2011.67	8.949	-3.846	1999.04
1346	9.009	-3.951			5	8.826	-4.621	2011.85	8.960	-3.919	1999.13
1347	9.031	-3.848			4	8.919	-4.005	2012.03	8.952	-4.038	1999.21
1348	9.021	-3.743			3	8.886	-4.035	2012.21	8.940	-4.116	1999.29
1349	9.036	-3.936			2	8.900	-4.288	2012.39	8.923	-4.148	1999.38
1350	9.006	-3.777			1	8.878	-4.372	2012.58	8.888	-4.394	1999.46
									8.871	-4.525	1999.54
									8.891	-4.398	1999.63
									8.899	-4.390	1999.71
									8.884	-4.282	1999.79
									8.896	-4.089	1999.88
									8.938	-3.983	1999.96
									8.941	-3.956	2000.04
									8.970	-4.053	2000.13
									8.970	-4.058	2000.21
									8.964	-4.057	2000.29
									8.955	-4.110	2000.38
									8.926	-4.160	2000.46
									8.878	-4.208	2000.54
									8.868	-4.254	2000.63
									8.870	-4.282	2000.71
									8.878	-4.177	2000.79
									8.886	-4.123	2000.88
									8.895	-4.136	2000.96
									8.916	-4.085	2001.04
									8.940	-4.018	2001.13
									8.938	-4.065	2001.21
									8.919	-4.022	2001.29
									8.905	-4.065	2001.38
									8.869	-4.214	2001.46
									8.838	-4.338	2001.54
									8.835	-4.380	2001.63
									8.840	-4.421	2001.71
									8.827	-4.382	2001.79
									8.873	-4.225	2001.88
									8.928	-4.081	2001.96
									8.925	-4.204	2002.04
									8.907	-4.176	2002.13
									8.925	-4.344	2002.21
									8.930	-4.462	2002.29
									8.903	-4.425	2002.38
									8.880	-4.376	2002.46
									8.860	-4.379	2002.54
									8.844	-4.436	2002.63
									8.834	-4.527	2002.71
									8.845	-4.442	2002.79
									8.870	-4.279	2002.88
									8.889	-4.160	2002.96
									8.896	-4.156	2003.04
									8.903	-4.304	2003.13
									8.886	-4.200	2003.21
									8.894	-4.250	2003.29
									8.889	-3.707	2003.38
									8.879	-4.379	2003.46
									8.863	-4.420	2003.54
									8.854	-3.495	2003.63
									8.841	-4.274	2003.71
									8.857	-4.164	2003.79
									8.874	-4.066	2003.88
									8.890	-3.985	2003.96
									8.897	-3.992	2004.04
									8.900	-4.032	2004.13
									8.886	-4.055	2004.21
									8.874	-4.091	2004.29
									8.864	-4.161	2004.38
									8.856	-4.195	2004.46
									8.849	-4.193	2004.54
									8.840	-4.281	2004.63
									8.830	-4.395	2004.71

LC3			Age Model		Linear interpolation				Monthly Resampling		
Sample ID	Sr/Ca (mmol/mol)	$\delta^{18}O$ (‰)	Sample ID	Time Pointer (year.month)	Sample ID	Sr/Ca (mmol/mol)	$\delta^{18}O$ (‰)	Age (year.month)	Sr/Ca (mmol/mol)	$\delta^{18}O$ (‰)	Age (year.month)
									8.854	-4.141	2004.79
									8.849	-4.041	2004.88
									8.862	-4.039	2004.96
									8.896	-4.063	2005.04
									8.922	-4.040	2005.13
									8.912	-4.028	2005.21
									8.900	-4.100	2005.29
									8.883	-4.185	2005.38
									8.852	-4.157	2005.46
									8.850	-4.250	2005.54
									8.839	-4.393	2005.63
									8.807	-4.565	2005.71
									8.824	-4.448	2005.79
									8.827	-4.433	2005.88
									8.839	-4.378	2005.96
									8.882	-4.210	2006.04
									8.904	-4.037	2006.13
									8.897	-4.075	2006.21
									8.872	-4.092	2006.29
									8.861	-4.231	2006.38
									8.866	-4.452	2006.46
									8.851	-4.486	2006.54
									8.838	-4.599	2006.63
									8.835	-4.556	2006.71
									8.865	-4.542	2006.79
									8.845	-4.384	2006.88
									8.860	-4.344	2006.96
									8.894	-4.282	2007.04
									8.915	-4.214	2007.13
									8.931	-4.127	2007.21
									8.921	-4.199	2007.29
									8.910	-4.267	2007.38
									8.897	-4.332	2007.46
									8.881	-4.371	2007.54
									8.864	-4.378	2007.63
									8.846	-4.356	2007.71
									8.884	-4.323	2007.79
									8.884	-4.319	2007.88
									8.896	-4.096	2007.96
									8.887	-4.098	2008.04
									8.916	-4.016	2008.13
									8.896	-4.071	2008.21
									8.897	-3.946	2008.29
									8.902	-4.255	2008.38
									8.918	-4.233	2008.46
									8.897	-4.268	2008.54
									8.884	-4.237	2008.63
									8.848	-4.265	2008.71
									8.870	-4.266	2008.79
									8.900	-4.263	2008.88
									8.931	-4.259	2008.96
									8.961	-4.256	2009.04
									8.991	-4.253	2009.13
									8.910	-4.083	2009.21
									8.911	-4.203	2009.29
									8.915	-4.111	2009.38
									8.917	-4.192	2009.46
									8.891	-4.632	2009.54
									8.849	-4.472	2009.63
									8.882	-4.572	2009.71
									8.851	-4.634	2009.79
									8.923	-4.431	2009.88
									8.923	-4.283	2009.96
									8.939	-4.258	2010.04
									9.036	-4.265	2010.13
									9.005	-4.151	2010.21
									8.973	-4.036	2010.29
									8.953	-4.130	2010.38
									8.934	-4.266	2010.46
									8.919	-4.358	2010.54
									8.908	-4.389	2010.63
									8.899	-4.416	2010.71
									8.953	-4.134	2010.79
									8.940	-4.294	2010.88
									8.960	-4.214	2010.96
									8.929	-4.149	2011.04
									8.971	-3.950	2011.13
									8.939	-4.298	2011.21
									8.932	-4.449	2011.29

LC3			Age Model		Linear interpolation				Monthly Resampling		
Sample ID	Sr/Ca (mmol/mol)	$\delta^{18}O$ (‰)	Sample ID	Time Pointer (year.month)	Sample ID	Sr/Ca (mmol/mol)	$\delta^{18}O$ (‰)	Age (year.month)	Sr/Ca (mmol/mol)	$\delta^{18}O$ (‰)	Age (year.month)
									8.888	-4.449	2011.38
									8.864	-4.706	2011.46
									8.839	-4.812	2011.54
									8.851	-4.508	2011.63
									8.862	-4.327	2011.71
									8.840	-4.502	2011.79
									8.840	-4.531	2011.88
									8.882	-4.248	2011.96
									8.917	-4.007	2012.04
									8.902	-4.021	2012.13
									8.887	-4.034	2012.21
									8.892	-4.146	2012.29
									8.899	-4.262	2012.38
									8.892	-4.318	2012.46
									8.882	-4.357	2012.54

Table A2: Trace element and oxygen isotope data together with age model for *Diploria strigosa coral* core LC4 from the lagoon of Little Cayman. Table continues on the following pages.

LC4		Age Model		Linear interpolation			Monthly Resampling	
Sample ID	Sr/Ca (mmol/mol)	Sample ID	Time Pointer (year.month)	Sample ID	Sr/Ca (mmol/mol)	Age (year.month)	Sr/Ca (mmol/mol)	Age (year.month)
1	9.022	3	2012.46	665	9.032	1969.43	9.020	1969.46
2	9.016	10	2012.20	664	8.984	1969.54	8.984	1969.54
3	9.039	19	2011.63	663	9.011	1969.66	9.003	1969.62
4	9.091	30	2011.03	662	9.045	1969.75	9.029	1969.71
5	9.113	33	2010.63	661	9.036	1969.88	9.042	1969.79
6	9.109	41	2010.13	660	9.121	1969.97	9.036	1969.87
7	9.123	50	2009.71	659	9.088	1970.06	9.107	1969.96
8	9.153	58	2009.14	658	9.172	1970.13	9.097	1970.04
9	9.160	64	2008.71	657	9.140	1970.18	9.172	1970.12
10	9.187	72	2008.13	656	9.106	1970.23	9.119	1970.21
11	9.136	80	2007.66	655	9.102	1970.28	9.107	1970.29
12	9.139	84	2007.21	654	9.121	1970.33	9.072	1970.37
13	9.053	95	2006.62	653	9.073	1970.37	9.061	1970.46
14	9.077	101	2006.12	652	9.049	1970.41	8.989	1970.54
15	9.058	106	2005.64	651	9.066	1970.45	8.931	1970.62
16	9.083	114	2005.06	650	9.020	1970.50	8.899	1970.71
17	9.052	121	2004.64	649	8.980	1970.55	8.924	1970.79
18	9.017	125	2004.15	648	8.938	1970.60	9.009	1970.87
19	8.985	137	2003.72	647	8.924	1970.65	9.023	1970.96
20	9.006	143	2003.11	646	8.896	1970.69	9.115	1971.04
21	9.136	149	2002.67	645	8.909	1970.77	9.047	1971.12
22	9.150	155	2002.21	644	8.945	1970.82	9.069	1971.21
23	9.241	164	2001.70	643	9.009	1970.87	9.059	1971.29
24	9.182	168	2001.22	642	9.006	1970.93	9.047	1971.37
25	9.261	180	2000.72	641	9.037	1970.98	9.021	1971.46
26	9.247	187	2000.13	640	9.116	1971.04	9.004	1971.54
27	9.249	196	1999.68	639	9.054	1971.09	8.958	1971.62
28	9.258	203	1999.13	638	9.042	1971.12	8.980	1971.71
29	9.196	213	1998.57	637	9.081	1971.17	9.008	1971.79
30	9.267	216	1998.20	636	9.068	1971.21	9.016	1971.87
31	9.231	226	1997.65	635	9.073	1971.27	9.039	1971.96
32	9.104	239	1996.71	634	9.052	1971.30	9.063	1972.04
33	9.069	247	1996.14	633	9.036	1971.35	9.086	1972.12
34	9.127	253	1995.72	632	9.056	1971.40	9.113	1972.21
35	9.218	261	1995.18	631	9.032	1971.44	9.096	1972.29
36	9.277	268	1994.62	630	9.005	1971.49	9.033	1972.37
37	9.263	278	1994.12	629	9.007	1971.54	8.994	1972.46
38	9.236	282	1993.63	628	8.989	1971.58	8.983	1972.54
39	9.256	285	1993.22	627	8.958	1971.62	8.954	1972.62
40	9.263	294	1992.64	626	8.955	1971.68	8.954	1972.71
41	9.291	305	1991.71	625	9.001	1971.73	8.975	1972.79
42	9.200	312	1991.20	624	9.008	1971.80	8.998	1972.87
43	9.261	320	1990.70	623	9.010	1971.85	9.054	1972.96
44	9.282	330	1990.20	622	9.033	1971.93	9.099	1973.04
45	9.126	343	1989.73	621	9.045	1971.99	9.085	1973.12
46	9.104	350	1989.13	620	9.057	1972.03	9.096	1973.21
47	9.099	358	1988.66	619	9.087	1972.09	9.070	1973.29
48	9.075	362	1988.13	618	9.086	1972.14	9.052	1973.37
49	9.030	372	1987.68	617	9.113	1972.21	9.016	1973.46
50	9.024	382	1987.13	616	9.101	1972.28	8.981	1973.54

LC4		Age Model		Linear interpolation			Monthly Resampling	
Sample ID	Sr/Ca (mmol/mol)	Sample ID	Time Pointer (year.month)	Sample ID	Sr/Ca (mmol/mol)	Age (year.month)	Sr/Ca (mmol/mol)	Age (year.month)
51	9.086	390	1986.69	615	9.063	1972.35	8.942	1973.62
52	9.085	395	1986.19	614	8.997	1972.40	8.965	1973.71
53	9.136	405	1985.63	613	8.992	1972.48	9.041	1973.79
54	9.179	421	1984.69	612	8.981	1972.56	9.038	1973.87
55	9.202	428	1984.21	611	8.954	1972.62	9.095	1973.96
56	9.205	435	1983.66	610	8.955	1972.69	9.110	1974.04
57	9.233	448	1982.60	609	8.950	1972.76	9.090	1974.12
58	9.309	458	1982.12	608	8.990	1972.81	9.110	1974.21
59	9.250	461	1981.66	607	8.990	1972.86	9.106	1974.29
60	9.177	480	1980.68	606	9.042	1972.94	9.081	1974.37
61	9.136	486	1980.13	605	9.072	1972.99	8.990	1974.46
62	9.207	495	1979.68	604	9.101	1973.05	9.005	1974.54
63	9.166	501	1979.20	603	9.084	1973.12	8.986	1974.62
64	9.016	512	1978.60	602	9.089	1973.19	9.073	1974.71
65	9.061	518	1978.17	601	9.102	1973.22	9.064	1974.79
66	9.081	528	1977.60	600	9.078	1973.27	9.027	1974.87
67	9.148	534	1977.08	599	9.056	1973.33	9.088	1974.96
68	9.190	546	1976.76	598	9.050	1973.39	9.112	1975.04
69	9.208	553	1976.10	597	9.018	1973.43	9.092	1975.12
70	9.202	561	1975.73	596	9.012	1973.50	9.084	1975.21
71	9.199	569	1975.04	595	8.979	1973.54	9.112	1975.29
72	9.229	576	1974.58	594	8.946	1973.59	9.017	1975.37
73	9.179	583	1974.22	593	8.938	1973.65	9.009	1975.46
74	9.177	593	1973.65	592	8.968	1973.71	8.977	1975.54
75	9.121	603	1973.12	591	9.039	1973.78	8.932	1975.62
76	9.127	610	1972.69	590	9.049	1973.84	8.899	1975.71
77	9.109	617	1972.21	589	9.033	1973.87	8.973	1975.79
78	9.036	626	1971.68	588	9.122	1973.91	9.012	1975.87
79	9.061	640	1971.04	587	9.074	1974.00	9.062	1975.96
80	9.015	646	1970.69	586	9.124	1974.06	9.095	1976.04
81	9.086	658	1970.13	585	9.088	1974.12	9.106	1976.12
82	9.046	664	1969.54	584	9.107	1974.18	9.083	1976.21
83	9.158			583	9.111	1974.22	9.076	1976.29
84	9.162			582	9.092	1974.27	9.084	1976.37
85	9.138			581	9.123	1974.32	9.100	1976.46
86	9.128			580	9.084	1974.36	9.049	1976.54
87	9.149			579	9.070	1974.42	8.983	1976.62
88	9.130			578	8.979	1974.46	8.954	1976.71
89	9.143			577	9.004	1974.51	8.992	1976.79
90	9.161			576	9.007	1974.58	9.027	1976.87
91	9.072			575	8.984	1974.63	9.155	1976.96
92	9.105			574	9.075	1974.70	9.108	1977.04
93	9.043			573	9.046	1974.77	9.101	1977.12
94	9.025			572	9.097	1974.84	9.132	1977.21
95	9.014			571	8.985	1974.90	9.142	1977.29
96	9.127			570	9.096	1974.96	9.111	1977.37
97	9.084			569	9.113	1975.04	9.074	1977.46
98	9.156			568	9.091	1975.13	9.005	1977.54
99	9.137			567	9.082	1975.20	9.005	1977.62
100	9.174			566	9.113	1975.29	9.027	1977.71
101	9.190			565	9.011	1975.38	9.070	1977.79
102	9.146			564	9.009	1975.46	9.098	1977.87
103	9.133			563	8.970	1975.56	9.116	1977.96
104	9.099			562	8.921	1975.64	9.170	1978.04
105	9.037			561	8.892	1975.73	9.150	1978.12
106	9.007			560	8.955	1975.78	9.150	1978.21
107	9.018			559	9.019	1975.83	9.152	1978.29
108	9.074			558	9.012	1975.87	9.141	1978.37
109	9.100			557	9.055	1975.92	9.055	1978.46
110	9.132			556	9.065	1975.97	9.066	1978.54
111	9.197			555	9.090	1976.01	9.052	1978.62
112	9.262			554	9.096	1976.05	9.059	1978.71
113	9.277			553	9.114	1976.10	9.092	1978.79
114	9.312			552	9.087	1976.18	9.093	1978.87
115	9.234			551	9.074	1976.27	9.071	1978.96
116	9.251			550	9.084	1976.38	9.154	1979.04
117	9.189			549	9.104	1976.48	9.142	1979.12
118	9.123			548	9.020	1976.58	9.155	1979.21
119	9.096			547	8.967	1976.65	9.118	1979.29
120	9.069			546	8.943	1976.76	9.108	1979.37
121	9.058			545	8.996	1976.79	9.126	1979.46
122	9.087			544	8.973	1976.81	9.132	1979.54
123	9.229			543	8.997	1976.84	9.079	1979.62
124	9.197			542	9.031	1976.87	9.080	1979.71
125	9.255			541	9.020	1976.89	9.089	1979.79
126	9.222			540	9.078	1976.91	9.109	1979.87
127	9.193			539	9.105	1976.93	9.147	1979.96
128	9.214			538	9.173	1976.97	9.219	1980.04
129	9.265			537	9.135	1976.99	9.213	1980.12

LC4		Age Model		Linear interpolation			Monthly Resampling	
Sample ID	Sr/Ca (mmol/mol)	Sample ID	Time Pointer (year.month)	Sample ID	Sr/Ca (mmol/mol)	Age (year.month)	Sr/Ca (mmol/mol)	Age (year.month)
130	9.236			536	9.119	1977.02	9.153	1980.21
131	9.205			535	9.103	1977.05	9.150	1980.29
132	9.082			534	9.084	1977.08	9.121	1980.37
133	9.104			533	9.118	1977.17	9.087	1980.46
134	9.038			532	9.154	1977.26	9.052	1980.54
135	9.089			531	9.115	1977.36	8.991	1980.62
136	9.066			530	9.095	1977.44	9.005	1980.71
137	9.016			529	9.004	1977.52	9.007	1980.79
138	9.033			528	9.008	1977.60	9.105	1980.87
139	9.085			527	9.002	1977.65	9.198	1980.96
140	9.139			526	9.022	1977.70	9.218	1981.04
141	9.196			525	9.068	1977.75	9.184	1981.12
142	9.122			524	9.071	1977.80	9.218	1981.21
143	9.211			523	9.087	1977.85	9.194	1981.29
144	9.158			522	9.109	1977.90	9.118	1981.37
145	9.070			521	9.118	1977.98	9.099	1981.46
146	9.107			520	9.174	1978.03	9.070	1981.54
147	9.138			519	9.151	1978.08	9.029	1981.62
148	9.100			518	9.150	1978.17	9.013	1981.71
149	8.999			517	9.150	1978.25	9.031	1981.79
150	9.061			516	9.154	1978.32	9.058	1981.87
151	9.092			515	9.134	1978.40	9.094	1981.96
152	9.156			514	9.047	1978.46	9.148	1982.04
153	9.159			513	9.078	1978.53	9.195	1982.12
154	9.157			512	8.995	1978.60	9.155	1982.21
155	9.228			511	9.080	1978.64	9.158	1982.29
156	9.191			510	9.066	1978.69	9.184	1982.37
157	9.159			509	9.045	1978.74	9.107	1982.46
158	9.187			508	9.094	1978.79	9.052	1982.54
159	9.145			507	9.083	1978.83	9.020	1982.62
160	9.122			506	9.096	1978.89	9.059	1982.71
161	9.102			505	9.059	1978.94	9.107	1982.79
162	9.136			504	9.106	1979.01	9.129	1982.87
163	9.158			503	9.155	1979.04	9.142	1982.96
164	9.080			502	9.133	1979.08	9.201	1983.04
165	9.164			501	9.157	1979.20	9.141	1983.12
166	9.191			500	9.124	1979.28	9.174	1983.21
167	9.184			499	9.101	1979.34	9.143	1983.29
168	9.271			498	9.129	1979.47	9.158	1983.37
169	9.201			497	9.132	1979.54	9.159	1983.46
170	9.267			496	9.079	1979.61	9.117	1983.54
171	9.271			495	9.081	1979.68	9.070	1983.62
172	9.228			494	9.079	1979.73	9.054	1983.71
173	9.212			493	9.090	1979.78	9.065	1983.79
174	9.250			492	9.085	1979.83	9.094	1983.87
175	9.117			491	9.115	1979.89	9.142	1983.96
176	9.044			490	9.174	1979.94	9.194	1984.04
177	9.049			489	9.112	1979.99	9.188	1984.12
178	9.064			488	9.226	1980.03	9.229	1984.21
179	9.012			487	9.192	1980.08	9.180	1984.29
180	8.973			486	9.216	1980.13	9.159	1984.37
181	9.004			485	9.144	1980.22	9.129	1984.46
182	9.020			484	9.153	1980.33	9.115	1984.54
183	9.084			483	9.087	1980.42	9.070	1984.62
184	9.137			482	9.088	1980.51	9.062	1984.71
185	9.123			481	8.973	1980.60	9.116	1984.79
186	9.157			480	9.038	1980.68	9.202	1984.87
187	9.224			479	8.961	1980.74	9.228	1984.96
188	9.222			478	8.999	1980.78	9.224	1985.04
189	9.162			477	9.038	1980.84	9.242	1985.12
190	9.176			476	9.132	1980.89	9.178	1985.21
191	9.147			475	9.189	1980.92	9.168	1985.29
192	9.124			474	9.218	1981.04	9.174	1985.37
193	9.154			473	9.260	1981.07	9.151	1985.46
194	9.049			472	9.084	1981.10	9.097	1985.54
195	8.985			471	9.191	1981.12	9.083	1985.62
196	9.013			470	9.148	1981.14	9.090	1985.71
197	8.995			469	9.239	1981.17	9.139	1985.79
198	9.022			468	9.210	1981.22	9.161	1985.87
199	9.131			467	9.195	1981.29	9.208	1985.96
200	9.150			466	9.163	1981.31	9.251	1986.04
201	9.177			465	9.122	1981.35	9.208	1986.12
202	9.179			464	9.109	1981.43	9.234	1986.21
203	9.217			463	9.080	1981.51	9.201	1986.29
204	9.137			462	9.055	1981.59	9.125	1986.37
205	9.173			461	9.002	1981.66	9.164	1986.46
206	9.139			460	9.041	1981.84	9.140	1986.54
207	9.113			459	9.106	1981.99	9.092	1986.62
208	9.022			458	9.204	1982.12	9.089	1986.71

LC4		Age Model		Linear interpolation			Monthly Resampling	
Sample ID	Sr/Ca (mmol/mol)	Sample ID	Time Pointer (year.month)	Sample ID	Sr/Ca (mmol/mol)	Age (year.month)	Sr/Ca (mmol/mol)	Age (year.month)
209	8.994			457	9.152	1982.17	9.126	1986.79
210	9.002			456	9.158	1982.24	9.142	1986.87
211	8.974			455	9.158	1982.30	9.210	1986.96
212	9.002			454	9.127	1982.34	9.281	1987.04
213	8.974			453	9.198	1982.38	9.330	1987.12
214	9.048			452	9.116	1982.42	9.260	1987.21
215	9.139			451	9.103	1982.47	9.197	1987.29
216	9.193			450	9.093	1982.52	9.256	1987.37
217	9.093			449	9.022	1982.56	9.164	1987.46
218	9.113			448	9.015	1982.60	9.105	1987.54
219	9.124			447	9.027	1982.66	9.099	1987.62
220	9.092			446	9.100	1982.77	9.136	1987.71
221	9.104			445	9.128	1982.87	9.115	1987.79
222	9.050			444	9.136	1982.95	9.160	1987.87
223	9.055			443	9.218	1983.02	9.196	1987.96
224	8.991			442	9.137	1983.12	9.187	1988.04
225	8.961			441	9.189	1983.18	9.233	1988.12
226	8.958			440	9.140	1983.27	9.201	1988.21
227	9.024			439	9.153	1983.35	9.160	1988.29
228	9.008			438	9.168	1983.43	9.123	1988.37
229	9.052			437	9.143	1983.50	9.110	1988.46
230	9.083			436	9.092	1983.58	9.103	1988.54
231	9.121			435	9.051	1983.66	9.057	1988.62
232	9.097			434	9.056	1983.74	9.052	1988.71
233	9.091			433	9.074	1983.84	9.131	1988.79
234	9.121			432	9.125	1983.93	9.072	1988.87
235	9.129			431	9.170	1984.01	9.134	1988.96
236	9.058			430	9.222	1984.08	9.216	1989.04
237	8.994			429	9.166	1984.15	9.266	1989.12
238	8.976			428	9.230	1984.21	9.168	1989.21
239	8.942			427	9.178	1984.29	9.130	1989.29
240	8.960			426	9.169	1984.36	9.155	1989.37
241	8.976			425	9.112	1984.43	9.167	1989.46
242	9.057			424	9.145	1984.49	9.159	1989.54
243	9.066			423	9.104	1984.56	9.141	1989.62
244	9.078			422	9.064	1984.64	9.094	1989.71
245	9.138			421	9.060	1984.69	9.095	1989.79
246	9.162			420	9.067	1984.76	9.159	1989.87
247	9.171			419	9.142	1984.81	9.109	1989.96
248	9.159			418	9.184	1984.86	9.191	1990.04
249	9.103			417	9.235	1984.91	9.235	1990.12
250	9.075			416	9.226	1984.97	9.214	1990.21
251	9.020			415	9.223	1985.01	9.168	1990.29
252	8.956			414	9.225	1985.08	9.151	1990.37
253	9.015			413	9.243	1985.12	9.136	1990.46
254	9.005			412	9.180	1985.21	9.155	1990.54
255	8.989			411	9.126	1985.27	9.089	1990.62
256	9.005			410	9.211	1985.32	9.031	1990.71
257	9.083			409	9.169	1985.38	9.150	1990.79
258	9.216			408	9.162	1985.44	9.102	1990.87
259	9.130			407	9.130	1985.50	9.173	1990.96
260	9.095			406	9.081	1985.56	9.220	1991.04
261	9.147			405	9.083	1985.63	9.168	1991.13
262	9.145			404	9.088	1985.70	9.187	1991.21
263	9.095			403	9.105	1985.76	9.148	1991.29
264	9.172			402	9.147	1985.80	9.125	1991.38
265	9.065			401	9.148	1985.86	9.119	1991.46
266	9.017			400	9.183	1985.91	9.101	1991.54
267	8.981			399	9.207	1985.95	9.063	1991.63
268	9.093			398	9.218	1986.00	9.040	1991.71
269	9.003			397	9.276	1986.07	9.072	1991.79
270	8.977			396	9.195	1986.14	9.153	1991.88
271	8.993			395	9.241	1986.19	9.203	1991.96
272	9.069			394	9.201	1986.29	9.210	1992.04
273	9.102			393	9.120	1986.38	9.202	1992.13
274	9.145			392	9.182	1986.49	9.199	1992.21
275	9.166			391	9.114	1986.57	9.170	1992.29
276	9.180			390	9.063	1986.69	9.158	1992.38
277	9.170			389	9.141	1986.74	9.136	1992.46
278	9.241			388	9.129	1986.79	9.072	1992.54
279	9.173			387	9.092	1986.84	9.003	1992.63
280	9.089			386	9.150	1986.88	9.003	1992.71
281	9.032			385	9.181	1986.94	9.052	1992.79
282	9.032			384	9.272	1986.99	9.102	1992.88
283	9.049			383	9.284	1987.06	9.077	1992.96
284	9.092			382	9.334	1987.13	9.134	1993.04
285	9.155			381	9.292	1987.19	9.127	1993.13
286	9.119			380	9.197	1987.25	9.151	1993.21
287	9.152			379	9.197	1987.31	9.119	1993.29

LC4		Age Model		Linear interpolation			Monthly Resampling	
Sample ID	Sr/Ca (mmol/mol)	Sample ID	Time Pointer (year.month)	Sample ID	Sr/Ca (mmol/mol)	Age (year.month)	Sr/Ca (mmol/mol)	Age (year.month)
288	9.124			378	9.269	1987.36	9.083	1993.38
289	9.075			377	9.231	1987.41	9.054	1993.46
290	9.093			376	9.148	1987.47	9.042	1993.54
291	9.114			375	9.096	1987.53	9.033	1993.63
292	9.031			374	9.131	1987.58	9.032	1993.71
293	9.004			373	9.093	1987.63	9.045	1993.79
294	8.996			372	9.077	1987.68	9.088	1993.88
295	9.026			371	9.156	1987.72	9.147	1993.96
296	9.115			370	9.101	1987.76	9.198	1994.04
297	9.156			369	9.120	1987.80	9.240	1994.13
298	9.162			368	9.161	1987.85	9.176	1994.21
299	9.198			367	9.160	1987.89	9.161	1994.29
300	9.201			366	9.161	1987.93	9.105	1994.38
301	9.210			365	9.222	1987.98	9.030	1994.46
302	9.202			364	9.187	1988.02	8.977	1994.54
303	9.139			363	9.187	1988.08	9.092	1994.63
304	9.057			362	9.239	1988.13	8.984	1994.71
305	9.040			361	9.148	1988.32	9.021	1994.79
306	9.054			360	9.116	1988.39	9.083	1994.88
307	9.114			359	9.102	1988.55	9.141	1994.96
308	9.119			358	9.034	1988.66	9.117	1995.04
309	9.124			357	9.058	1988.72	9.146	1995.13
310	9.127			356	9.132	1988.79	9.117	1995.21
311	9.172			355	9.068	1988.83	9.119	1995.29
312	9.191			354	9.075	1988.90	9.200	1995.38
313	9.168			353	9.127	1988.95	9.072	1995.46
314	9.223			352	9.179	1989.00	8.996	1995.54
315	9.179			351	9.233	1989.06	8.999	1995.63
316	9.167			350	9.268	1989.13	9.013	1995.71
317	9.124			349	9.141	1989.23	8.962	1995.79
318	9.089			348	9.125	1989.32	9.036	1995.88
319	9.165			347	9.168	1989.40	9.086	1995.96
320	9.022			346	9.166	1989.50	9.139	1996.04
321	9.070			345	9.151	1989.59	9.168	1996.13
322	9.101			344	9.128	1989.66	9.164	1996.21
323	9.156			343	9.077	1989.73	9.140	1996.29
324	9.151			342	9.101	1989.77	9.075	1996.38
325	9.132			341	9.095	1989.79	9.064	1996.46
326	9.123			340	9.130	1989.83	9.032	1996.54
327	9.180			339	9.075	1989.85	8.968	1996.63
328	9.168			338	9.226	1989.89	8.942	1996.71
329	9.170			337	9.106	1989.93	8.983	1996.79
330	9.220			336	9.111	1989.97	9.034	1996.88
331	9.213			335	9.214	1990.01	9.128	1996.96
332	9.235			334	9.187	1990.05	9.114	1997.04
333	9.230			333	9.230	1990.09	9.092	1997.13
334	9.187			332	9.235	1990.13	9.100	1997.21
335	9.214			331	9.213	1990.17	9.114	1997.29
336	9.111			330	9.220	1990.20	9.080	1997.38
337	9.106			329	9.170	1990.25	9.038	1997.46
338	9.226			328	9.168	1990.30	9.013	1997.54
339	9.075			327	9.180	1990.35	8.990	1997.63
340	9.130			326	9.123	1990.40	8.961	1997.71
341	9.095			325	9.132	1990.45	9.034	1997.79
342	9.101			324	9.151	1990.50	9.056	1997.88
343	9.077			323	9.156	1990.56	9.097	1997.96
344	9.128			322	9.101	1990.61	9.118	1998.04
345	9.151			321	9.070	1990.65	9.097	1998.13
346	9.166			320	9.022	1990.70	9.187	1998.21
347	9.168			319	9.165	1990.78	9.152	1998.29
348	9.125			318	9.089	1990.86	9.097	1998.38
349	9.141			317	9.124	1990.91	9.037	1998.46
350	9.268			316	9.167	1990.93	8.990	1998.54
351	9.233			315	9.179	1990.99	8.991	1998.63
352	9.179			314	9.223	1991.05	8.976	1998.71
353	9.127			313	9.168	1991.12	8.996	1998.79
354	9.075			312	9.191	1991.20	9.080	1998.88
355	9.068			311	9.172	1991.25	9.139	1998.96
356	9.132			310	9.127	1991.33	9.157	1999.04
357	9.058			309	9.124	1991.40	9.206	1999.13
358	9.034			308	9.119	1991.45	9.179	1999.21
359	9.102			307	9.114	1991.51	9.177	1999.29
360	9.116			306	9.054	1991.64	9.151	1999.38
361	9.148			305	9.040	1991.71	9.115	1999.46
362	9.239			304	9.057	1991.78	9.017	1999.54
363	9.187			303	9.139	1991.85	9.002	1999.63
364	9.187			302	9.202	1991.94	8.994	1999.71
365	9.222			301	9.210	1992.04	9.050	1999.79
366	9.161			300	9.201	1992.13	9.134	1999.88

LC4		Age Model		Linear interpolation			Monthly Resampling	
Sample ID	Sr/Ca (mmol/mol)	Sample ID	Time Pointer (year.month)	Sample ID	Sr/Ca (mmol/mol)	Age (year.month)	Sr/Ca (mmol/mol)	Age (year.month)
367	9.160			299	9.198	1992.23	9.162	1999.96
368	9.161			298	9.162	1992.31	9.172	2000.04
369	9.120			297	9.156	1992.41	9.224	2000.13
370	9.101			296	9.115	1992.50	9.173	2000.21
371	9.156			295	9.026	1992.58	9.133	2000.29
372	9.077			294	8.996	1992.64	9.134	2000.38
373	9.093			293	9.004	1992.71	9.103	2000.46
374	9.131			292	9.031	1992.77	9.044	2000.54
375	9.096			291	9.114	1992.85	9.007	2000.63
376	9.148			290	9.093	1992.89	8.976	2000.71
377	9.231			289	9.075	1992.95	9.051	2000.79
378	9.269			288	9.124	1993.02	9.044	2000.88
379	9.197			287	9.152	1993.08	9.246	2000.96
380	9.197			286	9.119	1993.14	9.227	2001.04
381	9.292			285	9.155	1993.22	9.260	2001.13
382	9.334			284	9.092	1993.35	9.256	2001.21
383	9.284			283	9.049	1993.47	9.217	2001.29
384	9.272			282	9.032	1993.63	9.186	2001.38
385	9.181			281	9.032	1993.77	9.191	2001.46
386	9.150			280	9.089	1993.88	9.170	2001.54
387	9.092			279	9.173	1993.99	9.127	2001.63
388	9.129			278	9.241	1994.12	9.091	2001.71
389	9.141			277	9.170	1994.17	9.141	2001.79
390	9.063			276	9.180	1994.23	9.109	2001.88
391	9.114			275	9.166	1994.28	9.139	2001.96
392	9.182			274	9.145	1994.33	9.183	2002.04
393	9.120			273	9.102	1994.38	9.176	2002.13
394	9.201			272	9.069	1994.43	9.225	2002.21
395	9.241			271	8.993	1994.49	9.162	2002.29
396	9.195			270	8.977	1994.54	9.157	2002.38
397	9.276			269	9.003	1994.59	9.122	2002.46
398	9.218			268	9.093	1994.62	9.076	2002.54
399	9.207			267	8.981	1994.70	9.032	2002.63
400	9.183			266	9.017	1994.79	9.029	2002.71
401	9.148			265	9.065	1994.86	9.097	2002.79
402	9.147			264	9.172	1994.93	9.134	2002.88
403	9.105			263	9.095	1995.00	9.082	2002.96
404	9.088			262	9.145	1995.10	9.161	2003.04
405	9.083			261	9.147	1995.18	9.197	2003.13
406	9.081			260	9.095	1995.23	9.126	2003.21
407	9.130			259	9.130	1995.32	9.176	2003.29
408	9.162			258	9.216	1995.39	9.164	2003.38
409	9.169			257	9.083	1995.45	9.123	2003.46
410	9.211			256	9.005	1995.50	9.089	2003.54
411	9.126			255	8.989	1995.58	9.052	2003.63
412	9.180			254	9.005	1995.65	9.020	2003.71
413	9.243			253	9.015	1995.72	9.087	2003.79
414	9.225			252	8.956	1995.79	9.083	2003.88
415	9.223			251	9.020	1995.85	9.242	2003.96
416	9.226			250	9.075	1995.94	9.207	2004.04
417	9.235			249	9.103	1996.00	9.239	2004.13
418	9.184			248	9.159	1996.07	9.228	2004.21
419	9.142			247	9.171	1996.14	9.202	2004.29
420	9.067			246	9.162	1996.23	9.223	2004.38
421	9.060			245	9.138	1996.30	9.156	2004.46
422	9.064			244	9.078	1996.36	9.081	2004.54
423	9.104			243	9.066	1996.44	9.062	2004.63
424	9.145			242	9.057	1996.52	9.069	2004.71
425	9.112			241	8.976	1996.59	9.108	2004.79
426	9.169			240	8.960	1996.66	9.175	2004.88
427	9.178			239	8.942	1996.71	9.250	2004.96
428	9.230			238	8.976	1996.76	9.282	2005.04
429	9.166			237	8.994	1996.84	9.276	2005.13
430	9.222			236	9.058	1996.90	9.263	2005.21
431	9.170			235	9.129	1996.95	9.193	2005.29
432	9.125			234	9.121	1997.02	9.131	2005.38
433	9.074			233	9.091	1997.11	9.097	2005.46
434	9.056			232	9.097	1997.20	9.051	2005.54
435	9.051			231	9.121	1997.27	9.010	2005.63
436	9.092			230	9.083	1997.37	9.024	2005.71
437	9.143			229	9.052	1997.43	9.065	2005.79
438	9.168			228	9.008	1997.51	9.117	2005.88
439	9.153			227	9.024	1997.60	9.139	2005.96
440	9.140			226	8.958	1997.65	9.156	2006.04
441	9.189			225	8.961	1997.71	9.190	2006.13
442	9.137			224	8.991	1997.75	9.176	2006.21
443	9.218			223	9.055	1997.81	9.146	2006.29
444	9.136			222	9.050	1997.87	9.151	2006.38
445	9.128			221	9.104	1997.92	9.102	2006.46

LC4		Age Model		Linear interpolation			Monthly Resampling	
Sample ID	Sr/Ca (mmol/mol)	Sample ID	Time Pointer (year.month)	Sample ID	Sr/Ca (mmol/mol)	Age (year.month)	Sr/Ca (mmol/mol)	Age (year.month)
446	9.100			220	9.092	1997.98	9.126	2006.54
447	9.027			219	9.124	1998.00	9.015	2006.63
448	9.015			218	9.113	1998.07	9.034	2006.71
449	9.022			217	9.093	1998.14	9.096	2006.79
450	9.093			216	9.193	1998.20	9.125	2006.88
451	9.103			215	9.139	1998.32	9.140	2006.96
452	9.116			214	9.048	1998.44	9.146	2007.04
453	9.198			213	8.974	1998.57	9.131	2007.13
454	9.127			212	9.002	1998.66	9.162	2007.21
455	9.158			211	8.974	1998.71	9.159	2007.29
456	9.158			210	9.002	1998.75	9.106	2007.38
457	9.152			209	8.994	1998.80	9.051	2007.46
458	9.204			208	9.022	1998.83	9.078	2007.54
459	9.106			207	9.113	1998.90	9.043	2007.63
460	9.041			206	9.139	1998.96	9.054	2007.71
461	9.002			205	9.173	1999.01	9.062	2007.79
462	9.055			204	9.137	1999.08	9.121	2007.88
463	9.080			203	9.217	1999.13	9.122	2007.96
464	9.109			202	9.179	1999.21	9.178	2008.04
465	9.122			201	9.177	1999.29	9.222	2008.13
466	9.163			200	9.150	1999.38	9.199	2008.21
467	9.195			199	9.131	1999.45	9.202	2008.29
468	9.210			198	9.022	1999.53	9.202	2008.38
469	9.239			197	8.995	1999.60	9.167	2008.46
470	9.148			196	9.013	1999.68	9.107	2008.54
471	9.191			195	8.985	1999.72	9.064	2008.63
472	9.084			194	9.049	1999.79	9.021	2008.71
473	9.260			193	9.154	1999.84	9.182	2008.79
474	9.218			192	9.124	1999.89	9.174	2008.88
475	9.189			191	9.147	1999.93	9.157	2008.96
476	9.132			190	9.176	1999.98	9.222	2009.04
477	9.038			189	9.162	2000.03	9.297	2009.13
478	8.999			188	9.222	2000.09	9.239	2009.21
479	8.961			187	9.224	2000.13	9.208	2009.29
480	9.038			186	9.157	2000.23	9.195	2009.38
481	8.973			185	9.123	2000.32	9.157	2009.46
482	9.088			184	9.137	2000.39	9.099	2009.54
483	9.087			183	9.084	2000.50	9.086	2009.63
484	9.153			182	9.020	2000.57	9.028	2009.71
485	9.144			181	9.004	2000.64	9.046	2009.79
486	9.216			180	8.973	2000.72	9.099	2009.88
487	9.192			179	9.012	2000.76	9.130	2009.96
488	9.226			178	9.064	2000.80	9.266	2010.04
489	9.112			177	9.049	2000.84	9.256	2010.13
490	9.174			176	9.044	2000.88	9.262	2010.21
491	9.115			175	9.117	2000.91	9.239	2010.29
492	9.085			174	9.250	2000.95	9.267	2010.38
493	9.090			173	9.212	2001.00	9.253	2010.46
494	9.079			172	9.228	2001.05	9.166	2010.54
495	9.081			171	9.271	2001.08	9.072	2010.63
496	9.079			170	9.267	2001.12	9.085	2010.71
497	9.132			169	9.201	2001.16	9.102	2010.79
498	9.129			168	9.271	2001.22	9.207	2010.88
499	9.101			167	9.184	2001.33	9.248	2010.96
500	9.124			166	9.191	2001.46	9.259	2011.04
501	9.157			165	9.164	2001.57	9.220	2011.13
502	9.133			164	9.080	2001.70	9.249	2011.21
503	9.155			163	9.158	2001.76	9.253	2011.29
504	9.106			162	9.136	2001.80	9.193	2011.38
505	9.059			161	9.102	2001.85	9.148	2011.46
506	9.096			160	9.122	2001.92	9.036	2011.54
507	9.083			159	9.145	2001.97	8.986	2011.63
508	9.094			158	9.187	2002.03	9.055	2011.71
509	9.045			157	9.159	2002.10	9.069	2011.79
510	9.066			156	9.191	2002.15	9.076	2011.88
511	9.080			155	9.228	2002.21	9.057	2011.96
512	8.995			154	9.157	2002.30	9.139	2012.04
513	9.078			153	9.159	2002.33	9.145	2012.13
514	9.047			152	9.156	2002.41	9.176	2012.21
515	9.134			151	9.092	2002.50	9.125	2012.29
516	9.154			150	9.061	2002.58	9.113	2012.38
517	9.150			149	8.999	2002.67	9.039	2012.46
518	9.150			148	9.100	2002.80	9.022	2012.54
519	9.151			147	9.138	2002.87		
520	9.174			146	9.107	2002.92		
521	9.118			145	9.070	2002.98		
522	9.109			144	9.158	2003.04		
523	9.087			143	9.211	2003.11		
524	9.071			142	9.122	2003.21		

LC4		Age Model		Linear interpolation			Monthly Resampling	
Sample ID	Sr/Ca (mmol/mol)	Sample ID	Time Pointer (year.month)	Sample ID	Sr/Ca (mmol/mol)	Age (year.month)	Sr/Ca (mmol/mol)	Age (year.month)
525	9.068			141	9.196	2003.32		
526	9.022			140	9.139	2003.42		
527	9.002			139	9.085	2003.55		
528	9.008			138	9.033	2003.67		
529	9.004			137	9.016	2003.72		
530	9.095			136	9.066	2003.76		
531	9.115			135	9.089	2003.79		
532	9.154			134	9.038	2003.82		
533	9.118			133	9.104	2003.85		
534	9.084			132	9.082	2003.88		
535	9.103			131	9.205	2003.92		
536	9.119			130	9.236	2003.95		
537	9.135			129	9.265	2003.99		
538	9.173			128	9.214	2004.03		
539	9.105			127	9.193	2004.07		
540	9.078			126	9.222	2004.10		
541	9.020			125	9.255	2004.15		
542	9.031			124	9.197	2004.27		
543	8.997			123	9.229	2004.40		
544	8.973			122	9.087	2004.52		
545	8.996			121	9.058	2004.64		
546	8.943			120	9.069	2004.71		
547	8.967			119	9.096	2004.77		
548	9.020			118	9.123	2004.82		
549	9.104			117	9.189	2004.89		
550	9.084			116	9.251	2004.96		
551	9.074			115	9.234	2005.01		
552	9.087			114	9.312	2005.06		
553	9.114			113	9.277	2005.12		
554	9.096			112	9.262	2005.21		
555	9.090			111	9.197	2005.29		
556	9.065			110	9.132	2005.37		
557	9.055			109	9.100	2005.45		
558	9.012			108	9.074	2005.51		
559	9.019			107	9.018	2005.58		
560	8.955			106	9.007	2005.64		
561	8.892			105	9.037	2005.76		
562	8.921			104	9.099	2005.83		
563	8.970			103	9.133	2005.91		
564	9.009			102	9.146	2006.02		
565	9.011			101	9.190	2006.12		
566	9.113			100	9.174	2006.22		
567	9.082			99	9.137	2006.31		
568	9.091			98	9.156	2006.40		
569	9.113			97	9.084	2006.48		
570	9.096			96	9.127	2006.54		
571	8.985			95	9.014	2006.62		
572	9.097			94	9.025	2006.68		
573	9.046			93	9.043	2006.74		
574	9.075			92	9.105	2006.80		
575	8.984			91	9.072	2006.85		
576	9.007			90	9.161	2006.89		
577	9.004			89	9.143	2006.95		
578	8.979			88	9.130	2007.00		
579	9.070			87	9.149	2007.05		
580	9.084			86	9.128	2007.11		
581	9.123			85	9.138	2007.16		
582	9.092			84	9.162	2007.21		
583	9.111			83	9.158	2007.32		
584	9.107			82	9.046	2007.44		
585	9.088			81	9.086	2007.57		
586	9.124			80	9.015	2007.66		
587	9.074			79	9.061	2007.72		
588	9.122			78	9.036	2007.77		
589	9.033			77	9.109	2007.83		
590	9.049			76	9.127	2007.90		
591	9.039			75	9.121	2007.97		
592	8.968			74	9.177	2008.02		
593	8.938			73	9.179	2008.07		
594	8.946			72	9.229	2008.13		
595	8.979			71	9.199	2008.20		
596	9.012			70	9.202	2008.29		
597	9.018			69	9.208	2008.36		
598	9.050			68	9.190	2008.42		
599	9.056			67	9.148	2008.49		
600	9.078			66	9.081	2008.57		
601	9.102			65	9.061	2008.63		
602	9.089			64	9.016	2008.71		
603	9.084			63	9.166	2008.76		

LC4		Age Model		Linear interpolation			Monthly Resampling	
Sample ID	Sr/Ca (mmol/mol)	Sample ID	Time Pointer (year.month)	Sample ID	Sr/Ca (mmol/mol)	Age (year.month)	Sr/Ca (mmol/mol)	Age (year.month)
604	9.101			62	9.207	2008.83		
605	9.072			61	9.136	2008.92		
606	9.042			60	9.177	2008.99		
607	8.990			59	9.250	2009.07		
608	8.990			58	9.309	2009.14		
609	8.950			57	9.233	2009.21		
610	8.955			56	9.205	2009.30		
611	8.954			55	9.202	2009.35		
612	8.981			54	9.179	2009.43		
613	8.992			53	9.136	2009.49		
614	8.997			52	9.085	2009.56		
615	9.063			51	9.086	2009.63		
616	9.101			50	9.024	2009.71		
617	9.113			49	9.030	2009.77		
618	9.086			48	9.075	2009.83		
619	9.087			47	9.099	2009.88		
620	9.057			46	9.104	2009.91		
621	9.045			45	9.126	2009.96		
622	9.033			44	9.282	2010.01		
623	9.010			43	9.261	2010.05		
624	9.008			42	9.200	2010.11		
625	9.001			41	9.291	2010.13		
626	8.955			40	9.263	2010.20		
627	8.958			39	9.256	2010.25		
628	8.989			38	9.236	2010.30		
629	9.007			37	9.263	2010.36		
630	9.005			36	9.277	2010.42		
631	9.032			35	9.218	2010.51		
632	9.056			34	9.127	2010.57		
633	9.036			33	9.069	2010.63		
634	9.052			32	9.104	2010.80		
635	9.073			31	9.231	2010.89		
636	9.068			30	9.267	2011.03		
637	9.081			29	9.196	2011.10		
638	9.042			28	9.258	2011.16		
639	9.054			27	9.249	2011.20		
640	9.116			26	9.247	2011.27		
641	9.037			25	9.261	2011.32		
642	9.006			24	9.182	2011.38		
643	9.009			23	9.241	2011.42		
644	8.945			22	9.150	2011.45		
645	8.909			21	9.136	2011.50		
646	8.896			20	9.006	2011.55		
647	8.924			19	8.985	2011.63		
648	8.938			18	9.017	2011.66		
649	8.980			17	9.052	2011.70		
650	9.020			16	9.083	2011.76		
651	9.066			15	9.058	2011.81		
652	9.049			14	9.077	2011.88		
653	9.073			13	9.053	2011.96		
654	9.121			12	9.139	2012.04		
655	9.102			11	9.136	2012.11		
656	9.106			10	9.187	2012.20		
657	9.140			9	9.160	2012.23		
658	9.172			8	9.153	2012.25		
659	9.088			7	9.123	2012.30		
660	9.121			6	9.109	2012.34		
661	9.036			5	9.113	2012.38		
662	9.045			4	9.091	2012.42		
663	9.011			3	9.039	2012.46		
664	8.984			2	9.016	2012.50		
665	9.032			1	9.022	2012.54		